ABC Imagem Cardiovascular

Volume 36 | Number 1

January/February/March 2023

Sociedade Brasileira de Cardiologia
ISSN-2675-312X

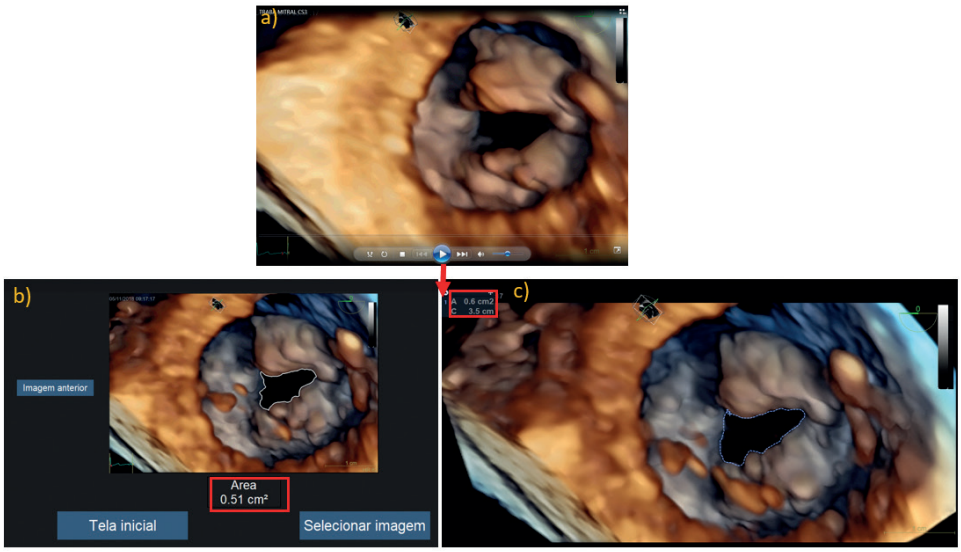

Figure 5 of the article: Automatic Measurement of the Mitral Valve Based on Echocardiography Using Digital Image Processing

DIC | SBC Sociedade Brasileira de Cardiologia 1943 | ABC Imagem Cardiovascular

Contents

Click on the title to read the article

Review Article

Case Report

Departament of Cardiovascular Imaging

President
André Luiz Cerqueira de Almeida - BA

Vice President of Echocardiography
Alex dos Santos Félix - RJ

Vice President of Nuclear Cardiology
Simone Cristina Soares Brandão - PE

Vice President of Vascular Echography
José Aldo Ribeiro Teodoro - SP

Vice President of Magnetic Resonance Imaging
Otávio Rizzi Coelho Filho - SP

Vice President of Computed Tomography
Márcio Sommer Bittencourt - SP

Vice President of Congenital Heart Disease and Pediatric Cardiology
Adriana Mello Rodrigues dos Santos - MG

Managing Director
Silvio Henrique Barberato - PR

Financial Director
Mohamed Hassan Saleh - SP

Journal Director
Daniela do Carmo Rassi Frota - GO

Board of Trustees

President
Fábio Villaça Guimarães Filho - SP

Members
Afonso Akio Shiozaki - PR
Bruna Morhy Borges Leal Assunção - SP
David Costa de Souza Le Bihan - SP
Jorge Andion Torreão - BA
José Luiz Barros Pena - MG
José Olimpio Dias Júnior - MG
Rafael Willain Lopes - SP

Scientific Committee

Coordinator
Alex dos Santos Félix - RJ

Members
Simone Cristina Soares Brandão - PE
José Aldo Ribeiro Teodoro - SP
Otávio Rizzi Coelho Filho - SP
Márcio Sommer Bittencourt - SP

Qualification Committee

Coordinator
Andrea de Andrade Vilela - SP
Antonio Tito Paladino Filho - SP

Adult Echo Members
Antônio Amador Calvilho Júnior - SP
Candice Machado Porto - BA
Eliza de Almeida Gripp - RJ
João Carlos Moron Saes Braga - SP
Rafael Modesto Fernandes – BA
Sandra Nívea dos Reis Saraiva Falcão - CE

Congenital Echo Members
Carlos Henrique de Marchi - SP
Daniela Lago Kreuzig - SP
Halsted Alarcão Gomes Pereira da Silva - SP
Márcio Miranda Brito - TO

Seniors
Fábio Villaça Guimarães Filho - SP
Maria Estefânia Bosco Otto - DF
Solange Bernades Tatani - SP

Communication, Information and Internet Committee

Coordinator
José Roberto Matos Souza - SP

Members
Fabio Roston
Issam Shehadeh

Committee of Institutional Relations, Fees and Advocacy

Coordinator
Marcelo Haertel Miglioranza - RS

Members
Wagner Pires de Oliveira Júnior - DF

Committee of Education and Accreditation

Coordinator
Edgar Bezerra de Lira Filho - SP

Intersociety Committee

Coordinator
Marcelo Luiz Campos Vieira - SP

DIC Youth Committee

Coordinator
Eliza de Almeida Gripp - RJ

Positioning and Guidelines Committee

Coordinator
Marcelo Dantas Tavares de Melo - PB

Consultant
José Luiz Barros Pena - MG

Representatives

ASE
José Luiz Barros Pena - MG

EACVI
Alex dos Santos Félix - RJ

SISIAC
Ana Cristina de Almeida Camarozano - PR

Board of Former Presidents
Jorge Eduardo Assef - SP
Arnaldo Rabischoffsky - RJ
Samira Saady Morhy - SP
Marcelo Luiz Campos Vieira - SP
Carlos Eduardo Rochitte -SP

Board of Directors – Year 2023 (Brazilian Society of Cardiology)

North/Northeast
Nivaldo Menezes Filgueiras Filho (BA)
Sérgio Tavares Montenegro (PE)

East
Denilson Campos de Albuquerque (RJ)
Andréa Araujo Brandão (RJ) – Presidente do Conselho Administrativo

State of São Paulo
Celso Amodeo (SP)
João Fernando Monteiro Ferreira (SP)

Center
Carlos Eduardo de Souza Miranda (MG) — Vice-presidente do Conselho Administrativo
Weimar Kunz Sebba Barroso de Souza (GO)

South
Paulo Ricardo Avancini Caramori (RS)
Gerson Luiz Bredt Júnior (PR)

Scientific Committee
Denilson Campos de Albuquerque (RJ)
Ibraim Masciarelli Francisco Pinto (SP)
Weimar Kunz Sebba Barroso de Souza (GO)

National Editorial Board

ABC Imagem Cardiovascular

Volume 36, Nº 1, January/February/March 2023

Indexing: Lilacs (Latin American and Caribbean Health Sciences Literature), Latindex (Regional Cooperative Online Information System for Scholarly Journals from Latin America, the Caribbean, Spain and Portugal) and DOAJ (Directory of Open Access Journals)

Address: Av. Marechal Câmara, 160 - 3º andar - Sala 330
20020-907 • Centro • Rio de Janeiro, RJ • Brasil
Phone.: (21) 3478-2700
E-mail: abcimaging@cardiol.br
https://www.abcimaging.org/

Commercial Department
Phone: (11) 3411-5500
E-mail: comercialsp@cardiol.br

Editorial Production
SBC - Scientific Department

Graphic Design and Diagramming
SBC - Scientific Department

Automatic Measurement of the Mitral Valve Based on Echocardiography Using Digital Image Processing

Genilton de França Barros Filho,[1] Israel Solha,[1] Ewerton Freitas de Medeiros,[1] Alex dos Santos Felix,[2] André Luiz Cerqueira de Almeida,[3] José Carlos de Lima Júnior,[1] Marcelo Dantas Tavares de Melo,[1] Marcelo Cavalcanti Rodrigues[1]

Universidade Federal da Paraíba,[1] João Pessoa, PB – Brazil
Instituto Nacional de Cardiologia,[2] Rio de Janeiro, RJ – Brazil
Departamento de Imagem Cardiovascular,[3] São Paulo, SP – Brazil

Abstract

Background: The evaluation of mitral valve area through multiplanar reconstruction in 3-dimensional echocardiography is restricted to specific software and to the experience of echocardiographers. They need to manually select the video frame that contains the maximum mitral valve opening area, as this dimension is fundamental to identification of mitral stenosis.

Objective: To automate the process of determining the maximum mitral valve opening area, through the application of digital image processing (DIP) in echocardiography tests, developing an open algorithm with video reading in avi format.

Method: This cross-sectional observational pilot study was conducted with 25 different echocardiography exams, 15 with normal aperture and 10 with rheumatic mitral stenosis. With the authorization of the Research Ethics Committee, all exams were performed and made available by 2 specialists who used 2 models of echocardiographic devices: Vivid E95 (GE Healthcare) and Epiq 7 (Philips), with multiplanar transesophageal probes. All videos in avi format were submitted to DIP using the image segmentation technique.

Results: The measurements obtained manually by experienced echocardiographers and the values calculated by the developed system were compared using a Bland-Altman diagram. There was greater agreement between values in the range from 0.4 to 2.7 cm².

Conclusion: It was possible to automatically determine the maximum mitral valve opening area, for cases from both GE and Philips, using only 1 video as input data. The algorithm has been demonstrated to save time on measurements when compared to the usual method.

Keywords: Mitral Valve; Echocardiography; Image Processing, Computer-Assisted.

Introduction

Valve diseases are important determinants of cardiovascular morbidity and mortality, with degenerative diseases of the mitral and aortic valves being the most prevalent, even though rheumatic disease still constitutes an important public health problem in Brazil. Echocardiography plays an important role in the diagnosis and severity assessment of valve diseases. It is able to determine anatomical and pathophysiological details that assist in planning the best intervention for each patient, and it has the advantages of being widely available and low cost, without requiring radiation or nephrotoxic contrast.[1]

Among the most common imaging tests, echocardiography is the most frequently used modality in the evaluation of mitral valve diseases. This is possible because it is a more readily available and widely used technique to assess function and structure. Echocardiography makes real-time imaging possible without the presence of ionizing radiation, serving today as a backbone in the field of cardiovascular imaging.[2]

The use of 3-dimensional echocardiography provides numerous advantages, such as the possibility of real-time navigation, image post-processing, and multiplanar reconstruction. It is especially important for the preoperative evaluation of patients who are candidates for valve repair or replacement surgery. It allows intraoperative monitoring of procedures, such as transcatheter aortic valve replacement[3] and implantation of clips for percutaneous mitral repair (Mitraclip). It also makes it possible to conduct procedures to treat rheumatic mitral stenosis, such as percutaneous mitral

Correspondência: Genilton de França Barros Filho •
Rua Luiza Dantas de Medeiros, 261, apt. 103 G. Postal code: 58073-040. José Américo, João Pessoa, PB - Brazil
E-mail: gfbfilho@gmail.com
Manuscript received December 18, 2022; revised manuscript January 27, 2023; accepted January 1, 2023
Editor responsible for the review: Daniela do Carmo Rassi Frota

DOI: https://doi.org/10.36660/abcimg.2023371i

Contents

balloon valvuloplasty, or even percutaneous implantation of a biological mitral valve prosthesis by transcatheter mitral valve replacement, in patients with degenerative mitral disease and calcification of the valve annulus, or percutaneous prosthesis implantation inside a dysfunctional biological prosthesis (mitral valve-in-valve procedure). The procedures described have shown great evolution, with increasingly effective results due to the help of multimodal cardiac imaging in pre-procedure evaluation and during the intervention.[4,5]

During interventions, decisions must be be agile, and accurate information must be provided to the interventionist; therefore, the quality of communication between teams is essential. Through visual demonstration of structures, made possible by 3-dimensional reconstruction and rendering, with more accurate measurements that are less dependent on angulations, such as those obtained by multiplanar reconstruction, it is possible to obtain better results, with greater efficiency and lower rate of complications.[5]

There is significant variation in the human interpretation of echocardiographic data, in addition to errors in measurements, due to considerable inter-observer variability. The use of automated systems for the interpretation of cardiovascular images can be useful in improving the methods' diagnostic and prognostic performance, and the application of machine learning to medical images, with the help of specialists' interpretation, increases the reliability of the process due to the availability of various data structured by reports.[6]

The accurate evaluation of the mitral valve area by means of multiplanar reconstruction on 3-dimensional transesophageal echocardiography is totally dependent on the examiner's experience and expertise in using specific software, which may not be available on some platforms or may not even be very practical to use, thus consuming exam time.[6]

Digital image processing (DIP) has been gaining recognition in 2 main areas of application, namely, improving visual information from imaging for human interpretation and processing imaging data for storage, transmission, and representation, considering automatic machine perception.[7]

It consists of manipulation of images by a computer, with different applications, such as contrast enhancement, noise reduction, tracking objects and/or people, edge detection, pattern identification, classification and counting of objects and/or people, and many others.[7] Among multiple existing DIP techniques, image segmentation has been applied. This technique produces a binary image, with pixels of value 1, indicating they are part of the object under study, and pixels of value 0, indicating they are not. Thus, it is possible to divide an image into regions, identifying borders and discontinuities, for example.[8]

Several studies have contributed to the evolution of echocardiography analysis using computerized tools. For example, Sakamiya et al. created a platform for online monitoring of the contractile behavior of the heart, which are the main functional characteristics of cardiac tissue, simultaneously employing an image processing and piezoelectric detection system. They also evaluated the influence of medications such as isoproterenol and doxorubicin on the contractile behavior of the heart. The medication reactivity results provided by these 2 measurement systems were consistent with the previous reports they had, demonstrating the reliability of the developed platform and its potential for use in medication-related screening applications.[9]

Nizar et al. used a convolutional neural network for real-time detection of the aortic valve in echocardiography exams, with the purpose of assisting medical examination, since an automated detection system in an echocardiogram can improve the accuracy of the medical diagnosis and provide additional medical analysis from the resulting detection. Therefore, they concluded that this tool can be of great help for medical purposes.[10]

Ostvik et al. verified the possibility of applying artificial neural networks in the classification of transthoracic images obtained by echocardiography. The conclusion was satisfactory for the implementation in 2-dimensional echocardiography, and, for analysis of 3-dimensional echocardiography, studies still need to make gains in performance, seeing that it is conducted based on frames obtained during the procedure.[11]

Therefore, the objective of this project is to automate the determination of maximum mitral valve opening area, by applying DIP to echocardiography exams and developing an open algorithm with video reading in avi format.

Methods

Retrospective analyses were conducted in different echocardiography studies by experienced echocardiographers. The exams included patients who had "normal" mitral valves, that is, mitral valve openings in normal conditions, and patients with mitral valves affected by rheumatic stenosis.

For acquisition, the echocardiographers used 2 echocardiography device models, with multiplanar transesophageal probes: the Vivid E95 (GE Healthcare) and the Epiq 7 (Philips). Each has its particularities. The most considerable difference, in relation to this research, is the way in which the image scale is represented. The Philips echocardiograph draws green dots, and the distance between their centroids is indicated as a numerical value belonging to the metric scale. The General Electric (GE) brand echocardiograph represents the scale at the bottom right of the image.

After acquiring the exams saved as videos, they were submitted to DIP using the image segmentation technique, considering that a video is composed of a set of sequential static images. As a result, DIP identifies the maximum valve opening area, highlights its outline, and calculates its value.

An application was developed to facilitate the use of DIP. People unfamiliar with programming are able to use it, as it has an intuitive graphical interface. It was created with python language.

Finally, the results obtained by the application were compared with the results obtained by the echocardiographers, who manually selected the maximum valve opening area using specific software. To verify the correlation between both measurements, the Bland-Altman method was used.

Results

All exams obtained were saved in avi video format. A total of 25 videos were acquired, 22 from the GE echocardiography device and 3 from the Philips device. The number of tests used in the present study was limited by the study time and influenced by the pandemic, which made it difficult to acquire more tests.

The study model was retrospective, cross-sectional, and observational, acquired in accordance with the recommendations of the American Society of Echocardiography.[12] Planimetry was performed by multiplanar reconstruction with ventricular and atrial view, using EchoPac v.204 for GE devices and directly on the Epiq 7 device during the echocardiography for the Philips devices.

Figure 1 illustrates the interfaces of the developed application and how it functions.

When the application is opened, the home screen is displayed (Figure 1a). It displays 2 options: "Philips" and "General Electric". The user must select the button according to the source of the video to be used for analysis. If the video was saved from echocardiograms performed using Philips devices, the "Philips" button must be selected. If the exams were performed using General Electric devices, the "General Electric" button must be selected.

When selecting the "Philips" option, the screen in Figure 1b will be displayed. The user must click on the "Select Video" button to load the video to be analyzed and, subsequently, inform the numerical scale present in the video. For example, if the exam was performed and saved with a 5 mm scale in the grid, the user must enter a value of 0.5 in the "Scale [cm]" field. Finally, the "Play" button must be selected for the application to perform the entire DIP to identify and calculate the maximum valve opening area. Additionally, the screen displays some instructions to facilitate the use of the application and to optimize the results to be obtained.

If the "General Electric" option is selected on the initial screen (Figure 1a), the screen in Figure 1c will be displayed. This screen allows the user to choose how the video was saved. If it was saved with only the 3-dimensional view, the "Case 1" button must be selected. If it was saved with the 3-dimensional view and the frontal, lateral, and superior views, the "Case 2" button must be selected. This distinction is necessary, because the mode and characteristics of saved videos influence digital processing.

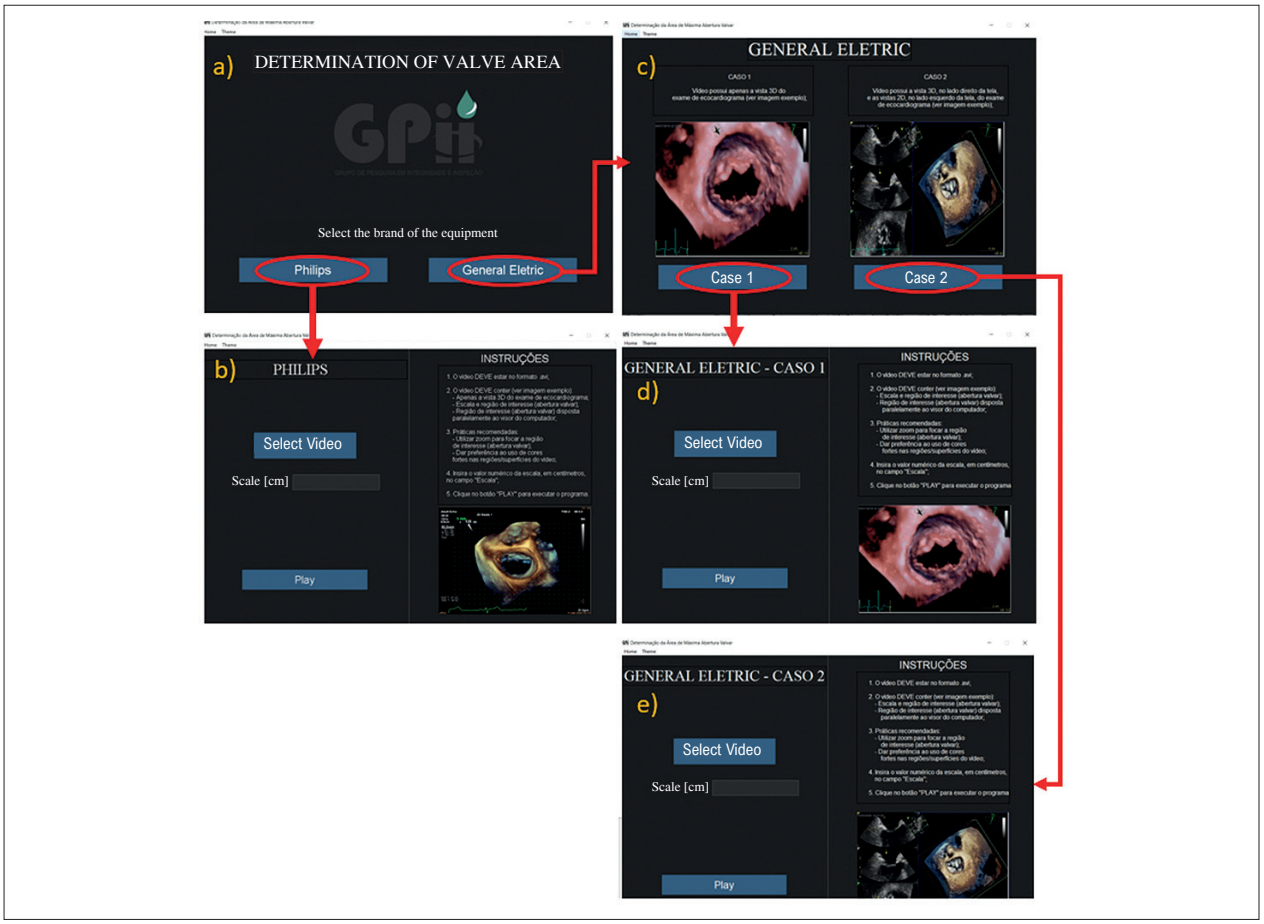

Figure 1 – *Screens of the developed application. a) Home screen; b) Screen for processing videos from Philips echocardiography devices; c) Screen for selecting options for video from GE echocardiography devices; d) Screen for processing videos with only the 3-dimensional view from GE echocardiography devices (Case 1); e) Screen for processing videos with 3-dimensional, lateral, superior, and frontal views from GE echocardiography devices (Case 2).*

The "Case 1" and "Case 2" buttons will display the screens in Figures 1d and 1e, respectively. They function in the same manner as the screen in Figure 1b, previously described.

After selecting the "Play" button in Figure 1b, Figure 1d, or Figure 1e, DIP transforms the video into a set of images (as in the example illustrated in Figure 2), also called frames, to analyze them separately and to identify the image that contains the maximum valve opening area. As all images are isolated, the frame rate (frames per second) of each video did not interfere with the results.

After digital processing, the application displays the result, as illustrated in Figure 3.

Figure 3a illustrates the first screen displayed after the application executes the DIP. The maximum valve opening area is identified and drawn (white outline). The value of the maximum area is also displayed. In the case shown in Figure 3a, the area is 4.45 cm ^{2}.

In order to make the results more accurate, the application allows the user to check the preceding and subsequent images, with the buttons "Previous image" and "Next image", respectively. They make it possible to verify the outlines that best correspond to reality.

In the result shown in Figure 3, although the outline in Figure 3a shows a satisfactory result, the outline in Figure 3b is more accurate and more consistent with the shape of the maximum valve opening. In fact, the maximum valve opening area became 4.5 cm^2.

The "Home screen" button returns to the initial screen of the application (Figure 1a) and the "Select image" button saves the results obtained.

Figures 4 and 5 represent comparisons between the results obtained by measuring the maximum valve opening area performed by the developed application and by an echocardiographer. Figure 4 characterizes a "normal" case, and Figure 5 displays a case with stenosis.

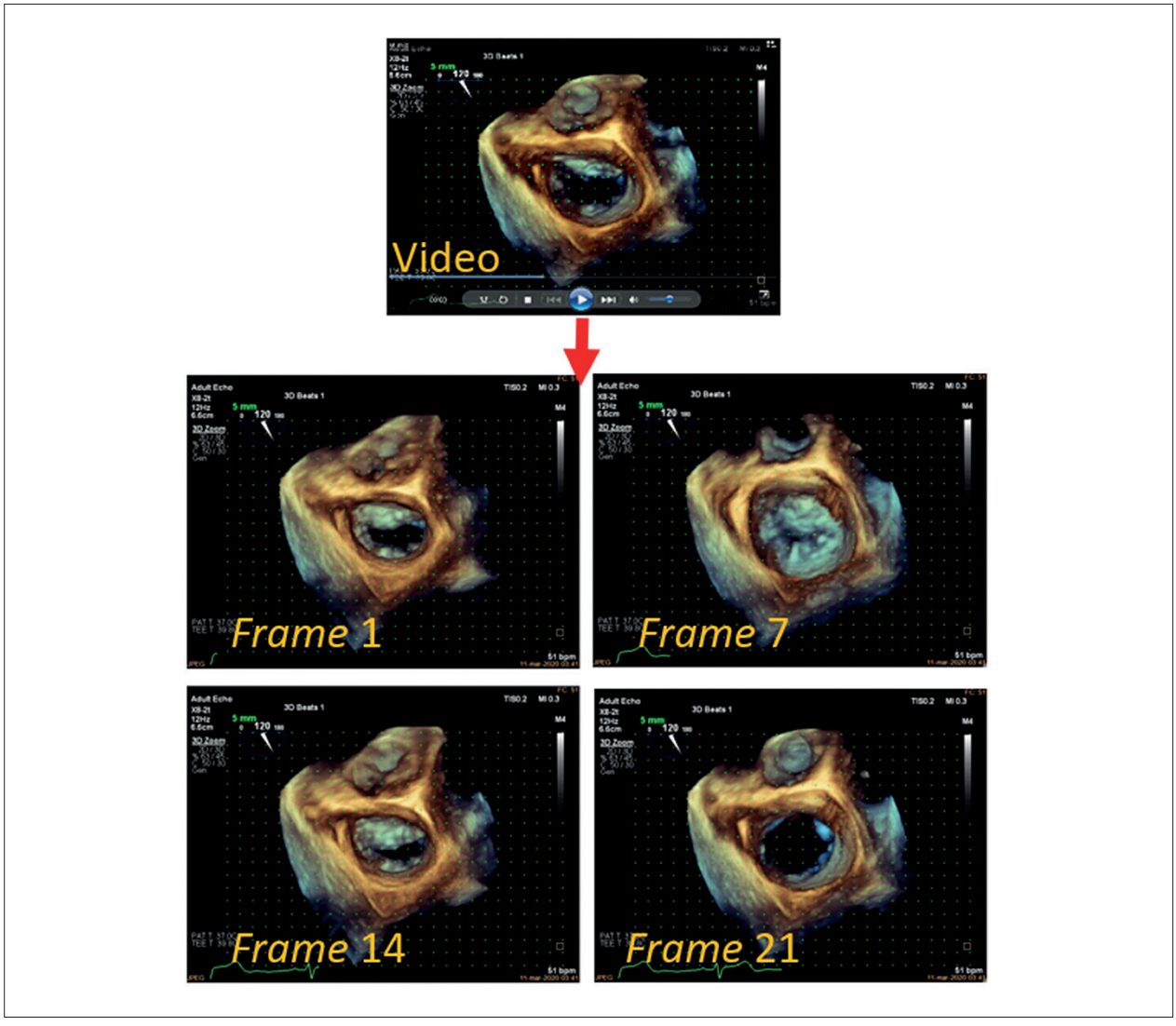

Figura 2 – *Example illustrating the transformation of a video into multiple images (frames).*

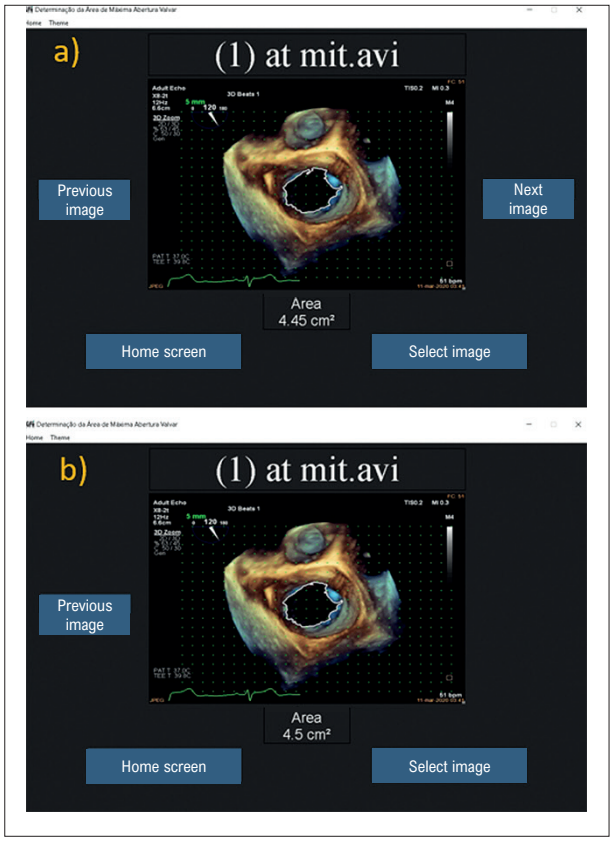

Figure 3 – *Results displayed by the developed application. a) Home screen; b) Final screen, with the image of the maximum valve opening selected.*

Analysis of Figures 4 and 5 reveals that the results were very close. For the "normal" case, the application provided the value of 4.59 cm² (Figure 4b), and the echocardiographer's measurement provided the value of 4.7 cm² (Figure 4c). In the case with stenosis, the application provided the value of 0.51 cm² (Figure 5b), and the echocardiographer's measurement provided the value of 0.6 cm² (Figure 5c).

Furthermore, it was observed that the adoption of some practices optimizes the results of the application, for example, saving videos highlighting the mitral valve region, applying zoom, and saving videos with few elements, preferably only the region of interest and the scale used. However, further tests would be needed to validate this finding.

With the identification of the maximum valve opening and the calculation of its value, the developed application is also able to detect whether or not the patient in the referred exam has stenosis.

Furthermore, the processing time of the application is relatively low, remaining under 3 minutes for the majority of analyses.

In order to verify the concordance of the results obtained by the application and by the echocardiographers' measurements, the Bland-Altman method was applied, as shown in Figure 6.

Using the Bland-Altman method, evaluating the cases with and without stenosis separately, agreement was found between the DIP and echocardiographers' measurements in obtaining the maximum valve opening area (Figure 6a

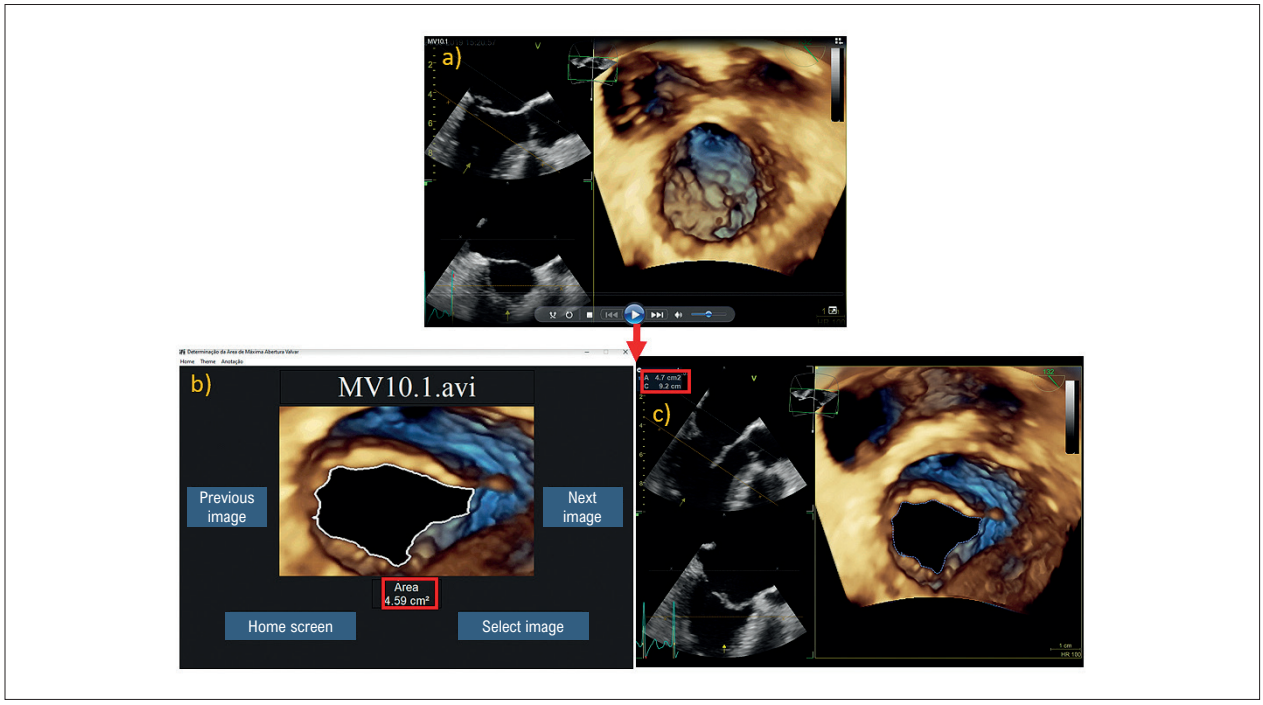

Figure 4 – *Comparison between the measurement of the developed application and the measurement of an echocardiographer, with manual selection by means of specific software. a) Analyzed video of a "normal" case; b) Result of the developed application: Area of 4.59 cm²; c) Result of the echocardiographer's measurement: Area of 4.7 cm².*

and Figure 6b). Combining all cases, only 2 were outside the acceptable range (Figure 6c). These results contribute to the validation of both the DIP technique employed and the developed application.

For cases without stenosis (Figure 6a), the greatest difference between measurements was 0.7 cm², while most remained within the range of −0.5 cm² to 0.5 cm². For cases with stenosis (Figure 6b), the greatest difference between measurements was 0.2 cm², and all remained within the range of −0.2 cm² to 0.2 cm². Analyzing all cases (Figure 6c), those with stenosis (points further to the left in Figure 6c) had smaller differences in measurements compared to those without stenoses (points further to the right in Figure 6c).

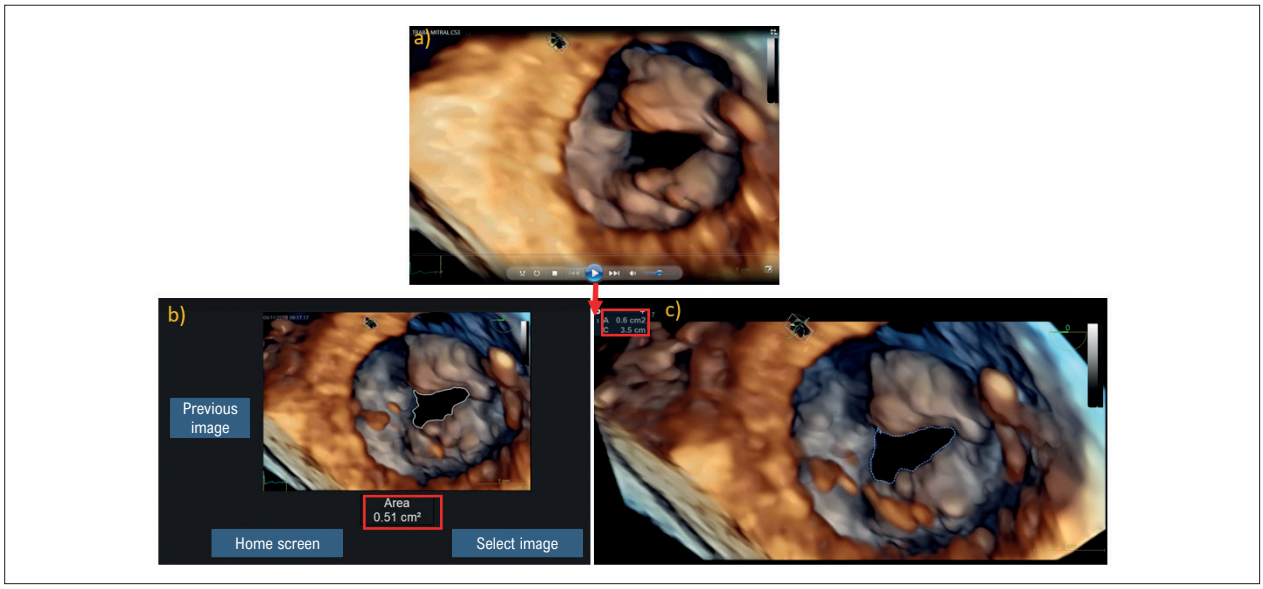

Figure 5 – *Comparison between the measurement of the developed application and the measurement of an echocardiographer, with manual selection by means of specific software. a) Analyzed video of a case with stenosis; b) Result of the developed application: Area of 0.51 cm²; c) Result of the echocardiographer's measurement: Area of 0.6 cm².*

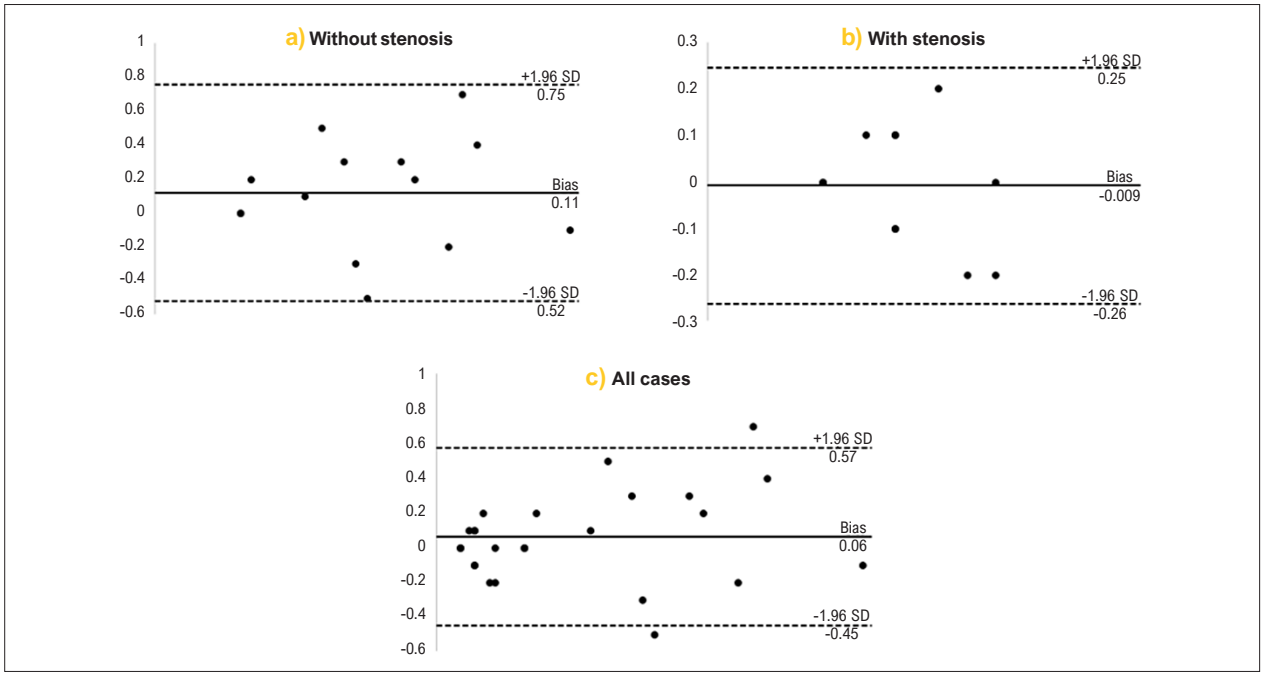

Figure 6 – *Bland-Altman method. a) Applied only to cases without stenosis; b) Applied only to cases with stenosis; c) Applied to all 25 tests used in this study.*

Discussion

This study stands out because it employs DIP, based on the image segmentation technique, to detect the maximum mitral valve opening area automatically, based on echocardiogram videos in avi format. Therefore, it contributes to the detection of mitral stenosis. A major differential is the application developed with python language, which allows easy access and easy handling of the DIP tools. It needs only be installed on a computer. The application's screens were developed to improve users' experience, and they do not require prior knowledge of programming.

The developed application is capable of analyzing more complex cases, such as patients with arrhythmias, because the automatic selection makes it possible to check each image in the video, highlighting the image with the maximum valve opening. Moreover, the more measurements that are performed with the developed application and compared with medical measurements, especially with different and atypical cases, the more it will be tested, allowing better assessment for its consolidation.

This automatic measurement has some advantages when compared with manual selection performed by echocardiographers, because the result can be heavily influenced by the moment when they pause the video to perform the analysis. This manual selection requires a great deal of the specialist's time, considering that they must be very careful to carry out a selection with as little error as possible and with maximum attention. Considering a full day of care, the accuracy of the selected regions will be greater for the first patients of the day, and they will decrease according to the echocardiographer's physical and mental fatigue, in addition to other external factors that may influence the measurement.

When conducting a survey of the literature, nothing similar was found. However, one of the great efforts of researchers is to ensure the automation of measurements in operator-dependent examinations for the investigation of various pathologies, with the aim of reducing or eliminating manual selection errors. Thus, Saine et al. presented a technique for automatic boundary detection of the left atrium and ventricle based on 2-dimensional echocardiograms, with the objective of determining the dilation area of these chambers in patients with mitral valve insufficiency.[13]

Melo et al. developed a semiautomated method that determines variation in ventricular area on dynamic 2-dimensional echocardiograms using DIP techniques such as time averaging, wavelet-based denoising, edge enhancement filtering, morphological operations, homotopy modification, and watershed segmentation. This method has become useful for analyzing global ventricular function by measurements of area.[14]

Mahadi et al. verified the use of DIP in 2-dimensional echocardiograms to transform scan slices into a set of pixels and thus determine the distance of points that could measure the diameter of a mitral valve in a given view.[15] Aquila et al. presented the use of a tool called Siemens eSie Valves which made it possible to automatically determine a series of parameters of the mitral valve annulus such as area, anteroposterior and posterolateral diameters, and intertrigonal distance. Therefore, this study compares existing anatomical alterations between functional and organic mitral regurgitation processes based on the automatic acquisition of valve measurements.[16]

Accordingly, this study offers another tool to combat possible human errors in measuring valve areas and to contribute to automation.

Conclusions

It was possible to automatically determine the maximum mitral valve opening area, for cases from both GE and Philips echocardiography devices, using only 1 video as input data.

As the application chooses the appropriate frame and calculates the area almost instantly, it can be intuitively concluded that it is faster than manual measurement.

This study shows interesting potential because it does not depend on specific software, and it has a good outlook for obtaining measurements remotely.

Author Contributions

Conception and design of the research: Barros Filho GF, Soares I, Medeiros EF, de Melo MDT, Rodrigues MC; acquisition of data: Felix AS, de Melo MDT; analysis and interpretation of the data: Barros Filho GF, Soares I, Medeiros EF, Felix AS, de Melo MDT, Rodrigues MC; statistical analysis: Barros Filho GF, Soares I, Medeiros EF; writing of the manuscript: Soares I, Medeiros EF; critical revision of the manuscript for intellectual content: Almeida ALC, Lima Júnior JC, de Melo MDT, Rodrigues MC.

Potential Conflict of Interest

No potential conflict of interest relevant to this article was reported.

Sources of Funding

This study was partially funded by Coordenação de Aperfeiçoamento de Pessoal de Nível Superior (CAPES).

Study Association

This article is part of the thesis of Doctoral submitted by Genilton de França Barros Filho, from Universidade Federal da Paraíba, Programa de Pós-Graduação em Engenharia Mecânica.

Ethics Approval and Consent to Participate

This study was approved by the Ethics Committee on Animal Experiments of the Colegiado do Comitê de Ética em Pesquisa com Seres Humanos - CEP/CCM/UFPB under the protocol number 3.858.742.

References

1. Tarasoutchi F, Montera MW, Grinberg M, Piñeiro DJ, Sánchez CR, Bacelar AC, et al. Brazilian Guidelines for Valve Disease - SBC 2011 / I Guideline Inter-American Valve Disease - 2011 SIAC. Arq Bras Cardiol. 2011;97(5 Suppl 1):1-67. doi: 10.1590/s0066-782x2011002000001.
2. Andreassen BS, Veronesi F, Gerard O, Solberg AHS, Samset E. Mitral Annulus Segmentation Using Deep Learning in 3-D Transesophageal Echocardiography. IEEE J Biomed Health Inform. 2020;24(4):994-1003. doi: 10.1109/JBHI.2019.2959430.
3. Reardon MJ, van Mieghem NM, Popma JJ, Kleiman NS, Søndergaard L, Mumtaz M, et al. Surgical or Transcatheter Aortic-Valve Replacement in Intermediate-Risk Patients. N Engl J Med. 2017;376(14):1321-31. doi: 10.1056/NEJMoa1700456.
4. El Sabbagh A, Eleid MF, Foley TA, Al-Hijji MA, Daly RC, Rihal CS, et al. Direct Transatrial Implantation of Balloon-Expandable Valve for Mitral Stenosis with Severe Annular Calcifications: Early Experience and Lessons Learned. Eur J Cardiothorac Surg. 2018;53(1):162-9. doi: 10.1093/ejcts/ezx262.
5. Mackensen GB, Lee JC, Wang DD, Pearson PJ, Blanke P, Dvir D, et al. Role of Echocardiography in Transcatheter Mitral Valve Replacement in Native Mitral Valves and Mitral Rings. J Am Soc Echocardiogr. 2018;31(4):475-90. doi: 10.1016/j.echo.2018.01.011.
6. Ghorbani A, Ouyang D, Abid A, He B, Chen JH, Harrington RA, et al. Deep Learning Interpretation of Echocardiograms. NPJ Digit Med. 2020;3:10. doi: 10.1038/s41746-019-0216-8.
7. Gonzalez RC, Woods RE. Processamento Digital de Imagens. São Paulo: Pearson Prentice Hall; 2010.
8. Jähne B. Digital Image Processing. Heidelberg: Springer; 2005.
9. Sakamiya M, Fang Y, Mo X, Shen J, Zhang T. A Heart-On-A-Chip Platform for Online Monitoring of Contractile Behavior via Digital Image Processing and Piezoelectric Sensing Technique. Med Eng Phys. 2020;75:36-44. doi: 10.1016/j.medengphy.2019.10.001.
10. Nizar MHA, Chan CK, Khalil A, Yusof AKM, Lai KW. Real-Time Detection of Aortic Valve in Echocardiography using Convolutional Neural Networks. Curr Med Imaging. 2020;16(5):584-91. doi: 10.2174/1573405615666190114151255.
11. Østvik A, Smistad E, Aase SA, Haugen BO, Lovstakken L. Real-Time Standard View Classification in Transthoracic Echocardiography Using Convolutional Neural Networks. Ultrasound Med Biol. 2019;45(2):374-84. doi: 10.1016/j.ultrasmedbio.2018.07.024.
12. Hahn RT, Saric M, Faletra FF, Garg R, Gillam LD, Horton K, et al. Recommended Standards for the Performance of Transesophageal Echocardiographic Screening for Structural Heart Intervention: From the American Society of Echocardiography. J Am Soc Echocardiogr. 2022;35(1):1-76. doi: 10.1016/j.echo.2021.07.006.
13. Saini K, Dewal ML, Rohit M. A Fast Region-Based Active Contour Model for Boundary Detection of Echocardiographic Images. J Digit Imaging. 2012;25(2):271-8. doi: 10.1007/s10278-011-9408-8.
14. Melo SA Jr, Macchiavello B, Andrade MM, Carvalho JL, Carvalho HS, Vasconcelos DF, et al. Semi-Automatic Algorithm for Construction of the Left Ventricular Area Variation Curve Over a Complete Cardiac Cycle. Biomed Eng Online. 2010;9:5. doi: 10.1186/1475-925X-9-5.
15. Mahadi LF, Ibrahim N, Zaluwi MT, Johan MHSM. Feature Detection of Mitral Valve Based on Image Processing Technique: A Review. J Phy: Conf Ser. 2019;1372(1):12071. doi: 10.1088/1742-6596/1372/1/012071.
16. Aquila I, Fernández-Golfín C, Rincon LM, González A, García Martín A, Hinojar R, et al. Fully Automated Software for Mitral Annulus Evaluation in Chronic Mitral Regurgitation by 3-Dimensional Transesophageal Echocardiography. Medicine. 2016;95(49):e5387. doi: 10.1097/MD.0000000000005387.

Heart Adaptation Mechanisms in Elite Female Athletes: Comparison With Healthy Individuals and Time of Training

José Maria Del Castillo,[1] Thiago Boschilia,[1] Nemi Sabeh Junior,[1] Carlos Antônio da Mota Silveira,[1] Djair Brindeiro Filho[1]

Escola de Ecografia de Pernambuco (ECOPE),[1] Universidade Católica de Pernambuco, Recife, PR – Brazil

Abstract

Background: Intense continuous exercise provokes adaptive remodeling phenotypes in athletes, the parameters of which can be evaluated through conventional echocardiography and myocardial deformation. We compared myocardial remodeling in female athletes (athlete group) with sedentary women of the same age range (control group) and between older and younger athletes.

Methods: A total of 57 female soccer players and 25 healthy sedentary women were selected. The athlete group was subdivided into a main group and those under 17 years of age (< 17 group). The dimensions and systolic and diastolic function of the cardiac chambers and myocardial deformation (longitudinal and circumferential, as well as radial strain and rotational mechanics) was determined through echocardiography, using the Z statistic with a significance level of p< 0.05.

Results: The mean age of the athlete, control, main, and < 17 groups was 22.1 (SD, 6.3); 21.2 (SD, 5.0); 26.5 (SD, 5.1); 16.5 (SD, 0.6) years, respectively. Weight, body mass index and heart rate were lower in the athlete group. Wall thickness, left ventricular mass index, left atrial (LA) volume, ejection fraction, and right ventricular dimensions were higher in athlete group, but remained within normal ranges. Regarding myocardial deformation, there was decreased radial strain, basal rotation, apical rotation, and twisting in the athlete group, suggesting a contractile reserve mechanism. These parameters were lesser in the main athlete group, who also had greater wall thickness, greater volume in the left atrium (LA) and larger size in the right ventricle (RV), suggesting that increased contractile reserve is related to longer time spent in the sport.

Conclusions: In female athletes who had undergone intense long-term training, we observed adaptive remodeling of the cardiac chambers and increased contractile reserve (at rest), and these changes were more pronounced in those with longer involvement in the sport.

Keywords: Echocardiography; Atrial Remodeling; Athletes.

Introduction

Intense sustained exercise leads to adaptive remodeling in the cardiac cavities. However, remodeling mechanisms differ according to activity type, as postulated by Morganroth in 1975:[1] anaerobic exercise (strength and short-duration) causes concentric remodeling, while aerobic exercise (resistance and long-duration) causes eccentric remodeling. In different sports there are many combinations between strength and resistance, resulting in combined phenotypes. Soccer, for example, involves an estimated 70% aerobic and 30% anaerobic activity.[2]

Mailng Address: José Maria Del Castillo •
Rua Jorge de Lima, 245, apto 303. Salute. Postal Code 51160-070. Imbiribeira, Recife, PE – Brazil
E-mail: castillojmd@gmail.com
Manuscript received December 17, 2022; revised manuscript January 27, 2023; accepted January 29, 2023
Editor responsible for the review: Daniela do Carmo Rassi Frota

DOI: https://doi.org/10.36660/abcimg.2023372i

In some athletes, remodeling results in different degrees of hypertrophy or myocardial dilation, sometimes resulting in a difficult differential diagnosis of hypertrophic or dilated cardiomyopathies. Based on research and diagnostic criteria, eligibility criteria for elite athletes with cardiac alterations have now been developed.[3] The selection of these criteria is extremely important, since the prevalence of sudden death among athletes is high.[4] In most athletes, however, physiological cardiac remodeling occurs within normal limits or below pathological values. The threshold between pathological and athletic hypertrophy is ≥ 16 mm for the interventricular septum. Athletes, in general, have a septal thickness ≤ 12 mm, with a septal thickness 13-15 mm and a septum/wall ratio < 1.3 considered a "gray zone".[5] As a further complication, the adaptive response to exercise is lower in women.[6]

Material and methods

To verify the adaptive response to habitual exercise at an intense level, we compared elite female athletes from the

Contents

national women's soccer team (athlete group), with healthy sedentary women of the same age range (control group).

To determine changes that occur as a function of time, we divided the athletes into two groups: one of players from the main team (main group) and another of players from the under-17 team (< 17 group).

The analysis was based on resting echocardiography, measuring and comparing several echocardiographic parameters. All parameters were analyzed according to current American Society of Echocardiography guidelines.[7]

Using transthoracic echocardiography, we analyzed a total of 57 athletes, which, as mentioned above, were subdivided into 2 groups: 32 older athletes (main group) and 25 younger athletes (< 17 group). A control group of 25 healthy sedentary women from the same age range was compared with the combined athlete group.

The analyzed demographic parameters were age, weight, height, body surface area, and body mass index. In a break between training sessions, we used transthoracic echocardiography at rest to determine heart rate, left ventricle (LV) diameter, end-diastolic thickness of the interventricular septum and free posterior wall, LV end-diastolic volume, ejection fraction, diameters of the aorta and left atrium, baseline right ventricle (RV) diameter, and end-expiratory inferior vena cava diameter. We calculated the LV mass, relative LV wall thickness, and left atrial (LA) volume. With Doppler ultrasound, we measured mitral flow, E wave, and A wave velocities, while with tissue Doppler imaging we measured the mean e' wave to peak mitral annulus velocity.

Using speckle tracking, a measure myocardial deformation, we determined: LV global longitudinal strain, LV systolic strain rate, and LV early diastolic strain rate, LV circumferential and radial strain, RV strain and longitudinal strain rate, baseline LV rotation, LV apical rotation, LA longitudinal strain, and right atrial (RA) longitudinal strain. The following parameters were indexed to body surface area: LV end-diastolic volume, LV mass, and LA volume. Twisting was calculated from LV basal rotation and apical rotation, which were obtained through speckle tracking.

The exams were performed by the same operator with a CX50 ultrasound machine (Philips Healthcare, Andover, MA, USA) and QLAB 15 software. In this quantitative descriptive study, statistical analysis was performed using the Z test for independent samples. Numerical data were analyzed in BioEstat 5.0, determining the mean, SD, and statistical difference with a significance level of < 5%. Sample variance was estimated to verify homogeneity.

Results

We divided the analysis into two parts: the first was a comparison of the combined athlete group with healthy controls, ie, sedentary women of the same age range; while the second was a comparison between the main and under-17 teams.

Table 1 compares echocardiographic data between the athlete and control groups, while Table 2 compares myocardial deformation parameters between the athlete and control groups. Table 3 compares echocardiographic data between the main and < 17 athlete groups, while Table 4 compares myocardial deformation parameters between the main and < 17 athlete groups.

Regarding echocardiographic parameters between the athlete and control groups, heart rate was significantly lower in the athlete group. End-diastolic thickness of the interventricular septum and free posterior wall, LA diameter, and RV diameter were significantly greater in the athlete group. LV mass index, LV diastolic volume, and indexed LA volume and LV ejection fraction were significantly higher among athletes than controls. In in 42% of the athlete group, the indexed LV volume was > 61 mL/m^2, which was considered the upper limit of normality, although the LV mass index and relative wall thickness were not characteristic of hypertrophy.

Regarding myocardial deformation in the athlete and control groups, LV global radial strain, RV global longitudinal strain, and LV basal and apical rotation and twisting were significantly greater in the control group.

Between the main and < 17 athlete groups, LV diastolic diameter was significantly greater in < 17 group, while end-diastolic thickness of the interventricular septum and free posterior wall, as well as LA and RV diameter, were significantly greater in the main group. Relative wall thickness was greater in the main group, while indexed LA volume was greater in the < 17 group. In the main group, mitral E wave velocity was significantly lower, mitral A wave velocity was significantly higher, and the E/A ratio was significantly lower, with no difference in the e' wave velocities of the mitral annulus or the E/e' ratio. Regarding strain parameters, LV longitudinal systolic and diastolic strain rate, LV radial strain, RV longitudinal strain rate, apical rotation, and twisting were significantly higher in the < 17 group.

Discussion

Comparing elite female athletes with healthy sedentary women of the same age range yielded some important observations: the athletes had lower weight, lower body mass index, and thinner bodies, but no difference in height. Thus, body mass index, rather than body surface area, allowed more efficient distinction of this body type, which has been observed in previous studies of obese and thin patients.[8,9]

The differences between the athlete and control groups show the heart's physiological adaptation to habitual intense exercise, such as lower heart rate, greater LV wall thickness and increased LA and RV diameters. Increased RV diameter, a frequent finding among highly trained athletes, is attributed to a disproportionate increase in right cardiac work during exercise due to the smaller decrease in pulmonary resistance in relation to systemic resistance.[10] Even without increased LV diastolic diameter, in 24 athletes (42%) LV end-diastolic volume indexed to body surface area was higher than normal (61 mL/m^2). However, no increase was observed when these values were indexed

Table 1 – Comparison between the athlete and control groups: demographic data, cavity dimensions, volumes, mass, and systolic and diastolic function

Parameter	Athletes (Mean ± SD)	Controls (Mean ± SD)	Z-score	P-value
Age (years)	22.14±6.29	21.24±5.02	0.6904	0.2450
Weight (kg)	60.02±6.71	65.24±6.21	3.4179	0.0003*
Height (cm)	166.05±7.98	164.24±6.48	1.0836	0.1393
Body surface (m^2)	1.67±0.13	1.69±0.09	1.1715	0.1207
Body mass index (Kg/m^2)	21.75±1.79	24.29±3.03	3.9007	< 0.0001*
HR (bpm)	62.95±9.01	75.28±8.69	5.8483	< 0.0001*
LVDD (mm)	45.82±2.25	45.12±2.62	1.1687	0.1213
DST (mm)	7.70±0.46	6.43±0.56	9.9477	< 0.0001*
DWT (mm)	7.67±0.48	6.40±0.58	9.5563	< 0.0001*
AoD (mm)	27.26±2.88	27.84±2.88	0.8344	0.2020
LAD (mm)	31.00±2.85	27.72±2.34	5.4571	< 0.0001*
RVDD (mm)	29.82±3.85	28.54±2.13	1.9342	0.0265*
IVCD (mm)	20.26±4.01	15.86±1.59	0.1320	0.4475
LV mass index (g/m^2)	68.67±8.01	54.69±8.35	7.0626	< 0.0001*
Relative thickness	0.34±0.03	0.29±0.03	1.057	0.15
LV/BS diastolic volume	59.74±10.84	51.30±9.41	13.588	< 0.0001*
LA/BS volume	21.73±5.94	20.86±5.77	3.161	0.0008*
LV ejection fraction (%)	63.45±5.99	59.57±7.55	4.5817	< 0.0001*
Mitral E wave (cm/s)	89.84±12.83	89.34±10.76	0.1818	0.4279
Mitral A wave (cm/s)	49.48±8.30	49.16±11.60	0.1227	0.4512
E/A Ratio	1.86±0.36	1.90±0.42	0.4677	0.3200
Tissue e' wave (cm/s)	18.40±2.50	18.48±1.62	0.8504	0.1976
Mean E/e' ratio	4.94±0.78	4.85±0.56	0.5692	0.2846

*HR: heart rate; LVDD: left ventricular diastolic diameter; DST: diastolic septal thickness; DWT: diastolic wall thickness; AoD: aorta diameter; LAD: left atrial diameter; RVDD: right ventricular diastolic diameter; IVCD: inferior vena cava diameter; LV/BS: left ventricle/body surface; LA/BS: left atrium/body surface; *: statistically significant.*

Table 2 – Comparison of myocardial strain parameters between the athlete and control groups

Parameter	Athletes (Mean ± SD)	Controls (Mean ± SD)	Z-score	P-value
LV global longitudinal strain (%)	-21.78±2.16	-21.52±2.28	0.061	0.48
LV systolic Longitudinal SR (s^{-1})	-1.18±0.38	-1.03±0.14	0.123	0.45
LV diastolic SR (s^{-1})	1.41±0.48	1.45±0.40	0.322	0.25
LV global circumferential strain (%)	-24.01±2.87	-22.97±3.20	0.051	0.48
LV global radial strain (%)	37.33±11.31	47.04±8.38	15.584	< 0.0001*
RV longitudinal strain (%)	-26.23±2.79	-28.12±3.02	2.326	0.01*
RV longitudinal SR (s^{-1})	-1.33±0.40	-1.18±0.16	0.223	0.41
LA basal rotation (°)	-4.63±1.83	-6.10±3.60	5.118	< 0.0001*
LA apical rotation (°)	3.66±1.68	13.10±6.00	17.227	< 0.0001*
LA twist (°)	8.30±2.43	16.10±6.40	14.570	< 0.0001*
LA longitudinal strain (%)	45.21±10.68	44.42±12.89	0.452	0.33
RA longitudinal strain (%)	41.77±10.23	40.18±13.01	0.256	0.40

*LV: left ventricle; SR: strain rate; RV: right ventricle; LA: left atrium; RA: right atrium; *: statistically significant.*

to height,[11] which seems to indicate that we are at one end of the normality curve, where a different methodology should be applied.

The LV mass index was also significantly higher in the athlete group than the control group, although remaining within normal limits, with a maximum value of 88.37 g/m^2 (normal value = ≤ 95 g/m^2). The fact that the athlete group had a higher indexed LA volume has been reported by other authors[7,12] and could be related to volume overload due to the sustained increase in cardiac output during training.[13]

Regarding myocardial deformation parameters, LV radial strain was lower in the athlete group, but was still within normal range (variation from 25% to 67%). One possibility is that this parameter increases during physical exertion, which could indicate a form of contractile reserve. Other authors have found increased radial strain in male athletes.[14] The lower RV longitudinal strain (varying from -19.40% to -31.90%) in the athlete group could be related to this

Table 3 – Comparison between the main and <17 athlete groups: demographic data, cavity dimensions, volumes, mass, and systolic and diastolic function

Parameter	Main group (Mean ± SD)	< 17 group (Mean ± SD)	Z-score	P-value
Age (years)	26.50±5.14	16.56±0.58	10.8571	< 0.0001*
Weight (kg)	60.44±6.70	59.48±6.83	0.5296	0.2982
Height (cm)	166.22±8.0	165.84±8.11	0.1759	0.4302
Body surface (m^2)	167.00±0.13	1.66±0.13	0.3644	0.3578
Body mass index (Kg/m^2)	21.87±1.96	21.59±1.58	0.5891	0.2779
HR (bpm)	62.69±10.82	63.28±6.18	0.2602	0.3973
LVDD (mm)	45.41±2.21	46.36±2.23	1.6063	0.0541
DST (mm)	7.97±0.18	7.36±0.49	5.9188	< 0.0001*
DWT (mm)	7.88±0.34	7.40±0.50	4.0839	< 0.0001*
AoD (mm)	27.66±3.05	26.76±2.62	1.1915	0.1167
LAD (mm)	32.47±2.17	29.12±2.52	5.2846	< 0.0001*
RVDD (mm)	31.91±3.48	27.16±2.39	6.0936	< 0.0001*
IVCD (mm)	20.55±4.41	19.44±3.43	1.0662	0.1432
LV mass index (g/m^2)	69.89±6.38	67.11±9.63	0.0144	0.4942
Relative thickness	0.35±0.02	0.32±0.02	5.1843	< 0.0001*
Diastolic volume LV/BS	58.14±9.02	61.79±12.70	0.0229	0.4909
LA/BS Volume	19.82±4.23	24.18±6.95	2.7632	0.0029*
Ejection fraction (%)	64.44±5.44	62.19±6.52	1.3879	0.0826
Mitral E wave (cm/s)	86.65±13.01	93.92±11.60	2.2257	0.0130*
Mitral A wave (cm/s)	51.25±9.29	47.21±6.30	1.9545	0.0253*
E/A ratio	1.73±0.37	2.01±0.30	3.1641	0.0008*
e' tissue wave (cm/s)	17.98±2.40	18.93±2.57	1.4260	0.0769
Mean E/e' ratio	4.88±0.88	5.01±0.62	0.6385	0.2616

*HR: heart rate; LVDD: left ventricular diastolic diameter; DST: diastolic septal thickness; DWT: diastolic wall thickness; AoD: aorta diameter; LAD: left atrial diameter; RVDD: right ventricular diastolic diameter; IVCD: inferior vena cava diameter; LV/BS: left ventricle/body surface; LA/BS: left atrium/body surface; *: statistically significant.*

Table 4 – Comparison of myocardial deformation parameters between the main and under-17 athlete groups

Parameter	Main group (Mean ± SD)	< 17 group (Mean ± SD)	Z-score	P-value
LV global longitudinal strain (%)	-21.58±2.56	-22.03±1.52	0.8379	0.2010
LV longitudinal systolic SR (s-1)	-1.00±0.10	-1.40±0.48	4.1393	< 0.0001*
LV diastolic SR (s-1)	1.19±0.15	1.69±0.60	4.0869	< 0.0001*
LV global circumferential strain (%)	-23.66±2.79	-24.46±2.97	1.0359	0.1501
LV global radial strain (%)	32.91±5.32	43.00±14.22	3.3697	0.0004*
RV longitudinal strain (%)	-26.38±3.04	-26.03±2.48	0.4727	0.3182
RV longitudinal SR (s-1)	-1.18±0.13	-1.51±0.54	2.9423	0.0016*
LV basal rotation (°)	-4.72±2.00	-4.51±1.62	0.4337	0.3322
LV apical rotation (°)	3.05±1.37	4.45±1.75	3.2836	0.0005*
LV twist (°)	7.78±2.45	8.96±2.28	1.8871	0.0296*
LA longitudinal strain (%)	46.31±11.39	43.80±9.74	0.8969	0.1849
RA longitudinal strain (%)	43.08±10.78	40.10±9.41	1.1102	0.1335

*LV: left ventricle; SR: strain rate; RV: right ventricle; LA: left atrium; RA: right atrium; *: statistically significant.*

cavity's larger dimensions, with increased end-systolic parietal stress, proportionally much greater than what the LV undergoes during effort. The increase in parietal stress was estimated at 125% for the RV and 14% for the LV.[15] The RV strain rate, however, did not decrease, suggesting that the chamber's longitudinal function is preserved.

The subject of rotational deformation is controversial. In our sample of athletes, all parameters were decreased (basal rotation, apical rotation, and twist). Some authors report that these indices are higher in athletes,[14,16] while others report a decrease in rotational mechanics, especially among athletes with a high aerobic and low anaerobic load.[17,18] Nevertheless, we hypothesize that, in addition to LV radial strain, rotational mechanics increase considerably during physical exertion, representing a form of contractile reserve.[19] Performing echocardiographic examinations during training, other authors have found that all rotational parameters gradually increase during exercise in proportion to exercise intensity.[20]

Our study was based on the assumptions that all of the athletes on the national team began playing on the junior teams and were subsequently promoted, undergoing the same type of intensive training prior to 17 years of age, as well as that the younger athletes would have different levels of adaptation from those on the main team, due to their greater age and training experience.

Comparing the athletes by career length (ie, main vs < 17 groups), significant differences were found in age, weight, height, body surface area, and body mass index. The main group had a smaller LV diastolic diameter and greater relative and end-diastolic thickness of the interventricular septum and free posterior wall. This seems to indicate adaptive concentric remodeling that remained within normal limits.

Indexed LA volume and RV size were also greater in the main group for the same reasons, ie, a sustained increase in LA cardiac output and lower reduction in RV pulmonary resistance.

Controlled studies in high-performance athletes involved in submaximal and supramaximal training found no increase in LV dimensions, although the diameter and indexed volume of the LA were increased.[21]

Some authors have reported that, due to disproportionate work during intense exercise, decompensation and a greater predisposition to arrhythmias occur in the RV.[22]

Among the diastolic function parameters in the main group, the mitral E wave velocity was lower, the A wave velocity higher, and the E/A ratio was lower. No differences were found regarding velocity in tissue Doppler imaging or the E/e' ratio. These data might be related to age-based physiological changes in the main group, although they had normal ventricular filling pressure.

The most interesting differences were in myocardial deformation. In longitudinal mechanics, although LV global longitudinal strain did not significantly differ, the systolic strain rate and the early diastolic strain rate were significantly higher in the < 17 group, suggesting greater efficiency in longitudinal strain and ventricular filling among younger athletes. Circumferential strain did not differ significantly between the groups.

Radial strain was higher in the < 17 group, suggesting greater efficiency or even decrease in older athletes, indicating better contractile reserve. RV longitudinal strain did not differ significantly between groups but, again, the RV strain rate was higher in the < 17 group.

Regarding rotational deformation, both the main and < 17 groups had decreased basal rotation, with no significant difference between groups, although the values were lower than those of the control group. Apical rotation, which was also lower among athletes than controls, was significantly lower in the main group, as was twisting. Reduced apical rotation and twisting at rest may indicate greater contractile reserve acquired through longer training, as has been reported by some authors, who found values similar to those of the present study.[19]

Conclusions

Compared to sedentary women in the same age group, elite female soccer athletes were thinner and had a lower heart rate.

There was a trend toward eccentric remodeling, greater RV diameter, LA diameter and indexed volume, and LV ejection fraction, although they were within normal limits. Myocardial deformation parameters showed lower LV radial strain, RV longitudinal strain, and rotational parameters (basal, apical, and twisting rotation).

Compared to the < 17 group, athletes from the main group had a smaller LV diameter, greater relative and parietal thickness, and tended to have concentric adaptation. The greater LA and RV dimensions in the main group of athletes, as well as the lower apical rotation and twisting, may correspond to a greater contractile reserve acquired through longer training.

Author contributions

Conception and design of the research: Castillo JMD, Boschilia T, Sabeh Júnior N, Silveira CAM; acquisition of data: Castillo JMD, Boschilia T, Sabeh Júnior N, Silveira CAM; analysis and interpretation of the data: Castillo JMD, Boschilia T, Sabeh Júnior N, Silveira CAM; statistical analysis: Castillo JMD, Boschilia T, Sabeh Júnior N, Silveira CAM; writing of the manuscript: Castillo JMD, Boschilia T, Sabeh Júnior N, Silveira CAM; critical revision of the manuscript for intellectual content: Castillo JMD, Boschilia T, Sabeh Júnior N, Silveira CAM; Brindeiro Filho D.

Potential Conflict of Interest

No potential conflict of interest relevant to this article was reported.

Sources of Funding

There were no external funding sources for this study.

Study Association

This study is not associated with any thesis or dissertation work.

Ethics Approval and Consent to Participate

This article does not contain any studies with human participants or animals performed by any of the authors.

References

1. Morganroth J, Maron BJ, Henry WL, Epstein SE. Comparative Left Ventricular Dimensions in Trained Athletes. Ann Intern Med. 1975;82(4):521-4. doi: 10.7326/0003-4819-82-4-521.
2. Guldal YK, Bilge M. The Examination According to the Position of Players of Aerobic and Anaerobic Capacity Relation in Professional Football Players. Eur J Phys Educ Sport Scien. 2019;5(3):84-97. doi: 10.5281/zenodo.2541664.
3. Maron BJ, Zipes DP. Introduction: Eligibility Recommendations for Competitive Athletes with Cardiovascular Abnormalities-General Considerations. J Am Coll Cardiol. 2005;45(8):1318-21. doi: 10.1016/j.jacc.2005.02.006.
4. Morentin B, Suárez-Mier MP, Monzó A, Molina P, Lucena JS. Sports-Related Sudden Cardiac Death due to Myocardial Diseases on a Population from 1-35 Years: A Multicentre Forensic Study in Spain. Forensic Sci Res. 2019;4(3):257-66. doi: 10.1080/20961790.2019.1633729.
5. Czimbalmos C, Csecs I, Toth A, Kiss O, Suhai FI, Sydo N, et al. The Demanding Grey Zone: Sport Indices by Cardiac Magnetic Resonance Imaging Differentiate Hypertrophic Cardiomyopathy from Athlete's Heart. PLoS One. 2019;14(2):e0211624. doi: 10.1371/journal.pone.0211624.
6. Petersen SE, Hudsmith LE, Robson MD, Doll HA, Francis JM, Wiesmann F, et al. Sex-Specific Characteristics of Cardiac Function, Geometry, and Mass in Young Adult Elite Athletes. J Magn Reson Imaging. 2006;24(2):297-303. doi: 10.1002/jmri.20633.
7. Lang RM, Badano LP, Mor-Avi V, Afilalo J, Armstrong A, Ernande L, et al. Recommendations for Cardiac Chamber Quantification by Echocardiography in Adults: An Update from the American Society of Echocardiography and the European Association of Cardiovascular Imaging. J Am Soc Echocardiogr. 2015;28(1):1-39.e14. doi: 10.1016/j.echo.2014.10.003.
8. Rosa EC, Moyses VA, Sesso RC, Plavnik FL, Ribeiro FF, Kohlmann NE, et al. Left Ventricular Hypertrophy Evaluation in Obese Hypertensive Patients: Effect of Left Ventricular Mass Index Criteria. Arq Bras Cardiol. 2002;78(4):341-51. doi: 10.1590/s0066-782x2002000400001.
9. Pfaffenberger S, Bartko P, Graf A, Pernicka E, Babayev J, Lolic E, et al. Size Matters! Impact of Age, Sex, Height, and Weight on the Normal Heart Size. Circ Cardiovasc Imaging. 2013;6(6):1073-9. doi: 10.1161/CIRCIMAGING.113.000690.
10. Paterick TE. The Athlete's Right Heart. J Phy Fit Treatment & Sports. 2018;5(2):555657. doi: 10.19080/JPFMTS.2018.05.555657.
11. Vasan RS, Larson MG, Levy D, Evans JC, Benjamin EJ. Distribution and Categorization of Echocardiographic Measurements in Relation to Reference Limits: The Framingham Heart Study: Formulation of a Height- and Sex-Specific Classification and its Prospective Validation. Circulation. 1997;96(6):1863-73. doi: 10.1161/01.cir.96.6.1863.
12. Moro AS, Okoshi MP, Padovani CR, Okoshi K. Doppler Echocardiography in Athletes from Different Sports. Med Sci Monit. 2013;19:187-93. doi: 10.12659/MSM.883829.
13. D'Ascenzi F, Anselmi F, Focardi M, Mondillo S. Atrial Enlargement in the Athlete's Heart: Assessment of Atrial Function May Help Distinguish Adaptive from Pathologic Remodeling. J Am Soc Echocardiogr. 2018;31(2):148-57. doi: 10.1016/j.echo.2017.11.009.
14. Eun LY, Chae HW. Assessment of Myocardial Function in Elite Athlete's Heart at Rest - 2D Speckle Tracking Echocardiography in Korean Elite Soccer Players. Sci Rep. 2016;6:39772. doi: 10.1038/srep39772.
15. Douglas PS, O'Toole ML, Hiller WD, Reichek N. Different Effects of Prolonged Exercise on the Right and Left Ventricles. J Am Coll Cardiol. 1990;15(1):64-9. doi: 10.1016/0735-1097(90)90176-p.
16. Małek ŁA, Barczuk-Falęcka M, Brzewski M. Cardiac Deformation Parameters and Rotational Mechanics by Cardiac Magnetic Resonance Feature Tracking in Pre-Adolescent Male Soccer Players. Cardiol Young. 2018;28(6):882-4. doi: 10.1017/S1047951118000343.
17. Nottin S, Doucende G, Schuster I, Tanguy S, Dauzat M, Obert P. Alteration in Left Ventricular Strains and Torsional Mechanics after Ultralong Duration Exercise in Athletes. Circ Cardiovasc Imaging. 2009;2(4):323-30. doi: 10.1161/CIRCIMAGING.108.811273.
18. Beaumont A, Grace F, Richards J, Hough J, Oxborough D, Sculthorpe N. Left Ventricular Speckle Tracking-Derived Cardiac Strain and Cardiac Twist Mechanics in Athletes: A Systematic Review and Meta-Analysis of Controlled Studies. Sports Med. 2017;47(6):1145-70. doi: 10.1007/s40279-016-0644-4.
19. Santoro A, Alvino F, Antonelli G, Caputo M, Padeletti M, Lisi M, et al. Endurance and Strength Athlete's Heart: Analysis of Myocardial Deformation by Speckle Tracking Echocardiography. J Cardiovasc Ultrasound. 2014;22(4):196-204. doi: 10.4250/jcu.2014.22.4.196.
20. Doucende G, Schuster I, Rupp T, Startun A, Dauzat M, Obert P, et al. Kinetics of Left Ventricular Strains and Torsion During Incremental Exercise in Healthy Subjects: The Key Role of Torsional Mechanics for Systolic-Diastolic Coupling. Circ Cardiovasc Imaging. 2010;3(5):586-94. doi: 10.1161/CIRCIMAGING.110.943522.
21. Mahjoub H, Le Blanc O, Paquette M, Imhoff S, Labrecque L, Drapeau A, et al. Cardiac Remodeling after Six Weeks of High-Intensity Interval Training to Exhaustion in Endurance-Trained Men. Am J Physiol Heart Circ Physiol. 2019;317(4):H685-H694. doi: 10.1152/ajpheart.00196.2019.
22. La Gerche A, Rakhit DJ, Claessen G. Exercise and the Right Ventricle: A Potential Achilles' Heel. Cardiovasc Res. 2017;113(12):1499-508. doi: 10.1093/cvr/cvx156.

Cardiovascular Imaging In Assessment Of Athletes

José Roberto Matos-Souza[1] *and Daniela do Carmo Rassi*[2]

Faculdade de Medicina,[1] *Unicamp, Campinas, SP – Brazil*

Faculdade de Medicina e Hospital das Clínicas, Universidade Federal de Goiás,[2] *Goiânia, GO – Brazil*

Short editorial related to the articles: "Mechanisms of Heart Adaptation in Elite Female Athletes: Comparison with Healthy Individuals and Training Time" and "My Approach to "Athlete'S Heart": Evaluation of the Different Types of Adaptation to Exercise"

Physical training is linked to a series of cardiac, morphological, and functional adaptations known as "athlete's heart".[1,2] An athlete can be considered a youth or adult amateur or professional who exercises regularly and participates in official sports competitions. The changes demonstrated depend on the duration, intensity, and type of training (isotonic versus isometric).[3]

In recent years, a large number of studies have been published, which have improved our ability to understand the characteristics of physiological cardiac remodeling in athletes.[4] Nevertheless, there are gaps regarding the differential diagnosis of athlete's heart, especially when it presents with a more intense expression. It can be difficult to differentiate this condition from inherited heart diseases such as hypertrophic, dilated, or arrhythmogenic cardiomyopathy and left ventricular non-compaction.[3,4]

Technological advances, such as 3-dimensional echocardiography, analysis of myocardial strain, cardiac magnetic resonance imaging, and multidetector computed tomography, have significantly improved the diagnostic capacity of current imaging modalities, allowing the identification of a greater number of pathological cardiovascular conditions that may affect the athlete population.[3]

The article by Mancuso[5] offers a review of interesting aspects regarding the most current division of sports modalities (skill, strength, endurance, and mixed) and their relationships with morphofunctional cardiac changes. The article indicates that most sporting disciplines are characterized by a varying degree of isometric and isotonic components; therefore, the original dichotomous classification into strength (isometric) or endurance (isotonic) disciplines is not applicable for most athletes. Moreover, it updates diagnostic criteria and describes the main challenges related to differential diagnoses.

Another interesting point concerning physical sporting activity and athlete's heart is the difference that may exist in terms of sex and training time.[3]

Women who practice sports regularly show similar cardiac adaptations compared to men, but generally to a lesser degree, in terms of absolute values. Female athletes exhibit modest absolute increases in left ventricular wall thickness and cavity size, as well as modest increases in right ventricular and bi-atrial cavity size in comparison with sedentary women.[3,6]

In relation to age, some differences have been reported in senior athletes compared to younger athletes. Master athletes show lower left ventricular volumes and mass compared to their younger counterparts, although both parameters are still higher compared to age-matched untrained controls.[7]

Castillo et al.[8] have presented an interesting study comparing a very specific group of women in professional soccer training. They conducted an evaluation between beginner and advanced athletes and compared them to a control group of sedentary women. The authors indicated differences between athletes and controls, as well as variations in young athletes, with regard to cardiac dimensions and strain evaluation. Myocardial strain analysis showed a decrease in radial strain, basal rotation, apical rotation, and twist. These data reveal yet another contribution of strain analysis to the understanding of cardiac physiology, with its intricate interaction between rotation and radial and longitudinal strain. This information provides clarification, especially when obtained by the same strain software and examiner.

In summary, the correct diagnosis of alterations that may be compatible with "athlete's heart" currently represents a well-recognized clinical need, especially on the part of cardiologists who work with cardiovascular imaging.

Keywords

Echocardiography; cardiac remodeling; myocardial deformation

Mailing Address: Daniela do Carmo Rassi •
Hospital São Francisco de Assis. R. 9-A, 110. St. Aeroporto. Postal Code 74075-250. Goiânia, GO – Brazil
E-mail: dani.rassi@hotmail.com
Editor responsible for the review: Marco Stephan Lofrano

DOI: https://doi.org/10.36660/abcimg.20230015i

References

1. Pelliccia A, Maron BJ, Spataro A, Proschan MA, Spirito P. The Upper Limit of Physiologic Cardiac Hypertrophy in Highly Trained Elite Athletes. N Engl J Med. 1991;324(5):295-301. doi: 10.1056/NEJM199101313240504.

2. Maron BJ, Pelliccia A. The Heart of Trained Athletes: Cardiac Remodeling and the Risks of Sports, Including Sudden Death. Circulation. 2006;114(15):1633-44. doi: 10.1161/CIRCULATIONAHA.106.613562.

3. Pelliccia A, Caselli S, Sharma S, Basso C, Bax JJ, Corrado D, et al. European Association of Preventive Cardiology (EAPC) and European Association of Cardiovascular Imaging (EACVI) Joint Position Statement: Recommendations for the Indication and Interpretation of Cardiovascular Imaging in the Evaluation of the Athlete's Heart. Eur Heart J. 2018;39(21):1949-69. doi: 10.1093/eurheartj/ehx532.

4. Niederseer D, Rossi VA, Kissel C, Scherr J, Caselli S, Tanner FC, et al. Role of Echocardiography in Screening and Evaluation of Athletes. Heart. 2020:heartjnl-2020-317996. doi: 10.1136/heartjnl-2020-317996.

5. Mancuso FJN. Como Eu Faço no Coração de Atleta: Avaliação dos Diferentes Tipos de Adaptação ao Exercício. Arq Bras Cardiol: Imagem Cardiovasc. 2023;36(1):e20230002. doi: 10.36660/abcimg.20230002.

6. Pelliccia A, Maron BJ, Culasso F, Spataro A, Caselli G. Athlete's Heart in Women. Echocardiographic Characterization of Highly Trained Elite Female Athletes. JAMA. 1996;276(3):211-5. doi: 10.1001/jama.276.3.211.

7. Bohm P, Schneider G, Linneweber L, Rentzsch A, Krämer N, Abdul-Khaliq H, et al. Right and Left Ventricular Function and Mass in Male Elite Master Athletes: A Controlled Contrast-Enhanced Cardiovascular Magnetic Resonance Study. Circulation. 2016;133(20):1927-35. doi: 10.1161/CIRCULATIONAHA.115.020975.

8. Castillo JM, Boschilia T, Sabeh N Jr, Silveira CAM, Brindeiro D Filho. Mecanismos de Adaptação do Coração em Atletas de Elite do Sexo Feminino: Comparação com Indivíduos Sadios e Tempo de Treinamento. Arq Bras Cardiol: Imagem Cardiovasc. 2023;36(1):e372. doi: 10.36660/abcimg.2023372.

Original Article

Incidental Tomographic Findings of Coronary Artery Calcifications: A Prevalence Study in Southern Brazil

Karen Rafaela Okaseski Scopel,[1] Tássia Machado Medeiros,[1,2] Bibiana Natalia Porto Maicá,[1] Maria Carbonari Velho,[1] Mariana Motta Dias da Silva,[3] Juliane Nascimento Mattos,[2] Guilherme Galante Heuser,[1,2] Eliane Roseli Winkelmann[1]

Universidade Regional do Noroeste do Estado do Rio Grande do Sul (UNIJUI),[1] Ijui, RS – Brazil
Hospital Noroeste Unimed/RS,[2] Ijui, RS – Brazil
Universidade Federal do Rio Grande do Sul (UFGRS),[3] Porto Alegre, RS – Brazil

Abstract

Introduction: Coronary artery calcifications (CAC) are shown to be a predictive factor of cardiovascular diseases. Computed tomography (CT) of the chest with a low-dose acquisition protocol is accurate in identifying CAC and provides incidental findings of these calcifications, which are commonly overlooked. This study will analyze the prevalence of incidental findings of calcification in coronary arteries in non-cardiac individuals undergoing chest CT.

Methods: Consecutive cross-sectional study of an analytical and descriptive nature. Individuals of both genders who underwent chest CT by referral, over 18 years of age and without heart disease were included. Data collection was carried out using medical records and a self-applied anamnesis form. The variables referring to the CAC and the extension of the impairment were obtained from the reassessment of the chest CT images available in the institution's system. The exams were anonymized and evaluated by two experienced radiologists. P≤0.05 was considered statistically significant.

Results: 397 exams were analyzed. A prevalence of calcifications was found in 176 (44%) of the cases. The existence of these coronary calcifications is related to age (p<0.001). Calcifications are related to gender (p = 0.03) with a higher odds ratio of development in men (odds ratio [OR] = 1.55). Smoking (p<0.001), sedentary lifestyle (p<0.001), systemic arterial hypertension (p<0.001), Diabetes Mellitus (p = 0.04), and dyslipidemia (p<0.001) showed a positive association.

Conclusion: The prevalence of incidental CAC findings was 44%; vary in greater numbers between mild and severe; higher odds ratio in males and increased prevalence with age. Therefore, chest CT proves to be an effective method to assess CAC, and together with the patient's clinical history, it can be used to measure risk factors for CVD and intervene in the outcome of the condition.

Keywords: Tomography, X-Ray Computed; Incidental Findings; Vascular Calcification; Coronary Vessels.

Introducton

Cardiovascular diseases (CVD) are among the main health problems in the world and, therefore, they should be prevented.[1] Thus, coronary artery calcifications (CAC), initially asymptomatic, have proven to be an alarming and predictive factor for these diseases.[2] They are characterized by a progressive and gradual pathophysiological process, which results in abnormal vasomotor responses and/or narrowing of the vessel lumen. These changes are strongly associated with advanced age, diabetes mellitus (DM), dyslipidemia, systemic arterial hypertension (SAH), male gender, and smoking.[3]

Computed tomography (CT) of the chest, used with low-dose acquisition protocols, was 97.13% accurate in identifying CAC and proved to be effective in detecting or excluding them.[4] This test, usually used for pulmonary diagnostic purposes, has been providing frequent incidental findings of calcifications, since there are cardiovascular conditions that can cause non-cardiac symptoms, such as dyspnea, chest pain, and hemoptysis. Thus, studies on these findings have been gaining space in the clinical and scientific scope.[2]

Despite the confirmation of the negative impacts of coronary calcifications, incidental cardiac findings on chest CT are still commonly neglected.[5-7] Thus, the prevalence of incidentalomas and their clinical relevance have been estimated in several studies and based on different contexts.[8,9] However, there are no studies of this nature in the northwest region of the state of Rio Grande do Sul; therefore, this research aimed to fill a gap regarding population-based information on the region under study in the clinical and scientific fields. In this perspective, the objective was to analyze the prevalence

Correspondência: Eliane Roseli Winkelmann •
Universidade Regional do Noroeste do Estado do Rio Grande do Sul (UNIJUI). Rua do Comércio, 2000. CEP: 98700-000. Bairro Universitário, Ijuí, RS – Brasil.
E-mail: elianew@unijui.edu.br
Manuscript received December 10, 2022; revised January 11, 2022; accepted January 16, 2023.
Editor responsible for the review: Leonardo Sara Silva.

DOI: https://doi.org/10.36660/abcimg.2023368i

Contents

of incidental findings of calcification in coronary arteries in non-cardiac patients undergoing chest CT.

Methods

Participants

This is a cross-sectional study of analytical and descriptive nature, developed in based on the Guidelines and Regulatory Norms for Research Involving Human Beings, in accordance with the Resolution of the National Health Council (*Conselho Nacional de Saúde* – CNS) No. 466/12 and approved by the Research Ethics Committee of UNIJUÍ (CAAE: 84431118.2.0000.5350). Individuals of both genders who underwent chest CT by referral were included. Individuals under 18 years of age, exams performed by referral from a cardiac physician, exams with technical difficulties for image evaluation and duplicate exams, that is, two or more exams performed by the same patient within an interval of less than 6 months, were excluded.

Data collection

It was carried out in medical records of a Hospital in the Northwest region of the state of Rio Grande do Sul, Brazil, between March 27th and October 5th, 2019. The variables age, gender, associated comorbidities (SAH, DM, and dyslipidemia), family history of heart disease, previous history of heart disease (Heart Failure, Acute Myocardial Infarction), smoking, physical inactivity, and the patient's symptomatology were collected from a self-administered anamnesis form with closed questions.

The variables referring to calcifications of the left coronary, left anterior descending, circumflex, and right coronary arteries, as well as the extent of their impairment, were obtained from the reassessment of the chest CT images available on the Picture Archiving and Communication System (PACS) (https://www.animati.com.br/animati-workstation/) of the institution. Also in this system, the reason for the medical referral to perform the examination described in the reports was obtained. Data were compiled by a single researcher for better quality and standardization of information.

Acquisition and Interpretation of Images

The device used to perform the exams was a 32-slice Alexion CT scanner (Toshiba, Otawara, Japan) using a low-dose acquisition protocol. The examinations were performed with the patient in the supine position and in apnea. The chest images were analyzed in axial sections, in soft tissue window and only in the non-contrast phase. The exams were anonymized (Advantage Workstation, version 4.6. GE Healthcare) so that previous data did not influence the analyses and the evaluators were completely blinded regarding the patient and each other. The analyses were performed by two previously trained radiologists with more than 5 years of experience in the area. First, the images were evaluated independently by the professionals. The images that showed disagreement between physicians were reanalyzed converging on a consensual result.

Coronary calcification score by visual scale

Following the protocol performed by Shemesh et al.,[10] four coronary arteries were evaluated: left main, left anterior descending, circumflex, and right. Each of them was classified and scored as absent (0), mild (1), moderate (2), or severe (3). It was characterized as mild when less than one third of the length of the entire artery was compromised, moderate when there were calcifications in one to two thirds of the artery, and severe when more than two thirds of the artery was calcified. After scoring, the results were added up, classified into: absent (0), mild (1-3), moderate (4-6), and severe (7-12).

Statistical analysis

Data collection was performed using Microsoft Office Excel 2010 and analysis using R Studio software (version 3.4.4). For the analysis of descriptive statistics, relative and absolute frequency, measures of central tendency and dispersion, were used. In the analytical statistics of the qualitative variables, the χ^2 test was used to test the hypothesis of dependence between the variables as well as to verify the adherence between them, considering statistically significant $p \leq 0.05$. In the analytical statistics of the quantitative variables, the prevalence of calcification findings was estimated. To determine the number of classes for the age variable, the Sturges Rule was used.

Inter-examiner agreement was estimated using Cohen's Kappa and the reference values for analysis described by Landis and Koch.[11] For the normality verification analysis, the Kolmogorov Smirnov test was used for the age variable along with the non-parametric Mann Whitney U test, considering statistically significant $p \leq 0.05$. The odds ratio was used to estimate the presence of calcification in relation to its predisposing variables.

Results

A total of 397 exams were analyzed, showing substantial inter-examiner agreement ($\kappa = 0.77$). Patients had a mean age of 61.88±16.26 years, with a predominance of females (52.14%). The commonly found reasons for referral were: changes in the respiratory system (n = 94), monitoring of a pulmonary nodule (n = 47), and lung cancer (n = 27).

Sedentary lifestyle (69.02%) and family history of heart disease (44.84%) are the most worrying among the main risk factors, while cancer is the leader in relation to previous diseases, reaching 38.29% of cases, followed by SAH (46.85%), with a higher prevalence in females (Table 1).

The population characterized above showed a prevalence of calcifications in 176 (44%) of the cases and it was found that the presence or absence of these coronary calcifications is related to age ($p < 0.001$). A greater occurrence of calcifications was observed in the age group between 76 and 84 years. However, the highest prevalence of calcification was from 92 to 100 years (100%), being more severe. Furthermore, it was possible to note that there is an increasing prevalence of calcifications above 68 years of age, reaching more than 60% of patients (Table 2). In the score used for the analysis of the arteries, seen in isolation, it was possible to verify that

Table 1 – Description of predisposing factors for the formation of arterial calcifications

	Female N = 207	Male N = 190	Total N = 397
Age mean±SD, years	**61.18±15.92**	**62.64±16.63**	**61.88±16.26**
Risk factors, N (%)			
Smoking	55 (13.85)	85 (21.41)	140 (35.26)
Sedentarism	153 (38.54)	121 (30.48)	274 (69.02)
Family history of heart disease	102 (25.69)	76 (19.14)	178 (44.84)
Family History of SAH	131 (33)	103 (25.94)	34 (58.94)
Prior Diseases, N (%)			
Cancer	73 (18.39)	79 (19.90)	152 (38.29)
Acute myocardial infarction	7 (1.76)	8 (2.02)	15 (3.78)
Cardiac insufficiency	17 (4.28)	21 (5.29)	38 (9.57)
Comorbidities, N (%)			
SAH	101 (25.44)	85 (21.41)	186 (46.85)
DM	24 (6.05)	24 (6.05)	48 (12.10)
Dyslipidemias	48 (12.09)	49 (12.34)	97 (24.43)

SD: standard deviation; SAH: Systemic Arterial Hypertension; DM: Diabetes Mellitus.

Table 2 – Visual scale analysis of coronary calcifications and their prevalence

Age	Absent	Mild	Moderate	Severe	Prevalence
18 ⊢27	11	0	0	0	0.00
27 ⊢35	15	0	0	0	0.00
35 ⊢43	28	4	0	0	0.13
43 ⊢51	31	3	0	2	0.14
51 ⊢59	39	13	0	2	0.28
59 ⊢68	44	20	11	5	0.45
68 ⊢76	36	31	11	13	0.60
76 ⊢84	11	18	7	14	0.78
84 ⊢92	6	6	8	5	0.76
92 ⊢101	0	0	0	3	1.00
Total	221	95	37	44	0.44

Table 3 – Relation of predisposing factors with coronary calcifications and the odds ratio of occurrence

Characteristics	p-value*	OR†	(95%)CI
Gender	0.03	-	-
Female	-	0.64	(0.42 – 0.98)
Male	-	1.55	(1.02 - 2.37)
Smoking	<0.001	2.45	(0.26 - 0.64)
Sedentarism	<0.001	2.97	(0.20 - 0.55)
Family history of heart disease	0.92	1.03	(0.64 - 1.48)
Family History of SAH	0.22	1.30	(0.50 - 1.18)
Cancer	0.47	1.17	(0.56 - 1.32)
SAH	<0.001	3.45	(0.19 - 0.45)
DM	0.04	1.93	(0.27 - 1.00)
Dyslipidemias	<0.001	2.65	(0.23 - 0.62)

**χ2 Test; † Odds Ratio; CI: confidence interval; SAH: Systemic Arterial Hypertension.*

the most compromised artery was the right coronary, in 193 (48.61%) of the cases.

Calcifications are related to gender ($p = 0.03$) with a higher odds ratio of development in men (odds ratio [OR] = 1.55). Still on the variables that influence the development of calcifications, smoking ($p < 0.001$), sedentary lifestyle ($p < 0.001$), SAH ($p < 0.001$), DM ($p = 0.04$), and dyslipidemia ($p < 0.001$) showed a positive association, with SAH (OR = 3.45) and sedentary lifestyle (OR = 2.97) having the highest odds ratio (Table 3). The results of the prevalence of CAC and the degree in relation to the age groups are graphically illustrated in Figure 1. Figure 2 represents the main findings of the study.

Discussion

The present study observed a 44% prevalence of incidental findings of CAC on chest CT in patients asymptomatic for heart disease, which increases with age and with greater chances of developing in males. It can also be observed that there is a direct relationship with risk factors and associated comorbidities, both closely linked to daily living habits. Regarding the diagnostic method, its effectiveness in the clinical and scientific scope can be seen, as in previous studies.

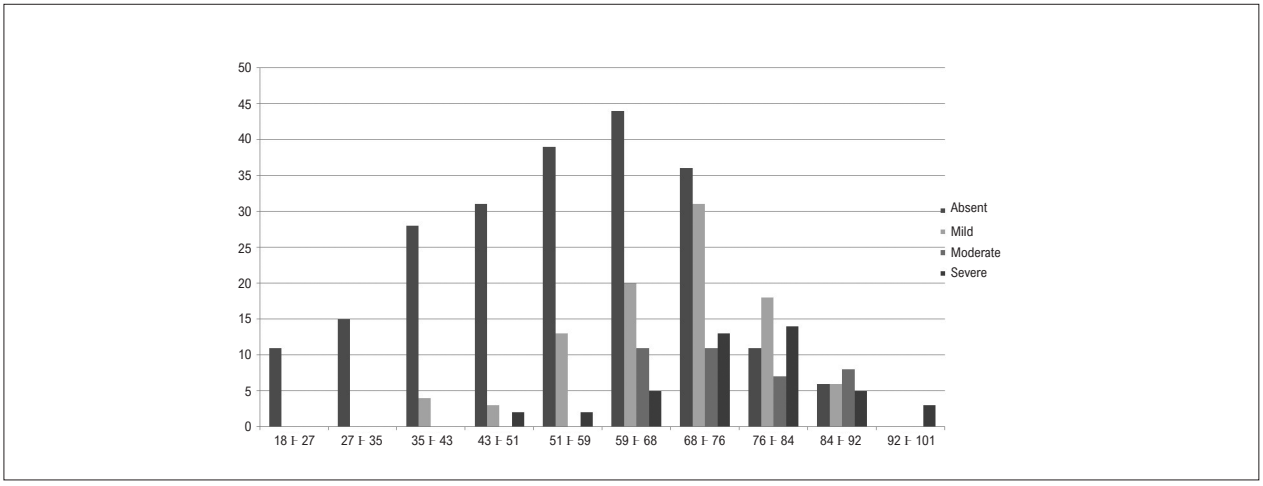

Figure 1 – *Graphical representation of the prevalence of CAC and the degree of involvement in relation to age.*

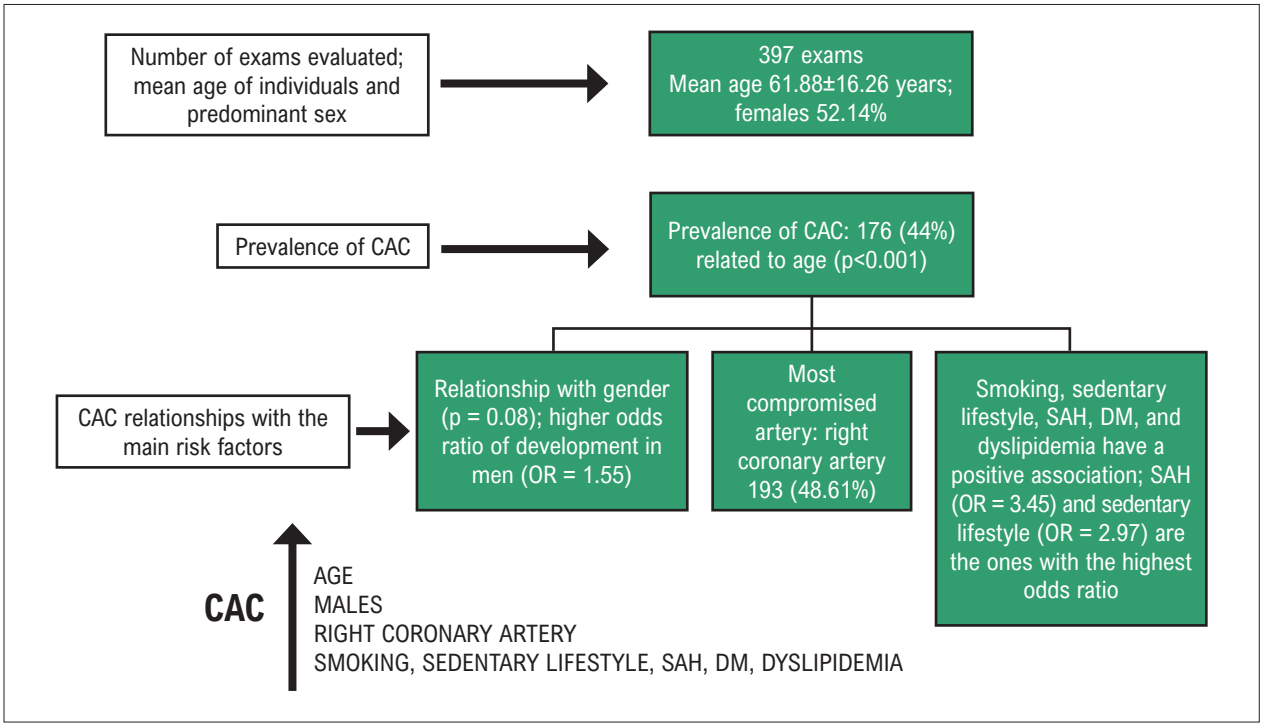

Figure 2 – *CAC: coronary artery calcification; DM: diabetes mellitus; SAH: systemic arterial hypertension; OR: odds ratio.*

In this line of analysis of coronary arteries, studies[6,7] with predominantly male population characterization, but similar mean age to our study, found that the prevalence of CAC in asymptomatic individuals is greater than 53%. These data are in line with what was presented in this research, with a predominance of mild and severe calcifications. In the analysis of calcifications in isolation, based on the score, the right coronary artery was shown to be the most compromised, unlike other studies that point to the anterior descending coronary artery.[12,13] However, this proximal compromise can cause reduction or blockage of the blood flow to a certain area of the myocardium,[14] whose outcome is one of the main causes of death.[15] This prevalence in asymptomatic patients is important, because when recognized early, helps in prevention, reduces the speed of disease progression, and reduces the associated morbidity and mortality.

Therefore, there are some factors that predispose the appearance of CAC. Among them, the present study found that men are more likely to develop CAC (OR = 1.55), as observed in previous studies;[5,10] however, there are studies that point out that these findings are independent of gender.[7] Another point that was proven statistically significant ($p < 0.001$) was the increasing prevalence with growing age. Other studies[5,7] present data in

line with these findings, which can be explained by the fact that these calcifications occur progressively, as a result of the sum of advancing age and complex biological processes, including genetics, risk factors, diseases acquired throughout life, and environmental factors.[16]

Furthermore, the study on the prevalence of CAC in Mexico corroborates what was previously shown and demonstrates that 27% of the participants have CAC, the majority being men (40%), followed by women (13%); both genders were older and had higher values of systolic and diastolic blood pressure, glucose, and LDL cholesterol.[17] In another recent study conducted in northern Brazil, a high prevalence of cardiovascular risk factors associated with coronary calcifications was observed, especially SAH (83.33%), dyslipidemia (62.22%), sedentary lifestyle (74.44%), and overweight (64.44%), being more prevalent in women, who were menopausal in the majority (90.48%).[18] Based on these data, the relevance of this topic can be seen and the relationship between CAC and the variables mentioned is confirmed.

Along these lines, SAH and dyslipidemia, as described in other studies,[12,19] are statistically significant and have high odds ratios. Studies show that a sedentary lifestyle[20] and smoking[21] have substantial impacts on risk factors, as found in this study. These data are of greater importance when considering that 80% of deaths from CVD could be avoided by quitting smoking habits and practicing physical activity regularly.[22]

The present study is a pioneer in the Northwest region of the State of Rio Grande do Sul and has a considerably large sample number for the collection period. However, the limitations of the study include divergences between the observers who analyzed the images, which can be explained by the fact that the exam was not performed with ECG-Gated Cardiac CT (image captured in cardiac diastole), making the analysis difficult; however, they were reassessed, reaching a consensus. The study population showed a selection bias, firstly because the study was carried out in a single hospital and secondly because the individuals included were referred due to clinical indications of different pathologies. The self-applied questionnaire can be considered a weakness, as individuals may omit or not fully understand what is being asked.

Conclusion

The incidental findings of CAC in asymptomatic individuals for heart disease undergoing chest CT showed a prevalence of 44% in the interior of the Northwest of the state of Rio Grande do Sul, Brazil. These vary between mild and severe, with a higher odds ratio in males and an increase in prevalence with age. Therefore, chest CT proves to be an effective method to assess CAC, along with the patient's clinical history, and can be used to measure risk factors for CVD and intervene in the outcome of the condition.

This study is a pioneer in this region and shows the importance of future investigations, surveys and/or evaluations of patients with CVD.

Acknowledgment

To the Diagnostic Imaging Center of *Hospital Unimed Noroeste*, Rio Grande do Sul, for their availability to carry out the work, to *Universidade Regional do Noroeste do Estado do Rio Grande do Sul* (UNIJUI) for the opportunity to carry out the research, and to the National Council for Scientific and Technological Development (*Conselho Nacional de Desenvolvimento Científico e Tecnológico* – CNPq) for granting scientific initiation scholarships.

Author Contribution

Conception and design of the research: Scopel KRO, Heuser GG, Medeiros TM, Winkelmann ER; writing of the manuscript: Scopel KRO, Medeiros TM, Winkelmann ER; analysis and interpretation of the data: Medeiros TM, Velho MC, Mattod JN, Heuser GG; acquisition of data: Scopel KRO, Maicá BNPM; statistical analysis: Silva MMD; critical revision of the manuscript for intellectual content: Medeiros TM, Heuser GG, Winkelmann ER.

Potential Conflict of Interest

No potential conflict of interest relevant to this article was reported.

Sources of Funding

There were no external funding sources for this study.

Study Association

This study is not associated with any thesis or dissertation work.

Ethics Approval and Consent to Participate

This study was approved by the Ethics Committee of the Universidade Regional do Nororeste do Estado do Rio Grande do Sul under the protocol number 2.739.345 / CAAE: 84431118.2.0000.5350. All the procedures in this study were in accordance with the 1975 Helsinki Declaration, updated in 2013. Informed consent was obtained from all participants included in the study.

References

1. Sociedade Brasileira de Cardiologia. Diretrizes da Sociedade Brasileira de Cardiologia: Pocket Book 2009-2014. Rio de Janeiro: SBC; 2014.
2. Liberman M, Pesaro AEP, Carmo LS, Serrano CV. Calcificação Vascular: Fisiopatologia e Implicações Clínicas. Einstein. 2013;11(3):376-82. doi: 10.1590/S1679-45082013000300021.
3. Madhavan MV, Tarigopula M, Mintz GS, Maehara A, Stone GW, Généreux P. Coronary Artery Calcification: Pathogenesis and Prognostic Implications. J Am Coll Cardiol. 2014;63(17):1703-14. doi: 10.1016/j.jacc.2014.01.017.
4. Pelandré GL, Sanches NMP, Nacif MS, Marchiori E. Detection of Coronary Artery Calcification with Nontriggered Computed Tomography of the Chest. Radiol Bras. 2018;51(1):8-12. doi: 10.1590/0100-3984.2016.0181.
5. Jairam PM, Gondrie MJ, Grobbee DE, Mali WP, Jacobs PC, van der Graaf Y, et al. Incidental Imaging Findings from Routine Chest CT Used to Identify Subjects At High Risk of Future Cardiovascular Events. Radiology. 2014;272(3):700-8. doi: 10.1148/radiol.14132211.

6. Sverzellati N, Arcadi T, Salvolini L, Dore R, Zompatori M, Mereu M, et al. Under-Reporting of Cardiovascular Findings on Chest CT. Radiol Med. 2016;121(3):190-9. doi: 10.1007/s11547-015-0595-0.

7. Secchi F, Di Leo G, Zanardo M, Alì M, Cannaò PM, Sardanelli F. Detection of Incidental Cardiac Findings in Noncardiac Chest Computed Tomography. Medicine (Baltimore). 2017;96(29):e7531. doi: 10.1097/MD.0000000000007531.

8. Sconfienza LM, Mauri G, Muzzupappa C, Poloni A, Bandirali M, Esseridou A, et al. Relevant Incidental Findings at Abdominal Multi-Detector Contrast-Enhanced Computed Tomography: A Collateral Screening? World J Radiol. 2015;7(10):350-6. doi: 10.4329/wjr.v7.i10.350.

9. Verdini D, Lee AM, Prabhakar AM, Abbara S, Ghoshhajra B, Writing Group. Detection of Cardiac Incidental Findings on Routine Chest CT: The Impact of Dedicated Training in Cardiac Imaging. J Am Coll Radiol. 2018;15(8):1153-7. doi: 10.1016/j.jacr.2016.02.011.

10. Shemesh J, Henschke CI, Shaham D, Yip R, Farooqi AO, Cham MD, et al. Ordinal Scoring of Coronary Artery Calcifications on Low-Dose CT Scans of the Chest is Predictive of Death From Cardiovascular Disease. Radiology. 2010;257(2):541-8. doi: 10.1148/radiol.10100383.

11. Landis JR, Koch GG. The Measurement of Observer Agreement for Categorical Data. Biometrics. 1977;33(1):159-74.

12. Gabriel FS, Gonçalves LFG, Melo EV, Sousa ACS, Pinto IMF, Santana SMM, et al. Atherosclerotic Plaque in Patients with Zero Calcium Score at Coronary Computed Tomography Angiography. Arq Bras Cardiol. 2018;110(5):420-7. doi: 10.5935/abc.20180063.

13. Phillips WJ, Johnson C, Law A, Turek M, Small AR, Inacio JR, et al. Reporting of Coronary Artery Calcification on Chest CT Studies in Breast Cancer Patients at High Risk of Cancer Therapy Related Cardiac Events. Int J Cardiol Heart Vasc. 2018;18:12-16. doi: 10.1016/j.ijcha.2018.02.001.

14. Ouchi JD, Teixeira C, Ribeiro CAG, Oliveira CC. Arrival time of Infarcted Patient in the Intensive Care Unit: Importante of Fast Care Services. Ensaios Cienc Biol Agrar. Saúde. 2017; 21(2):92-7.

15. Brasil. Ministério da Saúde. Sistema de Informação sobre a Mortalidade. Brasília; Ministério da Saúde; 2013.

16. Shemesh J. Coronary Artery Calcification in Clinical Practice: What We Have Learned and Why Should It Routinely Be Reported On Chest CT? Ann Transl Med. 2016;4(8):159. doi: 10.21037/atm.2016.04.08.

17. Posadas-Romero C, López-Bautista F, Rodas-Díaz MA, Posadas-Sánchez R, Kimura-Hayama E, Juárez-Rojas JG, et al. Prevalence and Extent of Coronary Artery Calcification in an Asymptomatic Cardiovascular Mexican Population: Genetics of Atherosclerotic Disease Study. Arch Cardiol Mex. 2017;87(4):292-301. doi: 10.1016/j.acmx.2016.12.004.

18. Silveira EL, Cunha LM, Pantoja MS, Lima AVM, Cunha ANA. Risk Factors of Coronary Disease Among Patients Subjected to Myocardial Revascularization (ABG) in Joinville/SC. Rev Fac Ciênc Méd Sorocaba. 2018;20(3):172-8. doi: 10.13037/ras.vol18n65.6517.

19. Oliveira JL, Hirata MH, Sousa AG, Gabriel FS, Hirata TD, Tavares Ida S, et al. Male Gender and Arterial Hypertension are Plaque Predictors at Coronary Computed Tomography Angiography. Arq Bras Cardiol. 2015;104(5):409-16. doi: 10.5935/abc.20150028.

20. Delaney JA, Jensky NE, Criqui MH, Whitt-Glover MC, Lima JA, Allison MA. The Association Between Physical Activity and Both Incident Coronary Artery Calcification and Ankle Brachial Index Progression: The Multi-Ethnic Study of Atherosclerosis. Atherosclerosis. 2013;230(2):278-83. doi: 10.1016/j.atherosclerosis.2013.07.045.

21. Pham T, Fujiyoshi A, Hisamatsu T, Kadowaki S, Kadota A, Zaid M, et al. Smoking Habits and Progression of Coronary and Aortic Artery Calcification: A 5-Year Follow-Up of Community-Dwelling Japanese Men. Int J Cardiol. 2020;314:89-94. doi: 10.1016/j.ijcard.2020.05.016.

22. GBD 2017 Disease and Injury Incidence and Prevalence Collaborators. Global, Regional, and National Incidence, Prevalence, and Years Lived with Disability for 354 Diseases and Injuries for 195 Countries and Territories, 1990-2017: A Systematic Analysis for the Global Burden of Disease Study 2017. Lancet. 2018;392(10159):1789-1858. doi: 10.1016/S0140-6736(18)32279-7.

Radiotherapy-Induced Heart Disease: What Can We Evaluate?

Marcelo Goulart Paiva[1]

DASA - Hospital 9 de Julho,[1] *São Paulo, SP – Brasil*

Radiotherapy (RT) has been part of oncological treatment since 1899 and is currently used with more than 50% of all patients.[1] Breast, lung, esophagus, and lymphoma tumors are commonly submitted to RT treatment, showing improvements in the total survival and freedom from diseases. By contrast, when including mediastinal structures, such as the heart and blood vessels, in 10% to 30% of the patients, adverse cardiovascular events were observed after 5 and 10 years, defined as Radiation-Induced Heart Disease (RIHD).[2,3]

The RIHD spectrum includes pericardial diseases, coronary artery disease, valvar heart disease, cardiomyopathy, as well as conduction abnormality and dysautonomia, leading to an increase in the cardiovascular morbidity and mortality of the survivors.[4]

High-risk patients were those submitted to anterior chest RT, whose therapeutic planning involves the heart and the presence of one or more factors related to the patient, such as a person under 50 years of age, previous cardiovascular disease, cardiovascular risk factors, a tumor located close the heart, and factors related to the treatment itself, including total accumulated dose (> 30 Gy), total dose upon the heart (increase in cardiovascular risk from 1.5% to 7% for each 1 Gy), association with anthracyclines and the absence of cardioprotection.[2,5]

Ionizing radiation can damage all heart tissues and be responsible for micro and macrovascular lesions. The loss of endothelial cells, inflammatory response, and vascular lesion were detected early on, resulting in capillary rarefaction with a consequent ischemia, fibrosis, and systolic and diastolic dysfunctions. The macrovascular lesion appears through accelerated atherosclerosis, with endothelial dysfunction, macrophagic infiltration, inflammation, and intraplaque hemorrhage, which makes it more prone to rupture.[2]

The pre-RT evaluation should include, in addition to the anamnesis and physical exam, the multimodality of imaging exams in the study of the pre-existing cardiovascular disease. In the staging or therapeutic planning, a chest computed tomography (CT) is commonly taken, in which one can evaluate the presence of coronary calcification. The identification of this shows a good correlation with research dedicated to the study of calcium scores and to the stratification of the cardiovascular risk.[4] The transthoracic echocardiogram (TTE) should be considered in all patients to evaluate the ventricular dysfunction and to study the valvar and pericardial heart disease. Whenever possible, medical professionals should evaluate myocardial deformities by means of the global longitudinal strain.[4]

The presence of cardiovascular risk and coronary disease in women with breast cancer submitted to RT was associated with a 2-fold and 6-fold higher risk, respectively, of severe cardiovascular events during follow-up.[6] One study, conducted with patients with atherosclerotic plaque in the anterior descending artery, demonstrated that, when submitted to RT (average dose applied to the left ventricle > 5 Gy), the patients presented a high risk of cardiovascular events after an average follow-up of 9 years.[5] All of the patients identified as high risk prior to RT should be treated according to the cardiovascular prevention and treatment guidelines.

Faced with the high risk of RIHD, a wide range of imaging exams can be used for follow-up and diagnosis of cardiotoxicity. The choice for complementary exams will depend on the experience of each center and of the individual characteristics of the patient, such as comorbidities, RT characteristics, association or not with anthracycline, and the emergence of symptoms.

In the majority of asymptomatic cases, the TTE is recommended to evaluate abnormalities, in addition to the study of ischemia after 5 to 10 years and every 5 years thereafter. In patients considered to be of high risk, an earlier evaluation is recommended, between 6 and 24 months after the end of RT.[7] More recently, the evaluation of non-obstructive coronary artery disease by coronary CT angiography enabled the early implementation of preventive pharmacological measures, such as the use of statins.[1] In symptomatic patients, medical exams should follow the recommendation set forth in the guidelines for each pathology.

The TTE (Figure 1), as it is a widely available method that is non-invasive and does not use ionizing radiation, has quickly become the first option for port-RT patient follow-up. The use of diverse modalities and resources, such as the M mode, Doppler 2D and 3D, ultrasound contrast, stress echocardiography, and transesophageal echocardiography, enables the detection of critical structural and functional changes in the diagnosis of RIHD. The reduction of the global longitudinal strain in the segment exposed to RT (Figure 1.C) can be observed early and present a subclinical dysfunction with a worse diagnosis.[1,8,9] The appearance of a pericardial stroke (Figure 1.B) a few weeks after the end of RT was significantly diminished after the reduction in the total dose in more modern protocols; however, 10% to 20% of the cases can evolve into chronic and constrictive forms after 20 years. The findings that suggest constrictive

Keywords

Radiotherapy; Echocardiography; Cardiotoxicity

Mailing Address: Marcelo Goulart Paiva •
Rua Periquito 210/92B. Postal code: 04514-050. São Paulo, SP – Brazil
E-mail: mgpaiva123@gmail.com
Manuscript received October 15, 2022; revised October 17, 2022; accepted November 2, 2022
Editor responsible for the review: Daniela do Carmo Rassi Frota

DOI: https://doi.org/10.36660/abcimg.2023358i

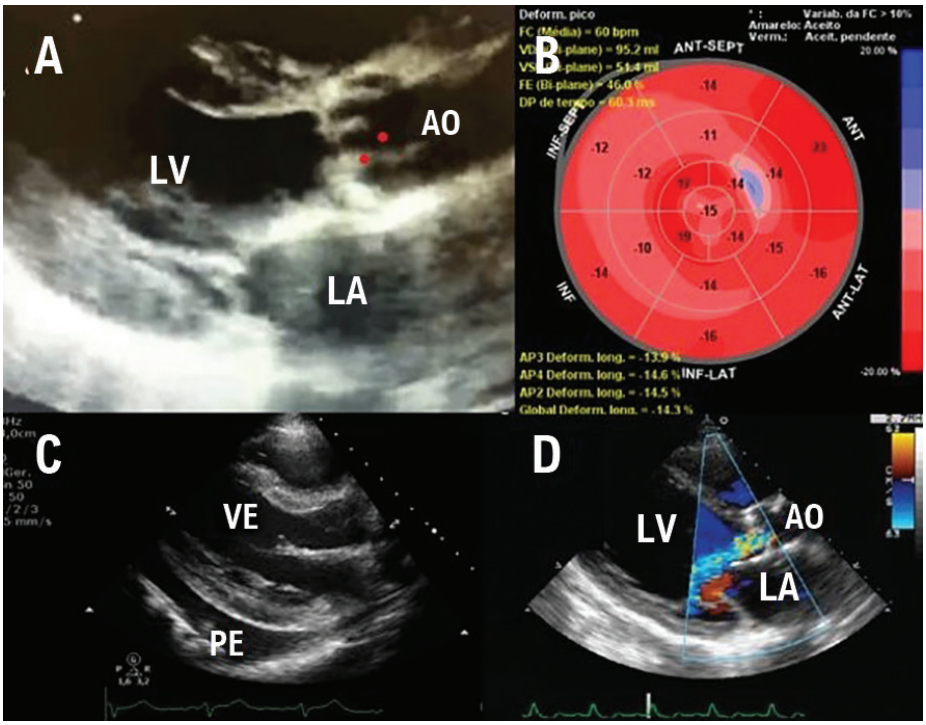

Figure 1 – *A) Longitudinal parasternal cut, valve-aortic calcification, mitroaortic fibrosis and anterior leaflet of the mitral valve, 72-year-old patient with a breast neoplasm; B) Polar Map of a 57-year-old patient and esophagogastric transition tumor; C) Longitudinal parasternal cut, presence of pericardial stroke, 32-year-old patient with Hodgkin lymphoma; D) longitudinal parasternal cut, presence of aortic insufficiency, 65-year-old patient with Hodgkin lymphoma. LV: left ventricle; PE: Pleural Effusion; AO: aorta; LA: left atrium*

pericarditis include pericardial thickening, septal bounce, restrictive patterns of diastolic filling, variation > 25% of the mitral inflow, plethora of inferior vena cava, and reversal of the expiratory diastolic flow in the hepatic veins.[2,7,11] The more common findings in the myocardial dysfunction are the change in the segmental contractility (normally on the lower wall), general hypokinesia, and signs of diastolic dysfunction. Changes in the segmental contractility are not necessarily related to the presence of coronary artery disease and the added evaluation by means of the stress echocardiogram can aid in the diagnosis.[12] It is important to remember that, to calculate the ejection fraction (EF), if possible, one should use 3D echocardiography, and, if this is not possible, always use the Simpson method in 2D. Despite the importance of EF, both in the diagnosis and in the follow-up of cardiotoxicity, one should not disregard the intraobserver and interobserver variability inherent to the method, as well as the influence of the pre-load and post-load. The subclinical dysfunction evaluated by the study of myocardial deformity, more commonly using the 2D speckle-tracking technique, presents more sensitive and earlier results, earlier even than the change in the EF. The study of the diastolic function is of utmost importance, as the emergence of heart failure with the EF preserved due to fibrosis and endothelial dysfunction is much more commonly observed.[2,4,8,10] The prevalence of moderate or severe valvar heart disease is rare in the first 10 years, with the preferential involvement being to that of the aortic valve, followed by the mitral valve. The echocardiographic findings range from the discrete thickening and calcification of the valve leaflets to more characteristic findings, such as the thickening and calcification of the mitroaortic curtain, a more significant involvement of the valve leaflets (aortic and anterior leaflets of the mitral valve) without commissural fusion, which enables a differential diagnosis with rheumatic carditis (Figure 1.A). Functionally, the regurgitant lesions (Figure 1.D) are more common; however, after 20 years, an increase in the incidence of valvar stenosis can be observed.[2,4,7,12,13]

Cardiac magnetic resonance Imaging (CMRI) is especially useful in cases in which the echocardiograph window is limited, and the evaluation of the ventricular function is adopted as the gold standard. The use of delayed enhancement by gadolinium injection, T1 map, and the increase in the extracellular volume, allow for the myocardial tissue characterization of the presence of fibrosis. The pericardial thickness, enhancement after contrast, the presence of a stroke, and findings suggestive of constriction in the cine-RM images suggest pericardial involvement. Evaluation of valvar heart lesions is also possible, with a higher precision for regurgitant lesions.[1,2,4]

Nuclear medicine (NM) can contribute to relevant information about the function and myocardial perfusion, both at rest and with stress (physical or pharmacological).

Editorial

The need to use radiation and the possible evaluation of the ventricular function by other methods has limited the use of NM to the study of perfusion, preferentially with ^{201}Tl and ^{99m}Tc. The prevalence of the defects of post-RT myocardial perfusion vary from 1% to 64%, depending on the irradiated ventricular volume, age, post-RT time, and methodology of the perfusion study. The distribution of the changes in the perfusion are not always correlated with obstructive coronary artery disease, often corresponding to changes in microcirculation. When changes in perfusion occur, an association among a deterioration of the ventricular function, the need for myocardial revascularization, and adverse cardiovascular events can be observed.[1,2,4]

As seen above, the identification of coronary calcification in studies performed for the staging of the oncological disease or the planning of RT, provides important information referent to the presence of atherosclerotic disease and the need to control cardiovascular risk factors. The use of CT angiography of the coronary arteries in the post-RT follow-up is still limited. In a study conducted with 31 patients with lymphomas after 24 years of RT treatment, CT angiography identified the presence of coronary disease in 12 patients and in the obstructive form in 3 patients, with only 1 identified in the functional exam used to study ischemia. The best moment for screening and the possibility of benefits in repeating the exam are still under debate. CT angiography appears to present a greater benefit than the isolated study of the calcium score, and the use of CT studies themselves can highlight false negative results.[1,2,4]

Despite the progress of RT techniques, RIHD is still common and can appear many years after the termination of the therapy. The simultaneous involvement of diverse heart structures, the comorbidities, and the limitations for invasive cardiovascular treatment reinforce the need for a rigorous control of cardiovascular risk factors, strategies of cardioprotection during RT, and the use of multimodality imaging (Figure 2) to reach an early diagnosis aimed at improving clinical results.[1,2,4,14]

Potential Conflict of Interest

No potential conflict of interest relevant to this article was reported.

Sources of Funding

There were no external funding sources for this study.

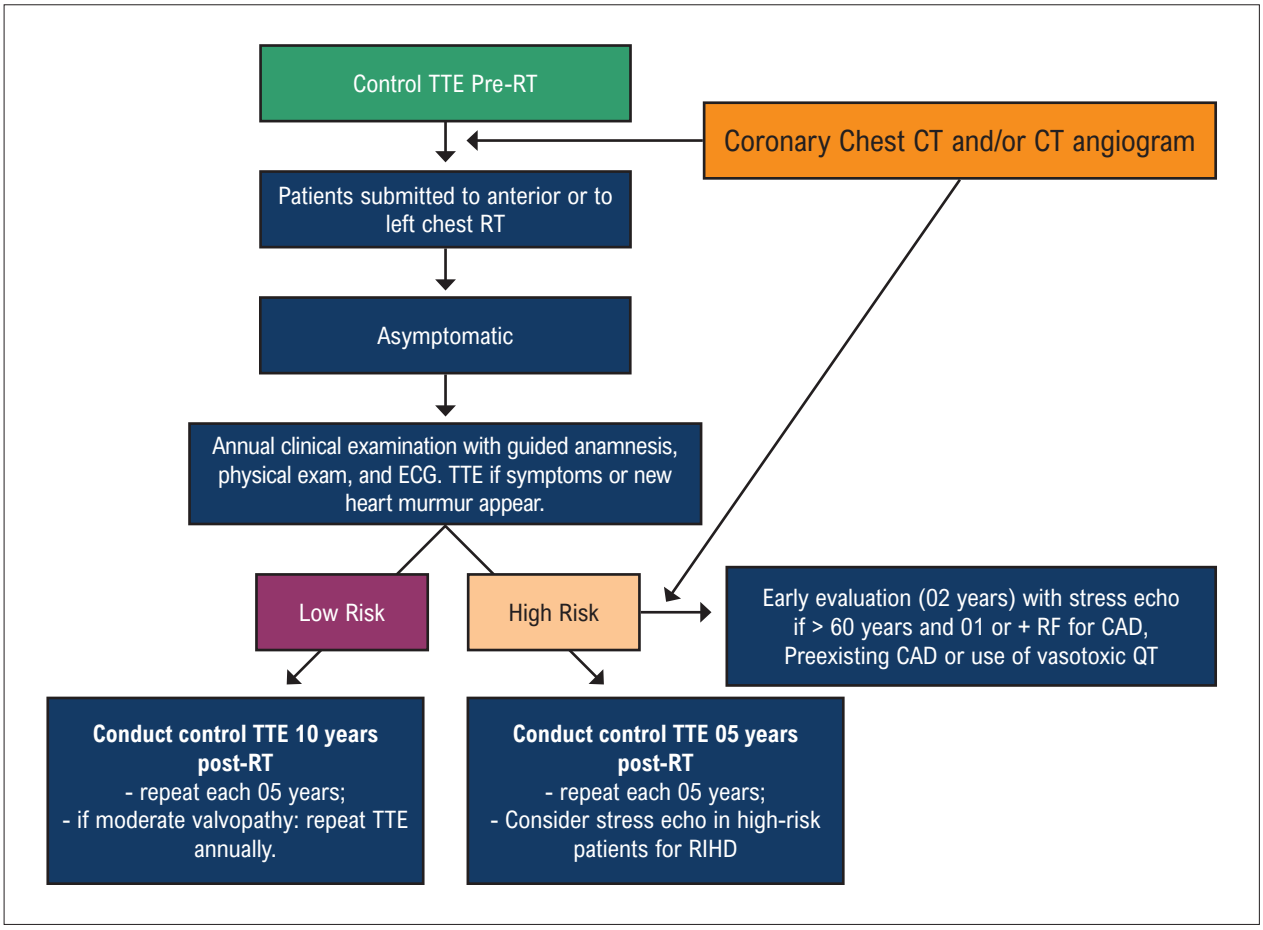

Figure 2 – *Adapted from the Brazilian Position Statement concerning the Use of Multimodal Imaging in Cardio-Oncology – 2021.7 RT: radiotherapy; TTE: transthoracic echocardiogram; ECG: electrocardiogram; CAD: coronary artery disease; RF: risk factor; QT: chemotherapy; RIHD: Radiation-Induced Heart Disease; CT: computed tomography.*

Study Association

This study is not associated with any thesis or dissertation work.

Author Contributions

Conception and design of the research, acquisition of data, analysis and interpretation of the data, writing of the manuscript, critical revision of the manuscript for intellectual content: Paiva MG.

Ethics Approval and Consent to Participate

This article does not contain any studies with human participants or animals performed by any of the authors.

References

1. Bergom C, Bradley JA, Ng AK, Samson P, Robinson C, Lopez-Mattei J, et al. Past, Present, and Future of Radiation-Induced Cardiotoxicity: Refinements in Targeting, Surveillance, and Risk Stratification. JACC CardioOncol. 2021;3(3):343-59. doi: 10.1016/j.jaccao.2021.06.007.
2. Lancellotti P, Nkomo VT, Badano LP, Bergler-Klein J, Bogaert J, Davin L, et al. Expert Consensus for Multi-Modality Imaging Evaluation of Cardiovascular Complications of Radiotherapy in Adults: A Report from the European Association of Cardiovascular Imaging and the American Society of Echocardiography. J Am Soc Echocardiogr. 2013;26(9):1013-32. doi: 10.1016/j.echo.2013.07.005.
3. Ganatra S, Chatur S, Nohria A. How to Diagnose and Manage Radiation Cardiotoxicity. JACC CardioOncol. 2020;2(4):655-60. doi: 10.1016/j.jaccao.2020.07.010.
4. Mitchell JD, Cehic DA, Morgia M, Bergom C, Toohey J, Guerrero PA, et al. Cardiovascular Manifestations from Therapeutic Radiation: A Multidisciplinary Expert Consensus Statement from the International Cardio-Oncology Society. JACC CardioOncol. 2021;3(3):360-80. doi: 10.1016/j.jaccao.2021.06.003.
5. van den Bogaard VAB, Spoor DS, van der Schaaf A, van Dijk LV, Schuit E, Sijtsema NM, et al. The Importance of Radiation Dose to the Atherosclerotic Plaque in the Left Anterior Descending Coronary Artery for Radiation-Induced Cardiac Toxicity of Breast Cancer Patients? Int J Radiat Oncol Biol Phys. 2021;110(5):1350-9. doi: 10.1016/j.ijrobp.2021.03.004.
6. Darby SC, Ewertz M, McGale P, Bennet AM, Blom-Goldman U, Brønnum D, et al. Risk of Ischemic Heart Disease in Women After Radiotherapy for Breast Cancer. N Engl J Med. 2013;368(11):987-98. doi: 10.1056/NEJMoa1209825.
7. Melo MDT, Paiva MG, Santos MVC, Rochitte CE, Moreira VM, Saleh MH, et al. Brazilian Position Statement on the Use of Multimodality Imaging in Cardio-Oncology - 2021. Arq Bras Cardiol. 2021;117(4):845-909. doi: 10.36660/abc.20200266.
8. Yu AF, Ho AY, Braunstein LZ, Thor ME, Lee Chuy K, Eaton A, et al. Assessment of Early Radiation-Induced Changes in Left Ventricular Function by Myocardial Strain Imaging After Breast Radiation Therapy. J Am Soc Echocardiogr. 2019;32(4):521-8. doi: 10.1016/j.echo.2018.12.009.
9. Villarraga HR, Herrmann J, Nkomo VT. Cardio-Oncology: Role of Echocardiography. Prog Cardiovasc Dis. 2014;57(1):10-8. doi: 10.1016/j.pcad.2014.05.002.
10. Hamza A, Tunick PA, Kronzon I. Echocardiographic Manifestations of Complications of Radiation Therapy. Echocardiography. 2009;26(6):724-8. doi: 10.1111/j.1540-8175.2008.00878.x.
11. Heidenreich PA, Schnittger I, Strauss HW, Vagelos RH, Lee BK, Mariscal CS, et al. Screening for Coronary Artery Disease After Mediastinal Irradiation for Hodgkin's Disease. J Clin Oncol. 2007;25(1):43-9. doi: 10.1200/JCO.2006.07.0805.
12. Hering D, Faber L, Horstkotte D. Echocardiographic Features of Radiation-Associated Valvular Disease. Am J Cardiol. 2003;92(2):226-30. doi: 10.1016/s0002-9149(03)00546-0.
13. Malanca M, Cimadevilla C, Brochet E, Iung B, Vahanian A, Messika-Zeitoun D. Radiotherapy-Induced Mitral Stenosis: A Three-Dimensional Perspective. J Am Soc Echocardiogr. 2010;23(1):108.e1-2. doi: 10.1016/j.echo.2009.08.006.
14. Dolmaci OB, Farag ES, Boekholdt SM, van Boven WJP, Kaya A. Outcomes of Cardiac Surgery After Mediastinal Radiation Therapy: A Single-Center Experience. J Card Surg. 2020;35(3):612-9. doi: 10.1111/jocs.14427.

How Can the Assessment of Myocardial Flow Reserve by Nuclear Medicine Change the Interpretation of Myocardial Perfusion Scintigraphy?

Ronaldo de Souza Leão Lima[1]
Universidade Federal do Rio de Janeiro,[1] *Rio de Janeiro, RJ – Brazil*

Myocardial perfusion scintigraphy (MPS) with single-photon emission computed tomography (SPECT) is important for the diagnosis and prognostic evaluation in patients with coronary artery disease (CAD).[1] MPS evaluates the presence, extent and degree of myocardial ischemia and/or infarction, usually through visual observation or semi-quantitative parameters. Despite its proven diagnostic and prognostic values, the relative nature of perfusion imaging may limit SPECT ability to identify patients with high-risk multivessel CAD.[2] Limitations regarding visual or semi-quantitative assessment of regional myocardial perfusion defects may result in underestimation or misdiagnosis due to "balanced" ischemia.

This limitation can be addressed by quantifying myocardial blood flow (MBF) or myocardial flow reserve (MFR) using tracer kinetics in positron emission tomography (PET).[3,4] PET is a well-validated non-invasive method for quantification of myocardial perfusion, demonstrating an incremental diagnostic and prognostic power compared to MPS in patients with suspected or known CAD.[5,6] PET then is considered the gold standard for non-invasive quantification of MBF and MFR.[7-9] However, the production of PET tracers is costly and the technology is not yet available in many countries.

The introduction of high-sensitivity cadmium-zinc-teluride (CZT) cameras for cardiology tests allows the dynamic acquisition of tomographic images to evaluate radiotracer kinetics, and opens a new era for measuring MBF and MFR.[10]

Quantification of MBF and MFR using dynamic CZT-SPECT in list mode is technically feasible and clinically useful.[11,12] The WATERDAY study[13] compared MBF and MFR obtained with 99mTc-sestamibi in CZT-SPECT with those obtained in a ^{15}O-water PET and fractional flow reserve (FFR). While stress and rest MBF were significantly overestimated with CZT-SPECT compared to PET, MFR was similar between the two techniques, which means that the quantification of MBF and MFR by dynamic 99mTc-sestamibi CZT-SPECT is clinically useful.[13] Acampa et al.[14] demonstrated that CZT-SPECT values are higher than those measured by 82Rb-PET imaging, with a moderate correlation between the two methods. CZT-SPECT showed good diagnostic accuracy for identifying obstructive CAD. Different studies have outlined the incremental value of MFR measurements in different categories of patients for diagnosis or prognosis.[14] In patients with multivessel CAD, where normal myocardial perfusion imaging (MPI) may not necessarily identify truly low-risk subgroups among high-risk cohorts, they often show reduced MFR.[14]

Despite the excellent diagnostic value of FFR, which quantifies pressure gradient through stenosis, it does not reflect microcirculation abnormalities. Unlike FFR, myocardial perfusion reserve (MPR) reflects flow in epicardial arteries and microvasculature. Therefore, FFR and MPR are not equivalent.[16]

It should be noted that several factors can affect the hemodynamic flow response to luminal stenosis, including lesion geometry and location and the presence of collateral vessels, impacting overall regional flow. In a study by our group, De Souza et al.[17] showed that both global MPR and MBF stress were reduced in patients with abnormal perfusion. In addition to assessing perfusion, this study demonstrated that overall MPR is inversely associated with CAD prognostic index (CADPI), a hierarchical index that includes the entire epicardial coronary tree and is related to overall cardiovascular risk.[17]

In this scenario, Panjer et al.[18] performed a systematic review and meta-analysis with the objective of evaluating the diagnostic accuracy of dynamic CZT-SPECT in coronary artery disease (CAD) compared to FFR and PET as a reference. To assess CZT-SPECT, the analysis yielded 0.79 sensitivity (95% CI 0.73–0.85) and 0.85 specificity (95% CI 0.74–0.92). Diagnostic odds ratio was 17.82 (95% CI 8.80–36.08, P \ 0.001). Positive likelihood ratio and negative likelihood ratio were 3.86 (95% CI 2.76–5.38, P<0.001) and 0.21 (95% CI 0.13–0.33, P<0.001), respectively. The results of this systematic review and meta-analysis emphasize the role of dynamic CZT-SPECT MPI with good sensitivity and specificity for diagnosing CAD compared to gold standards. The use of CZT-SPECT systems for measuring MPR is very attractive considering that in just one scan it is possible to obtain perfusion and functional parameters with results comparable to PET. However, what emerges from this meta-analysis is that the protocol used in different centers should be better standardized. The included studies use different methodologies in terms of dose administration, acquisition protocol, CZT cameras, radiotracers and software package used. Furthermore, in each study a different cutoff value was defined for the dynamic SPECT MPI. Seven studies compared with FFR and two used PET. To measure acquisition, MPI was performed with different types of CZT-SPECT cameras. Six studies used Discovery NM 530c (GE Healthcare, Chicago, IL, USA), one study (11.1%) used Discovery NM/CT 570c

Keywords

Coronary artery disease; Scintigraphy; Diagnosis.

Mailing Address: Ronaldo de Souza Leão Lima •
Rua Paissandu, 329/303. Postal code: 22210-080. Flamengo, Rio de Janeiro, RJ - Brazil
E-mail: ronlima@hotmail.com

DOI: https://doi.org/10.36660/abcimg.2023363i

(Alcyone technology, GE Healthcare, Haifa, Israel) and two studies (22.2%) used D-SPECT (Spectrum Dynamics, Palo Alto, California). Dual isotope administration was used in one study. Two studies used 201Tl as a radiotracer, and six studies (66.7%) used 99mTc-labeled markers. Different software was used for MBF quantification and MFR measurement, including internal software, with 4DM Corridor (INVIA, Ann Arbor, MI, USA) applied more often than others. Furthermore, the main limitation of this systematic review and meta-analysis, in addition to the typical limitations for this type of analysis, is the relatively small number of included studies and patients and inter-comparison heterogeneity.[19] In this regard, studies with a larger population and smaller variability between methodologies, such as different thresholds for MFR, myocardial radiotracer distribution, different reconstruction algorithms and applied flow models will be necessary to clearly demonstrate the additional clinical impact of MBF with CZT.

Myocardial flow reserve assessment using CZT can be useful in many clinical situations, as shown by PET (Table 1).

One of the main uses was demonstrated in the extremely high sensitivity to detect multivascular disease, as in the study by DiCarli et al., where normal MFR on PET virtually excluded the possibility of this event.[20] MFR evaluation by CZT-SPECT also allows for this increase in accuracy.[21]

The possibility of identifying microvascular disease as the cause of angina is useful for reducing investigation costs but also very important as a determinant of prognosis. MFR, both on PET and on CZT-SPECT, is a non-invasive modality for confirming this phenomenon.[22]

In preparation for pharmacological stress with dipyridamole or adenosine, abstinence from caffeine for at least 24 hours is recommended. However, when this preparation is not carried out properly, vasodilator response may be compromised and, consequently, induction of flow disparity. In traditional scintigraphy, this cannot be identified and may result in a "false-negative" result, but this inadequate response is detected by MFR evaluation.[23]

As more studies are published, leading to better standardization of MBF and MFR quantification by CZT-SPECT, it will become an important tool in the clinical practice of ischemic cardiomyopathies, adding to our understanding of this disease.

Table 1 – In which situations can myocardial flow reserve make a difference?

1) Patients with little ischemia who may have multivessel CAD.
2) Perfusion defects, but with artifact.
3) Normal perfusion but at high risk for CAD.
4) Identification of microvascular disease.
5) Determine vaso-stressor effectiveness.

Author Contributions

Writing of the manuscript: Lima RSL.

Potential Conflict of Interest

No potential conflict of interest relevant to this article was reported.

Sources of Funding

There were no external funding sources for this study.

Study Association

This study is not associated with any thesis or dissertation work.

Ethics Approval and Consent to Participate

This article does not contain any studies with human participants or animals performed by any of the authors.

References

1. Mastrocola LE, Amorim BJ, Vitola JV, Brandão SCS, Grossman GB, Lima RSL, et al. Update of the Brazilian Guideline on Nuclear Cardiology - 2020. Arq Bras Cardiol. 2020;114(2):325-29. doi: 10.36660/abc.20200087.
2. Lima RS, Watson DD, Goode AR, Siadaty MS, Ragosta M, Beller GA, et al. Incremental Value of Combined Perfusion and Function Over Perfusion Alone by Gated SPECT Myocardial Perfusion Imaging for Detection of Severe Three-Vessel Coronary Artery Disease. J Am Coll Cardiol. 2003;42(1):64-70. doi: 10.1016/s0735-1097(03)00562-x.
3. Muzik O, Duvernoy C, Beanlands RS, Sawada S, Dayanikli F, Wolfe ER Jr, et al. Assessment of Diagnostic Performance of Quantitative Flow Measurements in Normal Subjects and Patients with Angiographically Documented Coronary Artery Disease by Means of Nitrogen-13 Ammonia and Positron Emission Tomography. J Am Coll Cardiol. 1998;31(3):534-40. doi: 10.1016/s0735-1097(97)00526-3.
4. Parkash R, de Kemp RA, Ruddy TD, Kitsikis A, Hart R, Beauchesne L, et al. Potential Utility of Rubidium 82 PET Quantification in Patients with 3-Vessel Coronary Artery Disease. J Nucl Cardiol. 2004;11(4):440-9. doi: 10.1016/j.nuclcard.2004.04.005.
5. Zampella E, Acampa W, Assante R, Nappi C, Gaudieri V, Mainolfi CG, et al. Combined Evaluation of Regional Coronary Artery Calcium and Myocardial Perfusion by 82Rb PET/CT in the Identification of Obstructive Coronary Artery Disease. Eur J Nucl Med Mol Imaging. 2018;45(4):521-29. doi: 10.1007/s00259-018-3935-1.
6. Assante R, Acampa W, Zampella E, Arumugam P, Nappi C, Gaudieri V, et al. Prognostic Value of Atherosclerotic Burden and Coronary Vascular Function in Patients with Suspected Coronary Artery Disease. Eur J Nucl Med Mol Imaging. 2017;44(13):2290-98. doi: 10.1007/s00259-017-3800-7.
7. Johnson NP, Gould KL, Di Carli MF, Taqueti VR. Invasive FFR and Noninvasive CFR in the Evaluation of Ischemia: What Is the Future? J Am Coll Cardiol. 2016;67(23):2772-88. doi: 10.1016/j.jacc.2016.03.584.
8. Danad I, Uusitalo V, Kero T, Saraste A, Raijmakers PG, Lammertsma AA, et al. Quantitative Assessment of Myocardial Perfusion in the Detection of Significant Coronary Artery Disease: Cutoff Values and Diagnostic Accuracy of Quantitative [(15)O]H2O PET Imaging. J Am Coll Cardiol. 2014;64(14):1464-75. doi: 10.1016/j.jacc.2014.05.069.

9. Kajander SA, Joutsiniemi E, Saraste M, Pietilä M, Ukkonen H, Saraste A, et al. Clinical Value of Absolute Quantification of Myocardial Perfusion with (15)O-Water in Coronary Artery Disease. Circ Cardiovasc Imaging. 2011;4(6):678-84. doi: 10.1161/CIRCIMAGING.110.960732.

10. Wells RG, Timmins R, Klein R, Lockwood J, Marvin B, deKemp RA, et al. Dynamic SPECT Measurement of Absolute Myocardial Blood Flow in a Porcine Model. J Nucl Med. 2014;55(10):1685-91. doi: 10.2967/jnumed.114.139782.

11. Esteves FP, Raggi P, Folks RD, Keidar Z, Askew JW, Rispler S, et al. Novel Solid-State-Detector Dedicated Cardiac Camera for Fast Myocardial Perfusion Imaging: Multicenter Comparison with Standard Dual Detector Cameras. J Nucl Cardiol. 2009;16(6):927-34. doi: 10.1007/s12350-009-9137-2.

12. Bocher M, Blevis IM, Tsukerman L, Shrem Y, Kovalski G, Volokh L. A Fast Cardiac Gamma Camera with Dynamic SPECT Capabilities: Design, System Validation and Future Potential. Eur J Nucl Med Mol Imaging. 2010;37(10):1887-902. doi: 10.1007/s00259-010-1488-z.

13. Agostini D, Roule V, Nganoa C, Roth N, Baavour R, Parienti JJ, et al. First Validation of Myocardial Flow Reserve Assessed by Dynamic 99mTc-Sestamibi CZT-SPECT Camera: Head to Head Comparison with 15O-Water PET and Fractional Flow Reserve in Patients with Suspected Coronary Artery Disease. The WATERDAY study. Eur J Nucl Med Mol Imaging. 2018;45(7):1079-90. doi: 10.1007/s00259-018-3958-7.

14. Murthy VL, Naya M, Foster CR, Hainer J, Gaber M, Di Carli G, et al. Improved Cardiac Risk Assessment with Noninvasive Measures of Coronary Flow Reserve. Circulation. 2011;124(20):2215-24. doi: 10.1161/CIRCULATIONAHA.111.050427.

15. Acampa W, Zampella E, Assante R, Genova A, De Simini G, Mannarino T, et al. Quantification of Myocardial Perfusion Reserve by CZT-SPECT: A Head to Head Comparison with 82Rubidium PET Imaging. J Nucl Cardiol. 2021;28(6):2827-39. doi: 10.1007/s12350-020-02129-w

16. Zavadovsky KV, Mochula AV, Boshchenko AA, Vrublevsky AV, Baev AE, Krylov AL, et al. Absolute Myocardial Blood Flows Derived by Dynamic CZT Scan vs Invasive Fractional Flow Reserve: Correlation and accuracy. J Nucl Cardiol. 2021;28(1):249-59. doi: 10.1007/s12350-019-01678-z.

17. Souza ACDAH, Gonçalves BKD, Tedeschi AL, Lima RSL. Quantification of Myocardial Flow Reserve Using a Gamma Camera with Solid-State Cadmium-Zinc-Telluride Detectors: Relation to Angiographic Coronary Artery Disease. J Nucl Cardiol. 2021;28(3):876-84. doi: 10.1007/s12350-019-01775-z.

18. Panjer M, Dobrolinska M, Wagenaar NRL, Slart RHJA. Diagnostic Accuracy of Dynamic CZT-SPECT in Coronary Artery Disease. A Systematic Review and Meta-Analysis. J Nucl Cardiol. 2022;29(4):1686-97. doi: 10.1007/s12350-021-02721-8.

19. Cantoni V, Green R, D'Antonio A, Cuocolo A. Dynamic CZT-SPECT in Coronary Artery Disease: Where are we Now? J Nucl Cardiol. 2022;29(4):1698-701. doi: 10.1007/s12350-021-02752-1.

20. Naya M, Murthy VL, Taqueti VR, Foster CR, Klein J, Garber M, et al. Preserved Coronary Flow Reserve Effectively Excludes High-Risk Coronary Artery Disease on Angiography. J Nucl Med. 2014;55(2):248-55. doi: 10.2967/jnumed.113.121442.

21. Souza ACDAH, Gonçalves BKD, Tedeschi A, Lima RSL. Quantification of Coronary Flow Reserve with CZT Gamma Camera in the Evaluation of Multivessel Coronary Disease. Arq Bras Cardiol. 2018;111(4):635-37. doi: 10.5935/abc.20180196.

22. Ong P, Camici PG, Beltrame JF, Crea F, Shimokawa H, Sechtem U, et al. International Standardization of Diagnostic Criteria for Microvascular Angina. Int J Cardiol. 2018;250:16-20. doi: 10.1016/j.ijcard.2017.08.068.

23. Bateman TM, Heller GV, Beanlands R, Calnon DA, Case J, deKemp R, et al. Practical Guide for Interpreting and Reporting Cardiac PET Measurements of Myocardial Blood Flow: An Information Statement from the American Society of Nuclear Cardiology, and the Society of Nuclear Medicine and Molecular Imaging. J Nucl Med. 2021;62(11):1599-615. doi: 10.2967/jnumed.121.261989.

Hypothesis on the Pathogenesis of Sub-Epicardial Scar Associated with Myocarditis

João A. C. Lima,[1] David A. Bluemke,[1] Joshua Hare,[1] Katherine Wu,[1] Leonardo Sara,[2] Carlos E. Rochitte[3]

Johns Hopkins University School of Medicine,[1] Baltimore, MD – United States

Centro de Diagnóstico por Imagem (CDI),[2] Goiânia, GO – Brazil

Instituto do Coração da Faculdade de Medicina da Universidade de São Paulo (InCor - FMUSP),[3] São Paulo, SP – Brazil

The typical pattern of myocardial injury and subsequent fibrosis in patients with viral myocarditis is subepicardial.[1] However, other patterns of injury and scar, as detected by contrast enhanced magnetic resonance imaging (cMRI), commonly occur, including sub-endocardial injury mimicking the ischemic heart disease pattern, and mid-wall circumferential scar seen more often in patients with advanced disease and dilated cardiomyopathies. In patients with myocarditis, who present malignant arrhythmias in the scenario of a preserved left ventricle (LV) function, it is not uncommon to find the typical subepicardial scar pattern in the presence of normal or mildly abnormal LV systolic function.[2] However, the pathogenesis of sub-epicardial scars in patients with myocarditis accompanied or not by significant LV dysfunction remains obscure.

In addition to myocarditis, subepicardial myocardial scar is found in association with various disease processes that are not believed to be secondary to a virally induced myocardial injury. The list includes disease processes with disparate etiologies, such Duchenne and Fabry's disease, Chagas cardiomyopathy, and rheumatic heart disease, among others.[3-5] Therefore, different theories have been proposed to explain this pattern of scar formation in patients with different pathologies. Increase in excessive regional stress and local perfusion alterations have been postulated as contributing mechanisms, but both fall short as main mechanisms.[6] Calculated wall stress is greater at the level of the subendocardium, and reversible perfusion defects secondary to ischemia are commonly subendocardial. After scar formation, perfusion is diminished in proportion to capillary density reduction (fixed defect), but that does not implicate local ischemia as the pathogenetic mechanism underlying subepicardial scar formation.

The COVID-19 pandemic may, however, provide a working hypothesis to explain the pathogenesis of focal subepicardial myocardial fibrosis in patients with myocarditis. COVID,-19 cardiac involvement has been amply documented by biomarker, electrocardiographic, echocardiographic and pathologic studies conducted during the acute infection.[7] Myocardial dysfunction leading to clinically manifested heart failure is uncommon, but it can occur during acute SARS-Cov-2 infection. Moreover, cardiac magnetic resonance imaging (MRI) studies performed on COVID-19 convalescing patients with different degrees of systemic and pulmonary involvement during the acute phase have demonstrated different types, extents, anatomical distributions and degrees of severity of cardiac injury.[7-8] Frequently, in these studies, both pericardial leaflets appear hyperenhanced 10-20 minutes after gadolinium administration, suggesting pericardial inflammation (Figure 1). In some patients, the subepicardial myocardial layer contains areas of localized delayed enhancement, reflecting fibrosis and/or inflammation. These abnormalities can persist in repeated imaging performed later in the convalescing period (Figure 1) and resemble subepicardial injury commonly seen in patients with myocarditis due to other viral etiologies. These suggest that subepicardial damage may be related to pericardial inflammation in patients with myocarditis, either as an inflammatory process originated in the pericardial space or in association with pericardial inflammation as markers of pancardiac inflammation. The combination of pericardial inflammation and subepicardial injury or scar is also commonly seen in patients with rheumatic heart disease.[5]

Viral infection leading to pericardial inflammation is seen not only in SARS-CoV-2 infection, but also in diverse types of viral cardiac infections, including Coxsachie B viruses, known to cause acute myocarditis that may evolve to dilated cardiomyopathy (9). In addition, clinically manifested acute pericarditis is also attributed to viral infection, sometimes leading to chronic constrictive pericarditis. Importantly, significant acute viral myocarditis can be unassociated with ventricular systolic dysfunction and therefore, the true prevalence of subclinical viral cardiac involvement in the community, as in the case of SARS-CoV-2 infection, remains largely unknown. In COVID-19, while severe cardiac involvement in non-hospitalized patients appears to be uncommon, the true prevalence of cardiac and also pulmonary involvement in the community has not been established. Much of the information obtained in non-hospitalized individuals comes from MRI studies performed in athletes before resuming intense physical activity after COVID-19 infection.[10] Findings from these studies suggest that myo-pericardial as well as pleural and parenchymal pulmonary involvement is common, although their long-term clinical significance remains unknown.

This hypothesis brought forth here, like hypotheses in general, leads us to additional questions. Why would subepicardial damage, if extending inwards from the pericardial leafs by contiguity, or as a marker of myocardial inflammation, be so often

Keywords

Cardiac resonance; myocarditis; COVID-19; epicardial injury

Mailing Address: Leonardo Sara •
CDI (Centro de Diagnosticos por Imagem). Tomografia e Ressonancia Cardiovascular. Avenida Portugal, 1155. Postal code: 74150-030. Setor Marista, Goiânia, GO – Brazil
E-mail: leosara@hotmail.com

Manuscript received October 5, 2022; revised October 20, 2022; accepted November 3, 2022.
Editor responsible for the review: Daniela do Carmo Rassi Frota

DOI: https://doi.org/10.36660/abcimg.20230001i

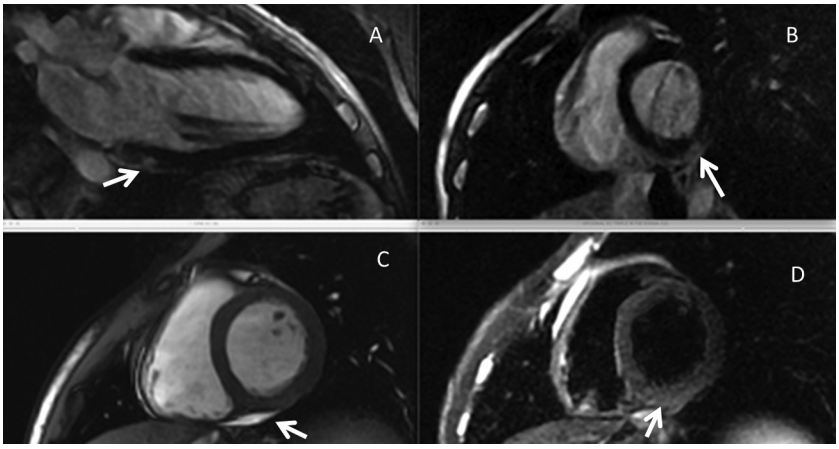

Figure 1 – *Example of patient with a post- COVID myocarditis- late gadolinium enhancement and evidence of active inflammation. Late gadolinium enhancement imaging (A and B) shows patchy areas of subepicardial enhancement in the basal inferior wall (white arrows). Short axis steady state free precession image (C) shows small pericardial effusion, and the T2-weighted image shows a small myocardial edema in the same region.*

limited to the subepicardium? Much attention has been given to the subepicardium for several reasons, including its proposed distinct embryologic origin.[11] Its pivotal role in preserving left ventricular geometry in the face of non-transmural ischemic injury or infarction is well recognized. If by contiguity, the preferential subepicardial localization of myocarditis associated injury can be explained by immediate adjacency to the pericardial space and leaflets. However, this contiguity hypothesis does not explain the other patterns, which not infrequently associate with viral myocardial disease. In addition, it does not take into full consideration the extent of infection and inflammation across the entire myocardium, frequently documented in processes associated with most pathogens, including SARS-CoV-2. Other pathways would have to be invoked to address those questions. In this regard, animal models of viral myocarditis do not reproduce the entire spectrum of disease typically seen in patients, highlighting the importance of clinical phenotypic COVID-19 studies during acute infection and convalescence. In the past, important pathophysiologic insights from endemic myocardial diseases, like Chagas heart disease, provided important insight into the pathogenesis of cardiac disease caused by diverse.[12] Initial observations from patients with COVID-19 or convalescing from SARS-CoV-2 infection suggest that the magnitude of pericardial involvement accompanied or not by subepicardial myocardial injury deserves further study.[7]

In conclusion, our hypothesis places emphasis on the pericardial inflammation as a possible answer to subepicardial injury in myocarditis, based on the findings in post-COVID patients. By analogy, pericardial and subepicardial involvement from myocardial diseases caused by other viruses and infectious pathogens should also be further investigated.

Author Contributions

Conception and design of the research: Lima JAC, Bluemke DA, Hare J, Wu K, Rochitte CE; acquisition of data: Lima JAC, Bluemke DA, Rochitte CE; analysis and interpretation of the data: Lima JAC, Bluemke DA, Hare J, Sara L, Rochitte CE; writing of the manuscript: Lima JAC, Sara L, Rochitte CE; critical revision of the manuscript for intellectual content: Lima JAC, Bluemke DA, Hare J, Wu K, Sara L, Rochitte CE.

Potential Conflict of Interest

No potential conflict of interest relevant to this article was reported.

Sources of Funding

There were no external funding sources for this study.

Study Association

This study is not associated with any thesis or dissertation work.

Ethics Approval and Consent to Participate

This article does not contain any studies with human participants or animals performed by any of the authors.

References

1. Ferreira VM, Schulz-Menger J, Holmvang G, Kramer CM, Carbone I, Sechtem U, et al. Cardiovascular Magnetic Resonance in Nonischemic Myocardial Inflammation: Expert Recommendations. J Am Coll Cardiol. 2018;72(24):3158-76. doi: 10.1016/j.jacc.2018.09.072.
2. Aquaro GD, Perfetti M, Camastra G, Monti L, Dellegrottaglie S, Moro C, et al. Cardiac MR with Late Gadolinium Enhancement in Acute Myocarditis with Preserved Systolic Function: ITAMY Study. J Am Coll Cardiol. 2017;70(16):1977-87. doi: 10.1016/j.jacc.2017.08.044.

3. Silva MC, Meira ZMA, Giannetti JG, Zatz M, Rochitte CE. Myocardial late enhancement in Duchenne and Becker individuals in the clinical milieu - Reply. J Am Coll Cardiol. 2007;50(20):2020-20. doi: 10.1016/j.jacc.2007.08.013

4. Senra T, Ianni BM, Costa ACP, Mady C, Martinelli-Filho M, Kalil-Filho R, et al. Long-Term Prognostic Value of Myocardial Fibrosis in Patients with Chagas Cardiomyopathy. J Am Coll Cardiol. 2018;72(21):2577-2587. doi: 10.1016/j.jacc.2018.08.2195.

5. Mavrogeni S, Schwitter J, van Rossum A, Nijveldt R, Aletras A, Kolovou G, et al. Cardiac Magnetic Resonance Imaging in Myocardial Inflammation in Autoimmune Rheumatic Diseases: An Appraisal of the Diagnostic Strengths and Limitations of the Lake Louise Criteria. Int J Cardiol. 2018;252:216-9. doi: 10.1016/j.ijcard.2017.11.032.

6. Wu KC, Weiss RG, Thiemann DR, Kitagawa K, Schmidt A, Dalal D, et al. Late Gadolinium Enhancement by Cardiovascular Magnetic Resonance Heralds An Adverse Prognosis in Nonischemic Cardiomyopathy. J Am Coll Cardiol. 2008;51(25):2414-21. doi: 10.1016/j.jacc.2008.03.018.

7. Gluckman TJ, Bhave NM, Allen LA, Chung EH, Spatz ES, Ammirati E, et al. 2022 ACC Expert Consensus Decision Pathway on Cardiovascular Sequelae of COVID-19 in Adults: Myocarditis and Other Myocardial Involvement, Post-Acute Sequelae of SARS-CoV-2 Infection, and Return to Play: A Report of the American College of Cardiology Solution Set Oversight Committee. J Am Coll Cardiol. 2022;79(17):1717-56. doi: 10.1016/j.jacc.2022.02.003.

8. Puntmann VO, Carerj ML, Wieters I, Fahim M, Arendt C, Hoffmann J, et al. Outcomes of Cardiovascular Magnetic Resonance Imaging in Patients Recently Recovered from Coronavirus Disease 2019 (COVID-19). JAMA Cardiol. 2020;5(11):1265-73. doi: 10.1001/jamacardio.2020.3557.

9. Pollack A, Kontorovich AR, Fuster V, Dec GW. Viral Myocarditis-Diagnosis, Treatment Options, and Current Controversies. Nat Rev Cardiol. 2015;12(11):670-80. doi: 10.1038/nrcardio.2015.108.

10. Petersen SE, Friedrich MG, Leiner T, Elias MD, Ferreira VM, Fenski M, et al. Cardiovascular Magnetic Resonance for Patients with COVID-19. JACC Cardiovasc Imaging. 2022;15(4):685-699. doi: 10.1016/j.jcmg.2021.08.021.

11. Tyser RCV, Ibarra-Soria X, McDole K, Arcot Jayaram S, Godwin J, van den Brand TAH, et al. Characterization of a Common Progenitor Pool of the Epicardium and Myocardium. Science. 2021;371(6533):eabb2986. doi: 10.1126/science.abb2986.

12. Rosenbaum MB. The Hemiblocks: Diagnostic Criteria and Clinical Significance. Mod Concepts Cardiovasc Dis. 1970;39(12):141-6.

Mitral Valve Area Quantification Using Digital Image Processing: Is That Feasible?

Edgar Daminello,[1] Paulo Pinto Alves Campos Vieira,[2] Cláudio Henrique Fischer,[1,3] Marcelo Luiz Campos Vieira[1,4]

Hospital Israelita Albert Einstein,[1] São Paulo, SP – Brazil

Universidade Santo Amaro (UNISA),[2] São Paulo, SP – Brazil

Universidade Federal de São Paulo (UNIFESP),[3] São Paulo, SP – Brazil

Instituto do Coração (InCor), Faculdade de Medicina da Universidade de São Paulo (FMUSP),[4] São Paulo, SP – Brazil

Regarding article "Automatic Measurement of Mitral Valve Based on Echocardiogram Using Digital Image Processing"

Echocardiography, since its initial descriptions in the 1950s, has evolved every decade with the incorporation of numerous new techniques, enabling structural cardiac analysis from multiple planes of spatial observation in real time. This occurred with the advent of nanotechnology, digital technology, application of modifiable algorithms based on the concept of machine learning and deep learning through the development of artificial intelligence (AI).[1-6] The use of AI is an ever-increasing reality in medicine as a whole, mainly in operator-dependent imaging areas, such as ultrasonography imaging.

In the concept of analyzing the confluence of a very large number of pieces of information (e.g. radiomics, metabolomics, proteomics) for the formation of data clusters with the aim of integrated patient observation, the formation of precision medicine, AI is used in a rational and organized way. The use of AI allows faster, more balanced and homogeneous observation of inputs, in the sense of minimizing inter and intraobserver errors.[1-6] In the specific echocardiographic evaluation, the use of AI presents a very wide range of applications, having been used for the acquisition of echocardiographic information for the quantification of left ventricular volumes and mass, analysis of biventricular systolic function, segmentation and qualification of the cusps, annulus and mitral valve apparatus, analysis of hypertrophic phenocopy (athletes, patients with hypertrophic cardiomyopathy), to predict the outcome of percutaneous hemodynamic procedures (e.g.: mitraclip).[1] We are currently working on a project in association with the University of Chicago for AI analysis of patients affected by transthyretin cardiac amyloidosis.

Regrettably, rheumatic disease remains, in the 2020s, a pathology of great epidemiological expression, especially in underdeveloped and developing countries.[7] Therefore, it seems highly appropriate and of special interest the echocardiographic analysis using AI and its various algorithms for interpreting patients suffering from rheumatic disease. Rheumatic disease is the most prevalent etiology of mitral valve stenosis, with mitral stenosis being the most expressive chronic lesion of rheumatic cardiac involvement.[7,8] Echocardiography is an essential diagnostic tool in the recognition and determination of the extent of cardiac involvement in rheumatic disease, especially in mitral valve dysfunction, by demonstrating typical findings such as reduced mobility due to leaflet thickening, commissural fusion, involvement of the subvalvular apparatus (shortening, thickening and fusion of the chordae tendineae) and valve and annulus calcification.[7-9] The progressive reduction of the valve area is accompanied by a gradual increase in left atrial pressure, pulmonary venous pressure and the onset of more common symptoms such as dyspnea.[7-9] The grading of mitral stenosis requires careful valve morphofunctional evaluation, as well as an accurate analysis of associated pathologies due to the implications in the therapeutic decision and the choice from different types of intervention (percutaneous or surgical approach in its multiple possibilities).[7-9]

Echocardiography is the first-line imaging technique for analyzing the mitral valve, offering numerous advantages over other analysis techniques (real-time analysis, devoid of radiation, based on three-dimensional projections, low cost, widely available); however, it has limitations, such as the great dependence on the quality of the acquired image, dependence on the cardiologist's experience during the acquisition and interpretation of images, especially in the three-dimensional study, which requires additional training and experience, for better multiplanar reconstruction of cardiac structures. Real-time three-dimensional echocardiography shows the leaflets in multiple planes, providing a more accurate identification of the most anatomical opening of the mitral valve.[7-9] Evaluation of valve segmentation, important in minimally invasive structural cardiac intervention, showed great progress in recent years, due to the applicability of AI to cardiovascular imaging tests.[4,9] This AI analysis of the mitral valve apparatus has evolved rapidly over the last few years, from the analysis that required many steps for its final elaboration to the semiautomatic, rapid and very expressive analysis of the mitral valve anatomy.[4,9] We are currently working on a project for the rapid semiquantitative analysis of the surgical results of patients with mitral valve disease due to fibroelastic etiology and valve prolapse, with pre and post-operative analysis after double teflon repair. This analysis shows the observation of more than 30 elements that constitute the mitral valve apparatus.

Keywords

Artificial intelligence; automated diagnosis; algorithm; echocardiography; mitral valve.

Mailing Address: Marcelo Luiz Campos Vieira •
Rua Nova York, 970, ap. 11. Postal code: 04560-002. Brooklin, São Paulo, SP – Brazil.
E-mail: mluiz766@terra.com.br
Manuscript received January 9, 2023; revised January 27, 2023; accepted January 30, 2023
Editor responsible for the review: Daniela do Carmo Rassi Frota

DOI: https://doi.org/10.36660/abcimg.2023376i

AI technology has the potential to optimize and revolutionize the practice of echocardiography, creating opportunities for standardization, improving accuracy and efficiency in cardiovascular imaging laboratories.[1-6] In recognition of this growing influence in echocardiography laboratories, Professor Vera Rigolin, from the Northwestern Memorial Hospital, Chicago, USA, introduced the concept of the four pillars of AI, namely: education, image acquisition, analysis and integration with clinical data.[5] These actions tend to minimize intra- and interobserver variability, inherent in the echocardiographic method, through the creation of protocols for the acquisition and analysis of images to quantify left ventricular ejection fraction, myocardial strain and grading valve lesion severity, among other application possibilities.[5]

AI-based digital image processing (DIP), a method proposed by Barros Filho et al.,[10] published in this issue of Arquivos Brasileiros de Cardiologia: Imagem Cardiovascular, has the purpose of improving the visual information of the mitral valve for analysis, automating the determination of the valve area by planimetry and transmitting and storing this information. Usually, image processing after acquisition tends to be hard work, requiring specific training and knowledge. The proposed DIP may eventually have a great clinical impact by minimizing this difficulty by using an easy, fast and intuitive language system with adequate reproducibility, with the potential to reduce human distraction and fatigue, inherent in complex and prolonged work, limiting intra- and inter-observer variability and assisting the interpretation of multiple and complex data.

Therefore, we recommend reading the article "Automatic Mitral Valve Measurement Based on Echocardiography Using Digital Image Processing,"[10] by Barros Filho et al., congratulating the group of researchers for the excellence of the investigation.

References

1. Daminello E, Vieira PPAC, Fischer CH, Vieira MLC. Aplicação da Inteligência Artificial em Imagem Cardiovascular: em Ecocardiografia. Rev Soc Cardiol Estado de São Paulo. 2021;31(4):388-93. doi: 10.29381/0103-8559/2022320139-44.
2. Narang A, Bae R, Hong H, Thomas Y, Surette S, Cadieu C, et al. Utility of a Deep-Learning Algorithm to Guide Novices to Acquire Echocardiograms for Limited Diagnostic Use. JAMA Cardiol. 2021;6(6):624-32. doi: 10.1001/jamacardio.2021.0185.
3. Chao CJ, Kato N, Scott CG, Lopez-Jimenez F, Lin G, Kane GC, et al. Unsupervised Machine Learning for Assessment of Left Ventricular Diastolic Function and Risk Stratification. J Am Soc Echocardiogr. 2022;35(12):1214-1225.e8. doi: 10.1016/j.echo.2022.06.013.
4. Pardi MM, Pomerantzeff PMA, Sampaio RO, Abduch MC, Brandão CMA, Mathias W Jr, et al. Relation of Mitral Valve Morphology to Surgical Repair Results in Patients with Mitral Valve Prolapse: A Three-Dimensional Transesophageal Echocardiography Study. Echocardiography. 2018;35(9):1342-50. doi: 10.1111/echo.14048.
5. Thachil R, Hanson D. Artificial Intelligence in Echocardiography: A Disruptive Technology for Democratizing and Standardizing Health. J Am Soc Echocardiogr. 2022;35(8):A14-A16. doi: 10.1016/j.echo.2022.06.001.
6. Seetharam K, Raina S, Sengupta PP. The Role of Artificial Intelligence in Echocardiography. Curr Cardiol Rep. 2020;22(9):99. doi: 10.1007/s11886-020-01329-7.
7. Pandian NG, Kim JK, Arias-Godinez JA, Marx GR, Michelena HI, Mohan JC, et al. Recommendations for the Use of Echocardiography in the Evaluation of Rheumatic Heart Disease: A Report from the American Society of Echocardiography. J Am Soc Echocardiogr. 2023;36(1):3-28. doi: 10.1016/j.echo.2022.10.009.
8. Silbiger JJ. Advances in Rheumatic Mitral Stenosis: Echocardiographic, Pathophysiologic, and Hemodynamic Considerations. J Am Soc Echocardiogr. 2021;34(7):709-722.e1. doi: 10.1016/j.echo.2021.02.015.
9. Vieira MLC, Branco CEB, Gazola ASL, Vieira PPAC, Benvenuti LA, Demarchi LMMF, et al. 3D Echocardiography for Rheumatic Heart Disease Analysis: Ready for Prime Time. Front Cardiovasc Med. 2021;8:676938. doi: 10.3389/fcvm.2021.676938.
10. Barros GF Filho, Solha I, Medeiros EF, Felix AS, Almeida ALC, Lima JC Jr, et al. Medição Automática de Valva Mitral a Partir de Ecocardiograma Utilizando Processamento Digital de Imagens. Arq Bras Cardiol: Imagem Cardiovasc. 2023;36(1):e371. doi: 10.36660/abcimg.2023371.

A Clinician's View of Tricuspid Regurgitation: What do I Need to Know? When to Intervene?

Tiago Bignoto[1]
Universidade de São Paulo,[1] *São Paulo, SP – Brazil*

Tricuspid valve dysfunction was considered a benign clinical situation for a long time, but with the advancement of diagnostic imaging methods and better clinical stratification of patients with structural heart disease, adequate classification of tricuspid regurgitation has become fundamental to decision making in the context of a Heart Team.[1]

The first assessment to be taken into account is the etiology of the dysfunction. With a low prevalence, the primary etiology, mainly due to rheumatic and congenital causes, has a well-established intervention flowchart, primarily based on the presence of symptoms or hemodynamic repercussions on the right side of the heart.[2]

The secondary etiology is the most prevalent, and it brings many challenges in its approach, as there are a number of conflicting publications regarding proposal of intervention.[3,4]

During the natural history of heart failure with reduced left ventricular ejection fraction, tricuspid insufficiency of at least moderate intensity is common, and it has an unfavorable impact on morbidity and mortality. In this context, even mild regurgitation that is considered progressive, with evolution between serial echocardiograms of 0.2 cm^2 in the effective regurgitation orifice (ERO) and 15 mL/beat in the regurgitant volume, has an unfavorable prognosis.[5]

Some clinical aspects must be taken into account when evaluating tricuspid insufficiency of functional etiology in order to select patients who may have worse prognosis, and, in this context, the criterion with the greatest impact is permanent atrial fibrillation.[5] This clinical condition leads to progressive dilation of the tricuspid annulus and is time-mediated; that is, the longer the patient spends in permanent fibrillation, the greater the dilation and, consequently, the greater the degree of reflux.[6]

Evaluation with multimodal diagnostic imaging methods is currently the recommended systematized approach, seeking anatomical and functional substrates of the tricuspid valve complex and the right ventricle.[7]

Keywords

Tricuspid Valve; Tricuspid Valve Insufficiency; Heart Valve Diseases

Mailing Address: Tiago Bignoto •
Instituto do Coração (InCor) Faculdade de Medicina da USP. Seção de Cardiopatia Estrutural. Avenida Dr. Enéas Carvalho de Aguiar, 44. Postal Code: 05.403-900. Cerqueira César, São Paulo, SP – Brazil
E-mail: tiagobignoto@yahoo.com.br
Manuscript received January 9, 2023; revised January 16, 2023; accepted January 26, 2023.
Editor responsible for the review: Daniela do Carmo Rassi Frota

DOI: https://doi.org/10.36660/abcimg.20230005i

Transthoracic echocardiography is the first test to be indicated to assess the presence, etiology, and severity classification of tricuspid insufficiency. This valve dysfunction is very sensitive to pre- and post-load, and attention should be paid to the volume status and clinical stability of heart failure during image acquisition.[7]

Understanding the limitations of the method, qualitative data, such as anatomical alterations and coaptation failure, and quantitative data, such as ERO and regurgitant volume calculated by proximal isovelocity surface area (PISA), should be analyzed together by an echocardiographer who has experience with structural heart disease. Services that have complementary 3-dimensional echocardiography should use the method to improve the accuracy of the assessment, and complementary transesophageal echocardiography often adds little information, except in limited thoracic acoustic windows.

Compared to other diagnostic imaging methods, cardiac magnetic resonance has excellent spatial resolution, and it is especially valuable for assessing right ventricular function. Due to the merely moderate correlation of quantitative assessment with echocardiography and the few data available in the literature on clinical impact, the use of the method is still limited.[8] Cardiac tomography is important in planning a possible structural intervention with assessment of the annular shape, perimeter, diameter, location, and trajectory of the right coronary artery.[7]

Efforts for adequate classification of tricuspid insufficiency are currently directed toward the following 2 main groups: those where it is possible to indicate the exact moment when the physiological limits were exhausted and the overload begins to negatively impact ventricular function, and those considered as having important tricuspid insufficiency, but well above the cutoff values. For the latter group, 2 new classifications have emerged, torrential and massive, which have negative prognostic and evolutionary impacts.[7,9]

After obtaining multimodality images and extensive discussion in a Heart Team, the criteria for indicating intervention in tricuspid insufficiency are aligned with the main international guidelines. As previously mentioned, primary tricuspid insufficiency in the presence of symptoms or hemodynamic repercussions on the right ventricle is a clear indication for intervention, valve repair being the first option. In the event that this is technically impossible, the implantation of a biological prosthesis is a viable alternative, even with the high prevalence of thromboembolic phenomena, which discourages the implantation of mechanical devices in this topography.[2,4]

Contents

Regarding functional etiology, if a patient has significant tricuspid regurgitation and a clear indication for intervention due to another reason, such as left-sided valve disease or even myocardial revascularization, the tricuspid lesion should be corrected during the same surgical time.[2,4,10]

The presence of a tricuspid annulus greater than or equal to 40 mm assessed by echocardiography through the apical 4-chamber window also indicates a concomitant approach at the same surgical time.[2,4,10]

The most challenging situation in the presence of functional tricuspid insufficiency is the isolated lesion, with no other indication for intervention. In this context, the data in the literature are controversial as to whether there is clear indication for the approach. Conventional surgery with repair and implantation of a semi-rigid ring does not apparently benefit survival when compared to optimized clinical treatment, but, in very symptomatic cases, valve correction improves functional class.[3,4]

The isolated approach may have a slightly clearer benefit in patients with very symptomatic functional tricuspid insufficiency in the presence of permanent atrial fibrillation or even in the presence of pacemaker electrodes altering the tricuspid valve dynamics. This fact has also led to a new etiological classification, creating a separate group within the secondary etiology for cases caused by the presence of this device.[4,7]

In an era of catheter-based technologies, the selection of a device based on the analysis of anatomical characteristics is essential to obtain the best results. Assessment of the regurgitation mechanism should include the annular, leaflet, and subannular components.[7]

In low-risk patients, surgery remains the gold-standard treatment for functional tricuspid insufficiency, but, in cases of high surgical risk, especially during the past decade when a large number of transcatheter devices were developed based on established surgical procedures, the clinical decision may be different.[7]

The greatest experience is related to valve repair with edge-to-edge clipping, in which the most robust data show a reduction in the degree of regurgitation, good echocardiographic evolution, and improved functional class, with little evidence of improvement in mortality, including cases considered to have torrential tricuspid insufficiency.[2,7]

Some annuloplasty devices can be used in patients whose leaflet tethering is less pronounced. The combination of procedures and devices may also be an interesting strategy, depending on the pre-procedure anatomical and functional evaluation.[7]

With the advancement of diagnostic methods and new devices for correcting tricuspid dysfunction, we will, in the coming years, be able to accompany a series of interesting data on clinical impact in the management of these patients, including changes in the level of recommendation for intervention depending on the clinical, anatomical, and functional characteristics, which will always be at the center of the discussion about tricuspid insufficiency.

Author Contributions

Conception and design of the research, writing of the manuscript and critical revision of the manuscript for intellectual content: Bignoto T.

Potential Conflict of Interest

No potential conflict of interest relevant to this article was reported.

Sources of Funding

There were no external funding sources for this study.

Study Association

This study is not associated with any thesis or dissertation work.

Ethics Approval and Consent to Participate

This article does not contain any studies with human participants or animals performed by any of the authors.

References

1. Prihadi EA, Delgado V, Leon MB, Enriquez-Sarano M, Topilsky Y, Bax JJ. Morphologic Types of Tricuspid Regurgitation: Characteristics and Prognostic Implications. JACC Cardiovasc Imaging. 2019;12(3):491-99. doi: 10.1016/j.jcmg.2018.09.027.
2. Tarasoutchi F, Montera MW, Ramos AIO, Sampaio RO, Rosa VEE, Accorsi TAD, et al. Update of the Brazilian Guidelines for Valvular Heart Disease - 2020. Arq Bras Cardiol. 2020;115(4):720-75. doi: 10.36660/abc.20201047.
3. Axtell AL, Bhambhani V, Moonsamy P, Healy EW, Picard MH, Sundt TM 3rd, et al. Surgery Does Not Improve Survival in Patients with Isolated Severe Tricuspid Regurgitation. J Am Coll Cardiol. 2019;74(6):715-25. doi: 10.1016/j.jacc.2019.04.028.
4. Otto CM, Nishimura RA, Bonow RO, Carabello BA, Erwin JP 3rd, Gentile F, et al. 2020 ACC/AHA Guideline for the Management of Patients with Valvular Heart Disease: Executive Summary: A Report of the American College of Cardiology/American Heart Association Joint Committee on Clinical Practice Guidelines. Circulation. 2021;143(5):e35-e71. doi: 10.1161/CIR.0000000000000932.
5. Spinka G, Bartko PE, Heitzinger G, Prausmüller S, Pavo N, Frey MK, et al. Natural Course of Nonsevere Secondary Tricuspid Regurgitation. J Am Soc Echocardiogr. 2021;34(1):13-19. doi: 10.1016/j.echo.2020.08.018.
6. Silbiger JJ. Atrial Functional Tricuspid Regurgitation: An Underappreciated Cause of Secondary Tricuspid Regurgitation. Echocardiography. 2019;36(5):954-7. doi: 10.1111/echo.14327.
7. Hahn RT, Badano LP, Bartko PE, Muraru D, Maisano F, Zamorano JL, et al. Tricuspid Regurgitation: Recent Advances in Understanding

Pathophysiology, Severity Grading and Outcome. Eur Heart J Cardiovasc Imaging. 2022;23(7):913-29. doi: 10.1093/ehjci/jeac009.

8. Zhan Y, Debs D, Khan MA, Nguyen DT, Graviss EA, Khalaf S, et al. Natural History of Functional Tricuspid Regurgitation Quantified by Cardiovascular Magnetic Resonance. J Am Coll Cardiol. 2020;76(11):1291-301. doi: 10.1016/j.jacc.2020.07.036.

9. Fortuni F, Dietz MF, Prihadi EA, van der Bijl P, De Ferrari GM, Knuuti J, et al. Prognostic Implications of a Novel Algorithm to Grade Secondary Tricuspid Regurgitation. JACC Cardiovasc Imaging. 2021;14(6):1085-95. doi: 10.1016/j.jcmg.2020.12.011.

10. Dreyfus GD, Martin RP, Chan KM, Dulguerov F, Alexandrescu C. Functional Tricuspid Regurgitation: A Need to Revise our Understanding. J Am Coll Cardiol. 2015;65(21):2331-6. doi: 10.1016/j.jacc.2015.04.011.

Contemporary Non-Invasive Imaging in Chronic Coronary Syndrome: What Stress Cardiovascular Magnetic Resonance has to Offer

Isabella Leo,[1,2] *Laura Torres Araujo,*[1] *Chiara Bucciarelli-Ducci*[1,3]

Royal Brompton and Harefield Hospitals, Guys' and St Thomas' NHS Trust,[1] *London – United Kingdom*
Department of Medical and Surgical Sciences, Magna Graecia University,[2] *Catanzaro – Italy*
School of Biomedical Engineering and Imaging Sciences, Faculty of Life Sciences and Medicine, King's College University,[3] *London – United Kingdom*

Non-invasive cardiac imaging has an established diagnostic and prognostic role in patients with suspected or known ischemic heart disease (IHD) and the imaging technology has significantly evolved over the years. Cardiovascular magnetic resonance (CMR) has emerged as a robust diagnostic and prognostic imaging modality and it currently represents a valid alternative to other existing and well-validated techniques, but also as a possible first-line strategy.

Major clinical practice guidelines have been increasingly incorporating stress CMR as a clinical test indicated in patients with chest pain, receiving a Class I recommendation first in the 2014 European Society of Cardiology (ESC) guidelines for revascularisation, followed by the 2017 ESC guidelines in the diagnosis and management of ST-elevation myocardial infarction which has been recommending CMR as an alternative test for left ventricular (LV) function when echocardiography is suboptimal, but also for the evaluation of myocardial viability and ischemia.[1] The recently published 2021 American Heart Association (AHA)/ American College of Cardiology (ACC) Guidelines also indicate stress CMR with class I recommendation in patients with acute and chronic chest pain and intermediate risk of coronary artery disease (CAD) (Table 1).[2]

Whilst CMR is the gold standard test for the calculation of left and right ventricular volumes, it is unique compared to other imaging modalities due to its ability to non-invasively characterize the myocardial tissue. Using T2-weighted sequences, CMR can visualize myocardial oedema, whilst the use of T1-weighted sequences with gadolinium-based contrast agents allow the delineation of presence and extent of myocardial scarring or fibrosis, thus determining myocardial viability. Finally, its high spatial resolution in stress perfusion (~ 2 mm, compared to ~ 10 mm of single-photon emission computed tomography [SPECT] and ~ 4 mm of positron emission tomography — PET), provides high diagnostic accuracy for the detection of myocardial ischemia (inducible perfusion defects).

Keywords

Cardiovascular Imaging; Cardiovascular Magnetic Resonance; Stress Imaging; Chronic Coronary Syndrome

Correspondência: Chiara Bucciarelli-Ducci •
Royal Brompton and Harefield Hospitals, Guys' and St Thomas' NHS Foundation Trust
Email: c.bucciarelli-ducci@rbht.nhs.uk
Artigo recebido em 2/1/2023; revisado em 6/1/2023; aceito em 9/1/2023.
Editor responsável pela revisão: Daniela do Carmo Rassi Frota

DOI: https://doi.org/10.36660/abcimg.20230004i

A multi-parametric CMR protocol that includes myocardial edema, viability and ischemia aims at identifying the cause of chest pain both in the acute and in the chronic setting. Clinical scenarios include identifying the ischemic territory, if any, in patients with known or suspected CAD, identify the culprit vessel (edematous territory) in patients with acute coronary syndrome and multivessel disease with unclear culprit lesion, and assess the extent of myocardial viability and hibernation to guide revascularization. In the acute setting, the presence of edema can guide clinical management such as the identification of recent and old infarction or determine the differential diagnosis in patients with suspected myocardial infarction and unobstructed coronary arteries (MINOCA), whether acute myocarditis, takotsubo cardiomyopathy, or small myocardial infarction. All these differentials can be achieved based on the different patterns of myocardial oedema and fibrosis which differ in each condition.

Finally, initial sequences covering the whole mediastinum and the upper portion of the abdomen are helpful in detecting some of the most common extracardiac causes of atypical chest pain, such as pleural effusion and hiatus hernia.

The CMR stress perfusion protocol is straightforward, with some similarities with the SPECT protocol. The stressor used is mainly a vasodilator, either adenosine at an infusion rate of 140 mcg/kg/min for 2 to 4 minutes (titrated to 210 mg/kg/min to maximize response) or regadenoson as a single injection of 0.4 mg.[3] At maximal vasodilation, contrast agent is injected and first pass perfusion images are acquired (typically 3 short-axis images: base, mid, apical), which are later repeated at rest for comparison. Contraindications are limited, and they include advanced second-degree atrioventricular block, systolic blood pressure < 90 mmHg or > 220/120 mmHg, severe sinus bradycardia (< 40 bpm), active bronchospasm or known hypersensitivity. Dobutamine is used in selected cases such as patients with severe asthmas or those with coronary anomalies and myocardial bridges, following a protocol similar to echocardiography with incremental doses up to a maximum of 40 μg/kg/min. Inducible myocardial perfusion defect, a surrogate for inducible myocardial ischemia, can be assessed qualitatively (visually) as hypointense "darker" (hypoperfused) areas (Figure 1). A semi-quantitative evaluation can complement the visual assessment. Recent technical developments include a respiratory motion corrected method with automated in-line perfusion mapping which provides a quantitative assessment of myocardial blood flow (MBF) and myocardial perfusion reserve (MPR) at a segmental or global level. This novel method has been validated against invasive angiography and demonstrated an excellent diagnostic performance and reproducibility.[4]

Table 1 – Role of cardiac magnetic resonance according to current European and United States Guidelines

	Clinical scenarios	Warranty period	High-risk markers	Added benefits
ESC guidelines	Chronic IHD including: patients with an inconclusive echocardiographic test. In high-risk asymptomatic adults. To prove myocardial ischemia before revascularization.	1 year	2 or more of 16 segments with stress perfusion defects or ≥3 dobutamine-induced dysfunctional segments.	Useful to establish other etiologies (myocarditis etc.)
ACC-AHA chest pain guidelines	Acute and chronic chest pain: Intermediate-risk patients with acute chest pain and no known CAD who are eligible for cardiac testing. Suspected scar. Suspected microvascular disfunction. Acute chest pain plus intermediate risk with known CAD. Patients with an inconclusive echocardiographic test (2a). Chronic: In intermediate to high risk patients with stable chest pain and no known CAD, it is effective for diagnosis of myocardial ischemia and for estimating risk of major adverse cardiac events (1b). Patients with obstructive CAD who have stable chest pain despite optimal medical treatment (1b). Patients with known extensive nonobstructive CAD with stable chest pain symptoms (2a). Patients with persistent stable chest pain and nonobstructive CAD, with the addition of MBFR measurement (2a).	1 year		Useful to establish other etiologies (myocarditis etc). Higher diagnostic accuracy for CMR versus other non-invasive methods. CMR followed by selective ICA had projected reduced costs by □25% when compared with direct referral to ICA.

AHA/ACC: American Heart Association/American College of Cardiology; CAD: coronary artery disease; CMR: cardiac magnetic resonance; ESC: European Society of Cardiology; ICA: invasive coronary angiography; MBFR: myocardial blood flow reserve; IHD: ischemic heart disease.

There is a wealth of literature and randomized clinical trials underpinning the clinical use of CMR in patients with IHD and its inclusion in all major clinical practice guidelines.

The Magnetic Resonance Imaging for Myocardial Perfusion Assessment in Coronary artery disease-2 (MR-IMPACT-2) study demonstrated higher sensitivity of stress CMR than SPECT in detecting CAD.[5] The Clinical Evaluation of Magnetic Resonance Imaging in Coronary Heart Disease (CE-MARC) trial was a head-to-head comparison of stress CMR and SPECT in patient with known or suspected CAD, using invasive angiography as gold standard. It demonstrated that stress CMR has increased diagnostic accuracy compared to SPECT, both in single and multivessel disease, as well as in males and females.[6] Further, the CE-MARC 2 trial demonstrated that the use of a functional test (SPECT or CMR) significantly reduced the probability of unnecessary coronary angiography in patients with known or suspected CAD (28% versus 7.5% and 7.1% when using stress CMR or SPECT, respectively as gatekeeper for invasive angiography).[7] Most recently, the MR Perfusion Imaging to Guide Management of Patients With Stable Coronary Artery Disease (MR-INFORM) trial randomized 918 patients with known or suspected CAD to either stress CMR evaluation or invasive fractional flow reserve obtaining similar clinical outcomes in the two groups, but the coronary revascularization rate was reduced when using CMR.[8] In terms of prognostication, data coming from the Stress CMR Perfusion Imaging in the United States (SPINS) study also proved that patients with a negative stress CMR or negative late gadolinium enhancement had very low annual rates of cardiovascular death or nonfatal myocardial infarction (< 1%) and coronary revascularization (1% to 3%) during the 5-year follow-up.[9] The non-invasive CMR-based approach has also proven to be cost-effective for healthcare systems, as demonstrated by consistent savings.[10]

Importantly, approximately half of patients with angina do not have evidence of obstructive CAD, and, if imaged

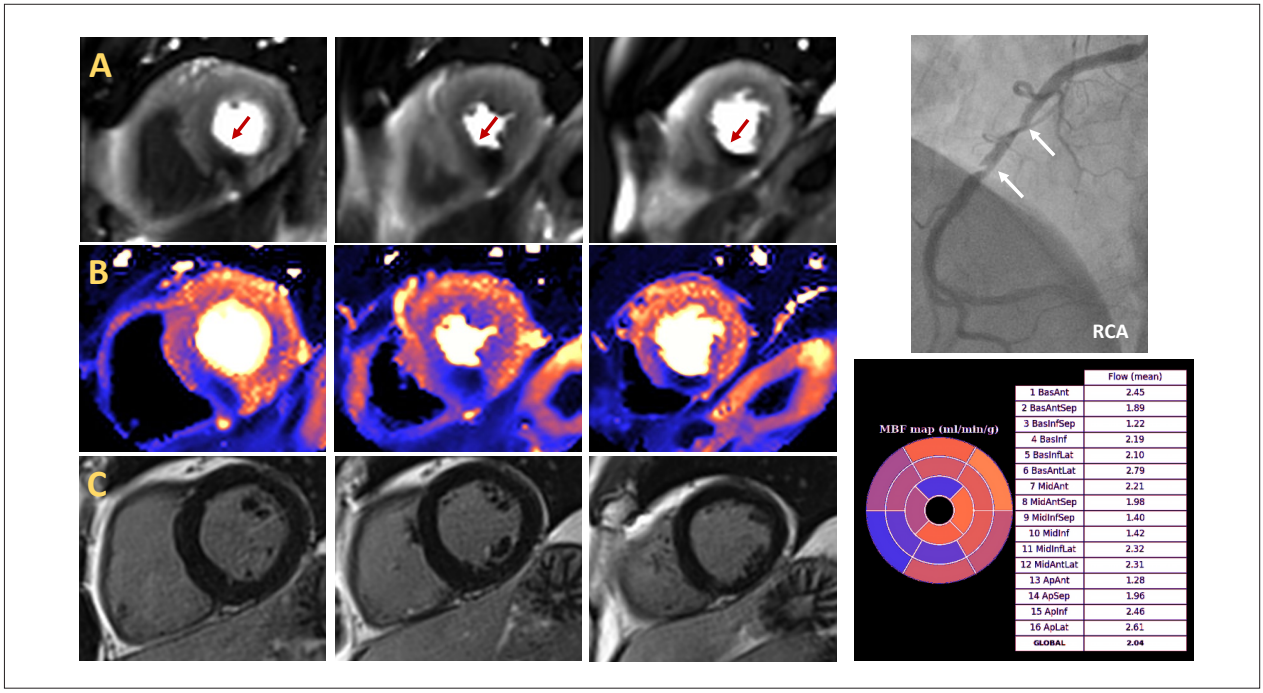

Figure 1 – *Cardiac magnetic resonance in a patient with angina. Stress first-pass perfusion images showed significant inducible myocardial perfusion defect during adenosine infusion in the RCA territory (A, red arrows). The perfusion defect was confirmed by automated in-line perfusion mapping (B, blue areas) and quantified as segmental stress myocardial blood flow (MBF map, bottom right). Late gadolinium enhancement images showed no myocardial infarction or scarring, with all segments fully viable (panel C). The patient was therefore referred for coronary angiography that demonstrated significant stenosis in the RCA. RCA: right coronary artery.*

adequately, there is demonstration of MVD.[11] This is more prevalent in women than in men and in patients with hypertension and diabetes. Quantitative stress CMR is increasingly used in patients with ischemia and unobstructed coronary arteries (INOCA) with excellent diagnostic accuracy. Recent data published by Kotecha and colleagues confirmed the usefulness of these non-invasive CMR parameters of MBF and MPR, with an additional potential role in discriminating between three-vessel disease and MVD, two conditions that are often hard to distinguish without an anatomical test.[4] A global stress MBF < 1.82 ml/g/min has in fact been proposed as a cut off to discriminate obstructive 3-vessel disease from MVD (area under the curve: 0.94; $p < 0.001$).[4]

Limitations of CMR include the relatively limited availability (although every MRI scanner has a cardiac package, often unused), high cost, limited access to existing MRI facilities, and a lack of trained CMR imaging specialists. In addition, there are some restrictions when performing CMR in patients with non-conditional devices, and the overall quality of the images acquired could be severely and unpredictably reduced in presence of metallic implants. Gadolinium-based contrast agents are relatively safe. However, caution should be used in presence of severe renal failure due to potential risk of nephrogenic systemic fibrosis and during pregnancy where a careful risk-benefit assessment is mandatory. Nevertheless, the role of CMR has evolved from mainly a research tool to a multi-purpose clinical tool with unquestionable advantages compared to other modalities. This recognized role of CMR in the recently published ESC and AHA/ACC chest pain guidelines is a testament that this technique is part of modern cardiology, and it is here to stay.

Author Contributions

Writing of the manuscript: Leo I, Araújo LT; critical revision of the manuscript for intellectual content: Bucciarelli-Ducci C.

Potential Conflict of Interest

No potential conflict of interest relevant to this article was reported.

Sources of Funding

There were no external funding sources for this study.

Study Association

This study is not associated with any thesis or dissertation work.

Ethics Approval and Consent to Participate

This article does not contain any studies with human participants or animals performed by any of the authors.

References

1. Ibanez B, James S, Agewall S, Antunes MJ, Bucciarelli-Ducci C, Bueno H, et al. 2017 ESC Guidelines for the Management of Acute Myocardial Infarction in Patients Presenting with ST-Segment Elevation: The Task Force for the Management of Acute Myocardial Infarction in Patients Presenting with ST-Segment Elevation of the European Society of Cardiology (ESC). Eur Heart J. 2018;39(2):119-77. doi: 10.1093/eurheartj/ehx393.
2. Gulati M, Levy PD, Mukherjee D, Amsterdam E, Bhatt DL, Birtcher KK, et al. 2021 AHA/ACC/ASE/CHEST/SAEM/SCCT/SCMR Guideline for the Evaluation and Diagnosis of Chest Pain: A Report of the American College of Cardiology/American Heart Association Joint Committee on Clinical Practice Guidelines. J Am Coll Cardiol. 2021;78(22):e187-e285. doi: 10.1016/j.jacc.2021.07.053.
3. Kramer CM, Barkhausen J, Bucciarelli-Ducci C, Flamm SD, Kim RJ, Nagel E. Standardized Cardiovascular Magnetic Resonance Imaging (CMR) Protocols: 2020 Update. J Cardiovasc Magn Reson. 2020;22(1):17. doi: 10.1186/s12968-020-00607-1.
4. Kotecha T, Martinez-Naharro A, Boldrini M, Knight D, Hawkins P, Kalra S, et al. Automated Pixel-Wise Quantitative Myocardial Perfusion Mapping by CMR to Detect Obstructive Coronary Artery Disease and Coronary Microvascular Dysfunction: Validation Against Invasive Coronary Physiology. JACC Cardiovasc Imaging. 2019;12(10):1958-69. doi: 10.1016/j.jcmg.2018.12.022.
5. Schwitter J, Wacker CM, Wilke N, Al-Saadi N, Sauer E, Huettle K, et al. MR-IMPACT II: Magnetic Resonance Imaging for Myocardial Perfusion Assessment in Coronary artery disease Trial: perfusion-cardiac magnetic resonance vs. single-photon emission computed tomography for the detection of coronary artery disease: a comparative multicentre, multivendor trial. Eur Heart J. 2013;34(10):775-81. doi: 10.1093/eurheartj/ehs022.
6. Greenwood JP, Maredia N, Younger JF, Brown JM, Nixon J, Everett CC. Cardiovascular Magnetic Resonance and Single-Photon Emission Computed Tomography for Diagnosis of Coronary Heart Disease (CE-MARC): A Prospective Trial. Lancet. 2012;379(9814):453-60. doi: 10.1016/S0140-6736(11)61335-4.
7. Greenwood JP, Ripley DP, Berry C, McCann GP, Plein S, Bucciarelli-Ducci C, et al. Effect of Care Guided by Cardiovascular Magnetic Resonance, Myocardial Perfusion Scintigraphy, or NICE Guidelines on Subsequent Unnecessary Angiography Rates: The CE-MARC 2 Randomized Clinical Trial. JAMA. 2016;316(10):1051-60. doi: 10.1001/jama.2016.12680.
8. Nagel E, Greenwood JP, McCann GP, Bettencourt N, Shah AM, Hussain ST, et al. Magnetic Resonance Perfusion or Fractional Flow Reserve in Coronary Disease. N Engl J Med. 2019;380(25):2418-28. doi: 10.1056/NEJMoa1716734.
9. Kwong RY, Ge Y, Steel K, Bingham S, Abdullah S, Fujikura K, et al. Cardiac Magnetic Resonance Stress Perfusion Imaging for Evaluation of Patients With Chest Pain. J Am Coll Cardiol. 2019;74(14):1741-55. doi: 10.1016/j.jacc.2019.07.074.
10. Moschetti K, Kwong RY, Petersen SE, Lombardi M, Garot J, Atar D, et al. Cost-Minimization Analysis for Cardiac Revascularization in 12 Health Care Systems Based on the EuroCMR/SPINS Registries. JACC Cardiovasc Imaging. 2022;15(4):607-625. doi: 10.1016/j.jcmg.2021.11.008.
11. Mileva N, Nagumo S, Mizukami T, Sonck J, Berry C, Gallinoro E, et al. Prevalence of Coronary Microvascular Disease and Coronary Vasospasm in Patients With Nonobstructive Coronary Artery Disease: Systematic Review and Meta-Analysis. J Am Heart Assoc. 2022;11(7):e023207. doi: 10.1161/JAHA.121.023207.

Left Atrial Strain in the Analysis of LV Diastolic Function: Ready to Use?

Antonio Amador Calvilho Júnior,[1,2] Jorge Eduardo Assef,[1] João Moron Saes Braga,[3] Andrea de Andrade Vilela,[1,4] Antonio Tito Paladino Filho,[1,5] Gustavo Nishida[1]

Instituto Dante Pazzanese de Cardiologia,[1] São Paulo, SP – Brazil
Conjunto Hospitalar de Sorocaba,[2] Sorocaba, SP – Brazil
Faculdade de Medicina de Marília,[3] Marília, SP – Brazil
Grupo Fleury,[4] São Paulo, SP – Brazil
Vila Nova Star,[5] São Paulo, SP – Brazil

Abstract

Left atrial (LA) dilation is a common indicator of diastolic dysfunction, and its analysis through a volume calculation reflects the cumulative effects of the left ventricular (LV) filling pressures. However, an increase in LA volume is not exclusive to diastolic dysfunction, which has also been observed in other clinical conditions. Thus, the evaluation of the LA strain enables a functional study of this chamber, adding to the morphological analysis through the volume calculation.

The LA strain, measured using the speckle tracking technique, brings information on the reservoir, conduction, and contractile functions of the LA, and is related to the LV function. Moreover, the changes in the LA strain precede the volumetric changes by nearly a decade, and correlate inversely with the degree of LA fibrosis – this has an important relationship with the diastolic dysfunction and its grading system. Albeit insufficient to explain its totality, LA fibrosis can partially justify the functional changes of this heart chamber and can favor the use of this variable as a complement to the current protocols for the analysis of the diastolic function.

Although further study is still warranted to establish other clinical applications, the LA strain stands out in the analysis of diastolic dysfunction and can be considered ready to use, offering a great potential to improve the evaluation of the overall cardiac function.

Introduction

The study of myocardial deformation can be considered definitely implemented in the current echocardiographic routine. Although some people believe this topic is recent, or in the research and pre-implementation stage, it is not true. The first studies of myocardial deformation are as old as the use of two-dimensional images in echocardiography, and the vast majority of these studies address left ventricular myocardial deformation. From the first experimental studies with sonomicrometry crystals directly inserted into the myocardium of dogs through the use of Doppler echocardiography, maturity was reached with the development of speckle tracking, a widely validated method for use in echocardiography and magnetic resonance imaging.[1–3]

Keywords

Echocardiography; Myocardium; Left Ventricular Dysfunction.

Mailing Address: Antonio Amador Calvilho Júnior •
Av. Dr. Dante Pazzanese, 500. Postal code: 04012-909. Vila Mariana São Paulo, SP – Brazil
E-mail: dr.calvilho@gmail.com
Manuscript received October 15, 2022; revised October 21, 2022; accepted November 2, 2022;
Editor responsible for the review: Daniela do Carmo Rassi

DOI: https://doi.org/10.36660/abcimg.2022357i

Multiplicity of speckle tracking variables in the assessment of different cardiac structures

Speckle tracking is the standard tool to study myocardial deformation by echocardiography and, when applied to the left ventricle (LV), provides a great amount of information that goes beyond the mere quantification of absolute deformation. Therefore, it is essential to standardize these measures.

The expression strain is used as a synonym for myocardial deformation, which reduced the applicability of the method to this measure, which is certainly incomplete, because speckle tracking also allows for the measurement of rotational variables, even enabling to estimate myocardial work. Although terminology is internationally standardized, misunderstandings are still frequent. In Brazil, for example, the expression "two-dimensional strain" is used to refer to speckle tracking, which is in disagreement with international standards.[4]

LV longitudinal strain is the most renowned measure for use in speckle tracking echocardiography (STE). Examples of its applicability include: determination of subclinical myocardial disease in apparently normal ventricles, early diagnosis of chemotherapy cardiotoxicity, differentiation between the main causes of increased myocardial thickness, risk segmentation in different heart diseases, and in a myriad of other clinical conditions affecting the myocardium.[5–8]

LV circumferential and radial deformations can also be measured by the same method; moreover, the velocity at which these deformations occur, the so-called strain rate, can also be obtained. Rotational variables measured at the basal, medial, and apical segments may also complement the assessment, as well as LV twist, which is the difference between LV basal and apical rotations.[4] These assessment methods have a complementary role to that of LV longitudinal strain and do not imply its replacement.

The right ventricle can also be assessed with regard to deformation; in this case, longitudinal strain of its free wall is the most validated and recommended measure.[9–12] The same applies to left atrial (LA) longitudinal strain, a promising approach for functional studies and the focus of this review, which will subsequently describe the peculiarities of this measure, focusing on the study of LV diastolic function (DF).

Contents

Quantification of cardiac mechanics and its studies in diastology

There is a significant number of publications on the complementation of DF analysis by techniques to quantify cardiac muscle mechanics, and the vast majority of these publications is related to the study of the LV with a focus on determining its filling pressure.[13–16] Despite the favorable results of these techniques, their effective implementation to this end did not occur, which may be explained, among other reasons, by the complexity of these analyses compared to the traditional measures of LV DF by Doppler echocardiography.[17]

However, although the assessment of LV filling pressure by STE is not part of 2016 recommendations for the assessment of DF, STE is indeed recommended to determine myocardial disease, especially LV global longitudinal strain, which may be used to determine myocardial disease and thus help in the initial analysis of DF.[18]

What is the role of LA in the assessment of LV DF?

Differently from other techniques to assess DF, which reveal cardiac hemodynamic status at the time of examination, the assessment of LA by calculating its volume reflects the cumulative effects of LV filling pressures.

The use of LA dimensions in clinical practice precedes even the first guidelines for the assessment of DF diastole by the American Society of Echocardiography (ASE), published in 2009.[19] Many studies showed that increased LA volume is closely related not only to diagnosis, but also to the prognosis of patients with diastolic dysfunction (DD).[20–28] However, it is important to emphasize that LA enlargement is not exclusive to DD and can also be observed in mitral valve disease, long-lasting arrhythmia, anemia, and intense and prolonged practice of physical activity. However, LA enlargement in patients with arterial hypertension is considered, by some authors, as a diagnostic feature of DD, even when not associated with other echocardiographic features of DD.[29]

From another perspective, the identification of normal-sized LA does not rule out the presence of DD, because recent or intermittent increases in LV filling pressure may not be sufficient to cause LA enlargement, which certainly makes it possible for this cavity to be assessed not only morphologically, but also functionally, more specifically by measuring its strain.

Functional analysis of the LA by speckle tracking and its potential applicability in diastology

Morphofunctional knowledge

Relationship between LA function and LV function

LA strain as measured by STE provides information on the reservoir, conduit, and contractile functions of this chamber (Figure 1). The usefulness of these measures is based on the close relationship between LA and LV functions. For example, the performance of reservoir and conduit functions is determined by, in addition to atrial compliance, ventricle relaxation and by transmitral pressure gradient.[30] The conditions that impair any aspect of atrial function, especially mechanical alterations that lead to abnormalities in pressure-volume relationships, may affect overall cardiac performance, leading to unfavorable symptoms and outcomes.[31]

Causes of LA dysfunction

The hemodynamic effects of ventricle diseases seem insufficient to explain all the changes leading to LA dysfunction, because, in some patients, this dysfunction occurs even in the absence of significant morphological and/or functional changes in the LV.[32] This is corroborated by studies with previously healthy populations, in which LA function and its remodeling were independently associated and preceded the clinical manifestation of heart failure.[33] Another aspect that favors functional studies of LA results from the fact that, although

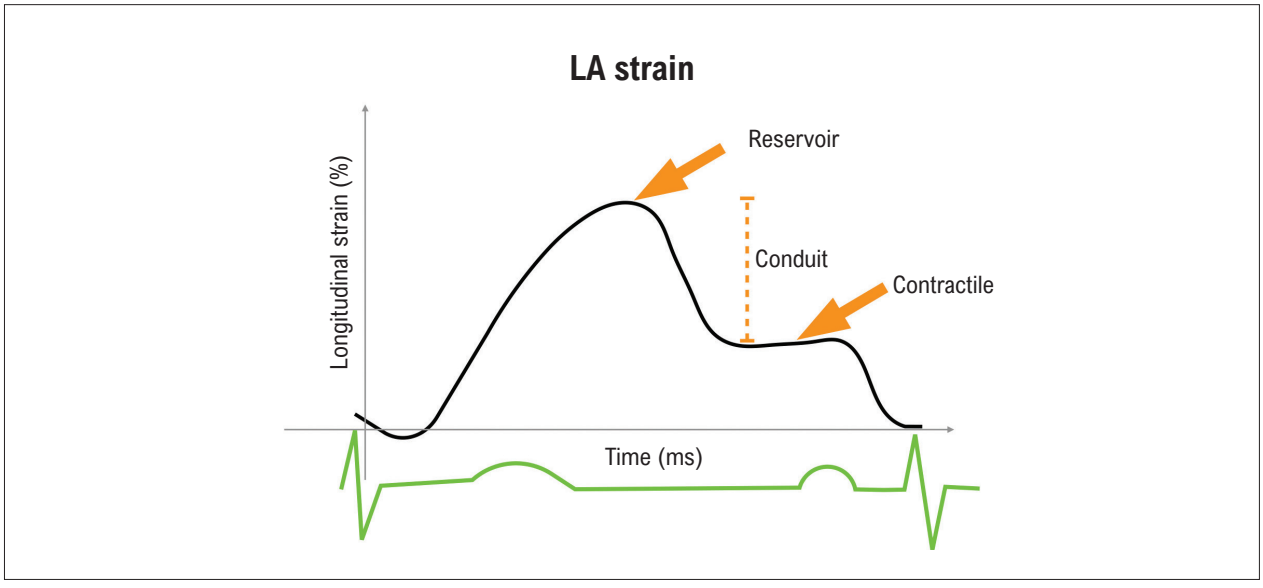

Figure 1 – *Phases of left atrial function evidenced by the study of longitudinal deformation. LA: left atrial.*

LA strain is not totally independent from load, myocardial deformation tends to be less affected by load than LA volume would be.[34] Furthermore, changes in LA strain precede volume changes in almost a decade.[35]

LA dysfunction is believed to result, at least in part, from LA myocardial fibrosis. This process has been associated with several biological factors, practically the same one that impact ventricular myocardium.[33] LA strain is inversely correlated with the degree of LA fibrosis (Figure 2).[36, 37] This association alone would not be sufficient to favor the use of this variable as a complementary tool in current protocols of DF analysis. However, LA function was shown to be a determinant factor of the time of decompensation of heart failure with preserved ejection fraction (HFpEF), one of the reasons for the discussion on the potential use of LA strain as a marker of elevated LV filling pressures.[38] However, although functional changes may be partially justified by LA fibrosis, it is insufficient to fully explain the phenomenon, which is one of the topics that justify studies on the applicability of LA strain in diastology.

Applicability of functional analysis of LA aimed at the study of LVDD

To apply the study of LA deformation in LV diastology, it is important to first consider the intended purpose, which may be:

1. To optimize the diagnosis of DD in general;

2. To determine the presence or absence of increased filling pressure.

A significant number of studies confirm the usefulness of measuring LA strain to diagnose DD by demonstrating a decrease in LA reservoir strain in critical situations such as hypertension, diabetes, and chronic kidney disease, even when LA volume and/or emptying pressure is still normal.[39–41] Similar findings were observed in a study of patients with hypertension, diabetes, or coronary disease, all of them with preserved LVEF, which revealed an increase close to 10% in the diagnosis of diastolic dysfunction when adding LA strain to the algorithm for DD detection used in the 2016 guidelines of ASE with the European Association of Cardiovascular Image (EACVI) (Figure 3).[42]

In addition to diagnosis, LA strain may also be applied to categorize DD, because both reservoir and conduit functions decrease as the grade of DD increases.[43] Analyses of ROC curve show that reservoir strain has high accuracy to grade DD compared to LV volume index.[44]

Despite this gradual and progressive reduction of reservoir and conduit functions, it should be observed that, a different behavior was observed in the first phases with regard to contractile function, which increases in DD grade 1 before decreasing, after grade 2.[44] Another interesting observation is that, in cases of changes in LV relaxation, there is an increase in the relative contribution of LA contractile function to its filling, while the conduit function decreases. When LV filling pressures increase significantly, the limits of LA preload are reached, and the LA will behave predominantly as a conduit.[45] Such characteristics would not necessarily be useful to make the use of LA strain effective in diastology, but its knowledge may help avoid mistaken interpretations by simplifying the effects of LV diastolic function on LA.

Standardization and atrial strain measures by speckle tracking

Despite measuring LA two-dimensional strain by STE is relatively simple and direct, methodological differences initially contributed to a certain variation in normal values. This was improved with the recent systematization and standardization proposed by several international societies and by the industry, which defined the longitudinal strain, which is the strain the direction tangential to the endocardial atrial border in an apical view, as the only one recommended. The same document advise against a segmental study; therefore, only the overall value obtained in the analyzed view.[46]

It is possible to combine measures obtained by the 4- and 2- chamber views to calculate global longitudinal LA strain, and it was even recommended in a previous consensus (Figure 4).[47] However, studies using a single view are acceptable, specifically the 4-chamber view in this case, due to its practicality. Results from a recent meta-analysis including 30 studies, totaling 2038 healthy individuals, provided the normal reference values currently accepted for LA strain during the reservoir, conduit, and contraction phases.[48]

Therefore, recommendation allows for the analysis to be conduct in an apical 4-chamber view, avoiding cavity shortening, and with the region of interest measuring nearly 3 mm in width.[46]

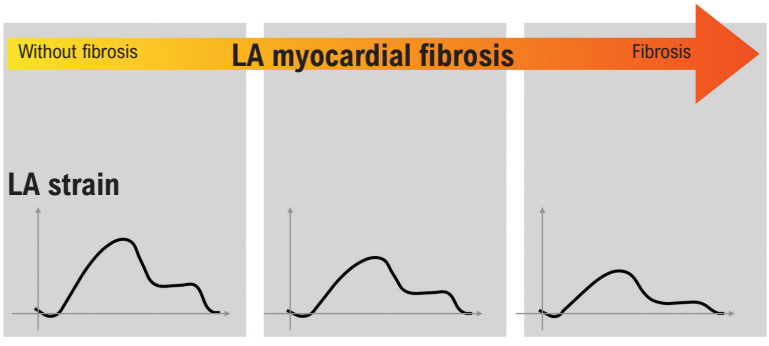

Figure 2 – *LA strain and myocardial atrial fibrosis. LA: left atrial*

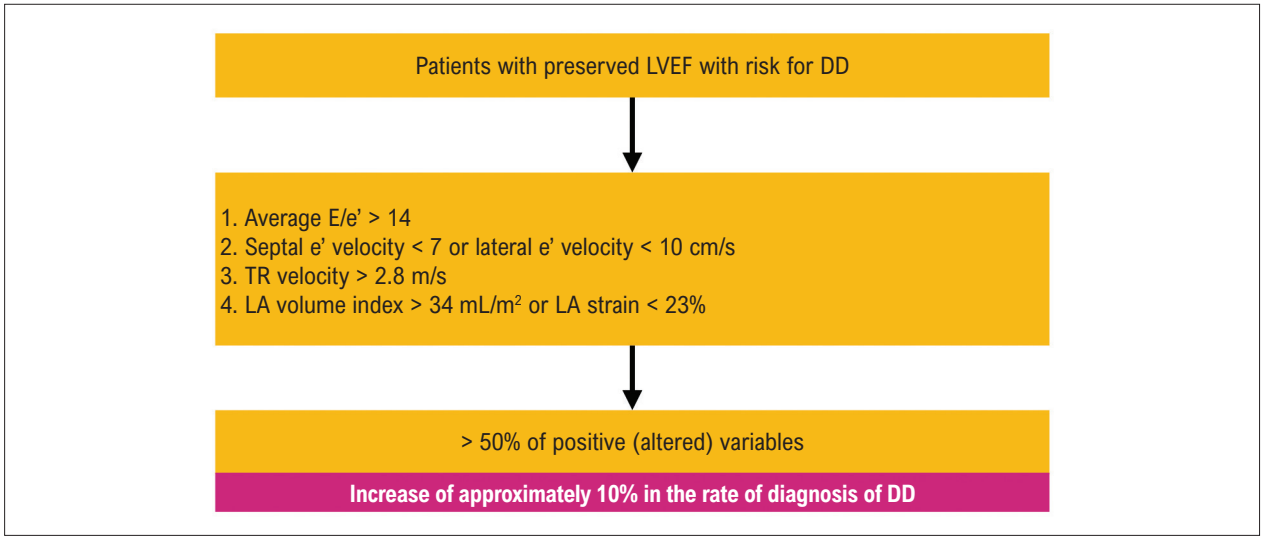

Figure 3 – *Increase in the diagnosis of DD by including LA strain to the algorithm. Adapted from Morris et al. (reference 42). E: E wave velocity of the transmitral flow in pulse Doppler; e': mitral annulus protodiastolic velocity in tissue Doppler; LA: left atrial; LVEF: left ventricular ejection fraction; TR: tricuspid regurgitation; DD: diastolic dysfunction.*

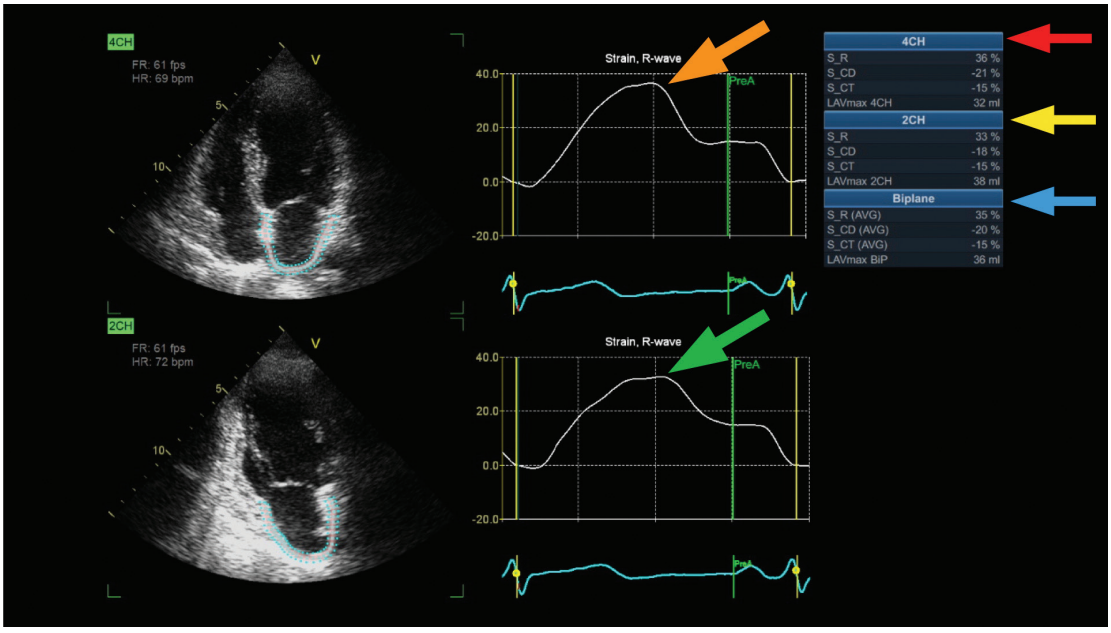

Figure 4 – *Measures of left atrial strain by speckle tracking. Orange and green arrows point to peak reservoir strains for the 4- and 2-chamber echocardiographic views, respectively. Red and yellow arrows indicate the automatic results for the reservoir, conduit, and contraction measures in the 4- and 2-chamber views, respectively, and the blue arrow highlights overall results (mean values) for the 2 views.*

Normal values of left atrial strain

As observed in Figure 1, LA deformation may be assessed by means of 2 peaks: maximum deformation (also known as reservoir strain) and atrial contraction deformation (also known as contractile strain), and the difference between these peaks, which is the third measure known as conduit strain. Normal values currently accepted derive from the aforementioned 2017 meta-analysis and are the following:[48]

- Reservoir strain 39% (95% confidence interval: 38% to 41%)
- Conduit strain 23% (95% confidence interval: 21% to 25%)
- Contractile strain 17% (95% confidence interval: 16% to 19%)

How to use altered LA strain values in diastology?

It would be convenient, with regard to diagnosis and classification of DD, that abnormal LA strain succeed elevated LV filling pressures, being a direct consequence of the latter. However, as previously shown, what actually occurs is the progressive reduction of LA strain as DD grade increases; therefore interpretation of the abnormality should be performed with caution and contextualized in the interest of the investigation.

Applicability of LA strain to determine cardiovascular prognosis

Abnormalities resulting from LA deformation may be studied in order to determine cardiovascular risks. In these cases, these abnormalities show an independent correlation with cardiovascular events.[49,50] Cutoff values found in these situations would not necessarily be useful to determine and categorize DD.

Applicability of LA strain to classify DD

Measures of LA deformation can also be used to help grade DD, which will also imply in determining prognosis, because, as already well established, the risk of cardiovascular events is directly correlated with grade of DD.[51,52]

Many studies were conducted to correlate reduction in LA myocardial deformation with increased LV filling pressures, especially pulmonary artery systolic pressure (PASP) and mean pulmonary capillary wedge pressure. One of these studies, conducted in 2009 by Kurt *et al.*, assessed the so-called LA stiffness, calculated as the ratio of E/e´ (average) to LA strain during systole (currently more often referred to as LA reservoir strain). These researchers showed that LA stiffness presented a good correlation with the invasive measure of PASP.[53] Subsequent studies started to focus on reservoir strain alone.

In 2019, Singh *et al*. showed that peak LA strain lower than 20% was able to accurately identify pre-A wave LV diastolic pressure higher than 15 mmHg, significantly improving the classification of DD made by current guidelines (2016), especially in individuals with preserved LVEF.[54] Similar results were published in 2021 by Inoue *et al.*, in whose study LA reservoir strain < 18% and LA contractile strain < 8% determined increased LV filling pressure better than LA volume and other conventional Doppler parameters.[55]

In 2020, an editorial published in *Journal of American College of Cardiology - Cardiovascular Imaging* by Jae Oh proposed a new diagnostic approach of DD. Of the proposals, the use of LA reservoir strain to differentiate undetermined cases.[56] In 2021, following exactly the same line, LA strain was included in an European consensus, in the case concerning the use of multimodality imaging in patients with HFpEF.[57] This incorporation took into account the 2016 algorithm for the analysis of DF and the results from the study by Inoue *et al.* (Figure 5).[55]

When not using LA strain to classify DD

In some situations, the measure of LA strain should not be considered, such as in limitations of echocardiographic images and in detriments to the analysis of two or more LA wall segments.

Similarly, patients with AF should not have their LA reservoir strain analyzed for the purpose of estimating LV filling pressure.[55] This also applies to patients who presented with episodes of AF for more than 48 hours in the 90 days before the test. Such fact results from the possible presence of LA myocardial stunning, a situation characterized by very low reservoir strain low values. Therefore, this measure should not be used to diagnose HFpEF when there is possibility of atrial stunning.

Final considerations

The importance of assessing LA function is unquestionable in several clinical situations and in specific patient populations. Considering the presented studies and the current technologies involved, the authors believe that LA strain is indeed ready to use, because it was shown that LA strain, especially its reservoir component, progressively decreases as LVDD worsens and may be useful in the reclassification of "undetermined" cases. Obviously, many questions remain to be answered regarding changes in LA function, especially in the context of diastology. However, this tool has potential for immediate use as a complementary diagnostic parameter.

The EACVI made a right decision when recommending the use of LA reservoir strain as an additional measure in cases when filling pressures would be classified as undetermined by the algorithm of the 2016 guidelines to assess DF.[57]

It is important to emphasize that the use of LA strain is not limited to diastology, as previously described. Changes in LA deformation are associated with prognostic implications in several scenarios, such as in the prediction of a cardioembolic event.[58] Furthermore, LA has been the focus of discussions and investigations that reinforce its role in a myriad of cardiovascular situations, including new concepts, such as the definition of atrial failure.[59]

Hence, there is a great potential in the use of LA myocardial deformation in the context of analysis of LV DF to improve the accuracy of algorithms employed in clinical practice.

Author Contributions

Writing of the manuscript: Calvilho Júnior AA, Assef JE and Braga JMS; conception and design of the research, acquisition of data and critical revision of the manuscript for intellectual content: Vilela AA, Paladino Filho AT and Nishida G.

Potential Conflict of Interest

No potential conflict of interest relevant to this article was reported.

Sources of Funding

There were no external funding sources for this study.

Study Association

This study is not associated with any thesis or dissertation work.

Ethics Approval and Consent to Participate

This article does not contain any studies with human participants or animals performed by any of the authors.

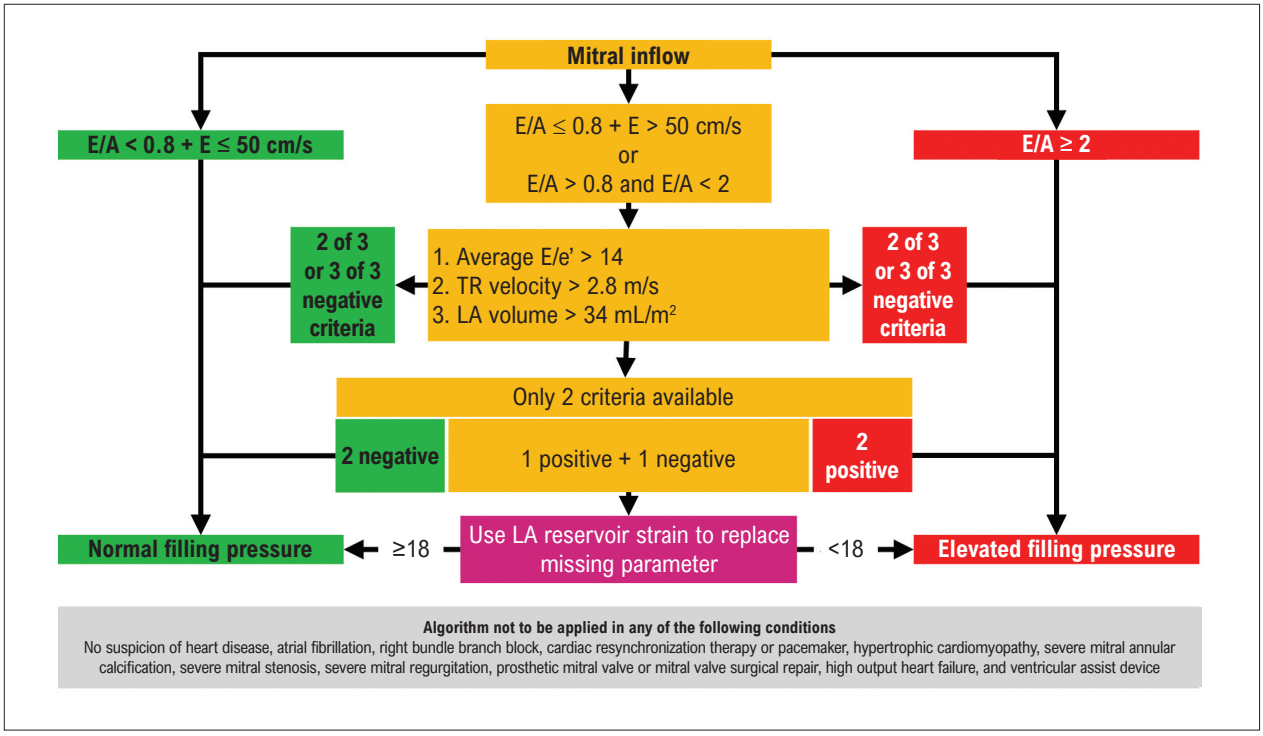

Figure 5 – *Algorithm proposed to grade DD using left atrial reservoir strain. Adapted from Smiseth et al. (reference 57). A: transmitral flow A wave velocity in pulse Doppler; E: E wave velocity of the transmitral flow in pulse Doppler, e': mitral annulus protodiastolic velocity in tissue Doppler; LA: left atrial; TR: tricuspid regurgitation.*

References

1. Mirsky I, Parmley WW. Assessment of Passive Elastic Stiffness for Isolated Heart Muscle and the Intact Heart. Circ Res. 1973;33(2):233-43. doi: 10.1161/01.res.33.2.233.
2. Urheim S, Edvardsen T, Torp H, Angelsen B, Smiseth OA. Myocardial Strain by Doppler Echocardiography. Validation of a New Method To Quantify Regional Myocardial Function. Circulation. 2000;102(10):1158-64. doi: 10.1161/01.cir.102.10.1158.
3. Stendahl JC, Parajuli N, Lu A, Boutagy NE, Guerrera N, Alkhalil I, et al. Regional Myocardial Strain Analysis Via 2D Speckle Tracking Echocardiography: Validation With Sonomicrometry and Correlation with Regional Blood Flow in the Presence of Graded Coronary Stenoses and Dobutamine Stress. Cardiovasc Ultrasound. 2020;18(1):2. doi: 10.1186/s12947-019-0183-x.
4. Mor-Avi V, Lang RM, Badano LP, Belohlavek M, Cardim NM, Derumeaux G, et al. Current And Evolving Echocardiographic Techniques for the Quantitative Evaluation of Cardiac Mechanics: ASE/EAE Consensus Statement on Methodology and Indications Endorsed by the Japanese Society of Echocardiography. J Am Soc Echocardiogr. 2011;24(3):277-313. doi: 10.1016/j.echo.2011.01.015.
5. Collier P, Phelan D, Klein A. A Test in Context: Myocardial Strain Measured by Speckle-Tracking Echocardiography. J Am Coll Cardiol. 2017;69(8):1043-56. doi: 10.1016/j.jacc.2016.12.012.
6. Halliday BP, Senior R, Pennell DJ. Assessing Left Ventricular Systolic Function: From Ejection Fraction to Strain Analysis. Eur Heart J. 2021;42(7):789-97. doi: 10.1093/eurheartj/ehaa587.
7. Almeida ALC, Gjesdal O, Mewton N, Choi EY, Teixido-Tura G, Yoneyama K et al. Speckle-Tracking pela Ecocardiografia Bidimensional – Aplicações Clínicas. Rev Bras Ecocardiogr Imagem Cardiovasc. 2013;26(1):38-49.
8. Oliveira AAA, Oliveira TA, Oliveira LA, Meneses GC, Bezerra GF, Martins AMC, et al. Association Between Angiopoietin-2 and Functional Cardiac Remodeling in Hemodialysis Patients with Normal Left Ventricular Ejection. J Clin Hypertens (Greenwich). 2022;24(4):502-12. doi: 10.1111/jch.14465.
9. Motoki H, Borowski AG, Shrestha K, Hu B, Kusunose K, Troughton RW, et al. Right Ventricular Global Longitudinal Strain Provides Prognostic Value Incremental to Left Ventricular Ejection Fraction in Patients With Heart Failure. J Am Soc Echocardiogr. 2014;27(7):726-32. doi: 10.1016/j.echo.2014.02.007.
10. Morris DA, Krisper M, Nakatani S, Köhncke C, Otsuji Y, Belyavskiy E, et al. Normal Range and Usefulness of Right Ventricular Systolic Strain to Detect Subtle Right Ventricular Systolic Abnormalities in Patients With Heart Failure: A Multicentre Study. Eur Heart J Cardiovasc Imaging. 2017;18(2):212-23. doi: 10.1093/ehjci/jew011.
11. D'Andrea A, Stanziola A, D'Alto M, Di Palma E, Martino M, Scarafile R, et al. Right Ventricular Strain: An Independent Predictor of Survival in Idiopathic Pulmonary Fibrosis. Int J Cardiol. 2016;222:908-910. doi: 10.1016/j.ijcard.2016.07.288.
12. Platz E, Hassanein AH, Shah A, Goldhaber SZ, Solomon SD. Regional Right Ventricular Strain Pattern in Patients With Acute Pulmonary Embolism. Echocardiography. 2012;29(4):464-70. doi: 10.1111/j.1540-8175.2011.01617.x.
13. Wang J, Khoury DS, Thohan V, Torre-Amione G, Nagueh SF. Global Diastolic Strain Rate For the Assessment of Left Ventricular Relaxation and Filling Pressures. Circulation. 2007;115(11):1376-83. doi: 10.1161/CIRCULATIONAHA.106.662882.
14. Dokainish H, Sengupta R, Pillai M, Bobek J, Lakkis N. Usefulness of New Diastolic Strain and Strain Rate Indexes For the Estimation of Left Ventricular Filling Pressure. Am J Cardiol. 2008;101(10):1504-9. doi: 10.1016/j.amjcard.2008.01.037. Epub 2008 Mar 21.

15. Nguyen JS, Lakkis NM, Bobek J, Goswami R, Dokainish H. Systolic and Diastolic Myocardial Mechanics In Patients With Cardiac Disease and Preserved Ejection Fraction: Impact of Left Ventricular Filling Pressure. J Am Soc Echocardiogr. 2010;23(12):1273-80. doi: 10.1016/j.echo.2010.09.008.

16. Wang J, Khoury DS, Yue Y, Torre-Amione G, Nagueh SF. Preserved Left Ventricular Twist and Circumferential Deformation, but Depressed Longitudinal and Radial Deformation in Patients with Diastolic Heart Failure. Eur Heart J. 2008;29(10):1283-9. doi: 10.1093/eurheartj/ehn141.

17. Calvilho AA Jr, Assef JE, Le Bihan D, Barretto RBM, Paladino ATF, Abizaid AAC, et al. E/E` Ratio Is Superior to Speckle Tracking For Detecting Elevated Left Ventricular End-Diastolic Pressure in Patients with Coronary Artery Disease and Preserved Ejection Fraction. Echocardiography. 2019;36(7):1263-72. doi: 10.1111/echo.14407.

18. Nagueh SF, Smiseth OA, Appleton CP, Byrd BF 3rd, Dokainish H, Edvardsen T, et al. Recommendations For The Evaluation of Left Ventricular Diastolic Function by Echocardiography: An Update from the American Society of Echocardiography and the European Association of Cardiovascular Imaging. J Am Soc Echocardiogr. 2016;29(4):277-314. doi: 10.1016/j.echo.2016.01.011.

19. Nagueh SF, Appleton CP, Gillebert TC, Marino PN, Oh JK, Smiseth OA, et al. Recommendations for the Evaluation of Left Ventricular Diastolic Function By Echocardiography. J Am Soc Echocardiogr. 2009;22(2):107-33. doi: 10.1016/j.echo.2008.11.023.

20. Tsang TS, Abhayaratna WP, Barnes ME, Miyasaka Y, Gersh BJ, Bailey KR, et al. Prediction of Cardiovascular Outcomes with Left Atrial Size: Is Volume Superior To Area Or Diameter? J Am Coll Cardiol. 2006;47(5):1018-23. doi: 10.1016/j.jacc.2005.08.077.

21. Pritchett AM, Jacobsen SJ, Mahoney DW, Rodeheffer RJ, Bailey KR, Redfield MM. Left Atrial Volume as an Index of Left Atrial Size: A Population-Based Study. J Am Coll Cardiol. 2003;41(6):1036-43. doi: 10.1016/s0735-1097(02)02981-9.

22. Tsang TS, Barnes ME, Bailey KR, Leibson CL, Montgomery SC, Takemoto Y, et al. Left Atrial Volume: Important Risk Marker of Incident Atrial Fibrillation in 1655 Older Men and Women. Mayo Clin Proc. 2001;76(5):467-75. doi: 10.4065/76.5.467.

23. Fatema K, Barnes ME, Bailey KR, Abhayaratna WP, Cha S, Seward JB, et al. Minimum Vs. Maximum Left Atrial Volume for Prediction of First Atrial Fibrillation or Flutter in an Elderly Cohort: A Prospective Study. Eur J Echocardiogr. 2009;10(2):282-6. doi: 10.1093/ejechocard/jen235.

24. Abhayaratna WP, Fatema K, Barnes ME, Seward JB, Gersh BJ, Bailey KR, et al. Left Atrial Reservoir Function As A Potent Marker for First Atrial Fibrillation or Flutter in Persons > Or = 65 Years Of Age. Am J Cardiol. 2008;101(11):1626-9. doi: 10.1016/j.amjcard.2008.01.051.

25. Moller JE, Hillis GS, Oh JK, Seward JB, Reeder GS, Wright RS, et al. Left Atrial Volume: A Powerful Predictor of Survival after Acute Myocardial Infarction. Circulation. 2003;107(17):2207-12. doi: 10.1161/01.CIR.0000066318.21784.43.

26. Beinart R, Boyko V, Schwammenthal E, Kuperstein R, Sagie A, Hod H, et al. Long-Term Prognostic Significance of Left Atrial Volume in Acute Myocardial Infarction. J Am Coll Cardiol. 2004;44(2):327-34. doi: 10.1016/j.jacc.2004.03.062.

27. Benjamin EJ, D'Agostino RB, Belanger AJ, Wolf PA, Levy D. Left Atrial Size and The Risk of Stroke and Death. The Framingham Heart Study. Circulation. 1995;92(4):835-41. doi: 10.1161/01.cir.92.4.835.

28. Takemoto Y, Barnes ME, Seward JB, Lester SJ, Appleton CA, Gersh BJ, et al. Usefulness of Left Atrial Volume in Predicting First Congestive Heart Failure in Patients > Or = 65 Years Of Age with Well-Preserved Left Ventricular Systolic Function. Am J Cardiol. 2005;96(6):832-6. doi: 10.1016/j.amjcard.2005.05.031.

29. Nagueh SF. Left Ventricular Diastolic Function: Understanding Pathophysiology, Diagnosis, and Prognosis With Echocardiography. JACC Cardiovasc Imaging. 2020;13(1 Pt 2):228-44. doi: 10.1016/j.jcmg.2018.10.038.

30. Bowman AW, Kovács SJ. Left Atrial Conduit Volume is Generated by Deviation from the Constant-Volume State of the Left Heart: A Combined MRI-Echocardiographic Study. Am J Physiol Heart Circ Physiol. 2004;286(6):H2416-24. doi: 10.1152/ajpheart.00969.2003.

31. Melenovsky V, Hwang SJ, Redfield MM, Zakeri R, Lin G, Borlaug BA. Left Atrial Remodeling and Function in Advanced Heart Failure with Preserved Or Reduced Ejection Fraction. Circ Heart Fail. 2015;8(2):295-303. doi: 10.1161/CIRCHEARTFAILURE.114.001667.

32. Habibi M, Chahal H, Opdahl A, Gjesdal O, Helle-Valle TM, Heckbert SR, et al. Association of CMR-Measured LA Function with Heart Failure Development: Results From the MESA Study. JACC Cardiovasc Imaging. 2014;7(6):570-9. doi: 10.1016/j.jcmg.2014.01.016.

33. Thomas L, Abhayaratna WP. Left Atrial Reverse Remodeling: Mechanisms, Evaluation, and Clinical Significance. JACC Cardiovasc Imaging. 2017;10(1):65-77. doi: 10.1016/j.jcmg.2016.11.003.

34. Genovese D, Singh A, Volpato V, Kruse E, Weinert L, Yamat M, et al. Load Dependency of Left Atrial Strain in Normal Subjects. J Am Soc Echocardiogr. 2018;31(11):1221-8. doi: 10.1016/j.echo.2018.07.016.

35. Boyd AC, Richards DA, Marwick T, Thomas L. Atrial Strain Rate is A Sensitive Measure of Alterations in Atrial Phasic Function in Healthy Ageing. Heart. 2011;97(18):1513-9. doi: 10.1136/heartjnl-2011-300134.

36. Kuppahally SS, Akoum N, Burgon NS, Badger TJ, Kholmovski EG, Vijayakumar S, et al. Left Atrial Strain And Strain Rate in Patients with Paroxysmal and Persistent Atrial Fibrillation: Relationship to Left Atrial Structural Remodeling Detected By Delayed-Enhancement MRI. Circ Cardiovasc Imaging. 2010;3(3):231-9. doi: 10.1161/CIRCIMAGING.109.865683.

37. Marrouche NF, Wilber D, Hindricks G, Jais P, Akoum N, Marchlinski F, et al. Association of Atrial Tissue Fibrosis Identified by Delayed Enhancement MRI and Atrial Fibrillation Catheter Ablation: The DECAAF Study. JAMA. 2014;311(5):498-506. doi: 10.1001/jama.2014.3.

38. Sanchis L, Gabrielli L, Andrea R, Falces C, Duchateau N, Perez-Villa F, et al. Left Atrial Dysfunction Relates To Symptom Onset in Patients with Heart Failure and Preserved Left Ventricular Ejection Fraction. Eur Heart J Cardiovasc Imaging. 2015;16(1):62-7. doi: 10.1093/ehjci/jeu165.

39. Morris DA, Takeuchi M, Krisper M, Köhncke C, Bekfani T, Carstensen T, et al. Normal Values and Clinical Relevance of Left Atrial Myocardial Function Analysed by Speckle-Tracking Echocardiography: Multicentre Study. Eur Heart J Cardiovasc Imaging. 2015;16(4):364-72. doi: 10.1093/ehjci/jeu219.

40. Mondillo S, Cameli M, Caputo ML, Lisi M, Palmerini E, Padeletti M, et al. Early Detection of Left Atrial Strain Abnormalities by Speckle-Tracking in Hypertensive and Diabetic Patients with Normal Left Atrial Size. J Am Soc Echocardiogr. 2011;24(8):898-908. doi: 10.1016/j.echo.2011.04.014.

41. Kadappu KK, Abhayaratna K, Boyd A, French JK, Xuan W, Abhayaratna W, et al. Independent Echocardiographic Markers of Cardiovascular Involvement in Chronic Kidney Disease: The Value of Left Atrial Function and Volume. J Am Soc Echocardiogr. 2016;29(4):359-67. doi: 10.1016/j.echo.2015.11.019.

42. Morris DA, Belyavskiy E, Aravind-Kumar R, Kropf M, Frydas A, Braunauer K, et al. Potential Usefulness and Clinical Relevance of Adding Left Atrial Strain to Left Atrial Volume Index in the Detection of Left Ventricular Diastolic Dysfunction. JACC Cardiovasc Imaging. 2018;11(10):1405-15. doi: 10.1016/j.jcmg.2017.07.029.

43. Singh A, Addetia K, Maffessanti F, Mor-Avi V, Lang RM. LA Strain for Categorization of LV Diastolic Dysfunction. JACC Cardiovasc Imaging. 2017;10(7):735-43. doi: 10.1016/j.jcmg.2016.08.014.

44. Brecht A, Oertelt-Prigione S, Seeland U, Rücke M, Hättasch R, Wagelöhner T, et al. Left Atrial Function in Preclinical Diastolic Dysfunction: Two-Dimensional Speckle-Tracking Echocardiography-Derived Results from the BEFRI Trial. J Am Soc Echocardiogr. 2016;29(8):750-8. doi: 10.1016/j.echo.2016.03.013.

45. Thomas L, Marwick TH, Popescu BA, Donal E, Badano LP. Left Atrial Structure and Function, and Left Ventricular Diastolic Dysfunction: JACC State-of-the-Art Review. J Am Coll Cardiol. 2019;73(15):1961-77. doi: 10.1016/j.jacc.2019.01.059.

46. Badano LP, Kolias TJ, Muraru D, Abraham TP, Aurigemma G, Edvardsen T, et al. Standardization of Left Atrial, Right Ventricular, and Right Atrial Deformation Imaging Using Two-Dimensional Speckle Tracking Echocardiography: A Consensus Document of the EACVI/ASE/Industry Task Force to Standardize Deformation Imaging. Eur Heart J Cardiovasc Imaging. 2018;19(6):591-600. doi: 10.1093/ehjci/jey042.

47. Lang RM, Badano LP, Mor-Avi V, Afilalo J, Armstrong A, Ernande L, et al. Recommendations for Cardiac Chamber Quantification by Echocardiography in Adults: An Update From the American Society of Echocardiography and the European Association of Cardiovascular Imaging. Eur Heart J Cardiovasc Imaging. 2015;16(3):233-70. doi: 10.1093/ehjci/jev014.

48. Pathan F, D'Elia N, Nolan MT, Marwick TH, Negishi K. Normal Ranges of Left Atrial Strain by Speckle-Tracking Echocardiography: A Systematic Review and Meta-Analysis. J Am Soc Echocardiogr. 2017;30(1):59-70.e8. doi: 10.1016/j.echo.2016.09.007.

49. Freed BH, Daruwalla V, Cheng JY, Aguilar FG, Beussink L, Choi A, et al. Prognostic Utility and Clinical Significance of Cardiac Mechanics in Heart Failure with Preserved Ejection Fraction: Importance of Left Atrial Strain. Circ Cardiovasc Imaging. 2016;9(3):10.1161/CIRCIMAGING.115.003754e003754. doi: 10.1161/CIRCIMAGING.115.003754.

50. Santos AB, Roca GQ, Claggett B, Sweitzer NK, Shah SJ, Anand IS, et al. Prognostic Relevance of Left Atrial Dysfunction in Heart Failure with Preserved Ejection Fraction. Circ Heart Fail. 2016;9(4):e002763. doi: 10.1161/CIRCHEARTFAILURE.115.002763.

51. Halley CM, Houghtaling PL, Khalil MK, Thomas JD, Jaber WA. Mortality Rate in Patients with Diastolic Dysfunction and Normal Systolic Function. Arch Intern Med. 2011;171(12):1082-7. doi: 10.1001/archinternmed.2011.244.

52. Kitzman DW, Little WC. Left Ventricle Diastolic Dysfunction and Prognosis. Circulation. 2012;125(6):743-5. doi: 10.1161/CIRCULATIONAHA.111.086843.

53. Kurt M, Wang J, Torre-Amione G, Nagueh SF. Left Atrial Function in Diastolic Heart Failure. Circ Cardiovasc Imaging. 2009;2(1):10-5. doi: 10.1161/CIRCIMAGING.108.813071.

54. Singh A, Medvedofsky D, Mediratta A, Balaney B, Kruse E, Ciszek B, et al. Peak Left Atrial Strain as a Single Measure for the Non-Invasive Assessment of Left Ventricular Filling Pressures. Int J Cardiovasc Imaging. 2019;35(1):23-32. doi: 10.1007/s10554-018-1425-y.

55. Inoue K, Khan FH, Remme EW, Ohte N, García-Izquierdo E, Chetrit M, et al. Determinants of Left Atrial Reservoir and Pump Strain and Use of Atrial Strain For Evaluation of Left Ventricular Filling Pressure. Eur Heart J Cardiovasc Imaging. 2021;23(1):61-70. doi: 10.1093/ehjci/jeaa415.

56. Oh JK, Miranda WR, Bird JG, Kane GC, Nagueh SF. The 2016 Diastolic Function Guideline: Is it Already Time to Revisit or Revise Them? JACC Cardiovasc Imaging. 2020;13(1 Pt 2):327-335. doi: 10.1016/j.jcmg.2019.12.004.

57. Smiseth OA, Morris DA, Cardim N, Cikes M, Delgado V, Donal E, et al. Multimodality Imaging in Patients with Heart Failure and Preserved Ejection Fraction: An Expert Consensus Document of the European Association of Cardiovascular Imaging. Eur Heart J Cardiovasc Imaging. 2022;23(2):e34-e61. doi: 10.1093/ehjci/jeab154.

58. Bhat A, Chen HHL, Khanna S, Mahajan V, Gupta A, Burdusel C, et al. Diagnostic and Prognostic Value of Left Atrial Function in Identification of Cardioembolism and Prediction of Outcomes in Patients with Cryptogenic Stroke. J Am Soc Echocardiogr. 2022;35(10):1064-76. doi: 10.1016/j.echo.2022.05.018.

59. Bisbal F, Baranchuk A, Braunwald E, Luna AB, Bayés-Genís A. Atrial Failure as a Clinical Entity: JACC Review Topic of the Week. J Am Coll Cardiol. 2020;75(2):222-232. doi: 10.1016/j.jacc.2019.11.013.

Echocardiographic Evaluation of a Patient in Circulatory Shock: A Contemporary Approach

Rafael Modesto Fernandes,[1,2,4] *Alexandre Costa Souza,*[2,3] *Bruno de Freitas Leite,*[1,2] *Jun Ramos Kawaoka*[1,2]

Hospital Aliança Rede D´Or,[1] *Salvador, BA – Brazil*
Instituto D´Or de Pesquisa e Educação (IDOR),[2] *Salvador, BA – Brazil*
Hospital São Rafael Rede D´Or,[3] *Salvador, BA – Brazil*
Escola Bahiana de Medicina e Saúde Pública,[4] *Salvador, BA – Brazil*

Abstract

Circulatory shock is characterized by a state of inefficient tissue oxygen supply and multiple organ dysfunction. Patients with circulatory shock require fast and assertive diagnosis and therapies to reduce its high lethality. Echocardiography has already been established as a fundamental method in managing patients with circulatory shock. It provides crucial assistance in etiological diagnosis, prognosis, hemodynamic monitoring, and volume estimation in these patients; its potential advantages include portability, absence of contrast or radiation, low cost, and real-time serial assessment. In the intensive care unit setting, it demonstrates a high correlation with invasive (pulmonary artery catheter) and minimally invasive (transpulmonary thermodilution) forms of hemodynamic monitoring. Currently, other techniques, such as pulmonary ultrasound and VExUS score, have been added to echocardiographic assessment, making the method more comprehensive and accurate. These techniques add relevant data to blood volume estimation in critical patients, influencing the probabilistic decision of fluid responsiveness and providing additional information in the diagnostic reasoning of the causes of shock, thus optimizing these patients' prognosis. Point of care ultrasound (POCUS) aims to make abilities to obtain information at the bedside more accessible to physicians who are not specialists in radiology, by means of ultrasound, which assists them in decision-making. This article addresses the diverse applications of echocardiography in patients with circulatory shock, including prognostic evaluation and etiological diagnosis by means of the parameters found in the main causes of shock, in addition to hemodynamic monitoring, evaluation of fluid responsiveness, and practical use of pulmonary ultrasound.

Introduction

The use of the echocardiogram is becoming more common in the daily practice of the intensive care unit (ICU), thus bringing several forms of application in the handling of the critical patient. Besides the many types of information that can be obtained by the examination, there are advantages brought by the method itself, such as portability, lack of contrast or radiation, low cost and serial evaluation in real-time.[1]

Circulatory shock is characterized by a state of inefficiency of the tissue oxygen offer, leading to cell failure and multiple organ dysfunction. Therefore, patients with such a condition require fast and assertive diagnosis and therapies for the reduction of its high lethality. The point of care ultrasound (POCUS) aims at making the skills to obtain bedside information more accessible for the physician that is not specialized in radiology, through the ultrasound, helping them in the decision-making process.[2] Complementation with a comprehensive echocardiography, performed by an imaging expert, makes this relationship even narrower and beneficial, optimizing the prognosis of the critical patient.

In this article, we describe several forms of application of the echocardiogram and POCUS in patients in circulatory shock, including diagnosis, prognosis, hemodynamic monitoring, fluid-responsiveness evaluation and use of a lung ultrasound.

Keywords

Circulatory shock; Diagnosis; Prognosis; Lung ultrasound; Fluid-responsiveness.

Mailing Address: Rafael Modesto Fernandes •
Hospital Aliança Rede D´Or. Avenida Juracy Magalhães Júnior, 2096. Postal Code 41920-180. Rio Vermelho, Salvador, BA – Brazil
E-mail: rafaelmodesto@cardiol.br
Manuscript received September 17, 2022; revised October 18, 2022; accepted December 22, 2022
Editor responsible for the review: Daniela do Carmo Rassi Frota

DOI: https://doi.org/10.36660/abcimg.20230013i

Echocardiographic evaluation by etiology

Cardiogenic shock

Cardiogenic shock is caused by a severe involvement of the myocardial function, leading to reduced cardiac output, tissue hypoperfusion and hypoxia. In patients hospitalized with acute heart failure (HF), the incidence of cardiogenic shock is of about 12%, and ischemic disease is responsible for approximately 80% of these cases. [3] Despite the significant advances in reperfusion therapy and circulatory support devices, mortality rates remain high, reaching up to 50%.[4]

Due to the multiplicity of causes and physiopathological mechanisms that lead to cardiogenic shock, its recognition is based on the combination of low cardiac output, signs of high filling pressure and structural and functional heart disease. The typical pattern includes low systolic volume associated with high left atrial pressure (increased mitral flow E-wave velocity and E/e' ratio).[5] The left atrium (LA) and left ventricle (LV) size may provide clues about the duration of the contractile involvement, and dilation indicates a stage of chronicity.

Contents

The LV ejection fraction (LVEF) is a traditional and practical parameter, besides a useful bedside guide to estimate systolic function. The interpretation needs to consider the preload effects (volemia), blood pressure (afterload), inotropics and vasopressors. The estimation of the LV systolic volume and cardiac output through the echocardiogram is well validated, being a useful parameter for the diagnosis of cardiogenic shock. The velocity time integral (VTI) of the left ventricular outflow tract (LVOT) can be used as a replacement for systolic volume, being a more practical parameter to be obtained, with lower interobserver variability. If it is higher than 18 cm, it is suggestive of proper systolic volume.[6]

In cardiogenic shock caused by ischemia, it is important to assess the associated mechanical complications: acute mitral insufficiency (MI), rupture of the interventricular septum (IVS) or the myocardial wall with or without formation of a pseudoaneurysm. All of these complications usually have a bimodal peak incidence.[7]

Cardiogenic shock associated with isolated right HF is characterized by low cardiac output associated with high right atrial pressure, dilated right atrium (RA) and dilated inferior (IVC) and superior vena cava, without significant pulmonary hypertension (PH), besides the finding of a dilated right ventricle (RV) with dysfunction. It is associated with inferior wall acute myocardial infarction (AMI), with proximal occlusion of the right coronary artery, and it is an adverse prognostic marker.[8]

Valvulopathy is a major cause of cardiogenic shock. The echocardiogram plays an essential role at identifying valvular disease, its severity and possible complications. Atrial fibrillation with high ventricular response in patients with mitral stenosis, significant valvular regurgitation due to infectious endocarditis or degenerative disease (chordae tendineae rupture) or aortic failure secondary to aortic dissection are some examples of acute causes, which lead to a challenge in the echocardiographic evaluation. Severe aortic stenosis can also be presented in cardiogenic shock, but it is usually secondary to acute decompensation in the context of subjacent severe chronic systolic dysfunction.[4]

There are many other conditions, such as stress cardiomyopathy, acute myocarditis, tachycardiomyopathy, which can be presented as cardiogenic shock. In these cases, the echocardiogram will show a compromised LV systolic function, with reduction of the VTI of the LVOT, suggesting the cardiogenic origin of the shock. The systolic dysfunction of the LV is usually characterized by diffuse hypokinesis, except for cardiopathies that can lead to segmental changes in contractility, such as ischemic cardiopathy or Takotsubo cardiomyopathy. Regional involvement is characteristic of the latter, showing apical ballooning and hypercontractility of basal segments.[9]

Acute pulmonary thromboembolism (APT)

In acute pulmonary embolism, there is a sudden increase in pulmonary vascular resistance (PVR), overlapping the capacity of the RV, which is adapted to a low-pressure regime. Consequently, there is acute dilation in the basal and medium regions of the RV, associated with a compromised systolic function. There is some preservation of the apical region of the RV, limited by the insertion of a lateral moderator band, in which systolic function is normal or increased. This finding, called "McConnell's sign",[10] is characteristic, but not pathognomonic, also occurring in RV infarction.

The RV prolongs its systolic time when faced with an afterload increase, so that the pressure in the RV exceeds the pressure in the LV at the end of the systole; such an effect is exacerbated by the underfilling of the left heart due to pulmonary oligoemia. Therefore, we find the paradoxical motion of the IVS with systolic rectification (observed at the parasternal short axis view when the LV takes on a D-shape during systole). The dilation of the RV is the keystone, and its association with the paradoxical septal motion defines the acute *cor pulmonale*. The dilation of the RV is promptly evaluated in the apical four chamber view, when the RV/LF ratio is >0.6; severe dilation is seen with a >1.0 proportion.[11] Acutely, the diameter of the pulmonary artery and the volume of the RA remain normal.

The evaluation of the LV is also informative in massive pulmonary thromboembolism (PTE), with small cavity and reduction of cardiac output. The presence of thrombus in the right chambers, IVC or pulmonary artery is occasionally seen, and reinforces PTE as a shock etiology – characterized as a low-flow obstructive shock, when VTI of the LVOT and cardiac output are typically low.[12]

The measures of the pulmonary artery systolic pressure (PASP), systolic function of the RV and PVR are useful to confirm the increased afterload of the RV, and especially to assess the effects of thrombolysis and other interventions.

• PASP is more commonly obtained through the peak tricuspid regurgitation velocity, using the modified Bernoulli equation. It is important to pay attention to the alignment and obtaining of accurate Doppler signals to prevent the underestimation of measures. In the absence of a reliable signal of tricuspid regurgitation, the pulmonary ejection acceleration time (PAAT) can be used. As a reference, a 70-90 ms PAAT indicates PASP > 70 mmHg. The presence of a mid-systolic notch at the pulse Doppler in the right ventricular outflow tract (RVOT) also indicates severe pulmonary arterial hypertension (PAH).[13] In acute pulmonary embolism with hemodynamic repercussion, we typically see PASP with mild to moderate increase.

• The systolic function of the RV can be normal, hyperdynamic, right after the pulmonary embolism insult, or hypodynamic in further stages. The tricuspid annular plane systolic excursion (TAPSE) is an acceptable and easy method to be used at the bedside, with a narrow learning curve (normal value ≥ 17 mm). The velocity of the lateral tricuspid annular plane at the tissue Doppler can also be used, and the value of < 9.5 cm/s means ventricular dysfunction. More accurate parameters should be used whenever possible, such as: variation of the fractional area (normal value ≥ 35%), right ventricular free wall longitudinal strain (normal value > 20%), and ejection fraction in the 3D echocardiogram (normal value ≥ 45%);

however, these are not always feasible for the critical ICU patient at bedside.[14]

• PVR: the gold standard for PVR is right heart catheterization; however, several methods have been proposed to estimate PVR using the echocardiogram, each one using the principle of pressure in relation to cardiac output (that is, the ratio between the pressure in the pulmonary arterial bed and cardiac output). The following formula, proposed by Abbas and collaborators, can be used:[15] PVR = TRV / VTI_{RVOT} x 10 + 0.16, in which TRV is the tricuspid regurgitation velocity, which corresponds to the transpulmonary pressure gradient, and VTI_{RVOT} is the VTI of the RV outflow tract, which corresponds to pulmonary blood flow (PBF). When compared to the PVR estimated by hemodynamics, the author obtained excellent correlation, R = 0.929. However, this calculation can be influenced by other factors, such as the variation of the alveolar pressure and pulmonary venous pressure: the increased pressure in the LA reduces PVR.

Therefore, in practical terms, the echocardiographic findings of RV dilation, paradoxical septal motion and McConnell sign suggest the diagnosis of PTE with obstructive shock as a cause, and the findings of elevated PSAP and PVR, together with reduced cardiac outflow and systolic function of the RV, support it, being an essential tool in the indication of thrombolysis.

Sepsis

Sepsis is the most prevalent cause of shock in an ICU, and it is closely related to cardiac injury in severe cases. In practice, septic shock has a distribution pattern, and is characterized in the echocardiogram by the presence of hyperdynamic ventricles and high cardiac output (normal or high VTI in RVOT associated with tachycardia).[16] However, the evolution with concomitant ventricular dysfunction is observed in 20-60% of the severe cases and is associated with worse outcomes.[17]

A major pathological contribution for shock in sepsis is peripheral vasoplegia. Systemic vascular resistance (SVR) can be calculated using the formula: SVR = (mean arterial pressure - ventral venous pressure / cardiac output) x 79.9 (dyn.s/cm^{-5}), and is typically reduced in these patients. Besides, hypovolemia is frequently associated as a consequence of the reduced effective circulating volume related to venous dilation and to the increased capillary permeability with losses for the third space. Heart dysfunction is mainly caused by the liberation of cytokines, mitochondrial dysfunction and tissue hypoxia, which lead to myocardial lesion.[17]

The spectrum of involvement in septic cardiomyopathy can range, including dysfunction in the LV and/or RV, global hypokinesia or changes in segmental contractility and subtle findings only identified with strain.[18] The diastolic dysfunction of the LV with high filling pressure is also very common in this scenario. A recent meta-analysis showed reduced e' wave associations and high E/e' ratio as predictors of higher mortality rates among critical patients with sepsis.[19]

Many patients with myocardial depression in sepsis do not require the use of inotropic agents, because cardiac output is adequate even at the presence of damaged cardiac function, due to the associated reduction of the LV afterload and its mild dilation.

It is important to highlight that contractile dysfunction is almost always reversible throughout the days, except in the presence of concomitant subjacent coronary artery disease or myocarditis. The reduction in the LV afterload may mask systolic dysfunction, which can become obvious only after the correction of hypotension.[20]

The echocardiogram plays a pertinent role in the evaluation of the valves in septic shock. Endocarditis or perivalvular abscesses can be the cause of shock. Transesophageal echocardiogram (TEE) is the technique of choice in the presence of such a suspicion, even though the transthoracic echocardiogram is still valuable in the acute scenario.

The RV can also be impacted by the combined effects of sepsis in contractility and higher RV afterload (acute respiratory distress syndrome [ARDS] and mechanical ventilation). In 20% of the patients, RV dysfunction is the prevalent characteristic.[21]

Finally, it is important to verify the presence of dynamic outflow tract and mid-ventricular obstructions in the LV, once the combination of the hyperdynamic state and hypovolemia can induce them and contribute with the genesis of hypotension.

Therefore, the bedside echocardiogram in patients with septic shock provides valuable information and can help with strategies to handle this context.

Cardiac tamponade

Pericardial effusion is the accumulation of fluid in the pericardial space beyond the physiological volume. It is especially related to inflammatory causes, post-operative periods of heart surgery and as a complication of percutaneous heart procedures. Cardiac tamponade is a clinical diagnosis that happens when the pressure made by the pericardial fluid overcomes the pressure in the heart chambers. The classical signs of the Beck's triad (hypotension, jugular venous distension and muffled heart sounds) have limited sensitivity, turning clinical diagnosis into a challenging task.[22]

The echocardiogram plays an essential role in the quantification of pericardial effusion, definition of the etiological suspicion and its repercussion in ventricular filling, especially in the finding of early changes that precede the clinical tamponade. In the physiopathology of cardiac tamponade, the velocity of the installation of the effusion plays an essential part, beyond its magnitude. This information becomes relevant in scenarios in which the fast installation of the small pericardial effusion (right ventricular free wall rupture after the infarction, hemopericardium as a complication during percutaneous heart procedures) is sufficient to determine hemodynamic involvement. The volemic status of the patient also contributes with

the occurrence of clinical repercussion, and this data is also accessible in a non-invasive manner, through the echocardiogram. Besides, the echocardiogram can be essential in urgent situations, to guide the subxiphoid puncture for pericardiocentesis (Marfan's puncture).

The first step in the diagnosis of pericardial effusion is to differentiate it from the pleural effusion. In the parasternal long axis window, pericardial effusion is in an anterior position in relation to the descending thoracic aorta, in a cross-sectional view; the pleural effusion is posterior to that structure (Figure 1). It is important to differentiate the epicardial fat from the pericardial effusion, which has lower echogenicity in comparison with the myocardium, and moves along with it.

The quantification of the pericardial effusion is based on the size of the layer of fluid measured in diastole. If the layer is smaller than 10 mm, the effusion is considered as mild; between 10-20 mm, moderate; and higher than 20 mm, it is a major pericardial effusion.[23] It becomes a challenge to accurately quantify and grade the effusion when its distribution is heterogeneous.

The presence of debris, mass or clots should also be reported in the exam's report, contributing with the etiological diagnosis and proper treatment.

In the patient with hemodynamic instability associated with pericardial effusion, some objective data from the M-mode analysis and bidimensional method, besides changes in blood flow by the Doppler, are able to determine the presence of restriction in ventricular filling.[23]

The following findings can be observed in patients with cardiac tamponade (Figure 1):

a. Paradoxical motion of the IVS: bulging of the IVS towards the LV during inspiration. Echocardiographic representation of ventricular interdependence, being the mechanism in charge of the pulsus paradoxus that is present in tamponade.

b. Diastolic collapse of the RA: sensitive and early finding because it is a low-pressure chamber. This finding has more value when the duration of the RA collapse is superior to one third of the cardiac cycle.

c. Diastolic collapse of the RV: less sensitive finding, however, more specific for the tamponade diagnosis.

d. Respiratory variation of the mitral flow E-wave (> 25%) and of the tricuspid flow E-wave (> 40%).

e. Reduction of systolic volume and cardiac output during inspiration (echocardiographic representation of the pulsus paradoxus).

f. Dilated inferior vena cava (IVC > 21 mm) associated with respiratory variation lower than 50%. This is a very sensitive finding in the tamponade diagnosis, however, little specific, since it can be present in other clinical conditions.

Hypovolemia

The echocardiogram may provide several objective parameters of hypovolemia, which help in the etiological diagnosis of shock and in the monitoring of the response after volemic repositioning.

In severe hypovolemia we can see the collapse of the LV at the end of systole, sign that is classically called "kissing walls". However, this finding is not specific for the diagnosis of hypovolemia, since it can be present in conditions of low SVR, hyperdynamic states with high cardiac output or use of inotropics. Among hypovolemic patients, it is also possible to find reduced final diastolic diameter of the LV, inferring low preload. On the other hand, the fixed bulging of the interatrial septum addressed to the RA suggests increased left atrial pressure and possible reestablishment of normovolemia.[24]

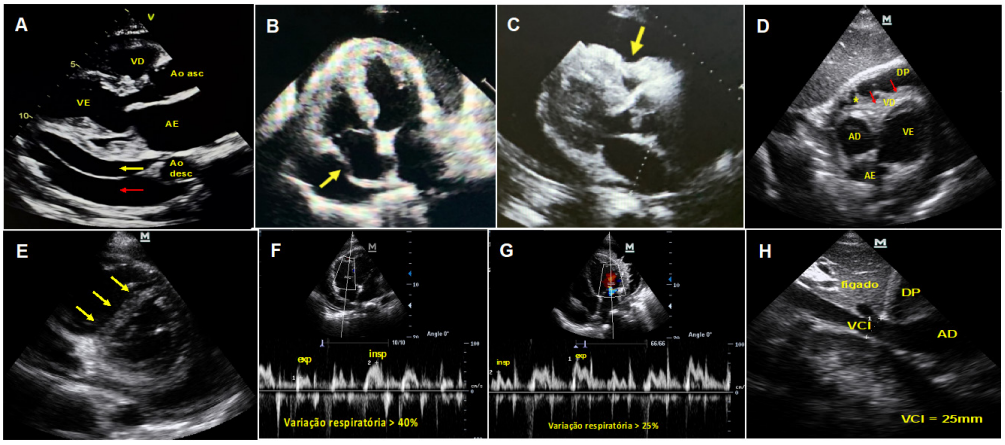

Figure 1 – *Evaluation of pericardial effusion and signs of cardiac tamponade. A. Differentiation between pericardial effusion (anterior to the descending aorta – yellow arrow) and pleural effusion (posterior to the descending aorta – red arrow). B. Transient collapse of the right atrium (arrow). C and D. Diastolic collapse of the right ventricle (arrow). There is presence of debris (asterisk). E. Paradoxical movement of the interventricular septum – displacement of interventricular septum towards the left ventricle during inspiration (echocardiographic representation of ventricular interdependence). F and G. Significant respiratory variation of E-waves of the mitral and tricuspid flow. H. Subcostal window showing plethoric inferior vena cava.*

Another parameter that is usually found among hypovolemic patients is collapsed IVC or with reduced dimensions. It is important to remember that in situations of right ventricular dysfunction, significant pericardial effusion, increased intra-abdominal pressure and in patients on mechanical ventilation, the use of IVC diameter and its respiratory variation becomes less reliable.[24]

Other common findings, however, not specific of hypovolemic shock, are VTI of LVOT below 18 cm, low systolic volume, low cardiac output and high SVR. One of the ways to distinguish it from a cardiogenic shock is to assess the filling pressure through the E/e' ratio, which will be reduced (E/e' < 8) in hypovolemic shock, besides the absence of dilation or LV dysfunction.[25]

The echocardiogram in hemodynamic monitoring

As observed, the echocardiogram can provide, in a non-invasive and serial manner, hemodynamic parameters using data from the Doppler and measures from the bidimensional method. In Figure 2, we describe how to classify the patient in circulatory shock profiles using echocardiographic parameters.

Besides showing high correlation with invasive (pulmonary artery catheterism) and minimally invasive forms (transpulmonary thermodilution) of hemodynamic monitoring, the echocardiogram presents the advantage of directly visualizing the heart structures and their functionalities.[24] Nowadays, other techniques, such as pulmonary ultrasound (PUS) and the VExUS score, have been added to the echocardiographic evaluation, making the method more comprehensive and accurate.[26,27]

The E/e' ratio, parameter that is exclusively obtained by the echocardiogram, has high correlation with the filling pressure of the left heart chambers, with significant prognostic value in the clinical context of the critical patient. Several studies have demonstrated that the E/e' ratio > 15 is predictive of an unfavorable outcome.[28]

The ventricular-arterial coupling (VAC) has become popular in the evaluation of the patient with cardiopathy. It is defined as the inter-relation between the left ventricular function and the arterial system, thus reflecting the global cardiovascular performance.[29] Mathematically, VAC is defined by the arterial elastance (Ea) divided by ventricular elastance at the end of the systole (Ees). Deriving from the Chen formula, the non-invasive measure of Ea and Ees is taken using simple data, such as systolic blood pressure, diastolic blood pressure, systolic volume, ejection fraction, time of total ejection and pre-ejection time. The normal values considered in consensus are: Ea = 2.2 ±0.8 mmHg/ml and Ees = 2.3 ±1.0 mmHg/ml. VAC (Ea/Ees) = 1 represents the ideal coupling, when there is the best ventricular work. Ea/Ees > 1 represents the ventricular-arterial decoupling, demonstrating inefficiency of the ventricular work. In the patient with decompensated HF, we can use VAC to guide therapy. When VAC >1 due to expressive increase in Ea, the therapy with vasodilators would reduces the Ea and, consequently, VAC. In the case of VAC > 1 due to reduction of Ees, therapy with inotropics would bring the ratio closer to the ideal value of 1.[30] As to the patient with septic shock, it is usual to see ventricular-arterial decoupling, especially due to expressive reduction of Ees. In this case, therapy with fluids and inotropics would restore the Ea/Ees ratio. On the other hand, the use of vasopressors alone would lead to worse coupling due to the isolated increase of Ea.[31]

Figure 3 shows how to measure the main echocardiographic parameters and their respective formulas.

Evaluation of fluid responsiveness

In-water resuscitation of the patient with circulatory shock aims at incrementing systolic volume and, consequently, cardiac output to improve tissue oxygenation. However, about half of the patients are considered as non-responsive to fluid therapy, and the early identification of this profile may prevent the risk of water overload.[32] Several parameters have been assessed as echocardiographic predictors of response to fluids. IVC is one of the classic parameters in the composition of the fluid responsiveness evaluation, and its plausibility is based on the lung-heart interaction. The variation of transpulmonary pressure while breathing is transmitted to the right cavities, making the venous return

SHOCK	IVC (RAP/CVP)	E/e' (PCP)	CO / CI	SVR	PVR
Hypovolemic	↓	↓	↓	↑	↓
Cardiogenic	↑	↑	↓	↑	↓
Distributive (septic)	↓	↓	↑↓	↓	↓
Pulmonary thromboembolism	↑	↑↓	↓	↑	↑
Cardiac tamponade	↑	↑↓	↓	↑	↓

Figure 2 – *Behavior of echocardiographic parameters according to type of shock. IVC: inferior vena cava; RAP: right atrium pressure; CVP: central venous pressure; PCP: pulmonary capillary pressure; CO: cardiac output; CI: cardiac index; SVR: systemic vascular resistance; PVR: pulmonary vascular resistance.*

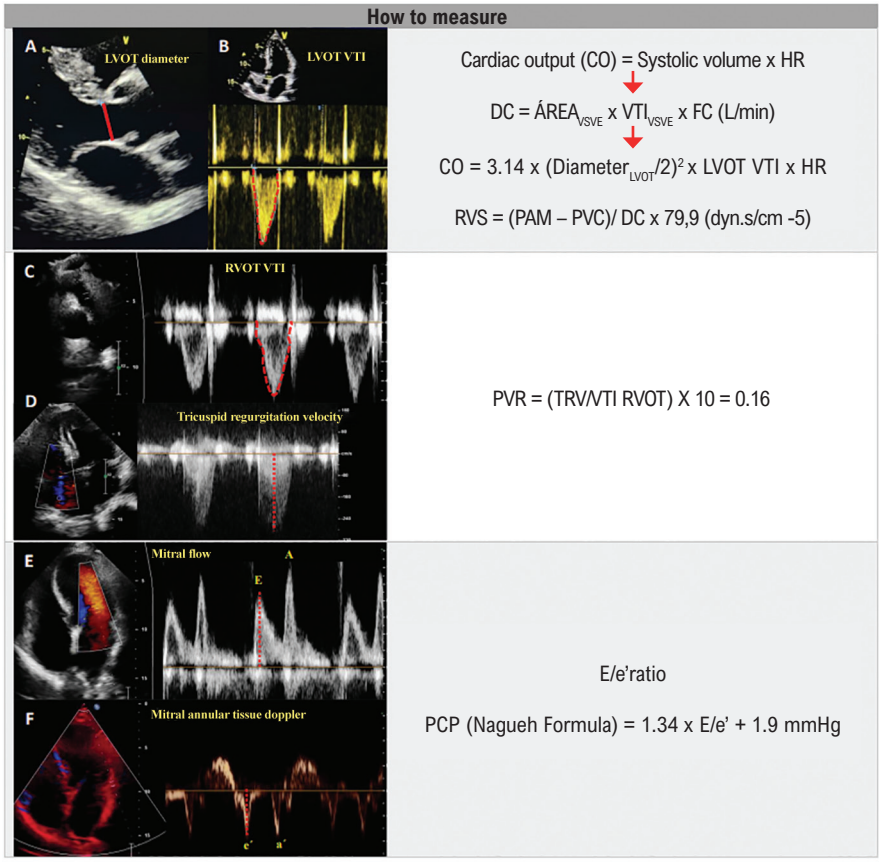

Figure 3 – *How to measure hemodynamic parameters with the echocardiogram. A and B: Cardiac output (CO) calculation, using the LVOT diameter (A) and LVOT VTI (B). Calculation of systemic vascular resistance, using CO, MAP and CVP estimation by the collapsibility index of the inferior vena cava; C and D: Calculation of pulmonary vascular resistance, using RVOT VTI (C) and tricuspid regurgitation velocity (D); E and F: Calculation of the E/e' ratio, using the E-wave mitral flow velocity (E) and the e'wave derived from the lateral mitral annular tissue Doppler (F). Calculation of PCP, using the E'e ratio by the Nagueh formula. CO: cardiac output; HR: heart rate; LVOT: left ventricle outflow tract; VTI: velocity time integral; SVR: systemic vascular resistance; PVS: pulmonary vascular resistance; TRV: tricuspid regurgitation velocity; RVOT: right ventricle outflow tract; PCP: pulmonary capillary pressure.*

vary. This ratio is influenced by the ventilatory mode and the complacence of the vena cava.[33]

IVC

The current recommendations suggest the evaluation of IVC to estimate the pressure inside the RA in non-ventilated patients, due to collapsing during inspiration: IVC diameter < 21 mm and collapsing > 50% suggests normal pressure (between 0 and 5 mmHg), whereas diameter > 21 mm and collapsing < 50% suggests high pressure (between 10 and 15 mmHg).(32) Vena cava diameter < 10 mm is common in states of hypovolemia and may indicate higher probability of response to fluids, whereas a diameter higher than 25 mm is associated with high volemic status and low probability of response to fluids. However, these static values are limited in the prediction of response to fluids, and the dynamic method based on the variation of IVC while breathing (distensibility index) allows to assess fluid-responsiveness more accurately. This calculation can be made using two different formulas, using the diameter of IVC at the end of inspiration and the end of expiration.[34] In ICUs with non-ventilated patients, the studies show high specificity, but low sensitivity.

Variation of systolic volume

The variation in systolic volume is a good indicator of fluid responsiveness, being easy to acquire and reproduce.[35] A variation in systolic volume higher than 12% was accurate to predict fluid responsiveness with values higher than 14%, being a strong predictor, and values below 10% with low correlation and response to volemic repositioning.

Even though static parameters have a limited value in the prediction of responsiveness to volume, such parameters can provide additional information for the probability evaluation in bedside decisions regarding resuscitation with fluids in the circulatory shock.

Cavity dimension

The presence of reduced LV dimensions with final diastolic area of the LV in the cross-sectional axis at the level of papillary muscles < 10 cm² with signs of hypercontractility (*"kissing walls"*) is a strong predictor of hypovolemia.[33]

The RV dilation after massive administration of fluids is usually seen in patients in volemic resuscitation, and it may work as one of the parameters for the adoption of protective ventilatory measures and interruption of the strategy of fluid administration.

Passive *leg raising* (leg elevation test)

A simple method used at bedside that uses the elevation of lower limbs at 45º and parameters of systolic volume or isolated VTI with variation above 10% suggests fluid responsiveness.[33] Echocardiogram remains as a practical instrument and with a valuable additional resource in the decision of administering fluids in the resuscitation of patients with acute circulatory failure, aiming at incrementing the systolic volume, and, consequently, cardiac output.

VExUS Ultrasound

The presence of right heart chamber overload, determining systemic venous congestion, has been underestimated in the evaluation at bedside of the critical patient due to the limitation of the traditional physical exam. The development of a tool addressed to systemic venous ultrasound (VExUS) and the growth of the *"point of care"* in the past decade enabled the use of a useful tool in the intensive care practice.[26]

Recent data guide the role of the VExUS score ultrasound for the evaluation of systemic congestion through the assessment of VCI and the venous flow of hepatic, renal and portal veins (Figure 4).

Under normal circumstances, the venous compartment is highly complacent with high capacitance; therefore, the more distal the heart, the more blunted the venous pulse, so that in smaller veins the flow becomes wavy, with a phasic nature. However, in states of right ventricular failure or overload in intravascular volume, the venous compartment is congested, and the limits of venous complacence are reached. Under these circumstances, the normal blunting of the venous pulse, due to the complacent nature of the smaller veins, is lost, and the pulsations are transmitted in a retrograde manner to the smaller veins.[36]

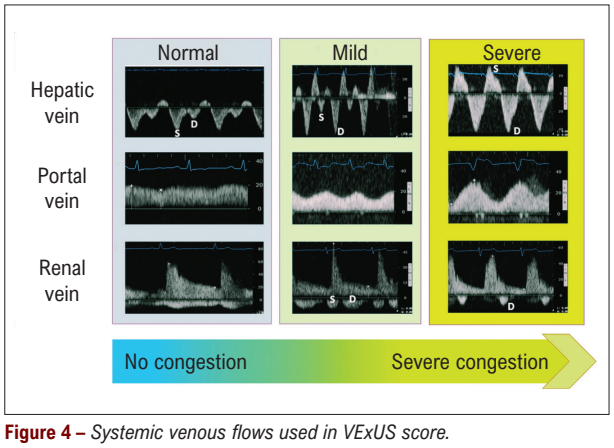

Figure 4 – *Systemic venous flows used in VExUS score.*

Hepatic venous circulation follows this path: portal vein, hepatic sinusoids, hepatic veins and IVC. Due to the distance from the heart, the normal portal venous flow is wavy and has a phasic nature. While the venous congestion increases, the retrograde flow of the hepatic vein generated by atrial contraction is transmitted by hepatic sinusoids and to the portal vein, where the impedance to the hepatoportal flow begins. This makes the normal wavy flow become progressively pulsatile, and this phenomenon is aggravated when there is systolic reversion of the venous return to the heart. Eventually, pulsatility becomes significant enough to cause a biphasic pattern. The intrarenal Doppler signal is usually a continuous monophasic flow below the baseline. With the increasing venous congestion, venous flow becomes pulsatile, and then progresses to an interrupted biphasic flow that is correlated with the S and D waves of the hepatic vein flow.[36]

PUS in shock

The use of a PUS has been highlighted in several clinical scenarios, and especially in critical intensive care patients. In patients with shock, it has a huge potential of helping the etiological diagnosis, besides providing information related to the level of lung involvement, associated congestion and/or complications related to mechanical ventilation.[37] Its feasibility at bedside, low cost, absence of radiation and obtention of this information in a serial manner are, without question, advantages of this method in relation to the others.

Technical aspects of PUS

PUS may require sectoral, convex or linear probes. Due to the physical principles inherent to the method, those transducers with lower frequency (sectoral and convex) will be ideal to assess lung parenchyma, whereas those with higher frequency will better visualize the subpleural and pleural space.[38] We should sweep using the ultrasound in several zones, and the disposition of the transducer can be perpendicular to the ribs, as well as along the intercostal spaces.

PUS can be performed both in the sitting and in the supine position; however, the position should be constant, because pulmonary fluid changes according to posture, and this must be written in the report. The device should be configured for the better processing of the image, adjusting frequency, depth, focus and gain appropriately. Each point should be assessed for at least one complete respiratory cycle.[38]

Many protocols have been validated in the literature, with the thoracic wall being divided in quadrants and the changes reported by sectors, or as a sum of each

region.[39] A more comprehensive and systematic approach is recommended whenever possible, dividing the thorax in 12 (upper and lower portion in the anterior, lateral and posterior region of each hemithorax), or 8 quadrants (excluding the posterior region). However, in emergency situations, requiring fast bedside answers, we can use a more focused and simple analysis. In this sense, a total of 6 quadrants is recommended: anterior, upper and posterolateral of each hemithorax.

Applicability of the PUS

The normal PUS image is characterized by lung sliding and by repetitions of hyperechogenic horizontal lines, called A Lines. The reduction in lung aeration due to inflammatory alveolar infiltration or congestion triggers the onset of vertical hyperechogenic lines, called B lines.[40]

PUS is more sensitive to detect pulmonary congestion when compared to the clinical exam and/or thoracic X-ray. Besides, the early detection of pulmonary congestion at bedside is essential to optimize the treatment and improve the prognosis of unstable patients with decompensated HF.[41] The detection of B lines is originated due to an artifact caused by the presence of extravasated fluid in the interstitium and pulmonary alveoli, reducing lung aeration. Therefore, other pathologies that lead to this physiopathological process can originate the same ultrasound image (viral pneumonitis and ARDS, for instance). Therefore, there are some signals suggesting that B lines are caused by congestion: 1) concordance with echocardiographic parameters of increasing filling pressures in the LV or increased atrial pressure; 2) thin pleural line with preserved sliding; 3) absence of subpleural involvement; 4) bilateral distribution of B lines, with prevalence in basal pulmonary segments; 5) coalescent B lines and absence of spared areas; 6) coexisting pleural effusion.[41]

Besides making the diagnosis of pulmonary involvement and its probable etiology, it is essential to quantify the level of B lines identified in PUS, monitoring the treatment and helping care management in a serial manner.

There are several ways described in the literature for that quantification.[41] The most practical way is to add the number of B lines visualized in the full sweep: 6 to 15 – mild; 16 to 30 – moderate; > 30 – major. Another validated way is to add up the score found in each studied zone, and the points would be discriminated as follows: 0 (absence or up to 3 B lines), 1 (> 3 B lines), 2 (coalescent B lines) and 3 (consolidation).

The quantification of B lines carried out by PUS is highly correlated with the findings of the computed tomography and in the evaluation by transpulmonary thermodilution.[42] The monitoring of pulmonary involvement and the serial bedside evaluation are useful tools in many situations, such as: 1) identifying the ideal moment for the weaning of invasive mechanical ventilation and as a predictor of a flawed extubation, 2) assessing the response after interventions, such as maneuvers of physical therapy recruitment, ideal positive end-expiratory pressure (PEEP) adjustment, therapeutic bronchoscopy, estimation of volemia and response after diuretic therapy and evolution of lung aeration after devices of pulmonary circulation assistance.

PUS is also accurate to diagnose other conditions associated with critical patients (pneumothorax, pleural effusion, pneumonia and pulmonary embolism). In Figure 5, we describe the normal pattern and the images found in several pathological situations.

Some algorithms were proposed in the literature to guide the diagnosis based on PUS.[43] We can emphasize the modified BLUE and FALLS protocols (Figure 6), both with excellent accuracy and an important tool in the etiological investigation of patients with respiratory failure and circulatory shock, respectively.

Limitations of the PUS

Even though the method is easier to execute than other modalities of ultrasound, it requires training and development of skills; its learning curve is relatively short.

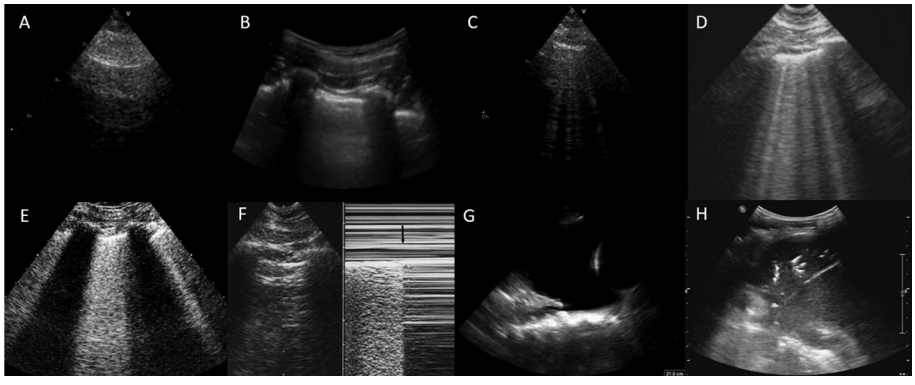

Figure 5 – *Normal and pathological findings in pulmonar ultrasound. Normal pulmonary ultrasound using a sector transducer (A) and a convex transducer (B). C. B lines in small quantity. D. B lines in large quantity with spared areas. E. B lines in large coalescent quantities. F. To the left, there are A lines in 2D and, to the right, the typical pattern of pneumothorax M-mode (arrow demonstrating lung point). G. Pleural effusion. H. Pneumonia.*

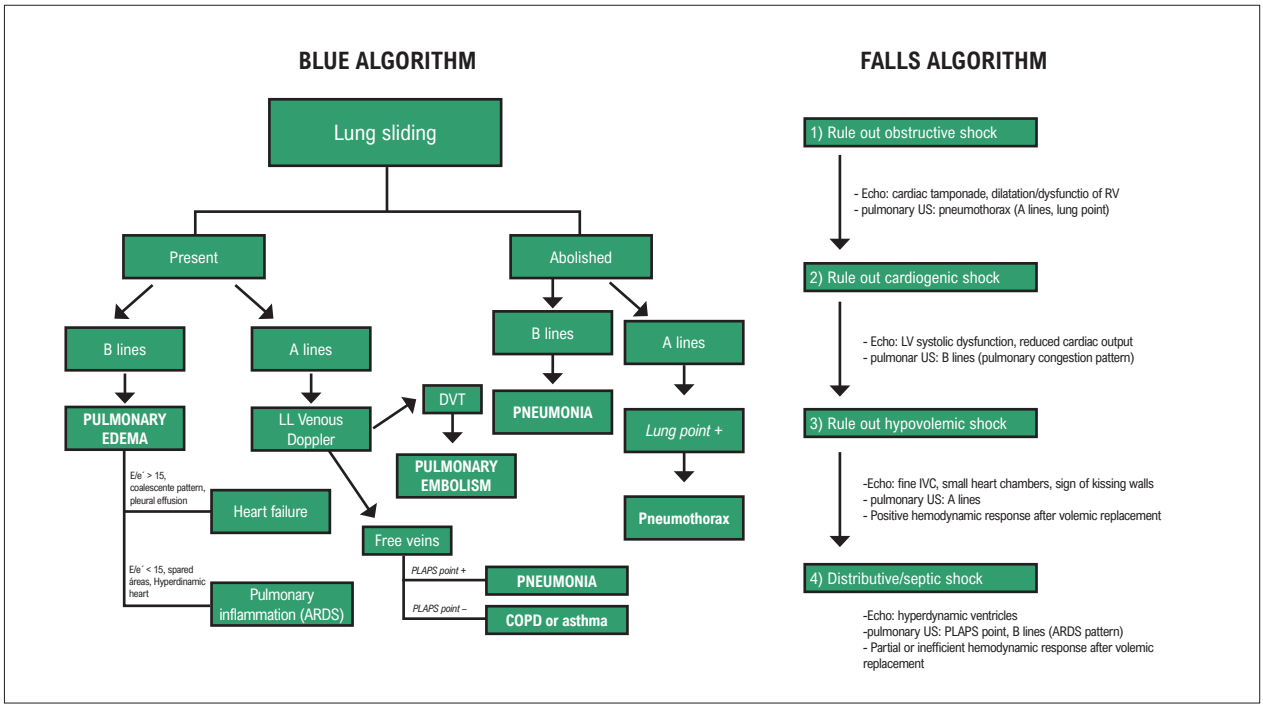

Figure 6 – *LL: lower limbs; ARDS: Acute respiratory distress syndrome; DVT: deep venous thrombosis; PLAPS: posterolateral alveolar and/or pleural syndrome; COPD: chronic obstructive pulmonar disease; RV: right ventricle; LV: left ventricle; IVC: inferior vena cava. Source: Adapted from Lichtenstein DA (2015).*[43]

The inter and intra-observer variability is small (lower than 5%), and the feasibility of the method is high. However, there may be difficulties related to the critical patient, such as inadequate acoustic window, difficulties in positioning, chest seals and/or presence of subcutaneous emphysema.[38]

PUS is very accurate to identify lung involvement and other comorbidities related to the critical patient. However, the findings should be interpreted within the context of each patient in the ICU, including clinical, laboratory parameters and other imaging exams.

Conclusions

The echocardiogram plays an essential role in the management of the patient in circulatory shock. It is a crucial help in etiological diagnosis, prognosis, hemodynamic monitoring and volemic estimation of these patients. Its application in a critical patient environment should be more and more incorporated to the daily practice.

Added to the strategy of bedside echocardiogram, the use of lung ultrasound and VExUS score may add relevant data to the estimation of volemia in a critical patient, thus influencing the probabilistic decision of fluid-responsiveness and aggregating information to the diagnostic logic of the causes of shock.

Potential Conflict of Interest

No potential conflict of interest relevant to this article was reported.

Sources of Funding

There were no external funding sources for this study.

Study Association

This study is not associated with any thesis or dissertation work

Author Contributions

Conception and design of the research and writing of the manuscript: Fernandes RM, Souza AC, Leite BF, Kawaoka JR; critical revision of the manuscript for intellectual content: Fernandes RM.

Ethics Approval and Consent to Participate

This article does not contain any studies with human participants or animals performed by any of the authors.

References

1. Vieillard-Baron A, Millington SJ, Sanfilippo F, Chew M, Diaz-Gomez J, McLean A, et al. A Decade of Progress in Critical Care Echocardiography: A Narrative Review. Intensive Care Med. 2019;45(6):770-8. doi: 10.1007/s00134-019-05604-2.
2. Rajamani A, Shetty K, Parmar J, Huang S, Ng J, Gunawan S, et al. Longitudinal Competence Programs for Basic Point-of-Care Ultrasound in Critical Care: A Systematic Review. Chest. 2020;158(3):1079-89. doi: 10.1016/j.chest.2020.03.071.

3. Follath F, Yilmaz MB, Delgado JF, Parissis JT, Porcher R, Gayat E, et al. Clinical Presentation, Management and Outcomes in the Acute Heart Failure Global Survey of Standard Treatment (ALARM-HF). Intensive Care Med. 2011;37(4):619-26. doi: 10.1007/s00134-010-2113-0.

4. van Diepen S, Katz JN, Albert NM, Henry TD, Jacobs AK, Kapur NK, et al. Contemporary Management of Cardiogenic Shock: A Scientific Statement from the American Heart Association. Circulation. 2017;136(16):e232-e268. doi: 10.1161/CIR.0000000000000525.

5. Nagueh SF, Smiseth OA, Appleton CP, Byrd BF 3rd, Dokainish H, Edvardsen T, et al. Recommendations for the Evaluation of Left Ventricular Diastolic Function by Echocardiography: An Update from the American Society of Echocardiography and the European Association of Cardiovascular Imaging. Eur Heart J Cardiovasc Imaging. 2016;17(12):1321-60. doi: 10.1093/ehjci/jew082.

6. Blanco P. Rationale for Using the Velocity-Time Integral and the Minute Distance for Assessing the Stroke Volume and Cardiac Output in Point-of-Care Settings. Ultrasound J. 2020;12(1):21. doi: 10.1186/s13089-020-00170-x.

7. Simoons ML, ten Cate FJ. Role of Echocardiography in Acute Coronary Syndromes. Eur J Echocardiogr. 2004;5(2):97-8. doi: 10.1016/j.euje.2004.01.004.

8. O'Rourke RA, Dell'Italia LJ. Diagnosis and Management of Right Ventricular Myocardial Infarction. Curr Probl Cardiol. 2004;29(1):6-47. doi: 10.1016/j.cpcardiol.2003.08.003.

9. Pieroni M, Bolognese L. Takotsubo (Stress) Cardiomyopathy. N Engl J Med. 2015;373(27):2689. doi: 10.1056/NEJMc1512595.

10. Sosland RP, Gupta K. Images in Cardiovascular Medicine: Mcconnell's Sign. Circulation. 2008;118(15):e517-8. doi: 10.1161/CIRCULATIONAHA.107.746602.

11. Jardin F, Dubourg O, Bourdarias JP. Echocardiographic Pattern of Acute Cor Pulmonale. Chest. 1997;111(1):209-17. doi: 10.1378/chest.111.1.209.

12. Bernard S, Namasivayam M, Dudzinski DM. Reflections on Echocardiography in Pulmonary Embolism-Literally and Figuratively. J Am Soc Echocardiogr. 2019;32(7):807-810. doi: 10.1016/j.echo.2019.05.007.

13. Tossavainen E, Söderberg S, Grönlund C, Gonzalez M, Henein MY, Lindqvist P. Pulmonary Artery Acceleration Time in Identifying Pulmonary Hypertension Patients with Raised Pulmonary Vascular Resistance. Eur Heart J Cardiovasc Imaging. 2013;14(9):890-7. doi: 10.1093/ehjci/jes309.

14. Lang RM, Badano LP, Mor-Avi V, Afilalo J, Armstrong A, Ernande L, et al. Recommendations for Cardiac Chamber Quantification by Echocardiography in Adults: An Update from the American Society of Echocardiography and the European Association of Cardiovascular Imaging. Eur Heart J Cardiovasc Imaging. 2015;16(3):233-70. doi: 10.1093/ehjci/jev014.

15. Abbas AE, Fortuin FD, Patel B, Moreno CA, Schiller NB, Lester SJ. Noninvasive Measurement of Systemic Vascular Resistance Using Doppler Echocardiography. J Am Soc Echocardiogr. 2004;17(8):834-8. doi: 10.1016/j.echo.2004.04.008.

16. De Backer D. Detailing the Cardiovascular Profile in Shock Patients. Crit Care. 2017;21(Suppl 3):311. doi: 10.1186/s13054-017-1908-6.

17. Vallabhajosyula S, Jentzer JC, Geske JB, Kumar M, Sakhuja A, Singhal A, et al. New-Onset Heart Failure and Mortality in Hospital Survivors of Sepsis-Related Left Ventricular Dysfunction. Shock. 2018;49(2):144-9. doi: 10.1097/SHK.0000000000000952.

18. Orde SR, Pulido JN, Masaki M, Gillespie S, Spoon JN, Kane GC, et al. Outcome Prediction in Sepsis: Speckle Tracking Echocardiography Based Assessment of Myocardial Function. Crit Care. 2014;18(4):R149. doi: 10.1186/cc13987.

19. Sanfilippo F, Corredor C, Arcadipane A, Landesberg G, Vieillard-Baron A, Cecconi M, et al. Tissue Doppler Assessment of Diastolic Function and Relationship with Mortality in Critically Ill Septic Patients: A Systematic Review and Meta-Analysis. Br J Anaesth. 2017;119(4):583-94. doi: 10.1093/bja/aex254.

20. Boissier F, Razazi K, Seemann A, Bedet A, Thille AW, de Prost N, et al. Left Ventricular Systolic Dysfunction During Septic Shock: The Role of Loading Conditions. Intensive Care Med. 2017;43(5):633-42. doi: 10.1007/s00134-017-4698-z.

21. Geri G, Vignon P, Aubry A, Fedou AL, Charron C, Silva S, et al. Cardiovascular Clusters in Septic Shock Combining Clinical and Echocardiographic Parameters: A Post Hoc Analysis. Intensive Care Med. 2019;45(5):657-67. doi: 10.1007/s00134-019-05596-z.

22. Roy CL, Minor MA, Brookhart MA, Choudhry NK. Does this Patient with a Pericardial Effusion Have Cardiac Tamponade? JAMA. 2007;297(16):1810-8. doi: 10.1001/jama.297.16.1810.

23. Klein AL, Abbara S, Agler DA, Appleton CP, Asher CR, Hoit B, et al. American Society of Echocardiography Clinical Recommendations for Multimodality Cardiovascular Imaging of Patients with Pericardial Disease: Endorsed by the Society for Cardiovascular Magnetic Resonance and Society of Cardiovascular Computed Tomography. J Am Soc Echocardiogr. 2013;26(9):965-1012.e15. doi: 10.1016/j.echo.2013.06.023.

24. McLean AS. Echocardiography in Shock Management. Crit Care. 2016;20:275. doi: 10.1186/s13054-016-1401-7.

25. Cecconi M, De Backer D, Antonelli M, Beale R, Bakker J, Hofer C, et al. Consensus on Circulatory Shock and Hemodynamic Monitoring. Task Force of the European Society of Intensive Care Medicine. Intensive Care Med. 2014;40(12):1795-815. doi: 10.1007/s00134-014-3525-z.

26. Rola P, Miralles-Aguiar F, Argaiz E, Beaubien-Souligny W, Haycock K, Karimov T, et al. Clinical Applications of the Venous Excess Ultrasound (Vexus) Score: Conceptual Review and Case Series. Ultrasound J. 2021;13(1):32. doi: 10.1186/s13089-021-00232-8.

27. Porter TR, Shillcutt SK, Adams MS, Desjardins G, Glas KE, Olson JJ, et al. Guidelines for the Use of Echocardiography as a Monitor for Therapeutic Intervention in Adults: A Report from the American Society of Echocardiography. J Am Soc Echocardiogr. 2015;28(1):40-56. doi: 10.1016/j.echo.2014.09.009.

28. Jentzer JC, Anavekar NS, Mankad SV, Khasawneh M, White RD, Barsness GW, et al. Echocardiographic Left Ventricular Diastolic Dysfunction Predicts Hospital Mortality After Out-Of-Hospital Cardiac Arrest. J Crit Care. 2018;47:114-120. doi: 10.1016/j.jcrc.2018.06.016.

29. Saeed S, Holm H, Nilsson PM. Ventricular-Arterial Coupling: Definition, Pathophysiology and Therapeutic Targets in Cardiovascular Disease. Expert Rev Cardiovasc Ther. 2021;19(8):753-61. doi: 10.1080/14779072.2021.1955351.

30. Vriz O, Fadl Elmula FM, Antonini-Canterin F. Noninvasive Assessment of Ventricular-Arterial Coupling in Heart Failure. Heart Fail Clin. 2021;17(2):245-54. doi: 10.1016/j.hfc.2020.12.003.

31. Monge García MI, Santos A. Understanding Ventriculo-Arterial Coupling. Ann Transl Med. 2020;8(12):795. doi: 10.21037/atm.2020.04.10.

32. Furtado S, Reis L. Inferior Vena Cava Evaluation in Fluid Therapy Decision Making in Intensive Care: Practical Implications. Rev Bras Ter Intensiva. 2019;31(2):240-47. doi: 10.5935/0103-507X.20190039.

33. Charron C, Caille V, Jardin F, Vieillard-Baron A. Echocardiographic Measurement of Fluid Responsiveness. Curr Opin Crit Care. 2006;12(3):249-54. doi: 10.1097/01.ccx.0000224870.24324.cc.

34. Airapetian N, Maizel J, Alyamani O, Mahjoub Y, Lorne E, Levrard M, et al. Does Inferior Vena Cava Respiratory Variability Predict Fluid Responsiveness in Spontaneously Breathing Patients? Crit Care. 2015;19:400. doi: 10.1186/s13054-015-1100-9.

35. Michard F, Teboul JL. Predicting Fluid Responsiveness in ICU Patients: A Critical Analysis of the Evidence. Chest. 2002;121(6):2000-8. doi: 10.1378/chest.121.6.2000.

36. Beaubien-Souligny W, Rola P, Haycock K, Bouchard J, Lamarche Y, Spiegel R, et al. Quantifying Systemic Congestion with Point-of-Care Ultrasound: Development of the Venous Excess Ultrasound Grading System. Ultrasound J. 2020;12(1):16. doi: 10.1186/s13089-020-00163-w.

37. Lichtenstein DA, Malbrain MLNG. Lung Ultrasound in the Critically Ill (LUCI): A Translational Discipline. Anaesthesiol Intensive Ther. 2017;49(5):430-36. doi: 10.5603/AIT.a2017.0063.

38. Stassen J, Bax JJ. How to Do Lung Ultrasound. Eur Heart J Cardiovasc Imaging. 2022;23(4):447-49. doi: 10.1093/ehjci/jeab241.

39. Kok B, Schuit F, Lieveld A, Azijli K, Nanayakkara PW, Bosch F. Comparing Lung Ultrasound: Extensive Versus Short in COVID-19 (CLUES): A Multicentre, Observational Study at the Emergency Department. BMJ Open. 2021;11(9):e048795. doi: 10.1136/bmjopen-2021-048795.

40. Lichtenstein D. Lung Ultrasound in the Critically ill. Curr Opin Crit Care. 2014;20(3):315-22. doi: 10.1097/MCC.0000000000000096.

41. Platz E, Jhund PS, Girerd N, Pivetta E, McMurray JJV, Peacock WF, et al. Expert Consensus Document: Reporting Checklist for Quantification of Pulmonary Congestion by Lung Ultrasound in Heart Failure. Eur J Heart Fail. 2019;21(7):844-51. doi: 10.1002/ejhf.1499.

42. Picano E, Scali MC, Ciampi Q, Lichtenstein D. Lung Ultrasound for the Cardiologist. JACC Cardiovasc Imaging. 2018;11(11):1692-705. doi: 10.1016/j.jcmg.2018.06.023.

43. Lichtenstein DA. BLUE-Protocol and FALLS-Protocol: Two Applications of Lung Ultrasound in the Critically ill. Chest. 2015;147(6):1659-70. doi: 10.1378/chest.14-1313.

Review Article

My Approach to "Athlete'S Heart": Evaluation of the Different Types of Adaptation to Exercise

Frederico José Neves Mancuso[1]
Universidade Federal de São Paulo, Escola Paulista de Medicina (UNIFESP/EPM),[1] São Paulo, SP – Brazil

Abstract

Exercise-induced adaptation may occur in amateur and professional athletes. This condition is commonly named "athlete's heart". The alterations observed include dilation of the heart chambers, increased myocardial thickness, improved ventricular filling, increased left ventricular trabeculation, dilation of the inferior vena cava, among others. These changes can also be observed in some heart diseases, such as dilated, hypertrophic and other cardiomyopathies (CMP). Thus, cardiac imaging tests are fundamental in identifying these alterations and in differentiating between "athlete's heart" and possible heart disease.

Introduction

Exercise-induced structural and/or functional heart alterations have been the object of study for more than 100 years, with their first reports appearing at the end of the nineteenth and the beginning of the twentieth century, referent to a dilated heart and a lower heart rate.[1] The development of complementary exams showed changes in electrocardiograms, chest X-rays, echocardiography, among other exams in athletes.[1]

Exercise-induced cardiac remodelling depends on a wide range of variables, including the type of exercise, the intensity, and the duration of training, generally with a "dose-effect" relation.[2] It is interesting to note that other variables are also involved in the adaptation, such as age, ethnicity, gender, and body size.[2]

The growing number of amateur and professional athletes periodically submitted to a cardiological evaluation before participating in activities or during the years of sports practice has led to a challenge in recognizing exercise-induced adaptation and its difference from potentially fatal heart conditions, such as hypertrophic cardiomyopathy (CMP), dilated CMP, arrhythmogenic right ventricular CMP, and non-compacted myocardium.[1]

Keywords

Athlete´s heart; ecocardiography; cardiomyopathy; adaptive cardiac remodeling

Mailing Address: Frederico José Neves Mancuso •
Rua Botucatu, 740 – 2º andar. Postal Code 04023-062. São Paulo – SP.
E-mail: fredmancuso@uol.com.br
Manuscript received January 8, 2023; revised January 9, 2023; accepted January 12, 2023.
Editor responsible for the review: Daniela do Carmo Rassi Frota

DOI: https://doi.org/10.36660/abcimg.20230002i

Types of exercise

Sports activities can be divided, in a simplified manner, into four categories: skill, power, endurance, and mixed. These activities mix, in greater or lesser quantity, isotonic (dynamic) and isometric (static) exercises, according to that described in Chart 1:[2]

In this sense, the type of exercise will result in the exercise-induced cardiac remodelling observed in these individuals' imaging exams. Thus, the greater the load of isotonic exercise, the greater the volume overload and the greater the possibility of observing a dilation in the heart chambers. By contrast, the greater the pressure overload, the greater the possibility of finding a dilation in the myocardial thickness.[2]

It is also important to observe that no type of sport is purely isotonic or isometric. Therefore, physical activities can present a greater or lesser predominance of one type of exercise, such as that mentioned above.[2] The classification adapted from the European Association of Cardiovascular Imaging and from the European Association of Preventive Cardiology is presented below, which shows the quantity of isometric and isotonic exercise associated with the main sports, as well as the intensity of the cardiac remodelling to them (Chart 2).[2]

Thus, it is possible to predict the exercise-induced cardiac remodelling that can be observed in the imaging exams[3] (Chart 3).

Other adaptations are observed with sports practice[4-6] (Chart 4).

Intensity and prevalence of exercise-induced cardiac remodelling

Though explained well in the literature and with a consensus regarding the exercise-induced cardiac remodelling described in this text, it is important to emphasize that not all of the athletes present these adaptations in imaging exams.[2,7,8]

For example, many studies conducted to evaluate the different ethnicities and modalities have shown the following

Chart 1 – Types of exercise and their alterations in cardiovascular physiology[2]

Type of exercise	Characteristic	Cardiac output	Peripheral vascular resistance	Result
Isotonic	Dynamic	Significant increase	Decrease	Volume overload
Isometric	Static	Slight increase	Increase	Pressure overload

Contents

Chart 2 – Characteristics of the exercises of different sports and intensity of the cardiac remodelling[2]

	Skill	Power	Endurance	Mixed
Isotonic	+/-	+/++	+++/++++	++/+++
Isometric	+/-	+++/++++	++/+++	++/+++
Cardiac remodelling	+/-	+/++	++++	++/+++
Sports	Table tennis, Karate, Golf, Yachting, Equestrianism	Weight lifting, Judo, Boxing, Short-distance running. Discus/Javelin throw, Olympic Gymnastics, Short-distance skating	Medium/Long-distance running, Medium/Long-distance cycling, Medium/Long-distance swimming, Triathlon, Canoeing/Rowing, Long-distance skating	Soccer, Volleyball Basketball, Tennis, Handball, Rugby, Water polo, Fencing

prevalence of left ventricular myocardial thickness ≥ 12 mm[2] (Chart 5).

One study evaluating elite athletes showed that 48% of them present a left ventricular diastolic diameter (LVDD) of above 55 mm, while only 14% present a LVDD ≥ 60 mm. The average LVDD among women was 48.4 ± 4.2 mm (varying from 38 to 66 mm), whereas among men the average was 55.4 ± 4.3 mm (varying from 43 to 70 mm). There was a correlation between the LVDD and the body surface area ($r = 0.76$; $p < 0.001$).[7] Figure 1 demonstrates an example of dilation of the left atrium and left ventricle in an amateur street race athlete.

It is important to highlight that in one study published by Caselli et al. in 2015 in the Journal of the American Society of Echocardiography, the left ventricular ejection fraction (LVEF) was normal throughout the studied population (1,145 Olympic athletes), with the lower limit for LVEF being 53%.[8]

This same study also showed that the left atrial diameter was larger than that of non-athletes; however, no differences were found when the diameter was indexed for the body surface area. Among athletes, 10% presented an LA diameter of above the reference values. In addition, 5.5% of the athletes presented an LVDD of above 60 mm and only 2.6% showed a myocardial thickness ≥ 13 mm.[8]

In children and adolescent athletes, one can also observe a dilation in the LA and LV, and a slight increase in the myocardial thickness.[9]

Differentiation between the exercise-induced adaptation and heart diseases

Some echocardiographic tools, such as the Tissue Doppler (TD) and cardiac magnetic resonance (CMR) aid in the differentiation between the "athlete´s heart" and heart diseases.[10,11]

The exercise-induced alterations do not reduce the speed of the wave e´ or increase the E/e´ ratio.[4]

Another important point, and which can aid in determining the differentiation in relation to heart diseases, is the absence of a decrease in myocardial deformation (Strain values) in the "athlete's heart", observing negative values of higher than -18%.[10]

Chart 3 – Cardiac remodelling according to the characteristic of the exercise[3]

	Isotonic (dynamic) Exercise	Isometric (static) Exercise
LV	Dilation	Minimum alteration in volume and without dilation
LV myocardial thickness	No alteration or minimal alteration	Increase
LV geometry	Excentric hypertrophy	Concentric hypertrophy
LA	Dilation	Dilation and/or hypertrophy
RV	Dilation	No alteration
RA	Dilation	No alteration

RV: right ventricle; LV: left ventricle; LA: left atrium; RA: right atrium.

Chart 4 – Adaptations observed with sports practice.[4-6]

Structure	Adaptation
Improved left ventricular filling	Wave e´ > 9 cm/s E/e´ Ratio < 6
Inferior vena cava	Dilation
Myocardial trabecular	Prominent trabeculations Increase in trabecular volume

Chart 5 – Prevalence of LV myocardial thickness ≥ 12 mm[2] according to ethnicity

Ethnicity	Prevalence
Blacks	18%
Caucasians	2%
Asians	2%
Arabs	< 1%

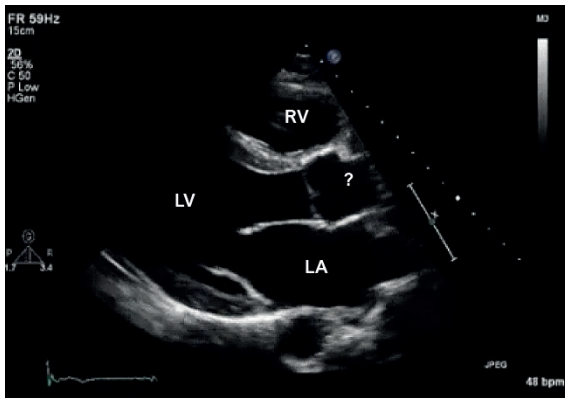

Figure 1 – *Longitudinal parasternal cut in an echocardiography exam of a 36-year-old man, amateur athlete in marathons (10 K, half-marathons, and marathons). We observed an increase in the diameter of the left atrium (LA) (45 mm) and the diastolic diameter of the left ventricle (LV) (60 mm). RV: right ventricle; LV: left ventricle; LA: left atrium; AO: aorta.*

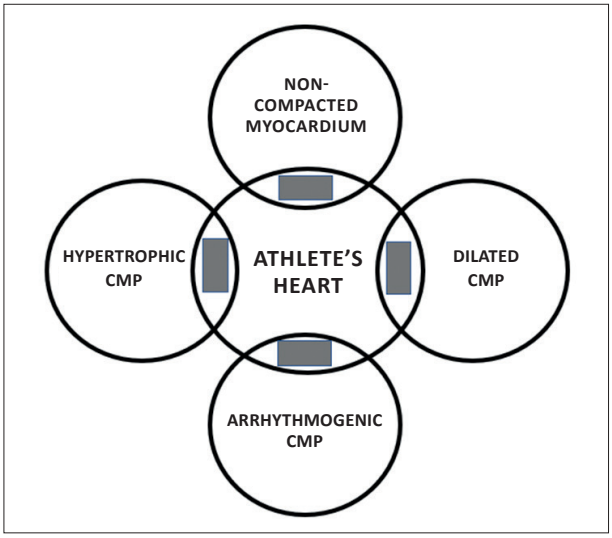

Figure 2 – *"Grey area" of the overlapping between the "athlete's heart" and some heart diseases (CMP).[2] CMP: cardiomyopathy.*

In questionable cases, the CMR is also very important in the differentiation between the athlete's heart and heart diseases, given that, in the athlete's heart, there is no delayed enhancement, no hypersignal in T1, or myocardial fat (this final concept in the differentiation from right ventricular arrhythmogenic CMP).[11]

According to the characteristics observed in each "athlete's heart", the diagnostic differentiation should be performed with hypertrophic CMP, dilated CMP, arrhythmogenic right ventricular CMP, and/or non-compacted myocardium. In some specific cases, this differentiation can be more challenging, since it can exist in a "grey area" with similar characteristics among the different heart diseases and the exercise-induced adaptations (Figure 2).[2,4]

Below are some points that aid in the differentiation in relation to each of the following heart diseases[2,4,11] (Chart 6).

Chart 6 – Elements that help in the differentiation between adaptation to exercise and cardiomyopathies[2,4,11]

Dilated myocardial thickness (13 to 16 mm) – Findings that suggest hypertrophic CMP
– Normal or reduced LVDD (< 54 mm)
– Segmental hypertrophy of the LV
– Obstruction of the left ventricular outflow tract
– Alteration of the diastolic function (wave e´ < 8.0 cm/s and/or E/A relation < 1.0)
– Left atrial dilation disproportional to the left ventricular dilation
– Delayed enhancement in the CMR
Heart chamber dilation – Findings that suggest dilated CMP
– Left ventricular dilation disproportional to the other heart chambers
– Left ventricular diastolic dysfunction
– Alteration in segmental contractility
– Reduced systolic volume
– Delayed enhancement in the CMR
Prominent Trabeculation in the LV – Findings that suggest non-compacted myocardium
– Left ventricular dilation disproportional to the other heart chambers
– Left ventricular systolic dysfunction
– Trabeculation associated with the thinning of the myocardial wall
– Delayed enhancement in the CMR
Heart chamber dilation – Findings that suggest arrhythmogenic right ventricular CMP
– Right ventricular dilation disproportional to the other heart chambers
– Alteration in segmental contractility of the right and/or LV
– Delayed enhancement in the right and/or LV in the CMR

CMP: cardiomyopathy; LV: left ventricle; LVDD: left ventricular diastolic diameter; CMR: cardiac magnetic resonance.

Conclusion

The regular and intense practice of physical activity can induce a wide range of cardiovascular adaptations, including electric, structural, and functional adaptations. These exercise-induced adaptations can often coincide with alterations observed in some heart diseases. Cardiac imaging plays a key role in the differentiation between the "athlete's heart" and pathological cardiovascular alterations, particularly in structural and functional evaluations.

Author Contributions

Conception and design of the research, acquisition of data, analysis and interpretation of the data, statistical analysis, obtaining financing, writing of the manuscript, critical revision of the manuscript for intellectual content: Mancuso FJN.

Potential Conflict of Interest

No potential conflict of interest relevant to this article was reported.

Sources of Funding

There were no external funding sources for this study.

Study Association

This study is not associated with any thesis or dissertation work.

Ethics Approval and Consent to Participate

This article does not contain any studies with human participants or animals performed by any of the authors.

References

1. Albaeni A, Davis JW, Ahmad M. Echocardiographic Evaluation of the Athlete's Heart. Echocardiography. 2021;38(6):1002-16. doi: 10.1111/echo.15066.
2. Pelliccia A, Caselli S, Sharma S, Basso C, Bax JJ, Corrado D, et al. European Association of Preventive Cardiology (EAPC) and European Association of Cardiovascular Imaging (EACVI) Joint Position Statement: Recommendations for the Indication and Interpretation of Cardiovascular Imaging in the Evaluation of the Athlete's Heart. Eur Heart J. 2018;39(21):1949-69. doi: 10.1093/eurheartj/ehx532.
3. Fulghum K, Hill BG. Metabolic Mechanisms of Exercise-Induced Cardiac Remodeling. Front Cardiovasc Med. 2018;5:127. doi: 10.3389/fcvm.2018.00127.
4. Sharma S, Merghani A, Mont L. Exercise and the Heart: The Good, the Bad, and the Ugly. Eur Heart J. 2015;36(23):1445-53. doi: 10.1093/eurheartj/ehv090.
5. D'Ascenzi F, Pelliccia A, Natali BM, Bonifazi M, Mondillo S. Exercise-Induced Left-Ventricular Hypertrabeculation in Athlete's heart. Int J Cardiol. 2015;181:320-2. doi: 10.1016/j.ijcard.2014.11.203.
6. Goldhammer E, Mesnick N, Abinader EG, Sagiv M. Dilated Inferior Vena Cava: A Common Echocardiographic Finding in Highly Trained Elite Athletes. J Am Soc Echocardiogr. 1999;12(11):988-93. doi: 10.1016/s0894-7317(99)70153-7.
7. Pelliccia A, Culasso F, Di Paolo FM, Maron BJ. Physiologic Left Ventricular Cavity Dilatation in Elite Athletes. Ann Intern Med. 1999;130(1):23-31. doi: 10.7326/0003-4819-130-1-199901050-00005.
8. Caselli S, Di Paolo FM, Pisicchio C, Pandian NG, Pelliccia A. Patterns of Left Ventricular Diastolic Function in Olympic Athletes. J Am Soc Echocardiogr. 2015;28(2):236-44. doi: 10.1016/j.echo.2014.09.013.
9. Pieles GE, Stuart AG. The Adolescent Athlete's Heart; A Miniature Adult or Grown-Up Child? Clin Cardiol. 2020;43(8):852-62. doi: 10.1002/clc.23417.
10. Paterick TE, Gordon T, Spiegel D. Echocardiography: Profiling of the Athlete's Heart. J Am Soc Echocardiogr. 2014;27(9):940-8. doi: 10.1016/j.echo.2014.06.008.
11. Maestrini V, Torlasco C, Hughes R, Moon JC. Cardiovascular Magnetic Resonance and Sport Cardiology: a Growing Role in Clinical Dilemmas. J Cardiovasc Transl Res. 2020;13(3):296-305. doi: 10.1007/s12265-020-10022-7.

My Approach to Right Ventricular Longitudinal Strain with Automated 2D and 3D Software

Lucas Arraes de França,[1,2] *Lucas Velloso Dutra*[3,4]
Hospital Israelita Albert Einstein,[1] *São Paulo, SP – Brazil*
Hospital Samaritano Paulista,[2] *São Paulo, SP – Brazil*
Hospital Sírio Libanês,[3] *São Paulo, SP – Brazil*
Hospital Edmundo Vasconcelos,[4] *São Paulo, SP – Brazil*

Abstract

Right ventricular strain analysis has emerged as an important diagnostic tool in the detection of early right ventricular systolic dysfunction not detected by conventional echocardiography techniques. Furthermore, it is capable of providing additional diagnostic and prognostic information to the traditional parameters for evaluating right ventricular systolic function in various pathologies. The echocardiography method of choice for its assessment is longitudinal strain derived from speckle-tracking. This method has been shown to be more sensitive for small changes in systolic function when compared to tricuspid annular plane systolic excursion, tissue Doppler imaging of the tricuspid annular s' wave, and right ventricular fractional area change. Advances in artificial intelligence and software with automated analysis have been introduced to this scenario with the aim of making the method simpler and quicker to apply, with lower inter- and intra-observer variability. The objective of this review article is to demonstrate the technique step by step, from image optimization and acquisition to interpretation of results, with illustrative figures of selected cases.

Introduction

The assessment of right ventricular (RV) systolic function has long been neglected. In recent years, there has been a great leap in the understanding of the importance of the RV in cardiac function. This has given rise to advanced non-invasive echocardiographic techniques that make functional assessment more accurate.

Several different acquired and congenital cardiac diseases can affect RV systolic function, leading to reduced stroke volume and cardiac output.

The analysis of RV systolic function has extremely peculiar characteristics. First, its complex geometry prevents two-dimensional (2D) volumetric analysis with the application of geometric assumptions routinely used to measure left ventricular volumes. The RV is composed of an inlet, body, apical region, and outflow tract (Figure 1), making it necessary, by means of 2D echocardiography, to use different views in different echocardiographic windows to assess its function, and it is impossible to estimate RV ejection fraction using 2D echocardiography. Furthermore, estimated RV systolic function is influenced by phasic changes in breathing and left ventricular mechanics that interfere with ventricular interdependence. It is also fundamental to understand that the myocardial contractility of the RV walls shows a different pattern of deformation in relation to the left ventricle. Finally, the RV myocardial wall is more trabeculated, which makes it more difficult to define its endocardial borders and the blood-tissue interface.[1]

RV systolic shortening occurs mainly due to the myocardial deformation of the fibers with longitudinal arrangement, which correspond to approximately 75%, and the contribution of the deformation of the radial fibers is very low. It is precisely for this reason that RV longitudinal strain has emerged in recent years as an

Keywords

Echocardiography; Myocardium; Left Ventricular Dysfunction.

Mailing Address: Lucas Arraes de França •
Av. Albert Einstein, 627/701. Postal code: 05652-900. Morumbi, São Paulo, SP - Brazil
E-mail: lucas.franca81@gmail.com
Manuscript received on November 15, 2022; reviewed on November 20, 2022; accepted on November 29, 2022.

DOI: https://doi.org/10.36660/abcimg.20230010i

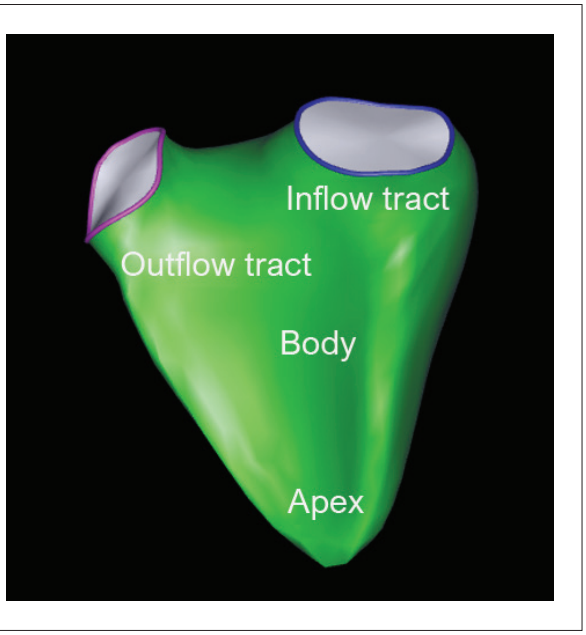

Figure 1 – *Three-dimensional reconstruction of the right ventricle using automated software demonstrating its peculiar geometry.*

Contents

important tool in the assessment of RV systolic function.[2]

There are two ways to study RV longitudinal strain: strain derived from tissue Doppler and strain derived from speckle-tracking. The second form is preferred and is widespread in the main echocardiography laboratories worldwide, due to the non-dependence on the angle between the longitudinal deformation and the ultrasound beam. Using the speckle-tracking technique, it is possible to measure RV free wall longitudinal strain (mean peak systolic strain of the 3 free-wall segments) and the 6-segment longitudinal strain (mean peak systolic strain of the 3 septum segments and the 3 segments of the free wall) (Figure 2). RV free wall longitudinal strain is the most validated technique due to the fact that left ventricular mechanics participate greatly in septal deformation.[3-5]

Initially, the existing software on the market for evaluating 2D strain derived from speckle-tracking were exclusively intended for evaluating left ventricular myocardial deformation, and analysis of the RV was performed using this same software, which often made the analysis difficult, leading to inaccurate results.

With technological advances and the emergence of artificial intelligence, it is now possible to analyze RV longitudinal strain in a completely automated manner, using 2D and 3D images with dedicated software for this purpose, with minimal need for adjustments.[1]

Clinical applicability

There are multiple clinical indications for evaluating RV systolic function by means of longitudinal strain. It plays an important role in several diseases involving the RV. It is already well documented in the literature that RV longitudinal strain has additional prognostic value to conventional echocardiographic parameters as a predictor of death and rehospitalization due to heart failure, detection of subtle involvement in patients with hypertrophic cardiomyopathy, and prediction of the development of this disease in family members. It is also able to predict survival of major cardiac events after acute myocardial infarction more accurately than the tricuspid annulus plane systolic excursion (TAPSE) and the RV fractional area variation (FAC),[2] RV longitudinal strain having a better correlation with magnetic resonance imaging in estimating its systolic function.[6-10]

RV longitudinal strain already demonstrates superiority to TAPSE in predicting events in different etiologies and degrees of pulmonary hypertension. In severe tricuspid insufficiency, it is an independent factor associated with all-cause mortality, demonstrating additional prognostic value to TAPSE and FAC. Finally, in congenital heart diseases such as tetralogy of Fallot, it is a sensitive parameter for detecting RV systolic dysfunction and a predictor of functional capacity on exertion and postoperative systolic dysfunction.[2,11]

Image acquisition

The quality of the images acquired is fundamental to obtain accurate results. The steps for acquiring ideal images for 2D longitudinal strain derived from speckle-tracking in automated software are as follows:

1. Acquire an apical 4-chamber view focused on the RV (Figure 3). Analysis in this view is preferable because of better visualization of the RV free wall. For acquisition, after performing a conventional 4-chamber apical view, it is

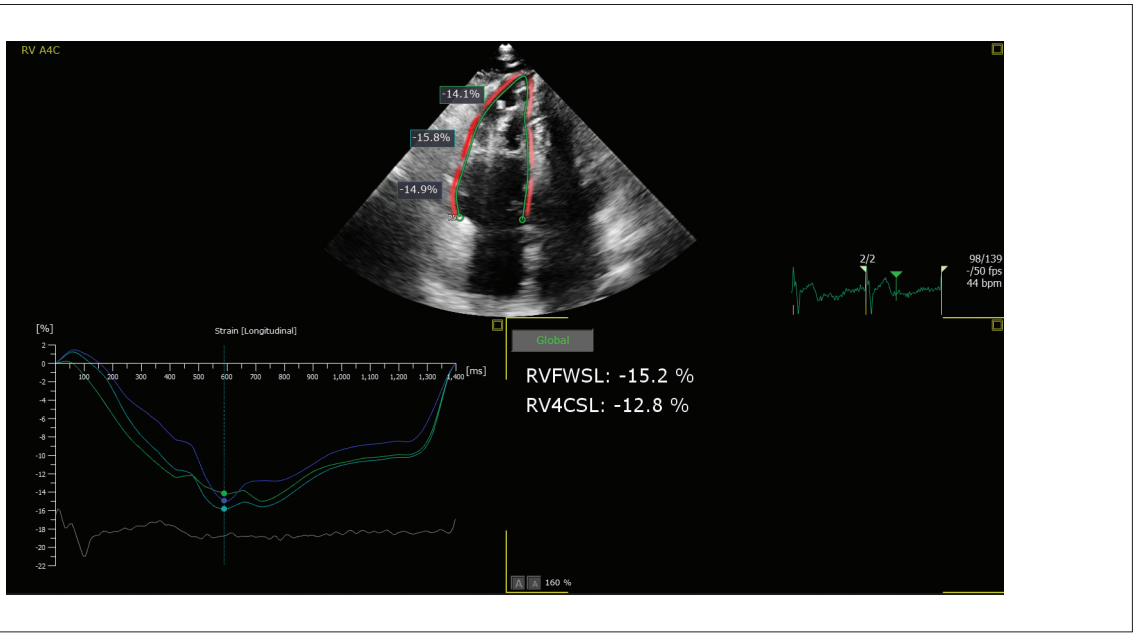

Figure 2 – *Analysis of free wall longitudinal strain and 6-segment longitudinal strain, estimated at –15.2% and –12.8%, respectively, in a patient with arrhythmogenic RV cardiomyopathy, using automated software.*

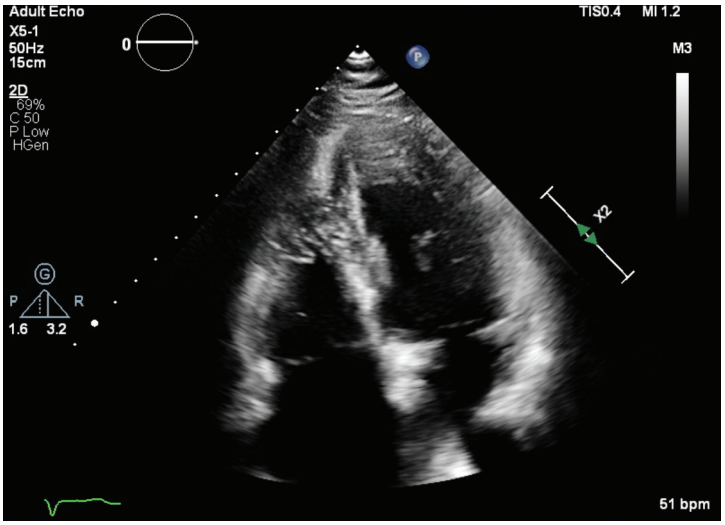

Figure 3 – *Apical 4-chamber view focused on the right ventricle.*

necessary to move the patient's right shoulder backwards and tilt the transducer toward the liver. In this manner, it is possible to keep the emitting ultrasound source close to the apex of the left ventricle with the RV properly positioned in the center of the image.

2. The image must have a frame rate between 50 and 80 Hz. To optimize the temporal resolution, it is necessary to reduce the sector width and the depth.

3. The image must be acquired after at least 2 to 3 cardiac cycles with the patient in expiratory apnea, with the goal of better subsequent recognition of the speckles by the software.

4. In the current automated software, it is not necessary to mark the effective time of RV systole (time from the peak of the R wave to the closure of the pulmonary valve), which was routinely done for analysis in non-automated software and usually acquired by means of pulsed Doppler of the RV outflow tract.

5. For accurate results, it is ideal for the patient to have a heart rate between 60 and 100 bpm and a regular heart rhythm. If the patient is in atrial fibrillation rhythm, heart rate variability between beats should not exceed 10%.[2,3]

When measuring RV longitudinal strain by means of 3D echocardiography with automated software that uses artificial intelligence, it is possible to measure RV free wall longitudinal strain from a "full volume" acquisition in the dynamic heart model (DHM) modality. The steps to acquire a large 3D pyramidal block that contains the entire RV geometry consist of the following:

1. Perform an apical 4-chamber view focused on the RV.

2. Activate the heart model (HM) acquisition mode, preferably with a double layout, paying attention to the fact that the lateral size of the 3D block and the width of the elevation contain the entire RV (Figure 4).

3. Ideally, the volume rate of the 3D block should be greater than 20 Hz, requiring adjustments to the width of the elevation and the lateral size to optimize the temporal resolution.

4. At least 2 to 3 cardiac cycles must be acquired, with the patient in expiratory apnea and preferably regular heart rhythm.[1,12]

Analysis of results

In recent years, despite demonstrating that the evaluation by RV longitudinal strain using the speckle-tracking method in 2D echocardiography has important implications for diagnosis, prognosis, and treatment of patients in different clinical contexts, its application in daily practice has been challenged by a lack of the standardization of methods, software, and reference values. A 2016 publication suggested cutoff values of −20.2% for the arithmetic mean of the 6-segment model (including the free wall and interventricular septum) and −23.3% for the 3-segment model (free wall).[13]

Since then, a task force[3] and a review article[14] have attempted to standardize the acquisition method, strengthening as a standard the acquisition of an apical 4-chamber view focused on the RV. However, in many articles published to date, evaluation began from the apical 4-chamber view. There is also a great variability of results depending on manufacturer, software developer, and sex (higher values for women).

Furthermore, data are limited for healthy individuals over 60 years of age and are still scarce and inconsistent for the pediatric population, with values ranging from −20.8% to −34.1%, with a mean of −30.1% in the 3-segment model (free wall), for example.

The use of automated software with artificial intelligence, in addition to optimizing the workflow, may help standardize the results in the future, reducing the interobserver difference.

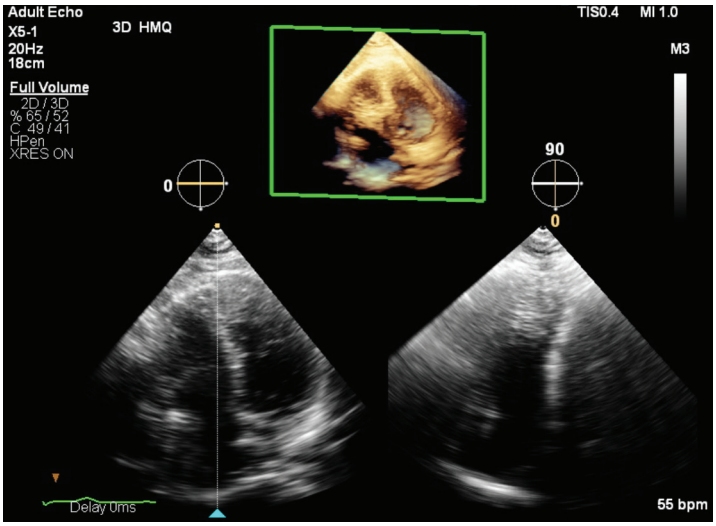

Figure 4 – *"Full volume" 3D acquisition in HM mode with dual layout.*

As previously mentioned, RV strain derived from speckle-tracking can be used to evaluate patients with pulmonary hypertension (including patients with acute or chronic pulmonary embolism), valve diseases (mitral stenosis, functional tricuspid insufficiency), and heart failure with reduced or preserved ejection fraction. A recent review article[15] cited the advantages of the method as an additional parameter in the assessment of RV systolic function, with high predictive value, high reproducibility, and mechanical assessment of the entire RV free wall thickness that are relatively load- and angle-independent. In addition, it has high availability, low cost, short acquisition time, and no need for advanced training, albeit with the disadvantages of lack of consensus regarding normality values and the 6- or 3-segment model, the need for a high temporal resolution, difficulty with limited echocardiographic windows and free wall visualization, and the need for stable heart rhythm. The applicability of RV longitudinal strain has shown to be more robust in studies focused on the assessment of pulmonary hypertension, heart failure with reduced ejection fraction, and tricuspid insufficiency. In other clinical contexts, such as heart failure with preserved ejection fraction, aortic stenosis, and mitral insufficiency, data remain scarce and further investigation is needed.[15]

Regarding the analysis of the results, instantaneous strain values are displayed on a percentage myocardial strain rate curve as a function of time. In the case of longitudinal strain, the curves are traced below the neutral horizontal line, considering the nadir as the maximum value (Figures 5, 6, 7, 8 and 9). By convention, systolic fiber shortening is represented by negative values, and lengthening is expressed by positive values. The result is shown in percentage values. Normal longitudinal strain values vary according to age, sex, and software. The lower limit of normality is −20.0% for the 3-segment model (free wall) and −18.2% for the 6-segment model, using TomTec automated software with images from Philips, Siemens, and General Electric ultrasound systems, as suggested in a recent study,[16] with a sample of 1,913 patients in which this system was used.

Another advantage of evaluating the free wall using the method of RV strain compared to traditional quantification methods is that we can analyze the strain values in the apical, middle, and basal segments, as exemplified in Figure 8 (non-compaction cardiomyopathy) and Figure 9 (hypertrophic cardiomyopathy, apical form), where the absolute values were notably reduced in the apical segments of both cases.

After acquiring a 3D pyramidal block of the RV, it is possible to perform an automated analysis using dedicated software (for example, 3D Auto RV by Philips). In addition to providing detailed information on 3D RV volumes and ejection fraction (Figure 10), it is possible to obtain 2D parameters from the 3D block, such as linear measurements and systolic function parameters, including TAPSE, FAC, and 2D strain in the model that includes the septum and free wall, as in the example below (Figure 11), with values of −17.6% and −18.9%, respectively.

Conclusion

Automated 2D and 3D software facilitates the workflow, making it possible to incorporate the method of 2D RV longitudinal strain into clinical practice. The results obtained in recent studies demonstrate a prognostic role in the clinical context of different diseases, such as heart failure with reduced ejection fraction, tricuspid insufficiency, and pulmonary hypertension.

A value of −20% is considered as the lower limit of normality for RV free wall strain, considering the latest literature data obtained with TomTec's "agnostic" automated software.[16]

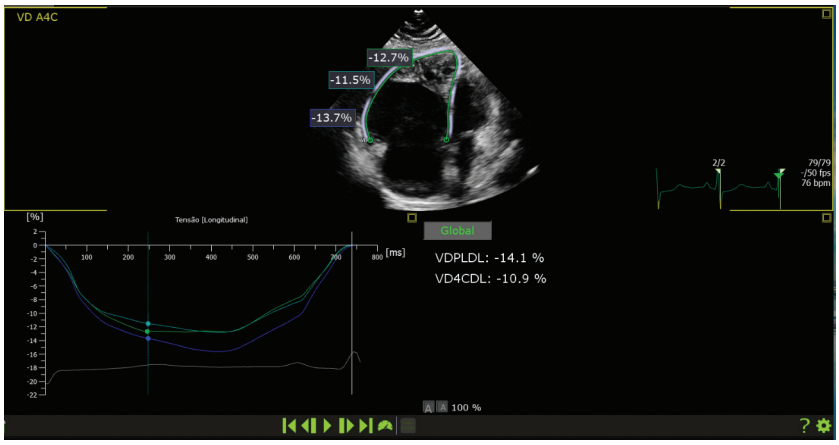

Figure 5 – *AutoStrain RV TomTec: Primary pulmonary hypertension (obtained value of –14.1% for free wall longitudinal strain).*

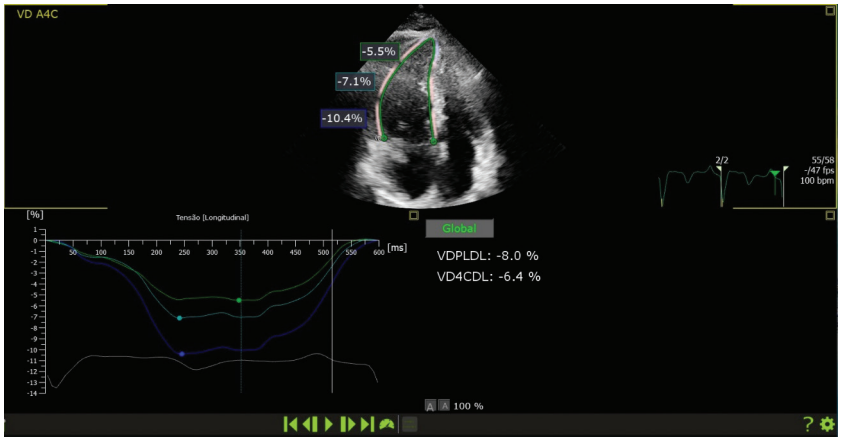

Figure 6 – *Pulmonary hypertension due to acute pulmonary thromboembolism (value of –8.0% obtained for free wall strain).*

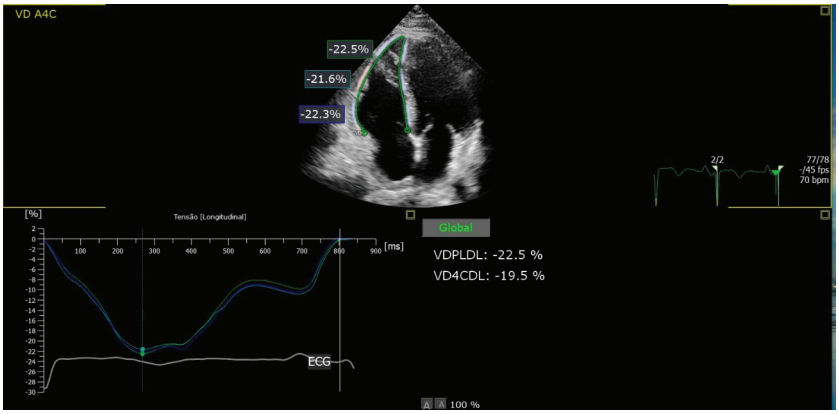

Figure 7 – *AutoStrain RV TomTec: examination performed on the same patient in Figure 6 with acute pulmonary thromboembolism two days after treatment with fibrinolytics and full anticoagulation (value of –22.5% obtained for free wall strain).*

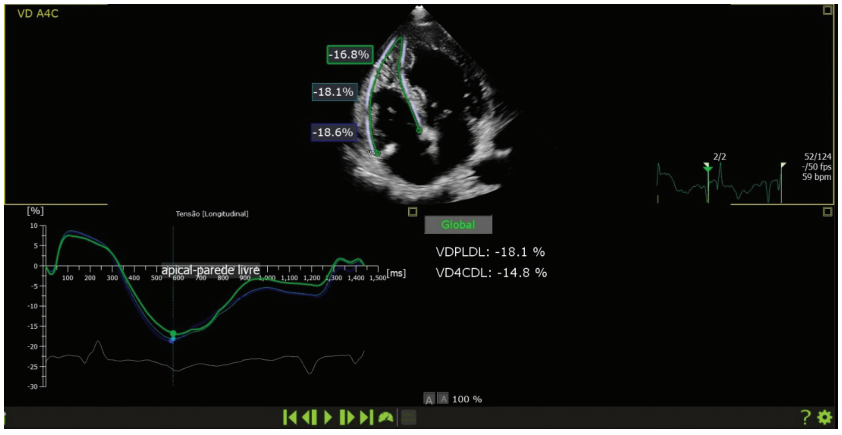

Figure 8 – *AutoStrain RV TomTec: non-compaction cardiomyopathy (value of –18.1% obtained for free wall strain).*

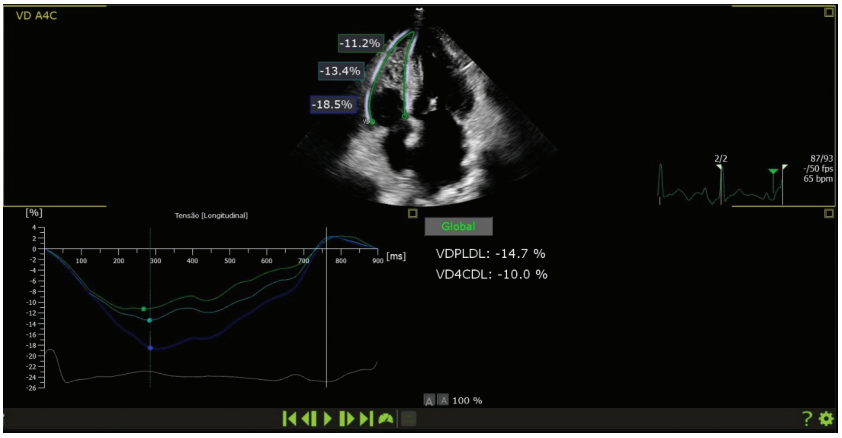

Figure 9 – *AutoStrain RV TomTec: apical form of hypertrophic cardiomyopathy (value of –14.7% obtained for free wall strain, with a lower absolute value in the apical segment).*

Figure 10 – *RV volumes and ejection fraction obtained automatically using the software 3D Auto RV (TomTec).*

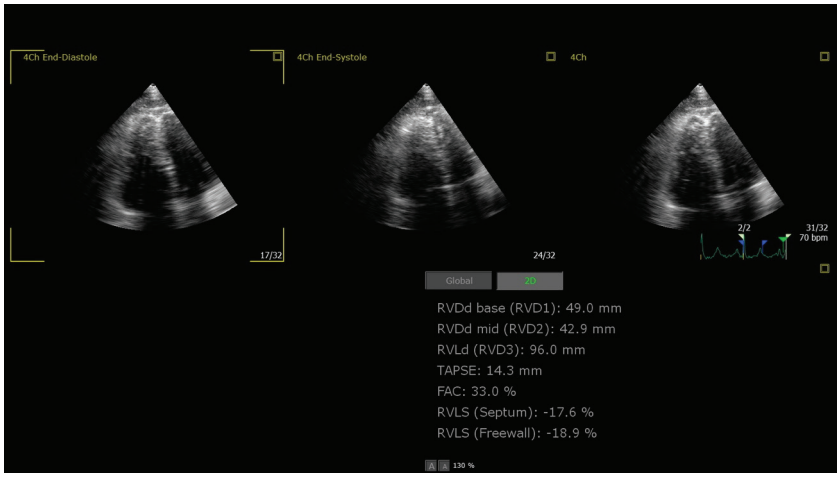

Figure 11 – *Information obtained automatically from a 2D image derived from the 3D volume, using the software 3D Auto RV (TomTec).*

Author contributions

Writing of the manuscript e critical revision of the manuscript for intellectual content: França LA, Dutra LV.

Potential Conflict of Interest

No potential conflict of interest relevant to this article was reported.

Sources of Funding

There were no external funding sources for this study.

Study Association

This study is not associated with any thesis or dissertation work.

Ethics approval and consent to participate

This study is not associated with any thesis or dissertation work.

References

1. Addetia K, Muraru D, Badano LP, Lang RM. New Directions in Right Ventricular Assessment Using 3-Dimensional Echocardiography. JAMA Cardiol. 2019 Sep 1;4(9):936-44. DOI: 10.1001/jamacardio.2019.2424.
2. Muraru D, Haugaa K, Donal E, Stankovic I, Voigt JU, Petersen SE, et al. Right ventricular longitudinal strain in the clinical routine: a state-of-the-art review. Eur Heart J Cardiovasc Imaging. 2022 Jun 21;23(7):898-912. DOI: 10.1093/ehjci/jeac022.
3. Badano LP, Kolias TJ, Muraru D, Abraham TP, Aurigemma G, Edvardsen T, et al. Industry representatives; Reviewers: This document was reviewed by members of the 2016–2018 EACVI Scientific Documents Committee. Standardization of left atrial, right ventricular, and right atrial deformation imaging using two-dimensional speckle tracking echocardiography: a consensus document of the EACVI/ASE/Industry Task Force to standardize deformation imaging. Eur Heart J Cardiovasc Imaging. 2018 Jun 1;19(6):591-600. doi: 10.1093/ehjci/jey042. Erratum in: Eur Heart J Cardiovasc Imaging. 2018 Jul 1;19(7):830-3. DOI: 10.1093/ehjci/jey042.
4. Voigt JU, Pedrizzetti G, Lysyansky P, Marwick TH, Houle H, Baumann R, et al. Definitions for a common standard for 2D speckle tracking echocardiography: consensus document of the EACVI/ASE/Industry Task Force to standardize deformation imaging. Eur Heart J Cardiovasc Imaging. 2015 Jan;16(1):1-11. DOI: 10.1093/ehjci/jeu184.
5. Prihadi EA, van der Bijl P, Dietz M, Abou R, Vollema EM, Marsan NA, et al. Prognostic Implications of Right Ventricular Free Wall Longitudinal Strain in Patients With Significant Functional Tricuspid Regurgitation. Circ Cardiovasc Imaging. 2019 Mar;12(3):e008666. DOI: 10.1161/CIRCIMAGING.118.008666.
6. Leong DP, Grover S, Molaee P, Chakrabarty A, Shirazi M, Cheng YH, et al. Nonvolumetric echocardiographic indices of right ventricular systolic function: Validation with cardiovascular magnetic resonance and relationship with functional capacity. Echocardiography. 2012;29(4):455-63. DOI: 10.1111/j.1540-8175.2011.01594.x.
7. Vizzardi E, Bonadei I, Sciatti E, Pezzali N, Farina D, D'Aloia A, et al. Quantitative analysis of right ventricular (RV) function with echocardiography in chronic heart failure with no or mild RV dysfunction: comparison with cardiac magnetic resonance imaging. J Ultrasound Med. 2015;34(2):247-55. DOI: 10.7863/ultra.34.2.247.
8. Lu KJ, Chen JX, Profitis K, Kearney LG, DeSilva D, Smith G, et al. Right ventricular global longitudinal strain is an independent predictor of right ventricular function: a multimodality study of cardiac magnetic resonance imaging, real time three-dimensional echocardiography and speckle tracking echocardiography. Echocardiography. 2015;32(6):966-74. DOI: 10.1111/echo.12783.

9. Focardi M, Cameli M, Carbone SF, Massoni A, De Vito R, Lisi M, et al. Traditional and innovative echocardiographic parameters for the analysis of right ventricular performance in comparison with cardiac magnetic resonance. Eur Heart J Cardiovasc Imaging. 2015;16:47-52. DOI: 10.1093/ehjci/jeu156.

10. Li YD, Wang YD, Zhai ZG, Guo XJ, Wu YF, Yang YH, et al. Relationship between echocardiographic and cardiac magnetic resonance imaging derived measures of right ventricular function in patients with chronic thromboembolic pulmonary hypertension. Thromb Res. 2015;135(4):602-6. DOI: 10.1016/j.thromres.2015.01.008.

11. Fine NM, Chen L, Bastiansen PM, Frantz RP, Pellikka PA, Oh JK, Kane GC. Outcome prediction by quantitative right ventricular function assessment in 575 subjects evaluated for pulmonary hypertension. Circ Cardiovasc Imaging. 2013 Sep;6(5):711-21. DOI: 10.1161/CIRCIMAGING.113.000640.

12. Medvedofsky D, Addetia K, Patel AR, Sedlmeier A, Baumann R, Mor-Avi V, Lang RM. Novel Approach to Three-Dimensional Echocardiographic Quantification of Right Ventricular Volumes and Function from Focused Views. J Am Soc Echocardiogr. 2015 Oct;28(10):1222-31. DOI: 10.1016/j.echo.2015.06.013.

13. Muraru D, Onciul S, Peluso D, Soriani MD, Cucchini U, Aruta P, et al. Sex and Method-Specific Reference Values for Right Ventricular Strain by 2 Dimensional Speckle-Tracking Echocardiography. Circ Cardiovasc Imaging. 2016;9(2):2003866. DOI: 10.1016/j.echo.2015.06.013.

14. Badano LP, Muraru D, Parati G, Haugaa K, Voigt JU. How to do right ventricular strain. Eur Heart J Cardiovasc Imaging. 2020;21(8):825. DOI: 10.1093/ehjci/jeaa126.

15. Tadic M, Nita N, Schneider L, Kersten J, Buckert D, Gonska B, et al. The Predictive Value of Right Ventricular Longitudinal Strain in Pulmonary Hypertension, Heart Failure, and Valvular Diseases. Front Cardiovasc Med. 2021;8:698158. DOI: 10.3389/fcvm.2021.698158.

16. Addetia K, Miyoshi T, Citro R, Daimon M, Gutierrez Fajardo P, et al. WASE Investigators. Two-Dimensional Echocardiographic Right Ventricular Size and Systolic Function Measurements Stratified by Sex, Age, and Ethnicity: results of the World Alliance of Societies of Echocardiography Study. J Am Soc Echocardiogr. 2021 Nov;34(11):1148-57.e1. DOI: 10.1016/j.echo.2021.06.013.

My Approach to Echocardiographic Assessment for Constrictive Pericarditis

Débora Freire Ribeiro Rocha,[1] Ana Caroline Reinaldo de Oliveira,[1] Verena Nunes e Silva,[1] João Batista Masson Silva[1]

Hospital das Clínicas da Universidade Federal de Goiás,[1] Goiânia, GO – Brazil

Abstract

Constrictive pericarditis (CP) is a condition in which scarring and loss of elasticity of the pericardium result in impaired ventricular filling, diastolic dysfunction, and right heart failure. The diagnosis of this pathology is challenging, with frequent need for multimodal imaging techniques, among which echocardiography represents the initial imaging modality for the diagnostic evaluation, in addition to allowing the differentiation of CP from restrictive cardiomyopathy (RCM) and other conditions that mimic constriction.

How I Perform Echocardiographic Assessment for CP

Introduction

Constrictive pericarditis (CP) is characterized by focal or global scarring and loss of elasticity of the pericardium with or without associated thickening. Abnormal pericardium prevents diastolic filling, causing elevation of systemic venous pressures, despite preserved myocardial function of the ventricles. Therefore, it results in right heart failure, with the classic manifestations of edema of the lower limbs, pulsatile hepatomegaly, ascites, pleural effusion, fatigue, and low tolerance for effort.[1,2]

The symptomatology of CP is not specific, and its manifestations can be confused with myocardial, coronary, pulmonary, or even gastrointestinal conditions, such as liver cirrhosis, RCM, endomyocardial fibrosis, among other pathologies, making the diagnosis challenging.[3,4]

Several conditions can lead to CP, including infectious etiologies, connective tissue diseases, trauma, metabolic disorders (uremia), iatrogenic etiologies (pericardiotomy, radiotherapy), neoplasms or even idiopathies.[5] In Europe and the United States, the most frequent etiology is idiopathic, followed by post-cardiac surgery, while in other parts of the world, such as Brazil, tuberculosis is more common.[5-7]

The pathophysiology of CP is related to the elevation and equalization of cardiac pressures, since the heart is located in a fixed space determined by the rigid pericardium, to exaggerated ventricular interdependence and to the dissociation of intrathoracic and intracardiac pressures.[6,7]

During inspiration, the rigid pericardium promotes the dissociation of intrathoracic and intracardiac pressures by preventing the decrease in intrathoracic pressure from being fully transmitted to the cardiac chambers. Thus, as the pressure in the extrapericardial pulmonary veins decreases during inhalation, there is attenuation of the pulmonary venous gradient toward the left atrium, contributing to the reduction of left ventricle (LV) filling.[5,6]

During inspiration, the decrease in LV filling allows for an increase in right ventricle (RV) filling with a deviation of the interventricular septum to the left, configuring ventricular interdependence. Consequently, fillings related to the left heart (mitral, aortic, and pulmonary venous flows) decrease, while fillings related to the right heart (tricuspid, hepatic, pulmonary artery, and inferior vena cava) increase. During expiration, all of the above mechanisms are reversed, except the superior vena cava (SVC) flow, which is not influenced by respiration in CP.[8]

The restriction to emptying of the left atrium during diastole results in an increase in its pressure and, subsequently, in pulmonary venous pressure.

In CP, there is no impairment of ventricular relaxation during the initial phase of diastole, with early filling being faster than normal due to increased driving force resulted from high atrial pressure. However, the myocardium cannot continue its relaxation after meeting the rigid pericardium during middle and late diastole, leading to increased end-diastolic pressure in the ventricles and atria.[8]

There are three subtypes of CP, namely transient, chronic, and effusive constrictive pericarditis. Transient CP is a temporary form of constriction due to underlying inflammation, which may resolve spontaneously or after drug treatment. Chronic CP results from chronic inflammation and permanent scarring, potentially necessitating surgical intervention. Effusive CP is characterized by the coexistence of constriction by the visceral pericardium and tense pericardial effusion, with elevated right atrial pressure persisting after pericardiocentesis.[7]

Pericardiectomy is the definitive treatment in refractory patients to clinical treatment, as it relieves pericardial containment and, in the absence of concomitant myocardial dysfunction, effectively restores diastolic filling.[9]

Keywords

Pericardium, Constrictive pericarditis, Heart failure.

Mailing Address: Débora Freire Ribeiro Rocha •
Rua 235, Quadra 68, Lote 285, Setor Leste Universitário. Postal Code: 74605-050. Goiânia, GO, Brazil.
E-mail: freire.debora17@gmail.com
Manuscript received November 25, 2022; revised December 1, 2022; accepted December 5, 2022.
Editor responsible for the review: Daniela do Carmo Rassi Frota

DOI: https://doi.org/10.36660/abcimg.2022366i

How to assess?

Suspicion of CP is based on clinical history and physical examination, and requires evaluation and confirmation by imaging and hemodynamic data.[6]

Echocardiography is the most commonly used imaging modality for the initial assessment of pericardial disease, as it is widely available, safe, fast, and inexpensive compared to other methods, aiding in the diagnosis of CP and excluding other causes of diastolic heart failure.[10]

Doppler echocardiographic findings in constriction:

• Increased pericardial thickness (≥ 3 mm), which may be absent in up to 12 to 18% of patients.[7] Due to the exacerbated pericardial refraction, even in normal individuals, it may be difficult to detect pericardial thickening and calcification, mainly by transthoracic echocardiogram, with the transesophageal echocardiogram having much higher sensitivity and specificity;

• During systole, restricted movement of the posterior wall of the left ventricle is observed due to pericardial adhesion. There is also an abrupt relaxation of the posterior wall with subsequent flattening of the endocardial movement during the rest of the diastole, which can be well observed in the M-mode;[6]

• Mitral *annulus reversus*, present in 74% of patients with CP, which represents the reversal of the normal ratio of early diastolic myocardial velocities with lateral e' smaller than septal e'.[6] The septal e' / lateral e' ratio ≥ 0.91 has a sensitivity (S) of 75% and specificity (E) of 85%[9] (Figures 1A, 1B, 1C and 1D);

• Normal or increased mitral inflow propagation velocity (> 100 cm/s) in Color M-Mode (S 74%; E 91%)[9] (Figure 2);

• Abnormal and oscillatory movement of the interventricular septum beat to beat, related to ventricular interdependence due to subtle differences in the timing of mitral and tricuspid valve opening and left and right atrial contraction (AC). In M-mode, a notch is observed at the beginning of diastole, followed by paradoxical movement and then normal movement of the interventricular septum[7] (Figure 3);

• Presence of a septal leap with respirophasic deviation of the interventricular septum toward the left ventricular cavity during inspiration (two-dimensional mode: S 62% and E 93%; M-mode: S 93% and E 69%)[9,11] (Video 1);

• Ventricular interdependence with respiratory variation ≥ 25% of peak mitral E wave velocity (S 88%; E 67%) or ≥ 40% of peak tricuspid E wave velocity (S 90%; E 88%) determined by pulsed wave Doppler at the level of the cuspid tips in an apical four-chamber view. The consensus for calculating the percentage of respiratory variation is (expiration - inspiration)/ expiration[9,12] (Figure 4A and 4B);

• Preserved or increased velocity e' of the septal mitral *annulus*, ≥ 9 cm/s (S 83%; E 81%);[7,9]

• Percent change in mitral flow E velocity between inspiration and expiration ≥ 14.6% (S 84%; E 73%);[11]

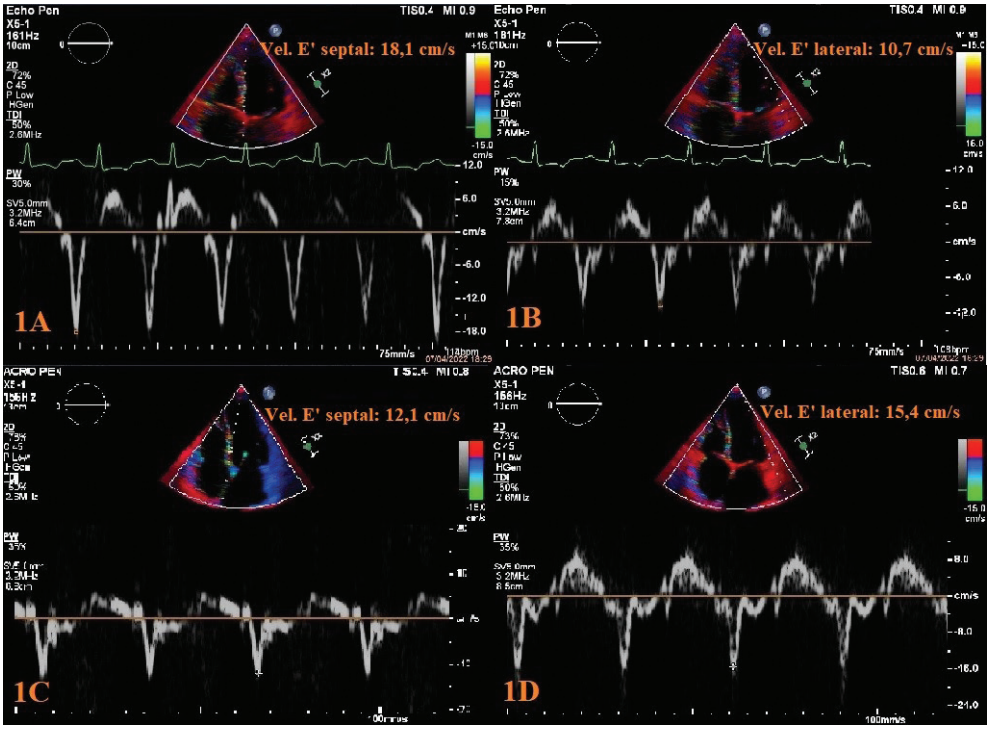

Figure 1 – *Tissue Doppler demonstrating the phenomenon of annulus reversus in Figures 1A and 1B, in which the velocity of the septal mitral annulus (18.1 cm/s) is greater than the lateral velocity (10.7 cm/s). After pericardiectomy, there was normalization of this relationship, with the septal velocity (12.1 cm/s) lower than the lateral velocity (15.4 cm/s), demonstrated in Figures 1C and 1D.*

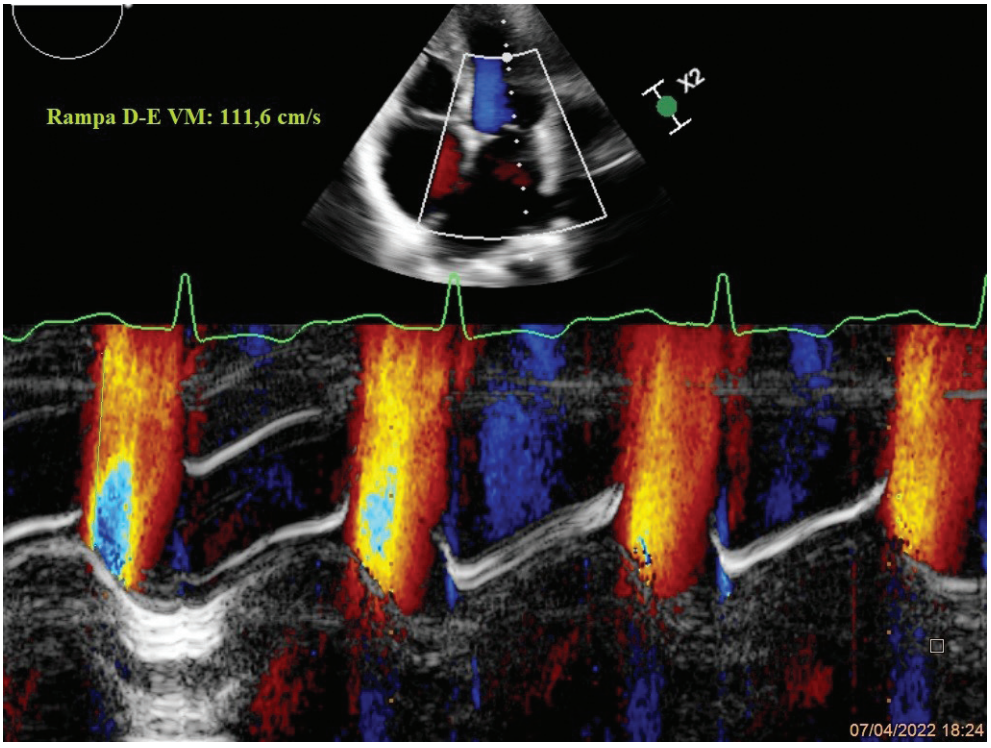

Figure 2 – *Color Doppler M-mode recording in a patient with CP. Note the rather steep propagation velocity (Vp) (> 100 cm/s), helping to differentiate between constrictive and restrictive physiology.*

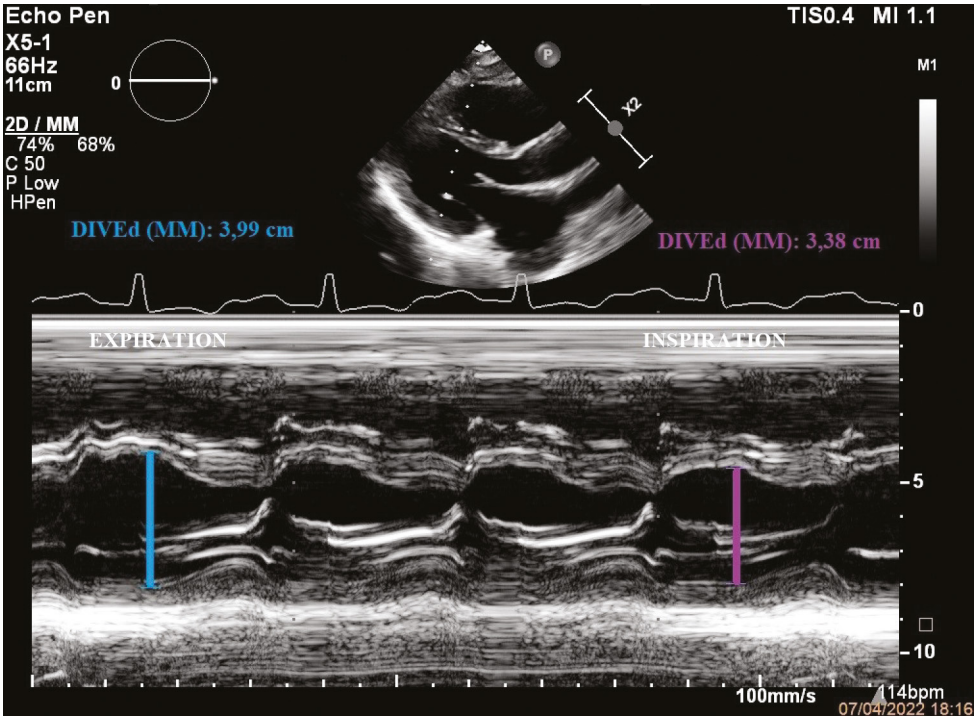

Figure 3 – *Beat-to-beat oscillatory movement of the interventricular septum and respirophasic movement recorded in windowed M mode parasternal long axis.*

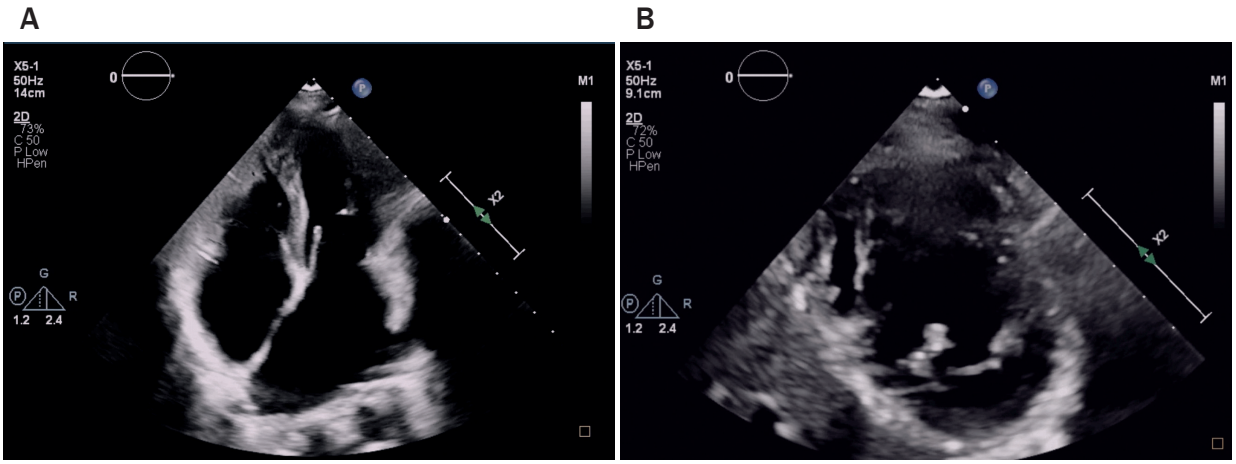

Video 1 – *Representation of the phenomenon of ventricular interdependence in a patient with CP. Note the deviation of the septum to the left during inspiration and shift to the right during expiration.*
Link video 1A: http://abcimaging.org/supplementary-material/2023/3601/ABC-366-video-1A.mp4
Link video 1B: http://abcimaging.org/supplementary-material/2023/3601/ABC-366-video-1B.mp4

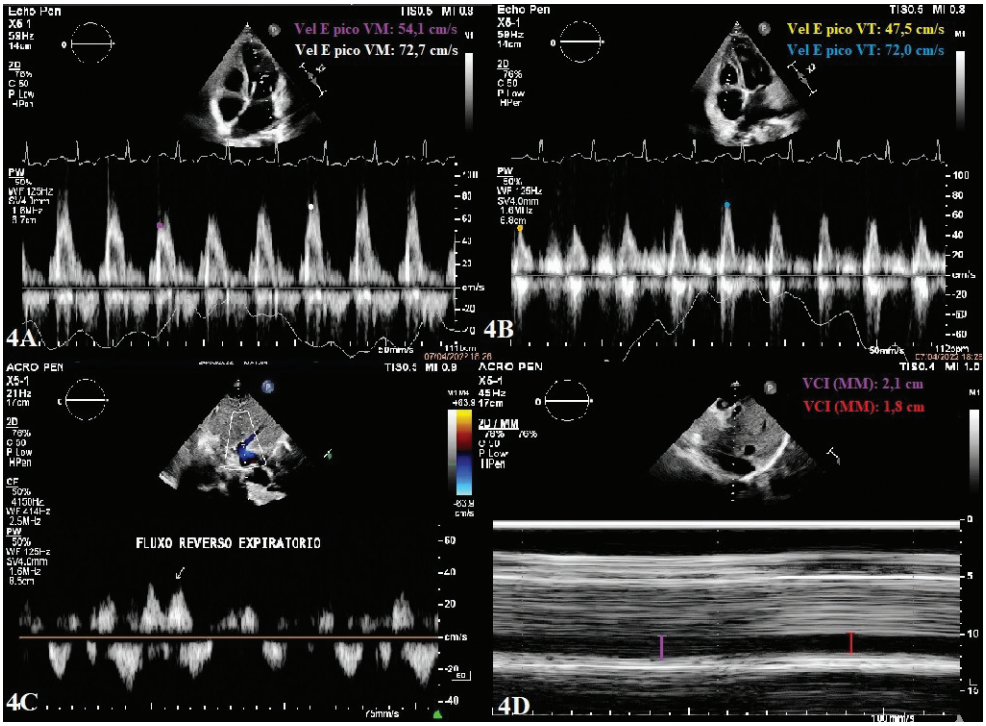

Figure 4 – *Demonstration of transmitral (4A) and transtricuspid (4B) flow variation during breathing in a patient with CP. In the same patient, note the presence of reverse flow in the hepatic vein during expiration (4C), as well as dilation of the inferior vena cava with reduced collapsibility (4D).*

• Marked increase in early diastolic filling velocity (E velocity) of mitral flow with a rapid deceleration and a decreased late diastolic filling velocity after AC (A velocity), resulting in increased E/A ratio (E/A > 2);[6]

• It is not uncommon to observe less typical patterns, in which there is a normal or inverted E/A ratio with exaggerated respiratory variation or in which only the tricuspid inflow reveals classic alterations;

• Exaggerated respiratory variation in the isovolumetric relaxation time of the left ventricle;

• In CP, the average of early diastolic myocardial velocities (lateral e' and septal e') is preserved, despite having higher filling pressures. Septal e' velocity increases progressively with the worsening of CP, causing a drop in the E/e' ratio despite the increase in pulmonary capillary pressure (PCP). This inverse relationship between PCP and E/e' is called *annulus paradoxus;*[7]

• During expiration, there is reduced forward diastolic flow in the hepatic vein with prominent telediastolic reverse flow and increased systolic forward flow on inspiration. High specificity mainly if reverse flow velocity is ≥ 0.8 m/s[7,11] (Figure 4C);

• Hepatic vein diastolic flow reversal ratio (expiratory diastolic reversal velocity divided by forward diastolic hepatic vein flow velocity) ≥ 0.79 is one of the most specific findings (S 76%; E 88%; PPV 96%; NPV 49%);[7,12]

• Dilation of the inferior vena cava (≥ 21 mm) and the suprahepatic vein with reduced respiratory variation (< 50%) (Figure 4D);

• The left atrium, which is only partially covered by the pericardium, may be enlarged. Enlargement of the right atrium may also occur (present in 61% of patients with CP);

• Premature opening of the pulmonary valve;

• Slight increase in pulmonary artery systolic pressure (generally not exceeding 50 mmHg);

• "Warm septum" sign on dot-tracking echocardiography: due to adhesion of the free walls by the diseased pericardium, mainly the lateral wall, the modular value of the longitudinal tension in these areas is reduced in relation to the septal wall, where it is increased (*strain reversus*).[6,7,13]

The classic findings of constriction are more prominent in euvolemic patients. If absent in patients with suspected CP, it is advised to reassess them after fluid replacement, if there is volume depletion, or to examine them in the sitting position, if there is volume overload.

Definitive diagnosis should be based on the combination of clinical and echocardiographic data, in addition to other complementary methods (e.g., computed tomography, magnetic resonance or invasive hemodynamic evaluation), when necessary.

Table 1 – Echocardiographic aspects in the differentiation between CP and RCM

Echocardiographic findings	CP	RCM
E/A Ratio	Increased (E/A> 2)	Increased (E/A> 2)
E deceleration time	Short (≤ 160 ms)	Short (≤ 160 ms)
Respiratory variation in mitral and tricuspid E-wave velocity	Δ VMi ≥ 25% Δ VTri ≥ 40%	Not variable
Velocity of annular e'	Normal	Reduced
Breathing movement of the interventricular septum	Present	Absent
Pulmonary hypertension	Rare	Frequent
Mitral inflow propagation velocity (color M-mode)	Increased (> 55 cm/s)	Reduced
LV isovolumetric relaxation time	Variable with breathing	Stable with breathing
Flow in the pulmonary veins	S > D, with small increment of D on expiration	S < D throughout the respiratory cycle
Diastolic reverse flow in the hepatic vein	During expiration	During inspiration
Flow in the SVC	S < D, with a slight reduction in D during expiration and no variation in AC with the respiratory cycle	S <<< D, with a decrease in D on expiration and an increase in AC on inspiration
Strain analysis	Reduced circumferential strain, torsion, and distortion velocity Overall normal longitudinal strain, although there may be *strain reversus*	Normal circumference strain Reduced longitudinal strain
Appearance of the pericardium	Glossy/thick	Normal
Atrial size	Normal or slightly dilated	Very dilated

S: velocity of the wave formed by the flow of the pulmonary veins towards the left atrium during ventricular systole; D: flow wave velocity from the pulmonary veins towards the left ventricle, using the left atrium as a conduit during ventricular diastole; ΔVMi: respiratory variation of E-wave velocity in the mitral valve; Δ VTri: respiratory variation of E-wave velocity in the tricuspid valve; E/A: ratio between the early diastolic velocity of the mitral flow (E) and the velocity of atrial contraction of the mitral flow (A).

How to differentiate CP and RCM

Both CP and RCM manifest themselves as a chronic clinical condition of volume overload, making the evaluation of multiple echocardiographic parameters important to establish the differential diagnosis, which has major implications for therapy and prognosis (Table 1).

In both conditions, increased E/A ratio with a shortened deceleration time can be noticed, however the respiratory variation in the velocity of the E wave is increased in constriction (> 25%), while in RCM it is normal or slightly variable (< 15%). In addition, this parameter tends to normalize in CP after pericardiectomy.[1]

Since RCM is a myocardial disease, it tends to have lower tissue (septal and lateral) Doppler velocities in contrast to CP.[1]

In CP, there is respirophasic movement of the interventricular septum, which is not usually present in RCM.

There is marked biatrial enlargement in RCM, but relatively normal or slightly increased sizes in CP.

Pulmonary hypertension is more common in RCM than in CP.

The left ventricular isovolumetric relaxation time is stable in RCM, while in CP there is exaggerated respiratory variation.[1]

Mitral valve propagation velocity with Color M-Mode is increased in CP (>55 cm/s), although reduced in RCM.[1]

In CP, during inspiration, the flow velocity in the pulmonary veins is predominantly systolic over diastolic, with a small increase in the latter in expiration, while in RCM, the flow in the pulmonary veins is consistently greater in diastole than in systole and persists throughout the respiratory cycle.[14]

In CP, there is an increase in diastolic reverse flow in the hepatic vein during expiration, while in RCM there may be reversal of diastolic flow in the hepatic vein during inspiration.[6]

In RCM, the flow in the SVC presents a much larger D wave than S wave, with a reduction in the D wave during expiration and an increase in reverse flow during AC during inspiration. In CP, the D wave is slightly larger than the S wave, with a slight reduction in the D wave during expiration and no change in the AC wave during the respiratory.[14]

CP is characterized by reduced circumferential strain, torsion, and shear rate, but with normal overall longitudinal strain despite regional differences. In RCM, there is reduced longitudinal strain but normal circumferential strain. This is due to the fact that subendocardial fibers, which are mainly responsible for longitudinal shortening, are more affected in RCM, while in CP there is greater involvement of subepicardial fibers, predominantly responsible for circumferential shortening.[6,7,9,13,15]

According to the study carried out at the Mayo Clinic between January 2008 and December 2010, whose population consisted of patients with surgically confirmed CP, it was concluded that echocardiography makes it possible to differentiate CP from RCM and severe tricuspid insufficiency. The three independent criteria most associated with the diagnosis of CP were: ventricular septal deviation related to breathing, preserved or increased e' velocity of the medial mitral *annulus*, and prominent reversal of the expiratory diastolic flow of the hepatic vein.[2,11] Each of these criteria was significantly associated with CP in the subgroup of patients with atrial fibrillation.[11]

According to the American Society of Echocardiography (2016), when the medial e' velocity of the mitral *annulus* is > 8 cm/s, mitral *annulus reversus* and hepatic vein expiratory flow reversal are present, RCM can be excluded and CP diagnosis can be established with confidence.[12]

Limitations of echocardiographic assessment in CP

The e' annular velocity through pulsed tissue Doppler may be reduced in cases of mitral valve replacement, severe annular calcification, and basal hypokinesia.

Diastolic dysfunction commonly associated with ischemia or advanced age can also make it difficult to interpret the mitral inflow pattern.

In aged and hypertensive patients, the LV cavity may be small, causing an increase in the propagation velocity of the mitral inflow despite the absence of CP.

A mitral flow pattern similar to that of CP can be seen in patients with chronic obstructive pulmonary disease, pulmonary thromboembolism, right ventricular infarction, shock, and large bilateral pleural effusion.

Diastolic posterior wall flattening during tachycardia may be difficult to detect.

In adolescents and young adults, the E/A ratio > 2 may be normal and they usually have mitral inflow propagation velocity > 100 cm/s and septal e' > 12 cm/s.

Conclusion

CP is an underdiagnosed cause of right and/or left ventricular failure caused by a reduction in the elasticity of the pericardium, resulting in impaired cardiac diastolic filling.[15] It has characteristic pathophysiological mechanisms, which can be identified with Doppler echocardiography, and this test is useful both for diagnostic confirmation and for follow-up of treated patients. The decision to perform additional tests, such as magnetic resonance imaging (MRI), computed tomography (CT) or invasive hemodynamic study, must be individualized.[11]

Author Contributions

Conception and design of the research: Oliveira ACR; writing of the manuscript: Rocha DFR, Oliveira ACR; critical revision of the manuscript for intellectual content: Silva JBM e Silva VN.

Potential Conflict of Interest

No potential conflict of interest relevant to this article was reported.

Sources of Funding

There were no external funding sources for this study.

Study Association

This study is not associated with any thesis or dissertation work.

Ethics Approval and Consent to Participate

This article does not contain any studies with human participants or animals performed by any of the authors.

References

1. Ardhanari S, Yarlagadda B, Parikh V, Dellsperger KC, Chockalingam A, Balla S, et al. Systematic Review of Non-Invasive Cardiovascular Imaging in the Diagnosis of Constrictive Pericarditis. Indian Heart J. 2017;69(1):57-67. doi: 10.1016/j.ihj.2016.06.004.
2. Ansari-Gilani K, Gilkeson RC, Kikano EG, Hoit BD. Multimodality Approach to the Diagnosis and Management of Constrictive Pericarditis. Echocardiography. 2020;37(4):632-6. doi: 10.1111/echo.14649.
3. Karima T, Nesrine BZ, Hatem L, Skander BO, Raouf D, Selim C. Constrictive Pericarditis: 21 Years' Experience and Review of Literature. Pan Afr Med J. 2021;38:141. doi: 10.11604/pamj.2021.38.141.22884.
4. Napolitano G, Pressacco J, Paquet E. Imaging Features of Constrictive Pericarditis: Beyond Pericardial Thickening. Can Assoc Radiol J. 2009;60(1):40-6. doi: 10.1016/j.carj.2009.02.034.
5. Klein AL, Abbara S, Agler DA, Appleton CP, Asher CR, Hoit B, et al. American Society of Echocardiography Clinical Recommendations for Multimodality Cardiovascular Imaging of Patients with Pericardial Disease: Endorsed by the Society for Cardiovascular Magnetic Resonance and Society of Cardiovascular Computed Tomography. J Am Soc Echocardiogr. 2013;26(9):965-1012.e15. doi: 10.1016/j.echo.2013.06.023.
6. Sohal S, Mathai SV, Lipat K, Kaur A, Visveswaran G, Cohen M, et al. Multimodality Imaging of Constrictive Pericarditis: Pathophysiology and New Concepts. Curr Cardiol Rep. 2022;24(10):1439-53. doi: 10.1007/s11886-022-01758-6.
7. Akyuz S, Yaylak B, Ergelen M, Uyarel H. Transient Constrictive Pericarditis: An Elusive Diagnosis. Future Cardiol. 2010;6(6):785-90. doi: 10.2217/fca.10.84. Erratum in: Future Cardiol. 2011;7(3):442.
8. Madeira M, Teixeira R, Costa M, Gonçalves L, Klein AL. Two-Dimensional Speckle Tracking Cardiac Mechanics and Constrictive Pericarditis: Systematic Review. Echocardiography. 2016;33(10):1589-99. doi: 10.1111/echo.13293.
9. van der Bijl P, Herbst P, Doubell AF. Redefining Effusive-Constrictive Pericarditis with Echocardiography. J Cardiovasc Ultrasound. 2016;24(4):317-23. doi: 10.4250/jcu.2016.24.4.317.
10. Alajaji W, Xu B, Sripariwuth A, Menon V, Kumar A, Schleicher M, et al. Noninvasive Multimodality Imaging for the Diagnosis of Constrictive Pericarditis. Circ Cardiovasc Imaging. 2018;11(11):e007878. doi: 10.1161/CIRCIMAGING.118.007878.
11. Argulian E, Halpern DG. "Hot Septum" Sign of Constrictive Pericarditis. JACC Case Rep. 2020;2(2):186-90. doi: 10.1016/j.jaccas.2019.12.024.
12. Welch TD, Ling LH, Espinosa RE, Anavekar NS, Wiste HJ, Lahr BD, et al. Echocardiographic Diagnosis of Constrictive Pericarditis: Mayo Clinic Criteria. Circ Cardiovasc Imaging. 2014;7(3):526-34. doi: 10.1161/CIRCIMAGING.113.001613.
13. Mertens LL, Denef B, De Geest H. The Differentiation between Restrictive Cardiomyopathy and Constrictive Pericarditis: The Impact of the Imaging Techniques. Echocardiography. 1993;10(5):497-508. doi: 10.1111/j.1540-8175.1993.tb00064.x.
14. Mastouri R, Sawada SG, Mahenthiran J. Noninvasive Imaging Techniques of Constrictive Pericarditis. Expert Rev Cardiovasc Ther. 2010;8(9):1335-47. doi: 10.1586/erc.10.77.
15. Gentry J, Klein AL, Jellis CL. Transient Constrictive Pericarditis: Current Diagnostic and Therapeutic Strategies. Curr Cardiol Rep. 2016;18(5):41. doi: 10.1007/s11886-016-0720-2.

Review Article

My Approach to Imaging in Sickle Cell Anemia

João Carlos Moron Saes Braga,[1,2,3] Fábio Villaça Guimarães Filho,[1,3,4] Alexandre Rodrigues,[1,3,4] Raphael Aparecido Barreto Silva[3,5]

Faculdade de Medicina e Enfermagem de Marília (Famema),[1] Marília, SP – Brazil
Universidade de São Paulo (USP),[2] São Paulo, SP – Brazil
Instituto do Coração de Marília (ICM),[3] Marília, SP – Brazil
Faculdade de Medicina de Botucatu (Unesp),[4] Botucatu, SP – Brazil
Instituto Dante Pazzanese de Cardiologia,[5] São Paulo, SP – Brazil

Abstract

Sickle cell disease (SCD) is recognized as a global problem in public health, characterized by the alteration in the red blood cells to the sickle form. Moreover, chronic anemia can also be observed through the change in the rheology of the red blood cells, leading to a scenario of inflammation and oxidative stress, making SCD a multisystem disease. Cardiac output (CO) proved to be high, leading to an overall increase in the heart chambers and an eccentric myocardial hypertrophy. These heart alterations were attributed only to adaptive reactions to chronic anemia. Recent studies have more clearly recognized an association with pulmonary hypertension (PH), left ventricular diastolic dysfunction, arrhythmias, and sudden death. Moreover, what has also arisen in this context is the hypothesis of the existence of a sickle-cell cardiomyopathy, characterized by diastolic dysfunction and restrictive physiology. The echocardiogram represents a key tool in determining cavitary volumes, diastolic dysfunction, and the estimation of pulmonary pressure, as well as constitutes a valuable resource in the diagnosis and therapeutic treatment of acute chest syndrome. The myocardial strain, rotational variables, myocardial work, and 3D echocardiography can be applied in an attempt to aid in the early detection of patients who are at a higher risk of developing complications and evolving to death related to SCD.

Introduction

Sickle cell disease (SCD) is the most prevalent hereditary hematological condition in the world, affecting about 5 million people, and it is estimated that 300,000 babies are born with SCD per year, being recognized by the World Health Organization (WHO) and Organization of the United Nations (UN) as a global public health concern.[1,2] A typical characteristic is the inheritance of mutant hemoglobin S, resulting from the replacement of a glutamic acid by a valine in position 6 of the beta chain, with consequent physical-chemistry modification in hemoglobin molecule.[3] SCD encompasses the homozygosity of hemoglobin S (SS), which constitutes sickle cell anemia (SCA), and associations with other hemoglobin variants, such as Hb C (SC), Hb D (SD), Hb E (SE), and interactions with thalassemias ($S\beta^0$, $S\beta^+$ and $S\alpha$). Sickle cell trait, heterozygosity for HbS, is not considered a disease.[4]

SCD is characterized by the strong tendency of mutant hemoglobin to polymerize, causing the red blood cell to change into a sickle shape, altering the erythrocyte membrane and the rheology of red blood cells, causing a scenario of intense hemolysis, occlusion of microvasculature, endothelial dysfunction, nitric oxide (NO) deficiency, inflammation, oxidative stress, increased neutrophil adhesiveness, activation of coagulation, making SCD a multisystem disease with high mortality, with a current average survival close to 50 years, even in developed countries.[5,6] Mortality results mainly from target-organ lesion, with a high incidence of sudden death in young adults and, currently, cardiopulmonary complications are the most common cause of death in this population[7] (Figure 1).

Cardiovascular manifestation of SCD

The regime of chronic anemia leads to adaptations that maintain adequate supply of oxygen to the tissues due to compensatory mechanisms. Non-hemodynamic mechanisms (stimulation of erythropoiesis) and hemodynamic mechanisms acting through afterload reduction (bradykinin, adenosine, NO) and preload increase (renin-angiotensin-aldosterone system) and even greater inotropic and chronotropic stimulation resulting from greater reflex sympathetic activity justify the increase in left ventricular function and the state of high cardiac output (CO).[8] These cardiac alterations classically found in SCD, such as enlargement of cardiac chambers, were only attributed to adaptive reactions to the chronic anemic state. Recent studies patently recognize the association with pulmonary hypertension (PH), left ventricular diastolic dysfunction, arrhythmia and sudden death and, in this context, the hypothesis of sickle cell cardiomyopathy characterized by diastolic dysfunction and restrictive physiology[9] (Figure 1). Coronary artery disease and cardiomyopathy secondary to iron overload are infrequent in these patients.[7] The most important aspects to be evaluated by echocardiography in SCD are presented below, as well as the indications for

Keywords

Sickle Cell Anemia; Diastolic Dysfunction; Pulmonary Hypertension

Mailing Address: João Carlos Moron Saes Braga •
Av. Vicente Ferreira, 780. Postal code: 17515-000. Cascata, Marília, SP - Brazil
E-mail: joaocbraga2002@yahoo.com.br
Manuscript received October 14, 2022; revised October 16, 2022; accepted December 22, 2022
Editor responsible for the review: Daniela do Carmo Rassi Frota

DOI: https://doi.org/10.36660/abcimg.20230009i

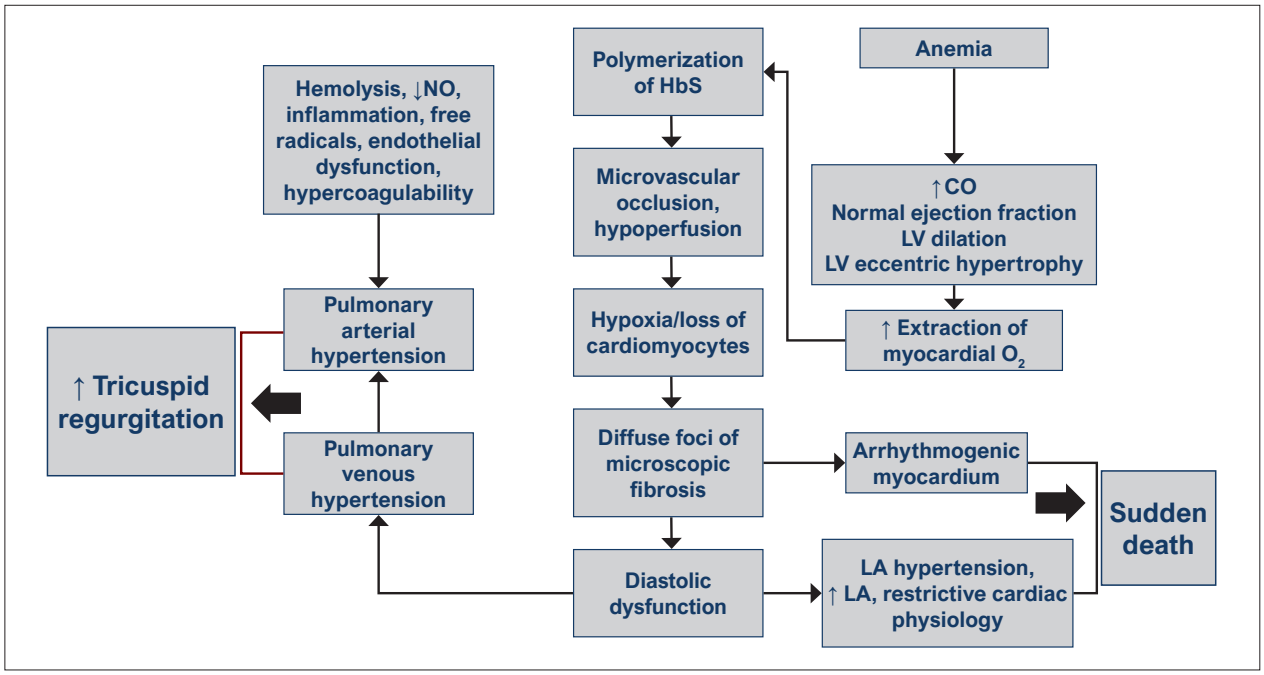

Figure 1 – *Mechanism proposed for sickle cell cardiomyopathy. Source: modified Rai et al. 2017.[7] LV: left ventricle; LA: left atrial; HbS: hemoglobin; NO: nitric oxide; O_2: oxygen; CO: cardiac output.*

echocardiography in the cardiological evaluation in this population (Table 1).

Quantification of the heart chambers

In SCD, CO is high due to increased systolic volume, with increased blood volume resulting from increased plasma volume and decreased peripheral resistance. Increased CO leads to enlargement of cardiac chambers globally, and eccentric-type myocardial hypertrophy. Abnormalities are of a progressive nature, and are more exuberant in the more advanced age groups. It is believed that right ventricle (RV) dilation occurs later and is less intense than that of the left cavities.

In order to properly quantify the cardiac chambers in this population, the internal linear measurement of the cardiac cavities and their walls should be carried out routinely and, ideally, cavity volumes must be measured by indexing the patient's body surface on two-dimensional echocardiography (Figure 2). Three-dimensional echocardiography, if available, can more accurately and reproducibly assess not only cavity volumes, but also left ventricle (LV) mass and function.

It is also relevant to highlight some difficulties related to the echocardiographic evaluation of this particular population, since most patients have body mass index significantly reduced, chronic pain with relative limitation of mobility and, often, tachycardia during the test.

Systolic function and myocardial strain

Left ventricular systolic function seems to be preserved in most patients with SCD, despite significant LV dilation,

Table 1 – Echocardiogram indications in the cardiac assessment of patients with SCD

Assessment of signs suggestive of PH and estimation of pulmonary pressure through maximum TRV.
Assessment of cavity diameters and volumes.
Assessment of ventricular hypertrophy.
Analysis of systolic function and diastolic function.
Assessment of heart murmur evaluation and associated valvopathy.
Analysis of cardiac impairment due to associated comorbidities.
Cardiological assessment in ACS helps detect transient elevations in pulmonary pressure and right ventricular dysfunction in the acute period.
Assessment of patients with clinical and laboratory criteria of disease severity.

PH: pulmonary hypertension; TRV: tricuspid regurgitation velocity; ACS: acute chest syndrome.

which is the rule in this population (Figure 2). Segmental abnormalities and coronary artery disease are rare.[9] When systolic dysfunction is present, it is mainly identified in older patients with associated diseases, such as systemic arterial hypertension and kidney disease.[10]

For many years, it has been considered that conventional parameters for measuring ejection fraction, due to their

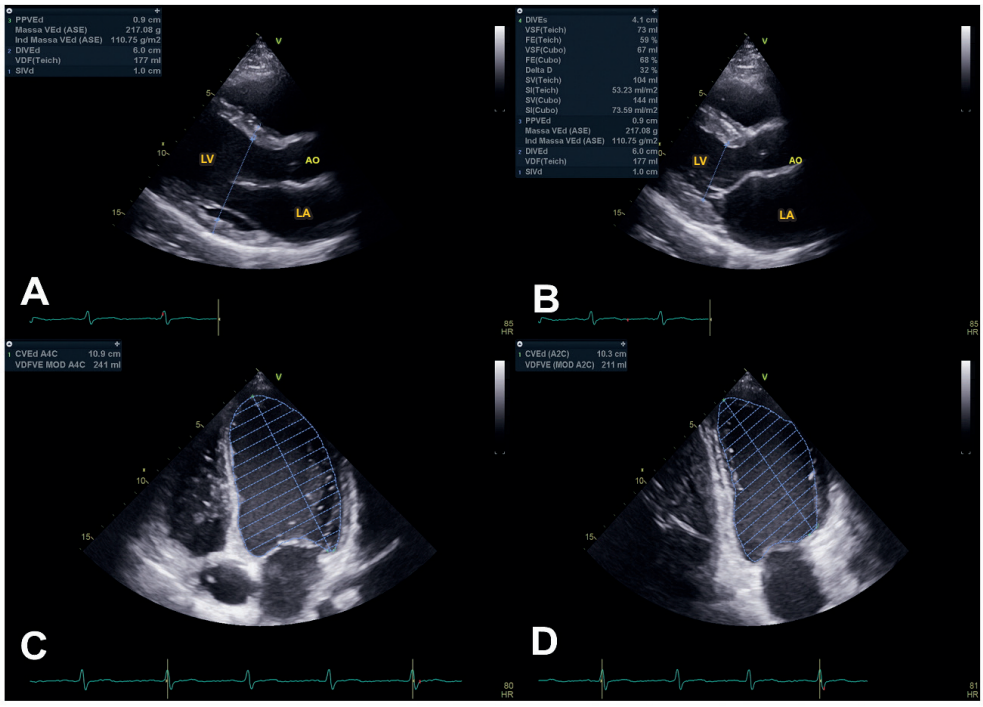

Figure 2 – *(A) Two-dimensional echocardiography (parasternal long-axis view) in a 20-year-old patient with SCA, showing left ventricular diastolic diameter of 60 mm. (B) Same patient, showing LA volume of 46 ml/m² (reference: <34 ml/m²). (C)/(D) Same patient, showing left ventricular volume of 118 ml/m² (reference: <74 ml/m²). LV: left ventricle; LA: left atrium; AO: aorta.*

great influence from pre- and after-load abnormalities, would not serve to assess systolic function in patients with SCD, hiding the intrinsic function of the cardiac muscle. Therefore, preference should be given to the assessment of biventricular systolic function using two-dimensional and three-dimensional strain, if available, rotational variables (twist and torsion) and myocardial work (Figure 3).[11-13]

Several factors can influence the analysis by myocardial strain in the context of SCD: ethnicity, race, sex, age and hemodynamic factors (hyperdynamic state and hypervolemia).[14] And there may be technical limitations for three-dimensional echocardiography: mobility difficulty and respiratory apnea in image acquisition, difficulty in image acquisition with high heart rate, and difficulty acquiring the full image in the large ventricles.

Diastolic dysfunction

LV diastolic dysfunction is common in patients with SCD, classically related to ventricular dilation and eccentric myocardial hypertrophy in response to chronic anemia, being an independent predictor of reduced exercise tolerance and mortality in these patients.[15] Recently, some experimental studies with anatomopathological analysis and cardiac resonance analysis have considered the possibility of myocardial fibrotic involvement due to the sequelae of microscopic ischemic events, resulting in restrictive ventricular filling and left atrial (LA) enlargement[9] (Figures 1 and 4).

Echocardiographic analysis of LV diastolic function is an integral part of the routine evaluation of patients with symptoms of dyspnea or heart failure. Diagnosis of diastolic dysfunction in this population is highly challenging, as patients usually have dilated LV and preserved ejection fraction, in addition to obvious signs of volume overload. To start the evaluation, it must be determined whether there is myocardial disease (evidence of relevant structural or functional heart disease, such as left ventricular hypertrophy — LVH — and/or systolic dysfunction) and, considering this determination, we suggest the evaluation of LV with routine two-dimensional strain for all patients. In addition, objective measures should be taken to assess filling pressures and diastolic function, which should be determined by analyzing echocardiographic variables, including mitral flow velocities, mitral annulus velocities, E/e' ratio, maximum tricuspid regurgitation velocity (TRV) and indexed LA volume. The four currently recommended variables and abnormal cutoff values are: 1) Mean E/e' ratio >14; 2) Abnormal velocity of septal e' <7 cm/sec or lateral e' <10 cm/sec; 3) Indexed LA volume >34 ml/m²; 4) Maximum tricuspid regurgitation (TR) speed >2.8 m/sec.[16]

PH

PH is a common serious complication in patients with SCD, being an important marker of mortality in these patients.[17] PH in SCD is mixed, having a pre-capillary

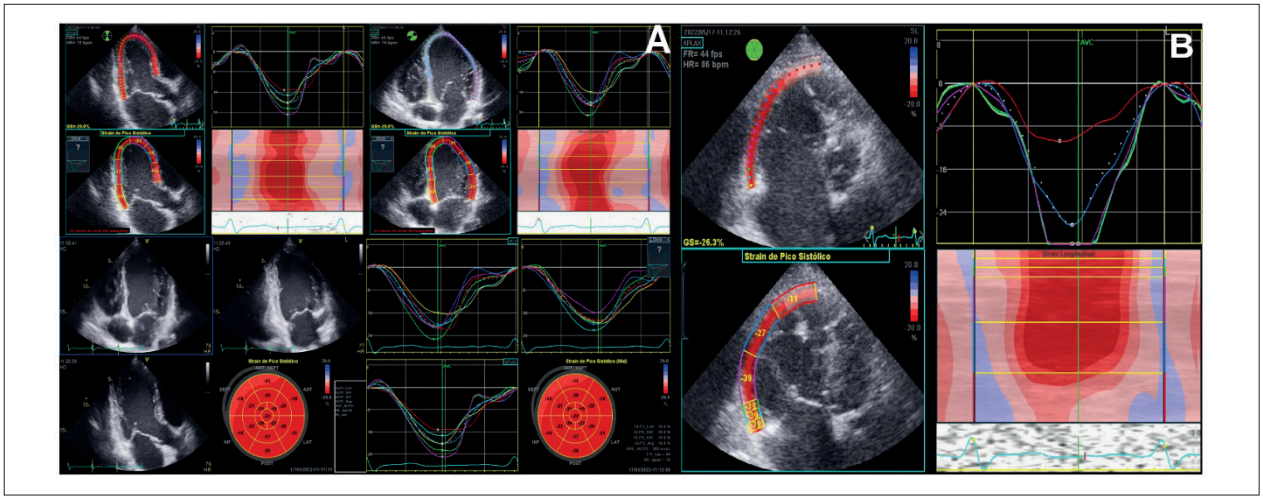

Figure 3 – *(A) Transthoracic echocardiogram (apical view) for analysis of the longitudinal strain in 20-year-old patient with SCA, showing preserved contractile function in each of the segments with LV global longitudinal Strain : -19.9 (Reference: <-16.9). (B) Same patient, showing preserved contractile function in each of the RV free wall segments, analysis of right ventricular longitudinal strain with RV free wall strain result: -26.3 (Reference: <-20).*

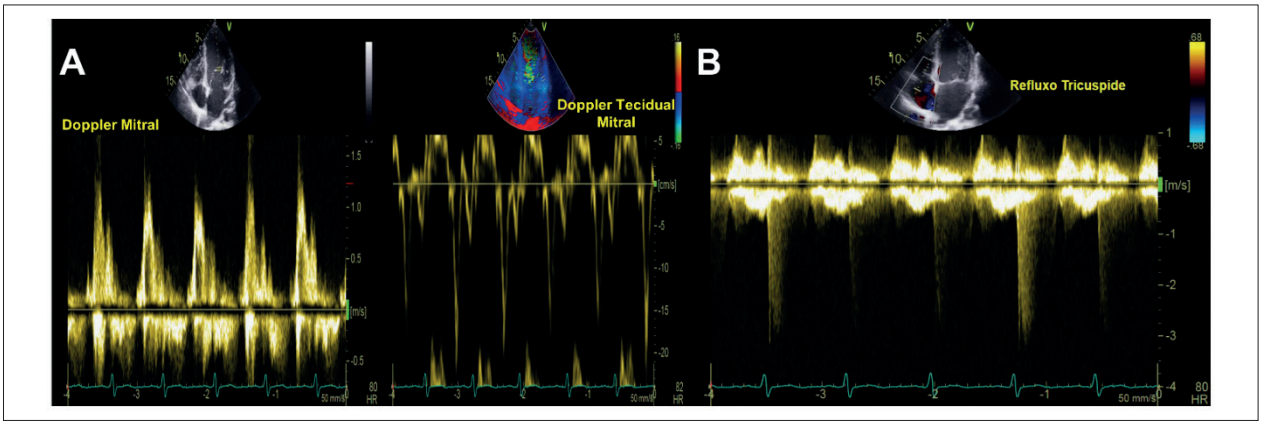

Figure 4 – *(A) Diastolic flow in 20-year-old patient with SCA. Note the septal E/e´ ratio of 21, resulting in a worse prognosis. (B) Same patient, showing TRV of 3.0 m/s, resulting in a worse prognosis.*

arterial component (pulmonary arterial hypertension — PAH) due to progressive increase in pulmonary vascular resistance (hemolysis, ↓NO, inflammation, free radicals, endothelial dysfunction, hypercoagulability, chronic thromboembolism) and a post-capillary venous component (venous pulmonary hypertension — VPH) (LV diastolic dysfunction). It is currently classified in PH group 5 due to multifactorial mechanisms (Figure 4). Estimation of pulmonary pressure by echocardiography is carried out mainly by measuring the TRV by which the pulmonary artery systolic pressure — PASP — is estimated (derived from the Bernoulli equation; PASP = 4 times the determination of TRV squared, then adding an estimated right atrial pressure). TRV greater than 2.9 m/s defines a subgroup of risk, occurring in approximately 10% of adults with SCD, and is associated with a relative risk of death of approximately 10, according to previous studies.[18] Intermediate TRV values between 2, 5 and 2.9 m/s remain a source of controversy. However, these patients also seem to have decreased exercise capacity and increased mortality with 4 risk ratio of death.[17] Although the vast majority of epidemiological studies conducted to date have shown that a mild to moderate elevation of RV systolic pressure (TRV ≥2.5 m/s) is common in adults with SCD, it is associated with a higher rate of risk of early death. The 2.5 m/s cutoff leads to hyperdiagnosis of PH, and higher TRV thresholds (>2.9 m/s) improves specificity.[18] Due to the high risk of developing PH, patients with SCD should undergo regular echocardiography scans at least every two or three years to identify the presence of increased pulmonary pressures.[19]

Acute chest syndrome

Acute chest syndrome (ACS) consists of a combination of signs and symptoms including dyspnea, chest pain, fever, cough and hypoxemia, associated with the emergence of a new pulmonary infiltrate. The etiology is complex and multifactorial, involving infectious and non-infectious causes

and in a high number of cases it is not possible to define the etiology. Diagnosis of ACS is extremely important due to significant morbidity and mortality and high recurrence. Echocardiography in this scenario is usually performed at the bedside and often shows a transient increase in pulmonary pressure and right ventricular dysfunction in the acute condition, having a fundamental diagnostic and prognostic application in this context. Patients with TRV ≥3 m/s on echocardiography during the acute event are at particularly higher risk of multiorgan failure and sudden death. Point-of-care lung ultrasound has also proven to be an important tool in ACS, reducing diagnostic radiation in the sickle cell population.[20]

Conclusions

SCD evolves with cardiovascular manifestations characteristically with restrictive cardiomyopathy (diastolic dysfunction, LA enlargement and preserved ejection fraction) and PH (pulmonary arterial hypertension and pulmonary venous hypertension). The echocardiogram is a fundamental instrument for determining cavity volumes, diastolic function, and estimating pulmonary pressure, and constitutes a valuable resource in the diagnosis and therapeutic management of ACS. Myocardial strain, rotational variables, myocardial work and 3D echocardiography can be used in an attempt to support the early identification of patients at greater risk of developing complications and death related to SCD.

Potential Conflict of Interest

No potential conflict of interest relevant to this article was reported.

Sources of Funding

There were no external funding sources for this study.

Study Association

This study is not associated with any thesis or dissertation work.

Author Contributions

Writing of the manuscript: Braga JCMS; critical revision of the manuscript for intellectual content: Guimarães Filho FV, Rodrigues A, Silva RAB.

Ethics Approval and Consent to Participate

This article does not contain any studies with human participants or animals performed by any of the authors.

References

1. Serjeant GR. Sickle-Cell Disease. Lancet. 1997;350(9079):725-30. doi: 10.1016/S0140-6736(97)07330-3.
2. Damy T, Bodez D, Habibi A, Guellich A, Rappeneau S, Inamo J, et al. Haematological Determinants of Cardiac Involvement in Adults with Sickle Cell Disease. Eur Heart J. 2016;37(14):1158-67. doi: 10.1093/eurheartj/ehv555.
3. Marotta CA, Wilson JT, Forget BG, Weissman SM. Human Beta-Globin Messenger RNA. III. Nucleotide Sequences Derived from Complementary DNA. J Biol Chem. 1977;252(14):5040-53.
4. Stuart MJ, Nagel RL. Sickle-Cell Disease. Lancet. 2004;364(9442):1343-60. doi: 10.1016/S0140-6736(04)17192-4.
5. Kaul DK, Fabry ME, Costantini F, Rubin EM, Nagel RL. In Vivo Demonstration of Red Cell-Endothelial Interaction, Sickling and Altered Microvascular Response to Oxygen in the Sickle Transgenic Mouse. J Clin Invest. 1995;96(6):2845-53. doi: 10.1172/JCI118355.
6. Piel FB, Steinberg MH, Rees DC. Sickle Cell Disease. N Engl J Med. 2017;376(16):1561-73. doi: 10.1056/NEJMra1510865.
7. Rai P, Niss O, Malik P. A Reappraisal of the Mechanisms Underlying the Cardiac Complications of Sickle Cell Anemia. Pediatr Blood Cancer. 2017;64(11). doi: 10.1002/pbc.26607.
8. Serjeant GR. Cardiovascular system. In: Serjeant GR, Serjeant BE, editors. Sickle Cell Disease. 3rd ed. Oxford: Oxford University Press; 1992.
9. Bakeer N, James J, Roy S, Wansapura J, Shanmukhappa SK, Lorenz JN, et al. Sickle Cell Anemia Mice Develop a Unique Cardiomyopathy with Restrictive Physiology. Proc Natl Acad Sci U S A. 2016;113(35):E5182-91. doi: 10.1073/pnas.1600311113.
10. Gordeuk VR, Sachdev V, Taylor JG, Gladwin MT, Kato G, Castro OL. Relative Systemic Hypertension in Patients with Sickle Cell Disease Is Associated with Risk of Pulmonary Hypertension and Renal Insufficiency. Am J Hematol. 2008 Jan;83(1):15-8. doi: 10.1002/ajh.21016.
11. Barbosa MM, Vasconcelos MC, Ferrari TC, Fernandes BM, Passaglia LG, Silva CM, et al. Assessment of Ventricular Function in Adults with Sickle Cell Disease: Role Of Two-Dimensional Speckle-Tracking Strain. J Am Soc Echocardiogr. 2014;27(11):1216-22. doi: 10.1016/j.echo.2014.07.014.
12. Ahmad H, Gayat E, Yodwut C, Abduch MC, Patel AR, Weinert L, et al. Evaluation of Myocardial Deformation in Patients with Sickle Cell Disease and Preserved Ejection Fraction Using Three-Dimensional Speckle Tracking Echocardiography. Echocardiography. 2012;29(8):962-9. doi: 10.1111/j.1540-8175.2012.01710.x.
13. Braga JC, Assef JE, Waib PH, de Sousa AG, de Mattos Barretto RB, Guimarães Filho FV, et al. Altered Left Ventricular Twist is Associated with Clinical Severity in Adults and Adolescents with Homozygous Sickle Cell Anemia. J Am Soc Echocardiogr. 2015;28(6):692-9. doi: 10.1016/j.echo.2015.01.019.
14. Marwick TH, Leano RL, Brown J, Sun JP, Hoffmann R, Lysyansky P, et al. Myocardial Strain Measurement with 2-Dimensional Speckle-Tracking Echocardiography: Definition Of Normal Range. JACC Cardiovasc Imaging. 2009;2(1):80-4. doi: 10.1016/j.jcmg.2007.12.007.
15. Sachdev V, Kato GJ, Gibbs JS, Barst RJ, Machado RF, Nouraie M, et al. Echocardiographic Markers of Elevated Pulmonary Pressure and Left Ventricular Diastolic Dysfunction are Associated with Exercise Intolerance in Adults and Adolescents with Homozygous Sickle Cell Anemia in the United States and United Kingdom. Circulation. 2011;124(13):1452-60. doi: 10.1161/CIRCULATIONAHA.111.032920.
16. Nagueh SF, Smiseth OA, Appleton CP, Byrd BF 3rd, Dokainish H, Edvardsen T, et al. Recommendations for the Evaluation of Left Ventricular Diastolic Function by Echocardiography: An Update From the American Society of Echocardiography and the European Association of Cardiovascular Imaging. J Am Soc Echocardiogr. 2016;29(4):277-314. doi: 10.1016/j.echo.2016.01.011.

17. Gladwin MT. Cardiovascular Complications and Risk of Death in Sickle-Cell Disease. Lancet. 2016;387(10037):2565-74. doi: 10.1016/S0140-6736(16)00647-4.

18. Gladwin MT, Sachdev V, Jison ML, Shizukuda Y, Plehn JF, Minter K, et al. Pulmonary Hypertension as a Risk Factor for Death in Patients with Sickle Cell Disease. N Engl J Med. 2004;350(9):886-95. doi: 10.1056/NEJMoa035477.

19. Ataga KI, Moore CG, Jones S, Olajide O, Strayhorn D, Hinderliter A, et al. Pulmonary Hypertension in Patients with Sickle Cell Disease: A Longitudinal Study. Br J Haematol. 2006;134(1):109-15. doi: 10.1111/j.1365-2141.2006.06110.x.

20. Daswani DD, Shah VP, Avner JR, Manwani DG, Kurian J, Rabiner JE. Accuracy of Point-of-care Lung Ultrasonography for Diagnosis of Acute Chest Syndrome in Pediatric Patients with Sickle Cell Disease and Fever. Acad Emerg Med. 2016;23(8):932-40. doi: 10.1111/acem.13002.

My Approach to Assessment After Tricuspid Interventions: Tips and Tricks

Bruna Morhy Borges Leal Assunção,[1,2] Arthur Cortez Gonçalves,[1] Lucas Velloso Dutra,[1,3] Renata de Sá Cassar[1,4]

Hospital Sirio-Libanes,[1] São Paulo, SP – Brazil

Instituto do Câncer do Estado de São Paulo (ICESP),[2] São Paulo, SP – Brazil

Hospital Edmundo Vasconcelos,[3] São Paulo, SP – Brazil

Instituto do Coracão do Estado de São Paulo (Incor),[4] São Paulo, SP – Brazil

Abstract

Severe tricuspid regurgitation (TR) is associated with high morbidity and mortality. Given that surgical treatment of TR alone has been associated with high mortality, transcatheter interventions in the tricuspid valve (TV) have been used for its treatment, with relatively lower risk. There is a delay in intervention for TR, and this is probably related to a limited understanding of the anatomy of the TV and the right ventricle, in addition to an underestimation of the severity of TR. In this scenario, it is necessary to have comprehensive anatomical knowledge of the TV, the pathophysiology involved in the mechanism of regurgitation, and more accurate grading. The TV has anatomical, histological, and spatial peculiarities that make its assessment more complex when compared to the mitral valve, requiring knowledge and training in the various echocardiographic techniques that will often be used in combination for accurate assessment.

This review will describe the anatomy of the TV, the role of echocardiography in the diagnosis, grading, and pathophysiology involved in TR; the main transcatheter treatment options currently available for TR; and the assessment of outcomes after transcatheter intervention by means of multiple echocardiographic modalities.

Introduction

Tricuspid regurgitation (TR) is a frequent echocardiographic finding that is present in 80–90% of normal individuals. Mild or minimal TR has no impact on clinical outcomes. However, moderate or severe TR is associated with worse prognosis regardless of left ventricular dysfunction or pulmonary arterial hypertension.[1]

The cause of TR may be related to the valve apparatus (primary TR) or the heart structure (secondary or functional TR), the latter being responsible for up to 90% of cases.[2]

In advanced stages, the conventional approach through open heart surgery may be indicated. Replacement of the diseased valve is performed with mechanical or biological valve prostheses. The choice of device depends on availability and on the age of the patient. Another surgical option is valve repair, mostly with the implantation of an associated valve annulus to reduce the size of the native valve annulus. Surgical repair mortality ranges from 13.9 to 33%. On average, operative mortality of tricuspid valve (TV) surgery is 19% at 30 days.[2] Due to advanced age and concomitant pathologies, many individuals with severe TR are considered inoperable or at prohibitive surgical risk, and only 18% of them are actually referred for valve surgery.[3]

Successful development and outcomes of transcatheter aortic valve implantation, followed by transcatheter therapies for mitral valve disease, have opened up a plethora of opportunities for transcatheter treatment of TR, a valvular heart disease traditionally considered benign and often left untreated.[4]

Current transcatheter treatment options mimic surgical techniques and include European-approved solutions such as leaflet approximation, direct annuloplasty, and heterotopic vena cava implantation, as well as transcatheter TV replacement systems not yet commercially available, using orthotopic valve implant.[4] (Figure 1) Compared to mitral procedures, transcatheter tricuspid valve interventions (TTVI) present several additional technical and anatomic challenges, including difficult visualization of the VT apparatus, variable anatomy with thinner valve leaflets, and a large coaptation gap. An algorithm for TTVI device selection was recently proposed.[4] (Figure 2)

The TV anatomy

TV is the largest of the four heart valves, and its area varies between 7 and 9 cm^2. Due to its large size and low pressure differences between the right atrium (RA) and right ventricle (RV), peak transvalvular diastolic velocities are typically smaller than 1 m/s with mean gradients <2 mmHg.[5] TV has anterior, septal, and posterior cusps. The anterior cusp is usually the largest, 2.2 cm wide. The septal and posterior cusps are notably smaller and measure approximately 1.5 and 2.0 cm, respectively.[6] In addition, it is the most apically positioned valve and, similar to the mitral valve, it consists of four components: the annulus fibrosus, the three cusps, the papillary muscles and the chordae tendineae.[7] The anterior papillary muscle has chordae for the anterior and posterior cusps, and the medial papillary muscle for the posterior and septal cusps. The septal wall provides chordae for the anterior and septal cusps. In addition, there may be accessory chordae connections to the RV free wall and to the moderator band.[8] The normal tricuspid annulus (TA) is triangular and saddle shaped.[8] When functional dilation occurs, the TA becomes more circular and planar, dilating from the septum to the lateral wall (Figure 3E).[9]

Keywords

Tricuspid valve; tricuspid regurgitation; transcatheter

Mailing Address: Bruna Morhy Borges Leal Assunção •
Rua Sabara, 315, apt 1003. Postal code: 01239-011. Higienópolis, São Paulo, SP - Brazil.
E-mail: brunaleal@gmail.com
Manuscript received November 30, 2022; revised manuscript December 1, 2022; accepted December 2, 2022.
Editor responsável pela revisão: Daniela do Carmo Rassi Frota

DOI: https://doi.org/10.36660/abcimg.20230006i

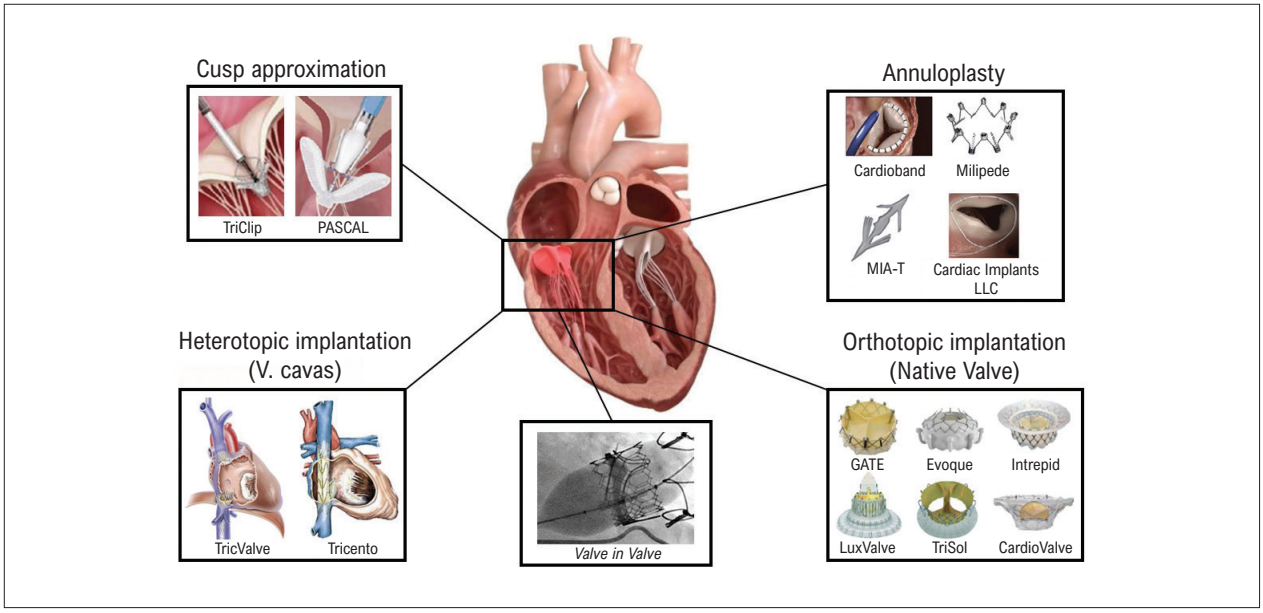

Figure 1 – *Current options for transcatheter TV intervention that are approved or under clinical evaluation. Adapted from Praz F, et al.[4]*

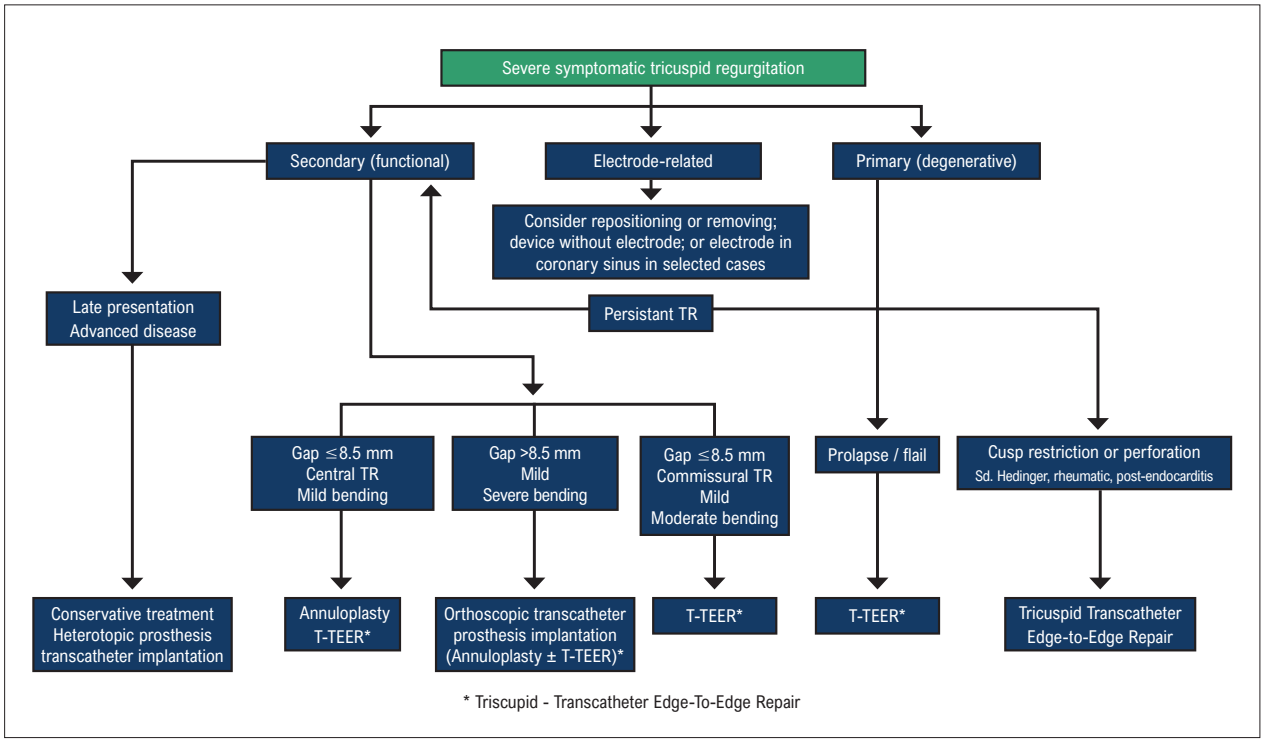

Figure 2 – *Algorithm for selecting the TTVI device. Adapted from Praz F, et al.[4] TR: tricuspid regurgitation.*

The role of echocardiogram

Echocardiography is routinely used in clinical practice to assess the severity of TR. This is done in an integrated way, using the color Doppler study by calculating the jet area, evaluating vena contracta width, calculating convergence flow, in addition to the size and direction of regurgitant jet.[10] On a two-dimensional transthoracic echocardiogram (2D TTE), the three cusps cannot be viewed simultaneously, requiring the acquisition of different echocardiographic windows. Through the longitudinal parasternal window via RV inlet, the anterior cusp will always be viewed in the proximal field, but in the distal field the septal cusp may be present (when the interventricular septum and/or the left ventricle are seen) or the posterior cusp (when the interventricular septum

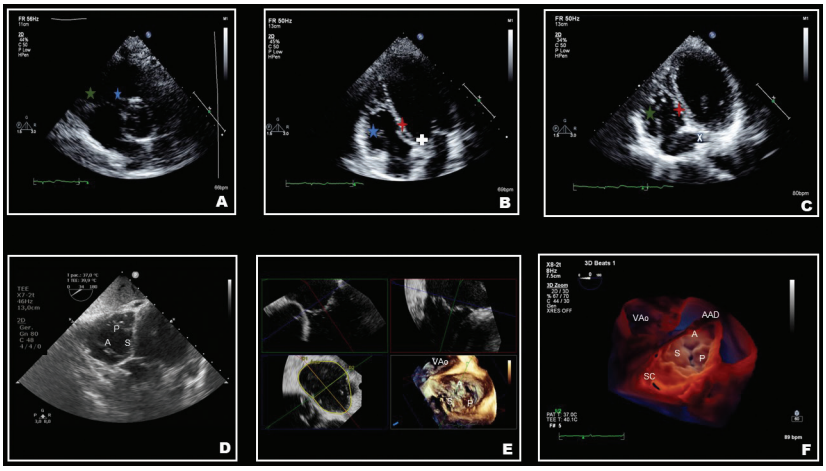

Figure 3 – *A) Parasternal short axis window (TTE). The leaflet adjacent to the free wall is posterior (green star) and the opposite leaflet adjacent to the aorta is anterior (blue star). B) Apical four-chamber window (TTE). The septal leaflet of the TV is adjacent to the septum (red star), while the opposite leaflet is anterior (blue star), once the aorta is displayed (white cross). C) Apical four-chamber window (TTE). The septal leaflet of the TV is adjacent to the septum (red star), while the opposite leaflet is posterior (green star), once the coronary sinus is displayed ("white X"). D) Transgastric short-axis view (TEE), which is the only two-dimensional view that generally provides simultaneous imaging of all three VT cusps. E) Evaluation of the measurements of the TA through multiplanar reconstruction (3D TEE). F) 3D TEE photorealistic rendering with transparency — atrial view of the TV and its relationships. (P: posterior cusp; S: septal cusp; A: anterior cusp); AoV: aortic valve; CS: coronary sinus; RAA: right atrial appendage)*

is not seen).[5] In the short-axis parasternal window, the cusp adjacent to the aorta is the septal (when the left ventricular outflow tract is seen) or anterior cusp (Figure 3A), and the cusp adjacent to the free wall is usually the posterior cusp (Figure 3A).[5] In the apical four-chamber window, the septal cusp will always be adjacent to the septum and the opposite cusp will be the anterior one when the transducer is angled anteriorly, and the aorta is seen (Figure 3B). However, if the transducer is angled posteriorly, displaying the coronary sinus, the opposite cusp will be the posterior one (Figure 3C).[5] The transesophageal echocardiogram (TEE) includes additional images, many of which are intended to improve TV image. Given the position of the heart in relation to the esophagus and stomach, the mid-esophagus, distal esophagus, transgastric, and deep transgastric views can bring the probe closer to the TV for two-dimensional (2D) and three-dimensional (3D) images.[11]

Multiple echocardiographic windows are needed to assess TV starting from the mid-esophageal plane. Four-chamber window displays the septal cusp and anterior cusp; Biplanar imaging can help clarify which cusp is displayed because the anterior cusp is normally seen adjacent to the aorta (Video 1). In the distal esophageal plane at the level of the coronary sinus, the posterior and anterior cusps are typically displayed. Advancing the TEE probe into the stomach and rotating approximately 20°–60° produces the transgastric short-axis view, which is the only two-dimensional view that generally provides simultaneous imaging of all three TV cusps (Figure 3D). Using the biplanar image, all cusp coaptation points can be seen. Advancing the TEE probe along with the right anterior flexion and returning the angle to 0°–20° produces a deep transgastric plane of the TV.[11]

Three-dimensional echocardiography significantly improved the accuracy of imaging and identification of cusps and associated anatomical components of the TV complex, eliminating the need for mental reconstruction of multiple 2D planes. Lang et al. suggested standardization of 3D acquisition of the VT, with the interatrial septum positioned inferiorly (at six o'clock), so that the anterior cusp is on the right, the posterior cusp on the left and the septal cusp on the distal field.[12] Due to the more anterior position of the right heart chambers, 3D TV images on TTE can be equal to or sometimes better than the 3D images on TEE. As in TTE, 3D TV images on TEE must have the interatrial septum positioned inferiorly as standard. Thus, the anterior cusp is on the left, the posterior cusp on the right and the septal cusp in the distal field (Figure 3F).

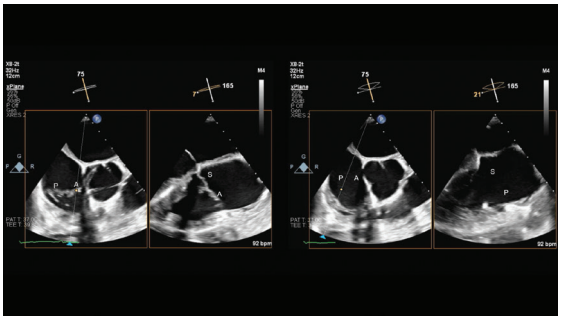

Video 1 – *Biplanar image through the middle esophageal plane (TEE). Commissural TV view (inlet and outlet of the RV), using a simultaneous orthogonal view for better identification of the cusps. (P: posterior cusp; S: septal cusp; A: anterior cusp)*
Link: http://abcimaging.org/supplementary-material/2023/3601/convite-Bruna-Leal-video_01.mp4

Post-procedure assessment

One of the main objectives of evaluating the success of percutaneous tricuspid procedure is evaluating residual TR. Similar to pre-procedure quantification, post-procedure assessment should attempt to quantify the severity of TR as much as possible. TR grading is well described both in the guidelines of the American Society of Echocardiography and in the European Cardiovascular Imaging Association.[13,14] In both documents, significant TR is defined as vena contracta diameter ≥0.7 cm; PISA radius >0.9 cm (when aliasing speed=28 cm/s); ERO≥40 mm^2; regurgitant volume ≥45 ml; inferior vena cava diameter >25 mm; RA area >18 cm^2, triangular shape of TR on continuous Doppler flow, in addition to reverse flow in hepatic veins. Measurement of 3D vena contracta area (VCA) has a good correlation with the regurgitant orifice area. A cut off >0.36 cm^2 for 3D VCA values has been shown to present 89% sensitivity and 84% specificity in predicting severe TR.[15] However, since patients undergoing TTVI often have an anatomical regurgitant area several times larger than an effective regurgitant orifice area (EROA) of 0.40 cm^2, an extended classification to include "massive" and "torrential" TR (both associated with harmful results) has been recently proposed (Table 1). To date, the complete elimination of TR after a percutaneous procedure is not achievable with currently available technology. However, most patients show significant improvement in functional class with reduction of at least two degrees of TR severity (e.g., from torrential to severe TR).[16]

While it is important to assess residual TR, equally important is the assessment of RV size and systolic function.[13] Including TA plane systolic excursion (TAPSE), RV fractional area change (FAC), tissue Doppler-derived lateral TA systolic wave velocity, RV myocardial performance index (MPI), myocardial strain indices, such as the global longitudinal strain or longitudinal strain of the 2D RV free wall, in addition to RV ejection fraction by the three-dimensional method. TAPSE values <17 mm, FAC <35%, S' <9.5 cm/s, RV free wall longitudinal strain <20% (absolute values), RV MPI by pulsed Doppler <0.43 s and 3D RV ejection fraction <45% are considered abnormal RV systolic function values[13] (Figure 4).

Significant TA dilation is defined by a diastolic diameter of ≥40 mm or >21 mm/m^2 by the apical four-chamber TTE window and is indicative of severe TR by the latest American Heart Association/American College of Cardiology guidelines.[19] Besides, TV thetering distance measurements (>0.76 cm) and TV thetering area (>1.63 cm^2) are predictors of TR recurrence after surgery.[20,21]

The TriClip system (Abbott Vascular, Abbott Park, Illinois) is an adaptation of the Abbott Vascular MitraClip system for the TV. The main objective of the tricuspid transcatheter edge-to-edge repair system is to restore coaptation between leaflets and reduce the regurgitant orifice area.[22] Quantification of TR severity can be challenging because TR jets are often deflected in multiple directions. Furthermore, it is important to inform the number of clips released, commissures/cusps captured and whether there is a single leaflet captured by the device. A mean transvalvular gradient <3 mmHg is acceptable after clip release.[2]

The FORMA Spacer System is a device that aims to fill the coaptation gap resulting from annulus and TV leaflet dilation. It consists of two pieces: a foam polymer balloon spacer placed in the regurgitant orifice, creating a surface for cusp coaptation and an anchorage system attached to the apex of the RV. After the FORMA procedure, it is difficult to quantify TR due to non-circular jets that appear around the device.[22] It is important to describe the percentage of device length in RV and RA.

RV inlet and outlet images are the main echocardiographic windows on TTE to assess device position (TriClip and FORMA). Short-axis parasternal and short-axis subcoastal windows are also helpful.[5] On TEE, the distal esophagus plane is typically the best for assessing regurgitant jet, leaflet capture by the clip, and tricuspid transvalvular gradients.[22] Transgastric planes are also useful for evaluating clip position, and Doppler scan in the deep transgastric planes.[5] The PISA method is generally not suitable for evaluating multiple regurgitant jets. A semiquantitative approach based on color Doppler and multiple echocardiographic windows might be required in such patients. The vena contracta area measured by 3D can also be useful in this context to assess the severity of residual TR after the procedure.[22]

There are two TTVI devices available in Brazil: TricValve and the Valve-in-Valve Tricuspid. TricValve (P&F Products & Features

Table 1 – Extended classification for grading TR. Adapted from Hahn et al.[17,18]

Parameters	Mild	Moderate	Moderate/ Severe	Severe	Massive	Torrential
Vena contracta width	< 3 mm	3–6.9 mm	6–6.9 mm	7–13 mm	14–20 mm	≥21 mm
EROA	20 mm^2	20–29 mm^2	30–39 mm^2	40–59 mm^2	60–79 mm^2	≥80 mm^2
Regurgitant volume	< 15 mL	15–29 mL	30–44 mL	40–59 mL	60–74 mL	≥75 mL
3D ECHO Regurgitant Fraction (MRI)*	< 25% (30%)*	< 25–44% (30–49%)*		< 45% (50%)*		
3D vena contracta				75–94 mm^2	95–114 mm^2	>115 mm^2

EROA: effective regurgitant orifice area; MRI: magnetic resonance imaging.

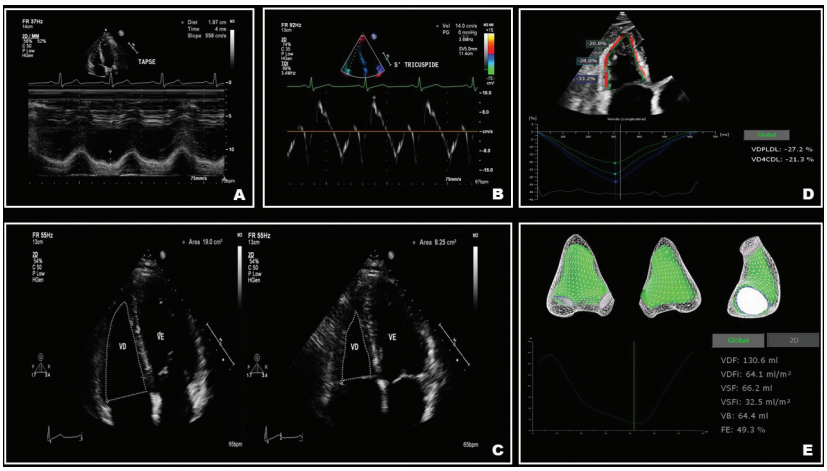

Figure 4 – *Quantitative parameters for assessing RV function (TTE): A) TA plane systolic excursion (TAPSE); B) RV fractional area change (FAC); C) lateral TA systolic wave velocity derived from tissue Doppler; D) 2D RV free wall longitudinal strain; E) and assessment of RV volumes and three-dimensional RV ejection fraction.*

Vertriebs GmbH, Vienna, Austria, in cooperation with Braile Biomedica, São José do Rio Preto, Brazil) consists of two self-expanding heterotopic bioprosthetic valves implanted in the superior and inferior vena cava and anchored in the cavo-atrial inflow. Transcatheter implantation of Valve-in-Valve Tricuspid through expandable balloon prosthesis consists of percutaneously treating dysfunction of TV bioprosthesis (Video 3). A recent pilot study carried out at Instituto do Coração do Hospital das Clínicas da Faculdade de Medicina da Universidade de São Paulo, from June 2015 to August 2022, evaluated 12 patients, most of them with congenital heart disease (66% Tetralogy of Fallot or Ebstein anomaly), who underwent percutaneous implantation of Valve-in-Valve in the tricuspid position due to symptomatic bioprosthesis dysfunction (50% NYHA functional class III-IV heart failure). The main mechanism of prosthetic dysfunction was failure (66%) and double prosthetic dysfunction (75%). Two expandable balloon prostheses were used: Inovare (Braile) in 10 patients and Sapien 3 (Edwards) in two patients. Mean length of stay was 12±5.4 days, with 67% of patients discharged in NYHA functional class I. There were no in-hospital or 29-month follow-up deaths; the predominant antithrombotic regimen was vitamin K antagonist in 10 (83%) and late bioprosthesis thrombosis occurred in one (8.3%) patient (Video 2), due to Covid-19 infection. One-year echocardiographic control showed a mean tricuspid gradient of 7.7±2.4 mmHg and one case with moderate paravalvular leak. This pilot retrospective registry demonstrated safety, efficacy and significant improvement in symptoms in the medium term.[23]

The presence of potential short- and long-term complications, such as device detachment, degeneration, annulus or leaflet rupture, endocarditis, pericardial effusion or cardiac tamponade, prosthetic thrombosis and perivalvular regurgitation in cases of tricuspid valve-in-valve), in addition to impairment of right coronary artery should be investigated and detected by TTE. In case of doubtful findings, 2D/3D TEE should be requested.[22]

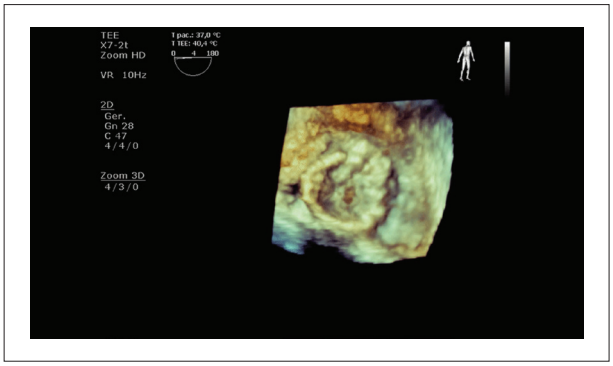

Video 2 – *3D TEE Tricuspid endoprosthesis (Valve-in-Valve) with restricted leaflet mobility.*
Link: http://abcimaging.org/supplementary-material/2023/3601/convite-Bruna-Leal-video_02.mp4

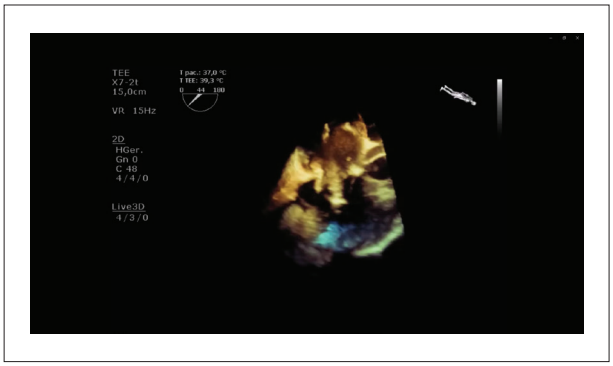

Video 3 – *Tricuspid Valve-in-Valve image (Edwards 3 prosthesis number 29): endoprosthesis placement on three-dimensional TEE image.*
Link: http://abcimaging.org/supplementary-material/2023/3601/convite-Bruna-Leal-video_03.mp4

Conclusion

Interest in TV has increased in a scenario of evidence that TR impacts morbidity and mortality of individuals. The complex anatomy and function of TV implies an evaluation using multiple windows and echocardiographic modalities (2D/3D TTE and 2D/3D TEE). After percutaneous TV intervention, residual TR, annulus size, RV function and size should be evaluated. The main complications include significant TR (single leaflet captured by the device), prosthesis thrombosis, endocarditis, pericardial effusion, and impairment of right coronary artery. Ideally, TTE should be performed at one, six and twelve months, and annually after the procedure.

Potential Conflict of Interest

No potential conflict of interest relevant to this article was reported.

Sources of Funding

There were no external funding sources for this study.

Study Association

This study is not associated with any thesis or dissertation work.

Author Contributions

Conception and design of the research: Assunção BMBL; writing of the manuscript: Assunção BMBL, Gonçalvez AC, Cassar RS; critical revision of the manuscript for intellectual content: Assunção BMBL, Gonçalvez AC, Cassar RS.

Ethics Approval and Consent to Participate

This article does not contain any studies with human participants or animals performed by any of the authors.

References

1. Nath J, Foster E, Heidenreich PA. Impact of Tricuspid Regurgitation on Long-Term Survival. J Am Coll Cardiol. 2004;43(3):405-9. doi: 10.1016/j.jacc.2003.09.036.
2. Izumi C. Isolated Functional Tricuspid Regurgitation: When Should We Go to Surgical Treatment? J Cardiol. 2020;75(4):339-43. doi: 10.1016/j.jjcc.2019.11.001.
3. Otto CM, Nishimura RA, Bonow RO, Carabello BA, Erwin JP, Gentile F, et al. 2020 ACC/AHA Guideline for the Management of Patients With Valvular Heart Disease: A Report of the American College of Cardiology/American Heart Association Joint Committee on Clinical Practice Guidelines. J Am Coll Cardiol. 2021;77(4):e25-e197. doi: 10.1016/j.jacc.2020.11.018.
4. Praz F, Muraru D, Kreidel F, Lurz P, Hahn RT, Delgado V, et al. Transcatheter Treatment for Tricuspid Valve Disease. EuroIntervention. 2021;17(10):791-808. doi: 10.4244/EIJ-D-21-00695.
5. Hahn RT. State-of-the-Art Review of Echocardiographic Imaging in the Evaluation and Treatment of Functional Tricuspid Regurgitation. Circ Cardiovasc Imaging. 2016;9(12):e005332. doi: 10.1161/CIRCIMAGING.116.005332.
6. Silver MD, Lam JH, Ranganathan N, Wigle ED. Morphology of the Human Tricuspid Valve. Circulation. 1971;43(3):333-48. doi: 10.1161/01.cir.43.3.333.
7. Antunes MJ, Barlow JB. Management of Tricuspid Valve Regurgitation. Heart. 2007;93(2):271-6. doi: 10.1136/hrt.2006.095281.
8. Rogers JH, Bolling SF. The Tricuspid Valve: Current Perspective and Evolving Management of Tricuspid Regurgitation. Circulation. 2009;119(20):2718-25. doi: 10.1161/CIRCULATIONAHA.108.842773.
9. Mahmood F, Kim H, Chaudary B, Bergman R, Matyal R, Gerstle J, et al. Tricuspid Annular Geometry: A Three-Dimensional Transesophageal Echocardiographic Study. J Cardiothorac Vasc Anesth. 2013;27(4):639-46. doi: 10.1053/j.jvca.2012.12.014.
10. Zoghbi WA, Adams D, Bonow RO, Enriquez-Sarano M, Foster E, Grayburn PA, et al. Recommendations for Noninvasive Evaluation of Native Valvular Regurgitation: A Report from the American Society of Echocardiography Developed in Collaboration with the Society for Cardiovascular Magnetic Resonance. J Am Soc Echocardiogr. 2017;30(4):303-71. doi: 10.1016/j.echo.2017.01.007.
11. Hahn RT, Abraham T, Adams MS, Bruce CJ, Glas KE, Lang RM, et al. Guidelines for Performing a Comprehensive Transesophageal Echocardiographic Examination: Recommendations from the American Society of Echocardiography and the Society of Cardiovascular Anesthesiologists. J Am Soc Echocardiogr. 2013;26(9):921-64. doi: 10.1016/j.echo.2013.07.009.
12. Lang RM, Badano LP, Tsang W, Adams DH, Agricola E, Buck T, et al. EAE/ASE Recommendations for Image Acquisition and Display Using Three-Dimensional Echocardiography. J Am Soc Echocardiogr. 2012;25(1):3-46. doi: 10.1016/j.echo.2011.11.010.
13. Lang RM, Badano LP, Mor-Avi V, Afilalo J, Armstrong A, Ernande L, et al. Recommendations for Cardiac Chamber Quantification by Echocardiography in Adults: an Update from the American Society of Echocardiography and the European Association of Cardiovascular Imaging. J Am Soc Echocardiogr. 2015;28(1):1-39.e14. doi: 10.1016/j.echo.2014.10.003.
14. Lancellotti P, Moura L, Pierard LA, Agricola E, Popescu BA, Tribouilloy C, et al. European Association of Echocardiography Recommendations for the Assessment of Valvular Regurgitation. Part 2: Mitral and Tricuspid Regurgitation (Native Valve Disease). Eur J Echocardiogr. 2010;11(4):307-32. doi: 10.1093/ejechocard/jeq031.
15. Chen TE, Kwon SH, Enriquez-Sarano M, Wong BF, Mankad SV. Three-Dimensional Color Doppler Echocardiographic Quantification of Tricuspid Regurgitation Orifice Area: Comparison with Conventional Two-Dimensional Measures. J Am Soc Echocardiogr. 2013;26(10):1143-52. doi: 10.1016/j.echo.2013.07.020.
16. Hahn RT, Thomas JD, Khalique OK, Cavalcante JL, Praz F, Zoghbi WA. Imaging Assessment of Tricuspid Regurgitation Severity. JACC Cardiovasc Imaging. 2019;12(3):469-90. doi: 10.1016/j.jcmg.2018.07.033.
17. Hahn RT, Zamorano JL. The Need for a New Tricuspid Regurgitation Grading Scheme. Eur Heart J Cardiovasc Imaging. 2017;18(12):1342-1343. doi: 10.1093/ehjci/jex139.
18. Hahn RT, Badano LP, Bartko PE, Muraru D, Maisano F, Zamorano JL, et al. Tricuspid Regurgitation: Recent Advances in Understanding Pathophysiology, Severity Grading and Outcome. Eur Heart J Cardiovasc Imaging. 2022;23(7):913-29. doi: 10.1093/ehjci/jeac009.
19. Nishimura RA, Otto CM, Bonow RO, Carabello BA, Erwin JP, Fleisher LA, et al. 2017 AHA/ACC Focused Update of the 2014 AHA/ACC Guideline for the Management of Patients with Valvular Heart Disease: A Report of the American College of Cardiology/American Heart Association Task Force on Clinical Practice Guidelines. Circulation. 2017;135(25):e1159-e1195. doi: 10.1161/CIR.0000000000000503.

20. Fukuda S, Song JM, Gillinov AM, McCarthy PM, Daimon M, Kongsaerepong V, et al. Tricuspid Valve Tethering Predicts Residual Tricuspid Regurgitation After Tricuspid Annuloplasty. Circulation. 2005;111(8):975-9. doi: 10.1161/01.CIR.0000156449.49998.51.

21. Raja SG, Dreyfus GD. Basis for Intervention on Functional Tricuspid Regurgitation. Semin Thorac Cardiovasc Surg. 2010;22(1):79-83. doi: 10.1053/j.semtcvs.2010.05.005.

22. Agricola E, Asmarats L, Maisano F, Cavalcante JL, Liu S, Milla F, et al. Imaging for Tricuspid Valve Repair and Replacement. JACC Cardiovasc Imaging. 2021;14(1):61-111. doi: 10.1016/j.jcmg.2020.01.031.

23. The Editorial Team (on behalf of the World Heart Federation). Abstract from the World Congress of Cardiology/Brazilian Congress of Cardiology 2022 [Internet]. Rio de Janeiro: World Heart Federation; 2022 [cited 2022 Dec 22]. Available from: https://world-heart-federation.org/world-congress-of-cardiology/rio-2022/

Role of Multimodality for the Diagnosis of Thrombosis at Late Follow-up of Patients Selected for TAVI: Review of a Case Series

Laila Caroline Oliveira Souza Barbosa Gomes,[1] *Alexandre Costa Souza,*[1] *Stephanie de Azevedo Drubi,*[1] *Bruna de Mattos Ivo Junqueira,*[1] *Mariana Lins Baptista Guedes Bezerra,*[1] *Rodrigo Vieira de Melo*[1]

Hospital São Rafael, Rede D'or,[1] *Salvador, BA – Brazil*

Introduction

The first transcatheter aortic valve implantation (TAVI) was performed by Alan Cribier in France in 2002 and the technique was introduced in Brazil in 2008. Since then, this modality has been consolidated and many patients have been approached using this technique. After more than 10 years of the first TAVI in Brazil, an increasing number of late complications appear in the cardiovascular imaging laboratory, with challenging anatomical and functional aspects in daily practice. Late thrombosis of aortic endoprosthesis may be one of the causes of dysfunction in the follow-up after TAVI. This clinical entity can assume a complex profile for accurate diagnosis and proper patient management, since it can have a variable presentation, ranging from subclinical leaflet thrombosis to limiting symptoms related to heart failure.[1] Transesophageal echocardiography (TEE), the additional resource of 3D echocardiography and high-resolution computed tomography (CT) play a complementary role in the diagnosis of this etiology through anatomical valve reconstruction with evidence of hypoattenuated leaflet thickening (HALT) with or without hypoattenuation affecting motion (HAM) of one or more prosthetic valve leaflets.[2,3] The risk of embolic events after diagnosis of leaflet thrombosis is still uncertain, especially for the central nervous system.[4,5] This case series presents two illustrative reports of aortic endoprostheses with high gradients and complementary aspects of the multimodality that direct the etiology to the diagnosis of late prosthesis thrombosis.

Case report

Case 1

Female patient, 87 years old, with stable coronary artery disease (CAD), history of coronary angioplasty and severe aortic stenosis, who underwent TAVI and definitive pacemaker implantation in 2019, was admitted in June/2022 due to chest pain. An electrocardiogram revealed no acute ischemic abnormalities and normal myocardial necrosis markers. The transthoracic echocardiogram (TTE) showed aortic valve with high gradients, mean of 43 mmHg, differing from the last test performed in 2021, and transesophageal echocardiogram (TEE) showed leaflet thickening with significant motion hypoattenuation of two of its mobile elements, suggestive of prosthesis thrombosis, with effective flow orifice estimated by 3D planimetry and 3D continuity equation to be 0.73 cm^2 and 0.48 cm^2/m^2, indexed by the body surface (Figures 2 and 3).[6] CT revealed advanced-grade HALT in the three leaflets: leaflet equivalent to that of the left coronary artery, involvement greater than 75% (grade 4); leaflet equivalent to that of the right coronary artery, involvement greater than 75% (grade 4). Full anticoagulation therapy was initiated and presented good evolution. The patient was discharged in June/2022, clinically stable and asymptomatic (Figures 1, 2, 3 and 4) for outpatient follow-up.

Case 2

Male patient, 70 years old, hypertensive, with virus C parenchymal liver disease and thrombocytopenia, bicuspid aortic valve with a history of TAVI five years prior and recent history of leaflet thrombosis with severe aortic stenosis, was taking Clopidogrel and direct oral anticoagulants (DOAC). The patient was hospitalized in June/22 with acute respiratory distress associated with cough and hemoptysis. Underwent CT angiography of the chest with negative result for pulmonary thromboembolism and a pattern suggestive of alveolar hemorrhage. During this hospitalization, a new transthoracic echocardiogram was performed with evidence of persistently high gradients of the aortic endoprosthesis (maximum: 50 mmHg and mean: 28 mmHg), with HALT improvement on CT. The patient was discharged after clinical compensation, stable and, due to the high risk of bleeding, was maintained without anticoagulation (Figure 5).

Discussion

Transcatheter aortic valve replacement is a safe treatment and not inferior to conventional surgery for patients with severe symptomatic aortic stenosis and intermediate to high surgical risk.[7,8] With the national experience in the long-term follow-up of patients undergoing TAVI, there is an increasing number of cases of prosthetic stenosis with increased gradients and transvalvular velocities. In these situations, transthoracic echocardiogram can support the screening and identification of high gradients, however, it has a limited role in the etiological investigation.

Keywords

Multimodality; Prosthesis thrombosis; Transcatheter Aortic Valve Replacement

Mailing Address: Laila Caroline Oliveira Souza Barbosa Gomes •
Hospital São Rafael, Av. São Rafael, 2152. Postal code: 41253-190. São Marcos, Salvador, BA – Brazil
E-mail: lailacarolines@gmail.com
Manuscript received November 26, 2022; revised January 31, 2023; accepted February 7, 2023
Editor responsible for the review: Daniela do Carmo Rassi Frota

DOI: https://doi.org/10.36660/abcimg.2023367i

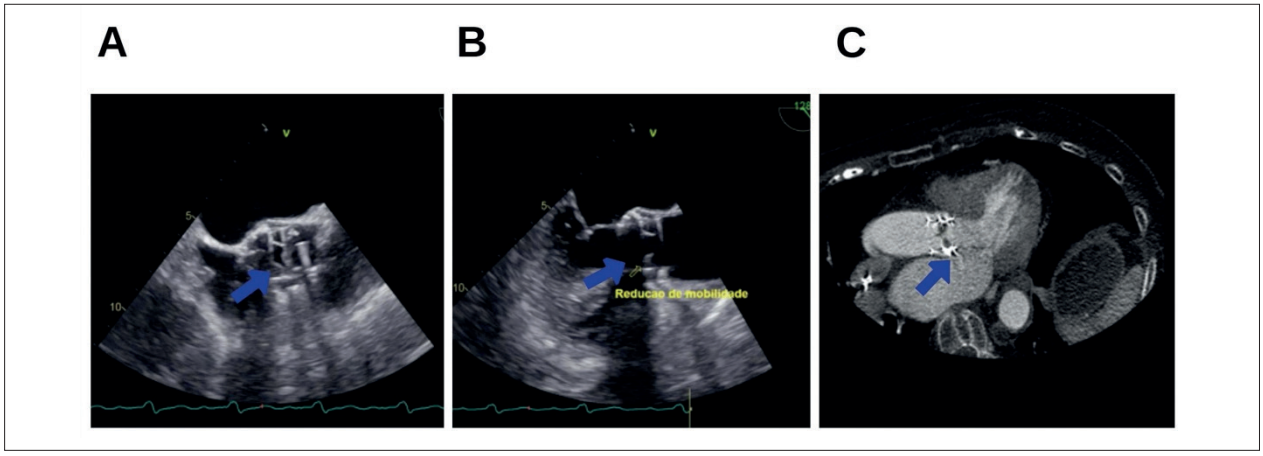

Figure 1 – *Images suggesting prosthesis thrombosis on TEE and cardiac CT. Reduced motion A and B: TEE at 45o and 130 o with evidence of leaflet thickening and reduced motion, respectively. C: HALT areas on cardiac CT.*

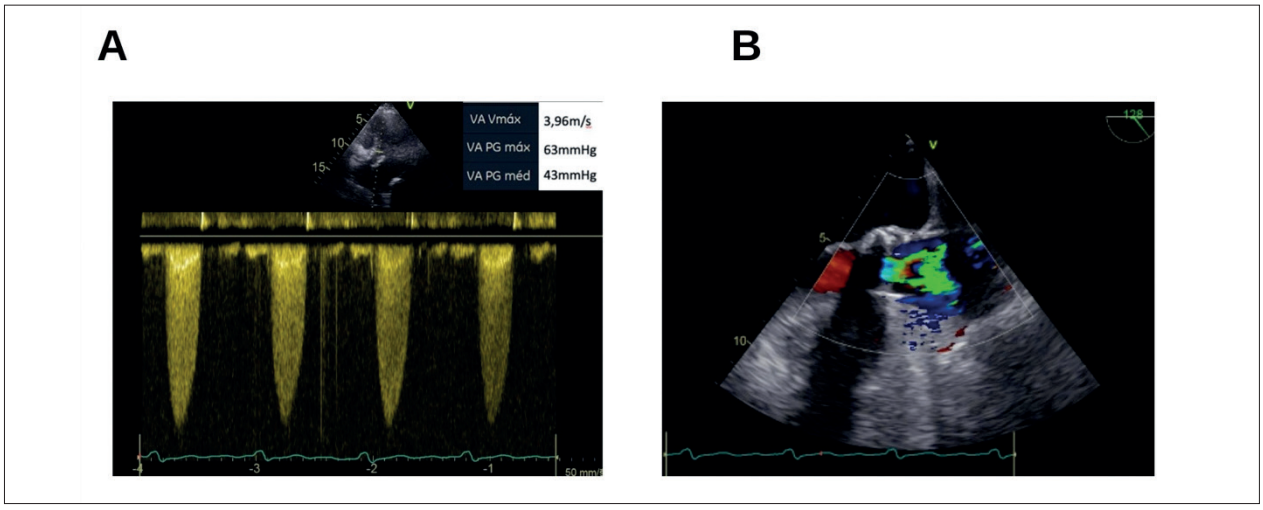

Figure 2 – *Echocardiographic findings of endoprosthesis dysfunction. A: High mean transprosthetic gradient at aortic position on transthoracic echocardiogram. B: TEE at 130o showing left ventricular outflow tract and aliasing on color Doppler flow through the endoprosthesis.*

Aortic endoprosthesis valve dysfunction is defined by transthoracic echocardiogram when there is a mean transvalvular gradient greater than 20 mmHg or greater than 50% of the previous mean baseline gradient.[2] Transesophageal echocardiography may have sensitivity comparable to cardiac CT in identifying signs of thrombosis, such as reduced leaflet motion, leaflet thickening, or even the identification of thrombi, especially in patients at increased risk of contrast nephropathy, which may contribute to the identification of the mechanism of prosthetic dysfunction.[2]

In this context, TEE can provide additional inputs in the evaluation of prosthesis dysfunction in the late follow-up of these patients. Real-time 3D complementation can be used in the evaluation of differential diagnoses of endoprosthesis dysfunction, especially for identifying images suggestive of endocarditis, mismatch, pannus and ascending aorta pathologies.

CT plays a crucial role in the complementary evaluation for the accurate diagnosis of post-TAVI prosthesis thrombosis. This test can identify prosthesis thrombosis through morphological criteria with a finding of HALT that may be associated with HAM, and the possibility of assessing the thrombotic load, a parameter that has been correlated with adverse clinical outcomes.[4,9,10] HALT can be classified according to the extent of leaflet involvement as <25%, 25–50%, 50–75% or >75%, with this assessment being performed on CT diastolic reconstructions (Figure 6). However, the presence of HALT is observed at similar rates for transcatheter and surgical prosthetic valves.[5,11]

Some elements are recognized as factors that may function as independent predictors of evolution to late thrombosis in the follow-up after TAVI. Some of these characteristics are based on clinical attributes, such as atrial fibrillation, chronic obstructive pulmonary disease, male gender, absence of postoperative treatment with

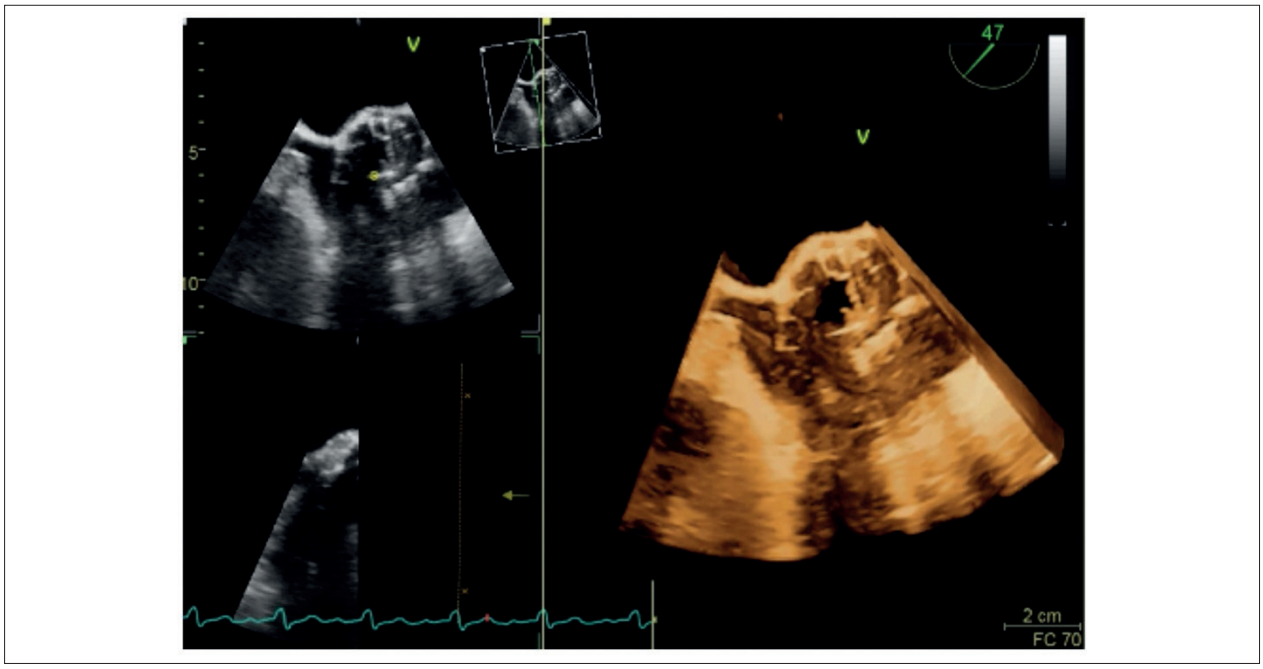

Figure 3 – *3D reconstruction of the aortic endoprosthesis. TEE at 45o with leaflet thickening and reduced motion (indicated by the arrow) with no images suggesting endocarditis.*

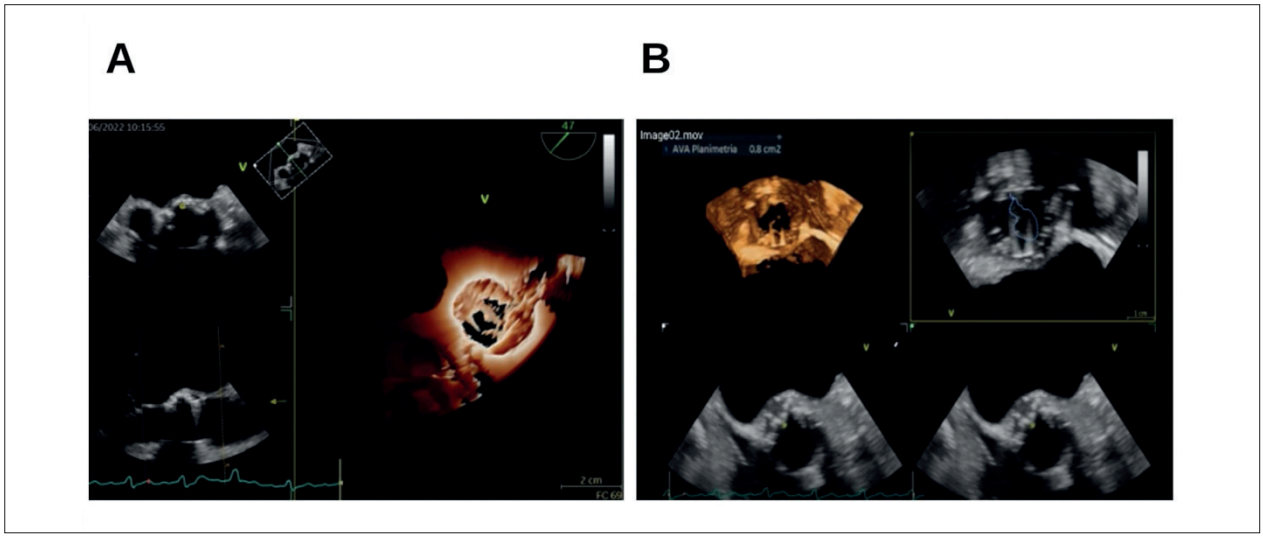

Figure 4 – *3D reconstruction of the aortic endoprosthesis. A: TEE at 45o with 3D reconstruction of the aortic endoprosthesis. B: estimation of effective flow orifice through 3D planimetry.*

antiplatelet agents, obesity and active smoking. Other factors are related to the intra-procedure, such as the smaller diameter of the implanted prosthesis, the supra-annular device implantation, balloon under-expansion and valve-in-valve procedure.[10,12,13] As for imaging methods, reduced left ventricular ejection fraction and paravalvular leak are strong predictors that may indicate a higher risk of thrombosis of an evolutionary prosthesis. Some studies describe a two-fold increase in late thrombosis in patients with at least mild leak.[11]

Symptomatic thrombosis of aortic valve endoprosthesis leaflets is rare, representing about 0.6 to 2.8% of reported cases,[8] contrasting with incidental finding in about 15–40% of subclinical thrombosis with evidence of HALT on cardiac CT, with a potential association with cerebrovascular events.[5,7,9] Optimal antithrombotic therapy is still the focus of clinical trials, with current guidelines recommending dual antiplatelet therapy (DAPT) for three to six months after TAVI and data regarding safety and longevity suggesting good durability in five years.[1,7] However, some studies suggest that subclinical

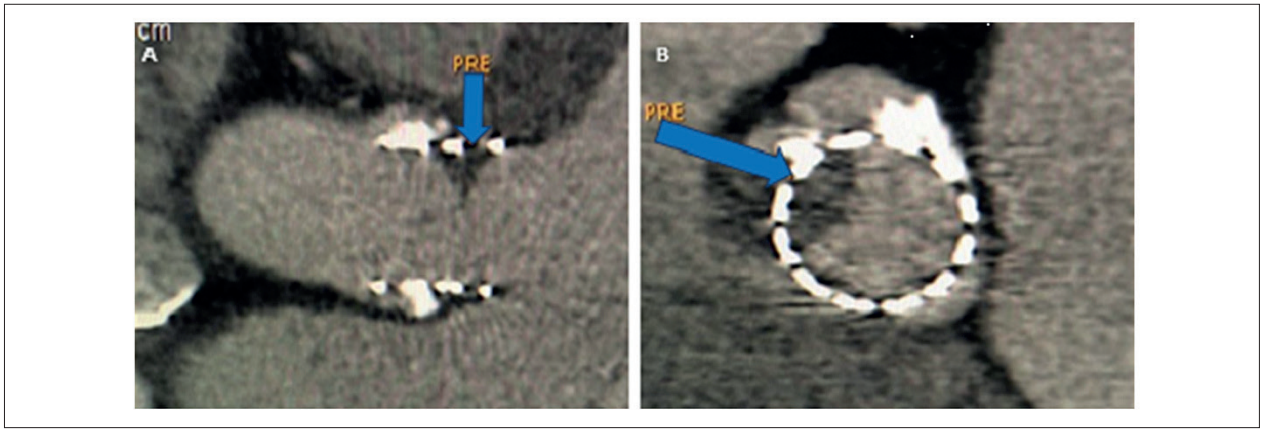

Figure 5 – *Multiplanar tomographic reconstruction A and B: long and short axis, respectively, showing non-coronary leaflet with grade 4 HALT. PRE: HALT before anticoagulation.*

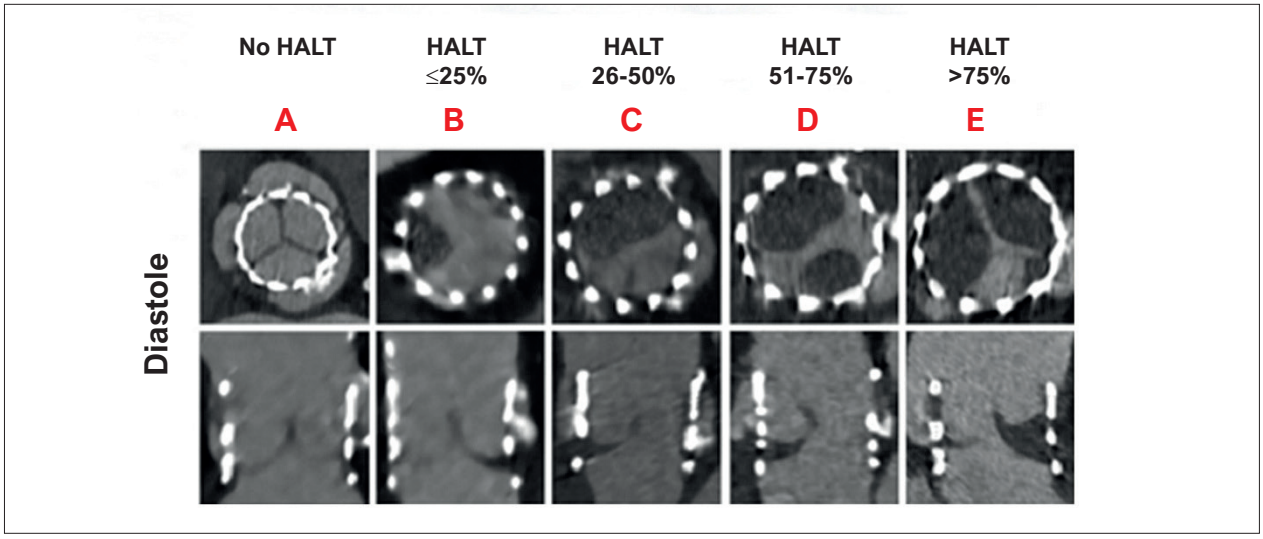

Figure 6 – *HALT classification through diastolic reconstruction by CT, cross-sectional and longitudinal axis. A: no leaflet involvement. B: leaflet involvement at ≤25%, C: 26–50%. D: 51–75%. E: >75%. HALT: hypoattenuated leaflet thickening.*

thrombosis is more common in those who did not receive anticoagulation, so that, after discontinuing DOAC, CT can reveal HALT in a variable degree, revealing its dynamic nature due to the potential of spontaneous progression or regression, even in asymptomatic patients.[1,5,7,11] However, the GALILEO trial demonstrated that the use of routine oral anticoagulants should be avoided after TAVI in order to prevent subclinical structural alterations, with well-established indications in view of the increased risk of death and bleeding.[14]

The follow-up of patients diagnosed with TAVI thrombosis and establishment of the indicated therapy are not well established in the literature. This follow-up is usually carried out systematically and periodically using serial transthoracic echocardiography with comparative assessment of transprosthetic systolic gradients and velocities, associated with complementary CT imaging to assess the quantitative reduction in leaflet thickening and improvement of leaflet motion[14] (Figure 7).

Conclusion

Aortic valve replacement with endoprostheses for the treatment of symptomatic aortic stenosis has raised the issue of long-term safety and longevity of the endoprosthesis. The use of multimodality in the follow-up of these patients has identified findings that vary from subclinical alterations to alterations that influence prognosis and symptoms. Based on a more accurate diagnosis of endoprosthesis dysfunction, through the combined findings of echocardiography and tomography, we can identify the precise mechanism of dysfunction in post-TAVI follow-up, allowing for more adequate quantification of leaflet involvement and motion restriction and earlier onset of specific therapy.[14]

Author Contributions

Conception and design of the research: Costa A, Gomes LC, Junqueira B; acquisition of data: Junqueira B, Drubi S;

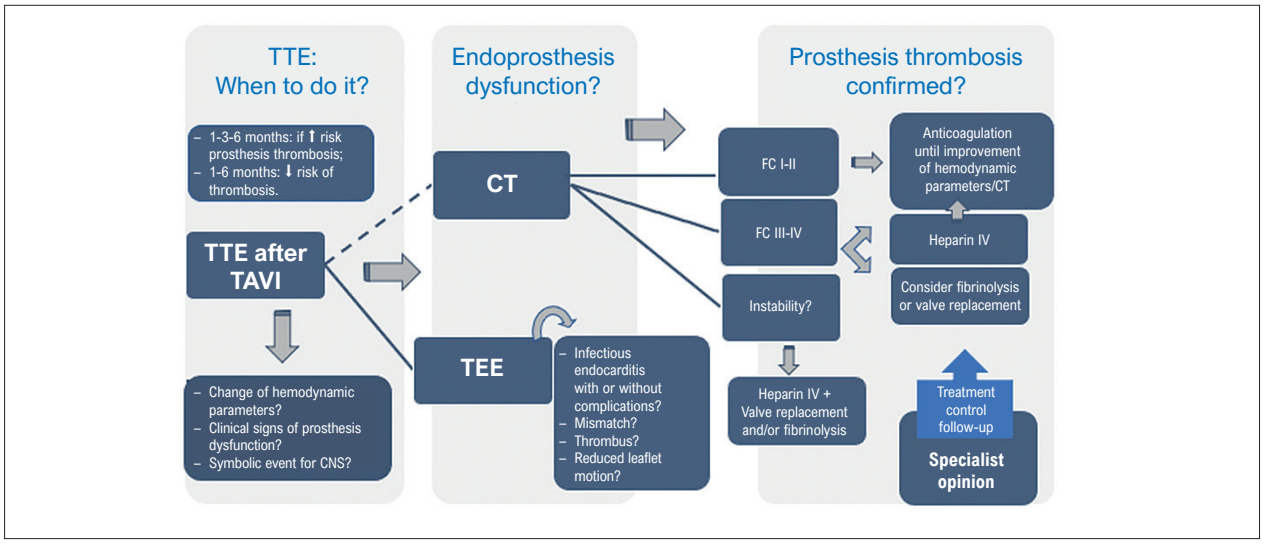

Figura 7 – *Algorithm for diagnosis and follow-up of prosthesis thrombosis after TAVI. TTE: Transthoracic echocardiography; CNS: central nervous system; TEE: transesophageal echocardiography; CT: computed tomography; FC: functional class according to NYHA; TAVI: transcatheter aortic valve implantation; IV: intravenous.*

writing of the manuscript: Gomes LC, Costa A, Drubi S; critical revision of the manuscript for intellectual content: de Melo RV, Guedes MB.

Potential Conflict of Interest

No potential conflict of interest relevant to this article was reported.

Sources of Funding

There were no external funding sources for this study.

Study Association

This study is not associated with any thesis or dissertation work.

Ethics Approval and Consent to Participate

The study with the ethical aspects set forth in the Declaration of Helsinki of 1975. As this is a review study, in which clinical data, exams and therapeutic procedures, already performed in the routine of the service due to clinical indication, were used, we request the waiver of the free and informed consent form.

References

1. Rheude T, Pellegrini C, Stortecky S, Marwan M, Xhepa E, Ammon F, et al. Meta-Analysis of Bioprosthetic Valve Thrombosis After Transcatheter Aortic Valve Implantation. Am J Cardiol. 2021;138:92-99. doi: 10.1016/j.amjcard.2020.10.018.
2. Mirsadraee S, Sellers S, Duncan A, Hamadanchi A, Gorog DA. Bioprosthetic Valve Thrombosis and Degeneration Following Transcatheter Aortic Valve Implantation (TAVI). Clin Radiol. 2021;76(1):73.e39-73.e47. doi: 10.1016/j.crad.2020.08.015.
3. Sondergaard L, De Backer O, Kofoed KF, Jilaihawi H, Fuchs A, Chakravarty T, et al. Natural History of Subclinical Leaflet Thrombosis Affecting Motion in Bioprosthetic Aortic Valves. Eur Heart J. 2017;38(28):2201-7. doi: 10.1093/eurheartj/ehx369.
4. Vollema EM, Kong WKF, Katsanos S, Kamperidis V, van Rosendael PJ, van der Kley F, et al. Transcatheter Aortic Valve Thrombosis: The Relation between Hypo-Attenuated Leaflet Thickening, Abnormal Valve Haemodynamics, and Stroke. Eur Heart J. 2017;38(16):1207-17. doi: 10.1093/eurheartj/ehx031.
5. Makkar RR, Blanke P, Leipsic J, Thourani V, Chakravarty T, Brown D, et al. Subclinical Leaflet Thrombosis in Transcatheter and Surgical Bioprosthetic Valves: PARTNER 3 Cardiac Computed Tomography Substudy. J Am Coll Cardiol. 2020;75(24):3003-15. doi: 10.1016/j.jacc.2020.04.043.
6. De Backer O, Dangas GD, Jilaihawi H, Leipsic JA, Terkelsen CJ, Makkar R, et al. Reduced Leaflet Motion after Transcatheter Aortic-Valve Replacement. N Engl J Med. 2020;382(2):130-9. doi: 10.1056/NEJMoa1911426.
7. Hansson NC, Grove EL, Andersen HR, Leipsic J, Mathiassen ON, Jensen JM, et al. Transcatheter Aortic Valve Thrombosis: Incidence, Predisposing Factors, and Clinical Implications. J Am Coll Cardiol. 2016;68(19):2059-69. doi: 10.1016/j.jacc.2016.08.010.
8. Yanagisawa R, Tanaka M, Yashima F, Arai T, Jinzaki M, Shimizu H, et al. Early and Late Leaflet Thrombosis after Transcatheter Aortic Valve Replacement. Circ Cardiovasc Interv. 2019;12(2):e007349. doi: 10.1161/CIRCINTERVENTIONS.118.007349.
9. Rashid HN, Michail M, Ihdayhid AR, Dowling C, Khav N, Tan S, et al. Clinical Predictors and Sequelae of Computed Tomography Defined Leaflet Thrombosis Following Transcatheter Aortic Valve Replacement at Medium-Term Follow-Up. Heart Vessels. 2021;36(9):1374-83. doi: 10.1007/s00380-021-01803-4.
10. Blanke P, Leipsic JA, Popma JJ, Yakubov SJ, Deeb GM, Gada H, et al. Bioprosthetic Aortic Valve Leaflet Thickening in the Evolut Low Risk Sub-Study. J Am Coll Cardiol. 2020;75(19):2430-42. doi: 10.1016/j.jacc.2020.03.022.
11. Pieniak K, Jędrzejczyk S, Domaszk O, Grodecki K, Rymuza B, Huczek Z, et al. Predictors and Biomarkers of Subclinical Leaflet Thrombosis after

Transcatheter Aortic Valve Implantation. J Clin Med. 2020;9(11):3742. doi: 10.3390/jcm9113742.

12. Tang L, Lesser JR, Schneider LM, Burns MR, Gössl M, Garberich R, et al. Prospective Evaluation for Hypoattenuated Leaflet Thickening Following Transcatheter Aortic Valve Implantation. Am J Cardiol. 2019;123(4):658-66. doi: 10.1016/j.amjcard.2018.11.012.

13. Brown R, Reid AB, Turaga M, Huang A, Maggiore P, MBBS, Sellers S, et al. Subclinical Leaflet Thrombosis Post Transcatheter Aortic Valve Replacement – An Update for 2020. Strutural Heart. 2020;4(5):369-81. doi: 10.1080/24748706.2020.1805534.

14. Dangas GD, Tijssen JGP, Wöhrle J, Søndergaard L, Gilard M, Möllmann H, et al. A Controlled Trial of Rivaroxaban after Transcatheter Aortic-Valve Replacement. N Engl J Med. 2020;382(2):120-9. doi: 10.1056/NEJMoa1911425.

Noblestitch Failure After Percutaneous Patent Foramen Ovale Closure in a Case Of Platypnea-Orthodeoxia Syndrome: Is this Device Suitable for All Patients?

Ana Rita Moura,[1] Mariana Silva,[2] Alberto Rodrigues,[2] João Carlos Silva,[3] José Ribeiro,[2] Daniel Caeiro,[2] Jorge Casanova,[3] Ricardo Fontes-Carvalho[2]

Hospital Distrital de Santarém,[1] Santarém – Portugal
Centro Hospitalar Vila Nova de Gaia/Espinho,[2] Vila Nova de Gaia – Portugal
Centro Hospitalar Universitário de São João,[3] Porto – Portugal

Introduction

Patent *foramen ovale* (PFO) is a common congenital cardiac lesion corresponding to a normal fetal interatrial communication that typically closes after birth with the fusion of the atrial *septum primum* to the *septum secundum*.[1] When the *foramen ovale* persists, it is usually asymptomatic and benign, with no need for treatment.[2] In rare cases, it can be implicated in the pathogenesis of some medical conditions, such as platypnea-orthodeoxia syndrome (POS). In this context, PFO closure may be indicated.[2]

Several occluder devices, traditionally based on a double-disc design, have shown that percutaneous PFO closure is possible.[3] Despite the proven efficacy, their use is not technically feasible for some patients. In addition, they have the potential to cause some complications.[4] NobleStitch EL (NS) is an alternative percutaneous PFO closure technique available in Europe, European Commission (EC) marked for cardiovascular suturing and PFO closure, and in the US, with Food and Drug Administration (FDA) clearance for vascular and cardiovascular suturing. It consists of a "deviceless" system with two dedicated suture delivery catheters.[5,6] To date, the experience with the NS device is limited, and we still lack information about its failure determinants, which could help select patients.[6-8]

Herein, we describe the case of a failed percutaneous PFO closure with NS that could add to the evidence that interatrial septum (IAS) anatomy may play a key role in the success of the procedure.

Clinical Case

We report the case of a 46-year-old man with a history of hypertension and acromegaly in the context of a pituitary adenoma, surgically removed in June 2020, and secondary panhypopituitarism developed after the procedure. He went to the emergency department complaining of 6-week exertional dyspnea. On examination, he was polypneic but hemodynamically stable, with no cardiac murmurs or adventitious lung sounds. Blood gases showed a severe type 1 respiratory failure, with a PaO2 of 33 mmHg in room air. Electrocardiogram (ECG) revealed no relevant anomalies in sinus rhythm. His blood test results had no significant abnormalities, with hemoglobin of 14 g/dL and no elevation of inflammatory parameters. A chest and abdominal computed tomography (CT) angiogram (Figure 1A) ruled out the diagnosis of pulmonary thromboembolism and interstitial lung disease. The results described an abnormality in the normal liver morphology, with atrophy of the fourth segment, and kyphoscoliosis, determining a deformity of the anterior right costal grid. The oxygen saturation obtained in pulse oximetry was lower while the patient was standing or sitting. POS was then established. The patient was admitted for further study.

A transthoracic echocardiogram (TTE – Figure 1B) showed left ventricular hypertrophy, aneurysmatic IAS, and mild aortic root ectasia of 39 mm. Additionally, it revealed an extrinsic compression of the right atrium by the ascending thoracic aorta and the liver. No other relevant findings were identified, including the stigma of pulmonary hypertension. Transesophageal echocardiography (TEE – Figure 1C; Video 1) corroborated the presence of PFO, which showed a spontaneous bidirectional flow. Right-sided catheterization confirmed that right chamber pressures were not increased; Qp/Qs in recumbent position was: 1.08.

Since the patient was clearly symptomatic, the decision was to proceed with percutaneous PFO closure. Given the marked right atrium deformation, he was considered a poor candidate for the placement of a traditional umbrella-like occluder device due to the high risk of wall erosion. The alternative chosen was the NS technique guided by fluoroscopy (Figure 2A) and TEE. Two sutures were placed due to the presence of a significant residual shunt after the first one (Figures 2B, 2C, and 2D; Video 2). After 3 days, the patient complained of recurrent dyspnea while standing. Re-evaluation TTE showed the persistence of patency of the *foramen ovale,* and TEE revealed two linear echogenic structures compatible with previously implanted devices at the *septum secundum*, but detached from the *septum primum* (Figure 3A and 3B; Video 3). The patient was subsequently referred to and accepted for surgical PFO closure with a bovine pericardium patch, which was performed without complications. Postoperative TEE showed no residual shunt. The patient was discharged after 6 days. At 6-month follow-up, he was asymptomatic, reporting a significant improvement in quality of life.

Keywords

Heart Defects, Congenital; Foramen Ovale, Patent; Platypneia-Ortthodeoxia Syndrome; NobleStich/methods; Atrial Septum.

Mailing Address: Ana Rita Baptista de Moura •
Av. Bernardo Santareno, nº 3737B. Postal code: 2005-177. Santarém - Portugal
E-mail: an.rita5@gmail.com
Manuscript received May 23, 2022; revised manuscript October 31, 2022; accepted November 29, 2022
Editor responsible for the review: Daniela do Carmo Rassi Frota

DOI: https://doi.org/10.36660/abcimg.2022309i

Contents

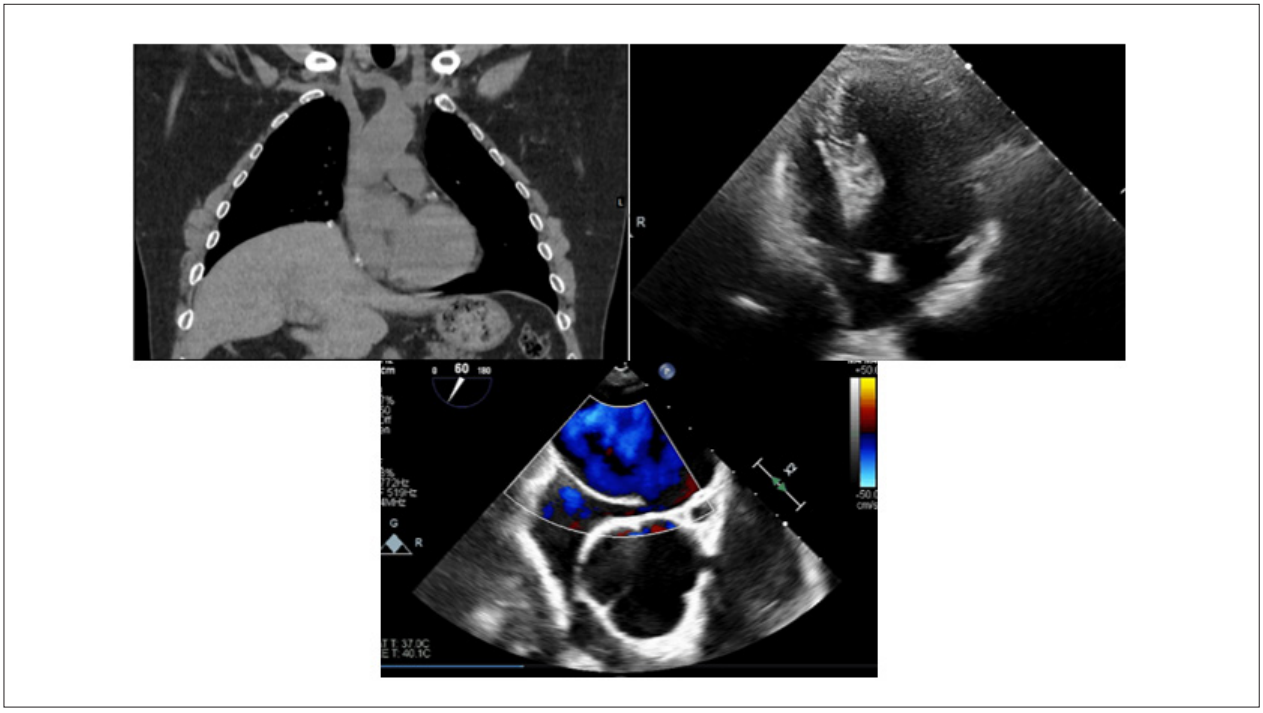

Figure 1 – *Pre-procedure percutaneous images. A: CT showing thoracic deformation with close relationship between right atrium and the liver; B: TTE showing right atrium compression; C: TEE mid-esophageal short axis view at 60º showing right atrium compression and PFO.*

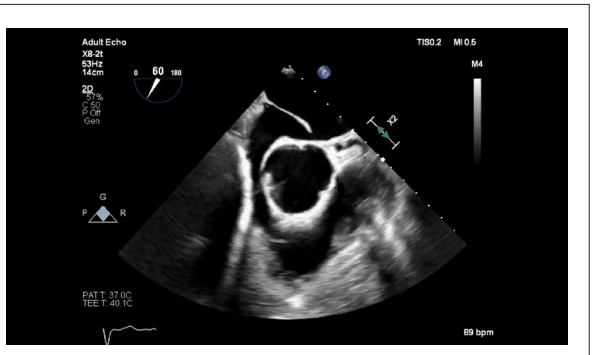

Video 1 – *Pre-procedure TEE showing right atrium compression and PFO with spontaneous bidirectional flow.*
Link: http://abcimaging.org/supplementary-material/2023/3601/ABC-309-video01.mp4

Discussion

POS is a rare syndrome caused by a right-to-left shunt (RLS) found in the heart or lungs. Most cases originate from an intracardiac shunt, which occurs when a structural component, such as interatrial communication, coexists with a functional component that favors an RLS in the upright position.[9] This can happen with conditions that affect the position and anatomy of the heart, dictating a transient increase in pressure in the right atrium and/or favoring the flow direction from the inferior vena cava directly through the septal defect, such as: aortic dilatation (one of the most common), diaphragmatic paralysis, post-pneumonectomy, kyphoscoliosis, prominent Eustachian valve or Chiari network, lipomatous hypertrophy of the IAS, or pericardial disease.[10]

In our patient, thromboembolic disease, arteriovenous malformations, and interstitial lung disease were excluded by chest CT as plausible causes of POS. In the absence of abnormal liver function tests, hepatopulmonary syndrome seemed also unlikely. The PFO described in TEE prevailed as the only reliable cause for the syndrome manifestation. In our case, aortic ectasia, thoracic deformation, and liver distortion seemed to be the structural cause interfering with the heart, favoring the appearance of intracardiac shunt.

The treatment for these patients consists of closing the atrial septal defect.[2] This option should be considered after ruling out other alternative causes of POS; when it has a significant impact on the patient's functional capacity; and there are no increased right chamber pressures.[2] Our patient met all these criteria.

Whenever possible, percutaneous closure is preferred. Double-disc occluder devices are the most used in these procedures;[3] however, they were not considered a good option for our patient, given the atypical anatomy of his right atrium, which did not have enough space to accommodate the device. Instead, we opted to use the NS device, which would allow us to overcome this limitation associated with classical devices; yet, the procedure was not successful.

To date, the experience with the NS device is limited, with only one published registry,[6] which seems to confirm the feasibility, safety, and efficacy of the procedure, with a documented closure rate (defined by RLS grade≤1) of 89% and a full closure rate of

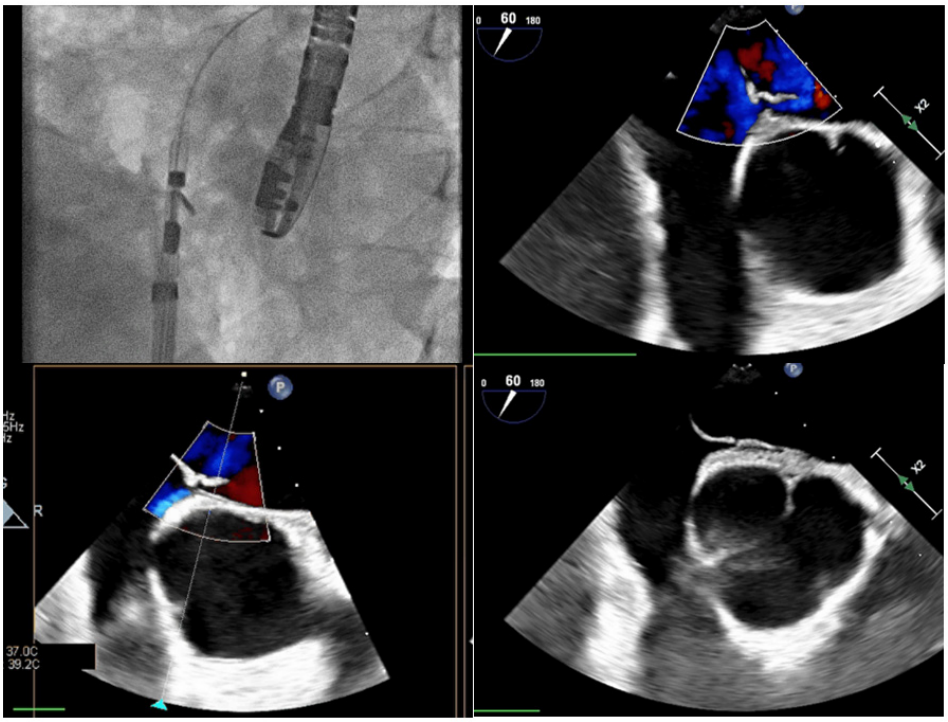

Figure 2 – *Peri-procedure percutaneous images. A: Fluoroscopic image with a suture delivery catheter of the NobleStitch system; B and C: TEE mid-esophageal short axis view at 60° revealing significant residual shunt after placement of the first suture; D: TEE using the same view with the two sutures in place.*

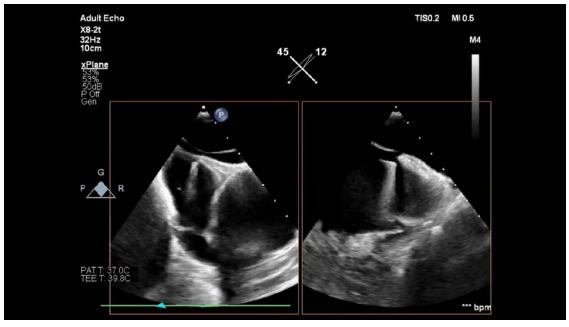

Video 2 – *Peri-procedure TEE images showing a significant residual shunt after placement of the first suture, which disappeared after the second suture was placed. Link: http://abcimaging.org/supplementary-material/2023/3601/ABC-309-video02.mp4*

75% at 12 months, results that are comparable with traditional devices. Nevertheless, we still lack experience and information on the determinants of residual RLS, which would help select patients with the most favorable anatomies for a suture-mediated closure technique.

In the previous registry,[6] the authors did not find a relevant correlation of significant RLS (grade≥2) or technique failure with the various baseline characteristics investigated. However, they highlighted that the presence of a wide redundant septum seemed to be a prevalent aspect in those patients. After a thorough literature search, we found only two case reports about NS failure. One was due to a septal tear, probably caused by the suture,[8] and the other was related to a significant residual RLS in an individual who also had an aneurysmatic IAS.[7]

Conclusions

POS is a rare condition that can have a significant impact on the patient's quality of life. When it is due to PFO-related intracardiac shunt, the defect closure is a curative treatment. Different percutaneous closure devices can be used. NS is an upcoming appealing alternative; yet, we still lack knowledge of the characteristics that should be considered in patient selection. Herein, we describe the case of another failed percutaneous PFO closure with NS that could add to the evidence that IAS anatomy may play a key role in the success of the procedure, with its use being less favorable in patients with aneurysmatic IAS.

Author Contributions

Conception and design of the research and writing of the manuscript: Moura AR; acquisition of data and analysis and interpretation of the data: Moura AR, Silva M, Rodrigues A, Silva JC, Ribeiro J, Caeiro D, Casanova J; critical revision of the manuscript for intellectual content: Silva M, Rodrigues A, Carvalho RF.

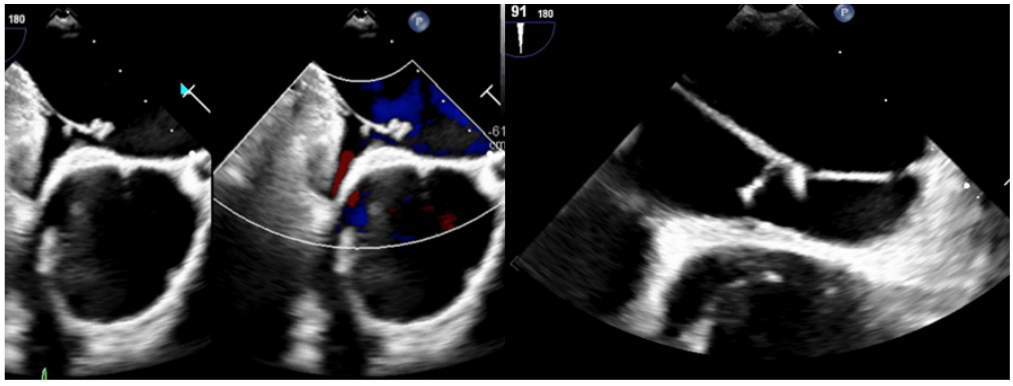

Figure 3 – *Post-procedure percutaneous images. TEE mid-esophageal short axis view at 60º with linear echogenic structures compatible with previously implanted devices at the septum secundum but detached from the septum primum and evident interatrial shunt.*

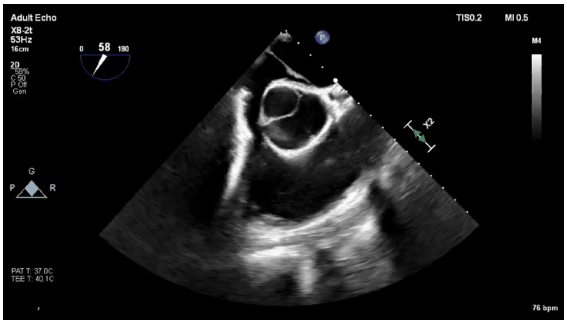

Video 3 – *Post-procedure TEE showing NS failure with the two previously implanted devices detached from the septum primum.*
Link: http://abcimaging.org/supplementary-material/2023/3601/ABC-309-video03.mp4

Potential Conflict of Interest

No potential conflict of interest relevant to this article was reported.

Sources of Funding

There were no external funding sources for this study.

Study Association

This study is not associated with any thesis or dissertation work.

Ethics Approval and Consent to Participate

This article does not contain any studies with human participants or animals performed by any of the authors.

References

1. Hara H, Virmani R, Ladich E, Mackey-Bojack S, Titus J, Reisman M, et al. Patent foramen ovale: current pathology, pathophysiology, and clinical status. J Am Coll Cardiol. 2005;46(9):1768-76. doi:10.1016/j.jacc.2005.08.038
2. Pristipino C, Germonpré P, Toni D, Sievert H, Meier B, D'Ascenzo F, et al. European position paper on the management of patients with patent foramen ovale. Part II - Decompression sickness, migraine, arterial deoxygenation syndromes and select high-risk clinical conditions [published correction appears in Eur Heart J. 2021 Jun 1;42(21):2102]. Eur Heart J. 2021;42(16):1545-53. doi:10.1093/eurheartj/ehaa1070
3. Giblett JP, Abdul-Samad O, Shapiro LM, Rana BS, Calvert PA. Patent Foramen Ovale Closure in 2019. Interv Cardiol. 2019;14(1):34-41. doi:10.15420/icr.2018.33.2
4. Merkler AE, Gialdini G, Yaghi S, Okin P, Iadecola C, Navi B, et al. Safety Outcomes After Percutaneous Transcatheter Closure of Patent Foramen Ovale. Stroke. 2017;48(11):3073-7. doi:10.1161/STROKEAHA.117.018501
5. Ruiz CE, Kipshidze N, Chiam PT, Gogorishvili I. Feasibility of patent foramen ovale closure with no-device left behind: first-in-man percutaneous suture closure. Catheter Cardiovasc Interv. 2008;71(7):921-6. doi:10.1002/ccd.21550
6. Gaspardone A, De Marco F, Sgueglia GA, Santis A, Iamele M, D'Ascoli E, et al. Novel percutaneous suture-mediated patent foramen ovale closure technique: early results of the NobleStitch EL Italian Registry. EuroIntervention. 2018;14(3):e272-e279. Published 2018 Jun 8. doi:10.4244/EIJ-D-18-00023
7. Trabattoni D, Gili S, Teruzzi G, Tamborini G. A severe right-to-left intracardiac shunt after NobleStitch failure: when a device is needed. Eur Heart J Case Rep. 2020;4(5):1-4. doi:10.1093/ehjcr/ytaa162
8. Baldetti L, Ferri LA, Ancona M, Bellini B, Visco E, Melillo F, et al. Interatrial Septal Tear After Patent Foramen Ovale Closure With the NobleStitch Device. JACC Cardiovasc Interv. 2019;12(16):e139-e140. doi:10.1016/j.jcin.2019.05.040
9. Rodrigues P, Palma P, Sousa-Pereira L. Platypnea-orthodeoxia syndrome in review: defining a new disease? Cardiology. 2012;123(1):15-23. doi:10.1159/000339872
10. Sanikommu V, Lasorda D, Poornima I. Anatomical factors triggering platypnea-orthodeoxia in adults. Clin Cardiol. 2009;32(11):E55-E57. doi:10.1002/clc.20461

Coronary-cavitary Fistula with Aneurysm in its Path: Case Report of Percutaneous Treatment

Carlos Alberto de Jesus,[1] Edileide de Barros Correia,[1] Líria Maria Lima da Silva,[1] Ibraim Masciarelli Francisco Pinto,[1] Mercedes Del Rosario Maldonado Andrade,[1] Andrezza Lobo de Alencar,[1] Marcelo Silva Ribeiro[1]

Instituto Dante Pazzanese de Cardiologia,[1] São Paulo, SP – Brazil

Abstract

The authors report the case of a 29-year-old, female patient with palpitations, chest pain, and dyspnea on exertion. The patient was diagnosed with right coronary fistula and underwent percutaneous correction of the fistulous tract with an Amplatzer prosthesis.

Introduction

Coronary artery fistula is a clinical condition characterized by an abnormal connection between one or more coronary arteries and heart chambers or large vessels adjacent to the heart. It has a prevalence of around 0.002% in the population, equally in both sexes, and it accounts for 14% of all coronary artery anomalies.[1-3]

Approximately 55% of cases of fistulas originate from the right coronary artery (or its branches) and 35% from the left coronary artery. In some cases, both arteries are involved. Most fistulas drain into the right ventricle, right atrium, and coronary sinus. Other drainage sites include the pulmonary artery, left atrium, left ventricle, and superior vena cava.[4]

The clinical picture varies according to the location and size of the fistula. Smaller fistulas usually occur without clinical repercussions, with the possibility of conservative treatment. On the other hand, large fistulas can generate a coronary steal mechanism, which causes functional myocardial ischemia and consequent angina or dyspnea on exertion. In these cases, invasive treatment with surgery or percutaneous closure of the fistula should be considered.[3]

Case report

A 29-year-old female patient, who was an active smoker with no previous comorbidities, came to the consultation complaining of chest pain and dyspnea on moderate exertion for a long time. She had begun follow-up with a cardiologist 7 years prior, when she presented with palpitations, which frequently persisted until she arrived at the reference service.

Upon physical examination, she was normotensive, in regular rhythm, well perfused, without edemas or jugular swelling; lung auscultation revealed no alterations, and cardiac auscultation revealed continuous murmur (+3/+6) in the right hemithorax.

There were no significant alterations in laboratory tests. Chest X-ray showed evidence of increased cardiac area. Admission electrocardiogram revealed atrial flutter rhythm. Transthoracic echocardiogram showed preserved ejection fraction (62% by Simpson's method), paradoxical movement of the interventricular septum (diastolic dysfunction suggestive of volume overload), preserved contractility in the other segments of the left ventricle, presence of pulmonary hypertension (pulmonary artery systolic pressure = 40 mmHg, estimated by tricuspid regurgitation), and heart valves without abnormalities. Dilation of the right coronary artery was observed, beginning in the right sinus of Valsalva (Figure 1A), with a very tortuous fistulous tract and the formation of a large aneurysm in the distal portion, draining into the right atrium, close to the inferior vena cava (Figure 1B), with systo-diastolic flow and velocity of approximately 1.15 m/s (Figure 1C). The aneurysmal portion of the right coronary artery measured 73 × 85 mm in its largest diameters, with an area of 46 cm² and marked slowing of the flow inside (spontaneous contrast), exerting compression on the right atrium (Figure 1D). There was presence of reverse holodiastolic flow in the descending thoracic aorta (secondary to the right coronary fistula to the right atrium).

The transthoracic echocardiogram findings were confirmed by chest angiography, and the patient was diagnosed with coronary-cavitary fistula with an aneurysm in its tract (fistula from the right coronary artery to the right atrium).

The patient was referred for cardiac catheterization, which did not show evidence of obstructive coronary lesions; however, it showed significant slowing of the distal flow of the right coronary artery, secondary to coronary steal of proximal flow through the fistulous tract to the aneurysmal portion (Figure 2A and 2B), which drained into the right atrium.

The decision was made to occlude the fistulous tract by means of a percutaneous procedure. Closing was performed with an 18 mm Amplatzer Vascular Plug II prosthesis, implanted shortly after the emergence of the fistulous tract,

Keywords

Cardiovascular Malformation; coronary vessel anomalies; vascular fistula; coronary aneurysm

Mailing Address: Andrezza Lobo •
Instituto Dante Pazzanese de Cardiologia. Avenida Dr. Dante Pazzanese, 500. Postal Code 04012-160. Vila Mariana, São Paulo, SP – Brasil.
E-mail: andrezzamed11@gmail.com
Manuscript received November 16, 2022; revised manuscript November 30, 2022; accepted December 1, 2022.
Editor responsible for the review: Simone Nascimento dos Santos

DOI: https://doi.org/10.36660/abcimg.2022364i

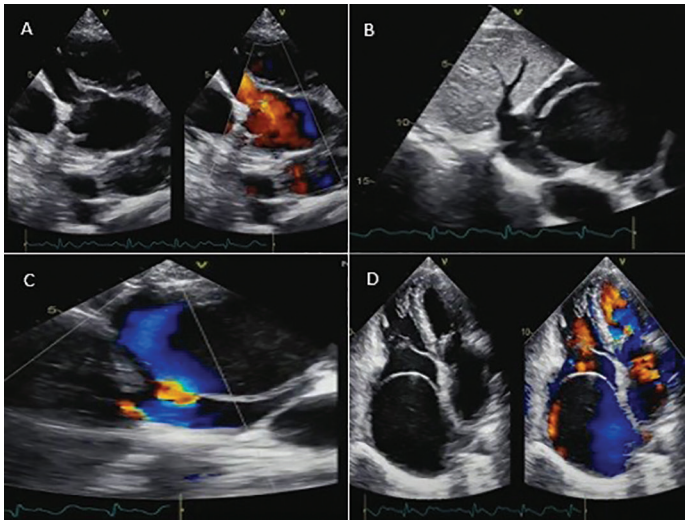

Figure 1 – *Longitudinal parasternal view of the aortic root at the emergence of the right coronary artery (important dilatation) in the sinus of Valsalva (A). Subcostal view showing the draining of the aneurysmal portion in the right atrium, close to the inferior vena cava (B) and Doppler with flow between the cavities (C). Apical 4-chamber transthoracic echocardiography window, with and without color mapping, Doppler showing flow within the aneurysm cavity (D).*

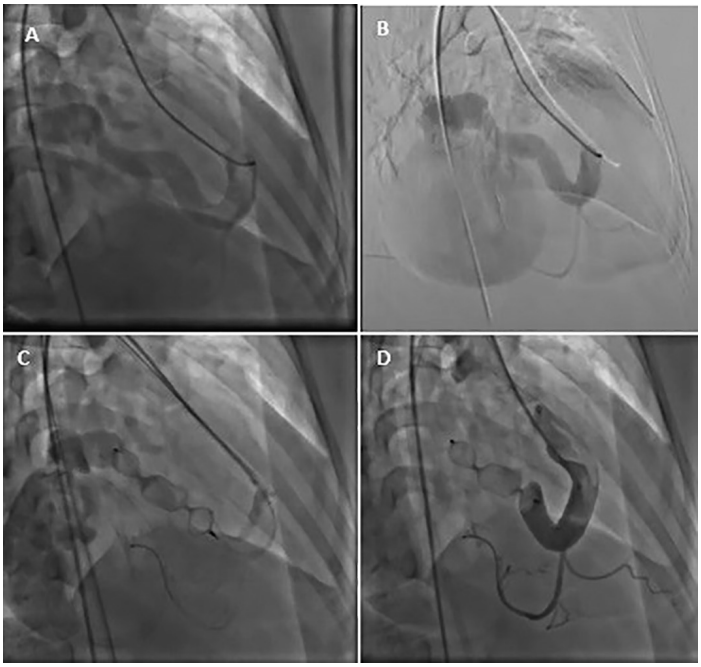

Figure 2 – *Dilated right coronary artery with a distal bed with normal caliber and low flow, shortly after the emergence of the fistula toward the aneurysmal portion (A). Right coronary fistula draining into an aneurysmal sac, image with digital subtraction for better delimitation of the structures (B). Amplatzer prosthesis positioned between the proximal and middle portion of the fistula (C). After release of the prosthesis and significant improvement in the distal flow of the right coronary artery (D).*

blocking the flow to the aneurysmal portion (Figure 2C). During the procedure, an important improvement was already observed in the distal flow of the right coronary artery shortly after implantation of the prosthesis (Figure 2D). The procedure took place without complications.

One day after the procedure, a control transthoracic echocardiogram was performed, which showed an aneurysmal portion with thrombotic content inside (Figure 3A), already with signs of rejection by the right atrium and without blood flow between the cavities (Figure 3B), in

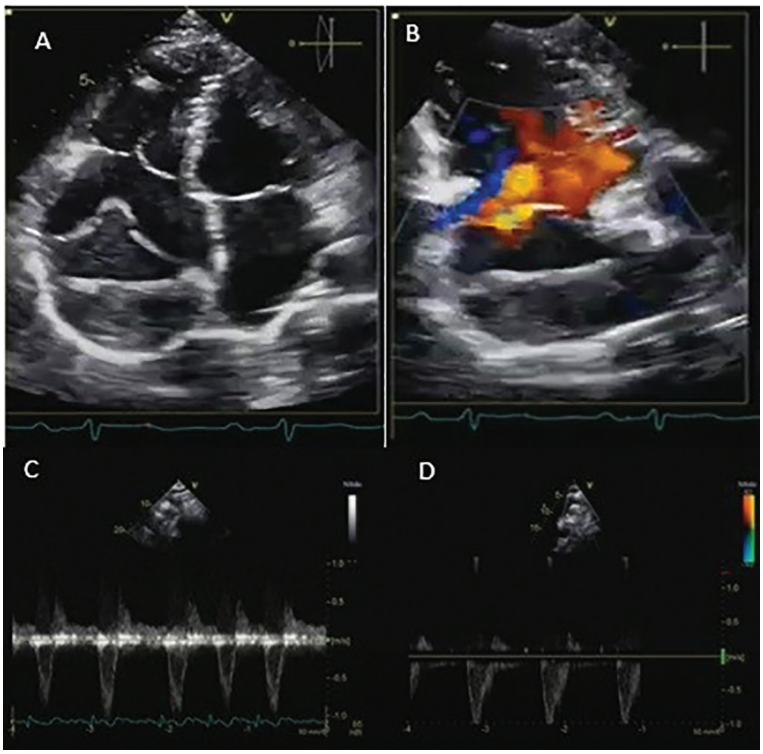

Figure 3 – *Apical 4-chamber view with the aneurysmal portion being rejected by the right atrium, with thrombotic content inside (A). Doppler showing that there is no more flow between the cavities (B). Tissue Doppler in descending thoracic aorta with reverse holodiastolic flow (before the procedure) (C) and subsequent control, without the initial findings (D).*

addition to significant improvement in reverse diastolic flow in the descending thoracic aorta (Figure 3C and 3D).

Discussion

Coronary fistula was first described in 1886, with the first report of successful surgical correction in 1947. From an embryological point of view, it appears to represent the persistence of embryonic intertrabecular spaces and sinusoids.[4-5] There is also an association of fistulas with other congenital anomalies, in approximately 20% of cases, such as tetralogy of Fallot, patent ductus arteriosus, and atrial and ventricular septal defects.[6]

In more than half of the cases, the fistula originates from the right coronary artery and is usually a dilated artery, with a long and tortuous tract before draining into the chamber or vessel. In approximately 19% of cases, it also presents with aneurysmal dilation. The most common drainage site is into the right heart chambers.[5]

The clinical picture is variable, and the majority of patients are asymptomatic. In the reported case, which is a high-caliber coronary-cavitary fistulous tract between the right coronary artery and the right atrium, during the entire cardiac cycle, the blood flow was directed to the right side, due to the greater pressure found in the arterioles and myocardial capillaries.[6] As there is continuity of the distal right coronary tract after the fistula, flow competition occurs in that territory, whose perfusion becomes compromised, promoting functional myocardial ischemia.

In asymptomatic cases, with small fistulas and without a high risk of complications, follow-up may be considered with an echocardiogram every 2 to 5 years. For symptomatic or asymptomatic patients with small fistulas and risk of complications or larger fistulas with hemodynamic repercussions, invasive treatment (surgical or percutaneous) is recommended.[6]

After the development of new hemodynamic techniques, there has been a great resurgence of indications for closing fistulas by means of the percutaneous technique. The main advantages compared to the surgical technique include lower costs of the procedure, shorter recovery time, reduced morbidity, better aesthetic results, fewer episodes of bleeding, fewer arrhythmias, fewer infections, and less myocardial ischemia.[7-8]

The first transcatheter coronary fistula closure occurred in 1983 by Reidy et al.[6] The main techniques used are coil embolization or occlusion devices. In the reported case, an 18 mm Amplatzer Vascular Plug II prosthesis was inserted between the proximal and middle thirds of the fistula; shortly thereafter, no residual shunt was observed, and there was significant improvement in distal coronary flow. The transthoracic echocardiogram performed one day after the procedure showed no complications and showed significant improvement in hemodynamic results (reduction of the

aneurysmal portion and absence of reverse diastolic flow in the descending thoracic aorta).

Six months after the procedure, angiography was scheduled to evaluate the involution of the aneurysmal sac, recovery of right atrial volume, and intracoronary thrombus. To date, the patient has shown clinical improvement, performing usual activities without limitations.

Author Contributions

Conception and design of the research: Silva LML and Correia EB; execution of images: Silva LML, Andrade MDRM, Jesus CA; acquisition and analysis and interpretation of the data: Andrade MDRM, Jesus CA, Ribeiro MS, Alencar AL. interventional procedure and provision of images: Ribeiro MS; writing of the manuscript: Alencar AL, Silva LML.

Potential Conflict of Interest

No potential conflict of interest relevant to this article was reported.

Sources of Funding

There were no external funding sources for this study.

Study Association

This study is not associated with any thesis or dissertation work.

Ethics Approval and Consent to Participate

This article does not contain any studies with human participants or animals performed by any of the authors.

References

1. Loukas M, Germain AS, Gabriel A, John A, Tubbs RS, Spicer D. Coronary Artery Fistula: A Review. Cardiovasc Pathol. 2015 May-Jun;24(3):141-8. doi: 10.1016/j.carpath.2014.01.010.
2. Challoumas D, Pericleous A, Dimitrakaki IA, Danelatos C, Dimitrakakis G. Coronary Arteriovenous Fistulae: A Review. Int J Angiol. 2014;23(1):1-10. doi: 10.1055/s-0033-1349162.
3. Abelin AP, Sarmento-Leite R, Quadros AS, Gottschall CAM. Fístula coronária. Rev Bras Cardiol Invas. 2008; 16 (2): 242-3.
4. Webb GD, Smallhorn JF, Therrien J. Doença cardíaca congênita. In: Zipes D, Libby P, Bonow RA, editors. Braunwald - Tratado de doenças cardiovasculares. 9th. Rio de Janeiro: Elsevier; 2013. p. 1499-500.
5. Parra-Bravo JR, Beirana-Palencia LG. Right Coronary Artery Fistula Opening Into Right Ventricle. Echocardiographic Findings and Interventional Management. Report of a Case. Arch Cardiol Mex. 2003;73(3):205-11.
6. Buccheri D, Chirco PR, Geraci S, Caramanno G, Cortese B. Coronary Artery Fistulae: Anatomy, Diagnosis and Management Strategies. Heart Lung Circ. 2018;27(8):940-51. doi: 10.1016/j.hlc.2017.07.014.
7. Oto A, Aytemir K, Çil B, Peynircioğlu B, Yorgun H, Canpolat U, et al. Percutaneous Closure of Coronary Artery Fistulae in Adults with Intermediate Term Follow-Up Results. J Interv Cardiol. 2011;24(3):216-22. doi: 10.1111/j.1540-8183.2010.00623.x.
8. Christmann M, Hoop R, Dave H, Quandt D, Knirsch W, Kretschmar O. Closure of Coronary Artery Fistula in Childhood: Treatment Techniques and Long-Term Follow-Up. Clin Res Cardiol. 2017;106(3):211-218. doi: 10.1007/s00392-016-1041-6.

Pulmonary Thromboembolism Associated with Paradoxical Embolism in a Patient with Patent Foramen Ovale

Arthur Barroso Vidal Vilarinho,[1] Danielly Bernardes Silva,[1] Ana Rosaria Medeiros Peres,[1] Rodolfo Loureiro Borges de Souza,[1] Carlos Eduardo de Sousa Amorelli,[1] Fábio Lemos Campedelli,[1] Luciano Moreira Alves,[1] Fabio Augusto Cypreste de Oliveira[1]

Hospital São Francisco de Assis, Serviço de Angiologia e Cirurgia Vascular, ANGIOGYN,[1] Goiânia, GO – Brazil

Introduction

Patent foramen ovale (PFO) is a pathological condition characterized by an opening in the interatrial septum, that allows blood to flow from one atrium to the other. It is found in approximately 25% of the adult population, with no hemodynamic implications in most cases.[1] However, due to persistence of the foramen, paradoxical embolism may occur as a cause of ischemic events; in some cases, closure of the PFO is indicated as a secondary prevention strategy for thromboembolic events.[2]

Studies have demonstrated an association between PFO and many clinical conditions, some potentially severe, such as ischemic stroke and pulmonary thromboembolism (PTE).[3]

Although paradoxical embolism is a well-documented consequence of PFO, the passage of blood clot through the PFO has been little documented in the literature.[3,4] Thus, the present study aimed to report a typical case of PTE associated with paradoxical embolism probably caused by PFO.

Clinical case

A 58-year-old male patient urgently admitted with severe dyspnea, which started about one week before, and got worse within the last hours before admission. The patient reported no other comorbidities.

The patient underwent computed tomography angiography of the chest, with a PTE protocol, which revealed bilateral PTE (Figure 1).

During hospitalization, the patient had abdominal pain; an abdominal magnetic resonance imaging was performed, which revealed splenic artery embolism, areas of multifocal infarcts, and absence of aortic lesions that may explain the embolism (Figure 2).

Full anticoagulation therapy with low molecular weight heparin was then initiated. In light of both arterial and venous thromboembolic events, transesophageal echocardiogram (TEE) was performed and revealed lipomatous interatrial septum, with bulging of the fossa ovalis region into the left right atrium, associated with delamination, with no evidence of interatrial tunnel or prominent Eustachian valve. Aired saline solution was infused, and right-to-left flow through the fossa ovalis was then observed (Figure 3).

The patient was regularly followed-up by the cardiology and vascular surgery staff. After excluding the presence of hematological disease, a percutaneous closure device was used to close the PFO (Figure 4).

Following device implantation, transthoracic echocardiogram confirmed complete closure of the PFO, with no residual flow. The patient was discharged with anticoagulation therapy and regular follow-up by the cardiology and vascular surgery staff.

Discussion

The presence of foramen ovale is essential in fetal life as it allows oxygenated blood to flow directly to systemic circulation, bypassing the lungs which are collapsed in this stage of life. However, with lung expansion at birth, fusion of the septa and closure of the foramen ovale occur around the first month of life. Nonetheless, in nearly 25% of the general population, complete closure of the foramen ovale does not occur, and it either remains patent throughout life or closes at first and then open in situations of right pressure overload.[3]

PFO may be diagnosed in association with PTE, and the concomitant presence of these both conditions is associated with systemic paradoxical embolism and greater severity of disease.[4] In patients with acute pulmonary embolism, right atrial pressure is increased, with elevates the risk of blood flow from the right to the left atrium through the PFO and thus potentially the risk of paradoxical embolism. Many prospective and retrospective observational studies have shown a high prevalence of stroke in patients with acute pulmonary embolism, and a disproportionately high prevalence of PFO among patients with acute pulmonary embolism who had a stroke.[5] In this case reported, the patient had PTE and probably progressed to systemic paradoxical embolism. Although the passage of the thrombus through the PFO could not be visualized, this was a potential causal factor based on the echocardiographic findings.

The foramen ovale can be defined as a risk factor for embolic events when it has specific echocardiographic features that become important in the therapeutic decision-making process.[6] Some characteristics of the PFO are associated with paradoxical

Keywords

Pulmonary Embolism; Splenic Infarction; Foramen Ovale; Paradoxical Embolism.

Correspondência: Arthur Barroso Vidal Vilarinho •
Rua 9A, n° 110, setor aeroporto. Postal code: 74110-110. Goiânia, GO - Brazil
E-mail: arthur.bvvilarinho@gmail.com
Artigo recebido em 9/9/2022; revisado em 15/9/2022; aceito em 17/12/2022
Editor responsável pela revisão: Daniela do Carmo Rassi Frota

DOI: https://doi.org/10.36660/abcimg.2023347i

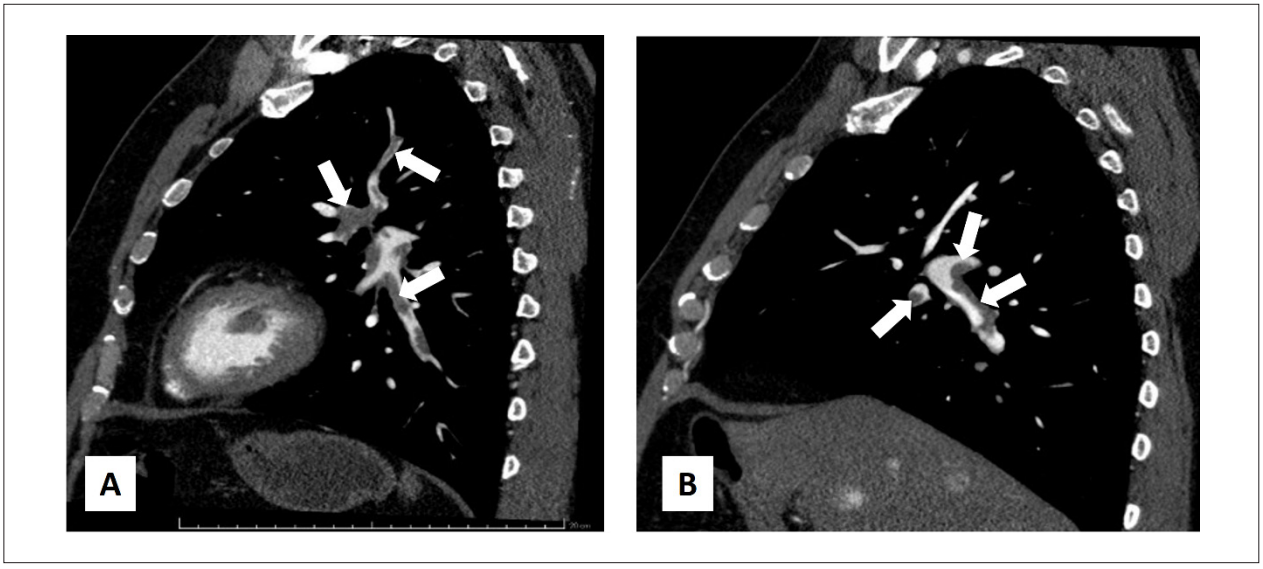

Figure 1 – *Sagittal sections of computed angiography showing several intraluminal filling defects in segmental and subsegmental branches of main pulmonary arteries (some of them indicated by white arrows), indicating bilateral PTE; A. left lung; B. right lung (arrows).*

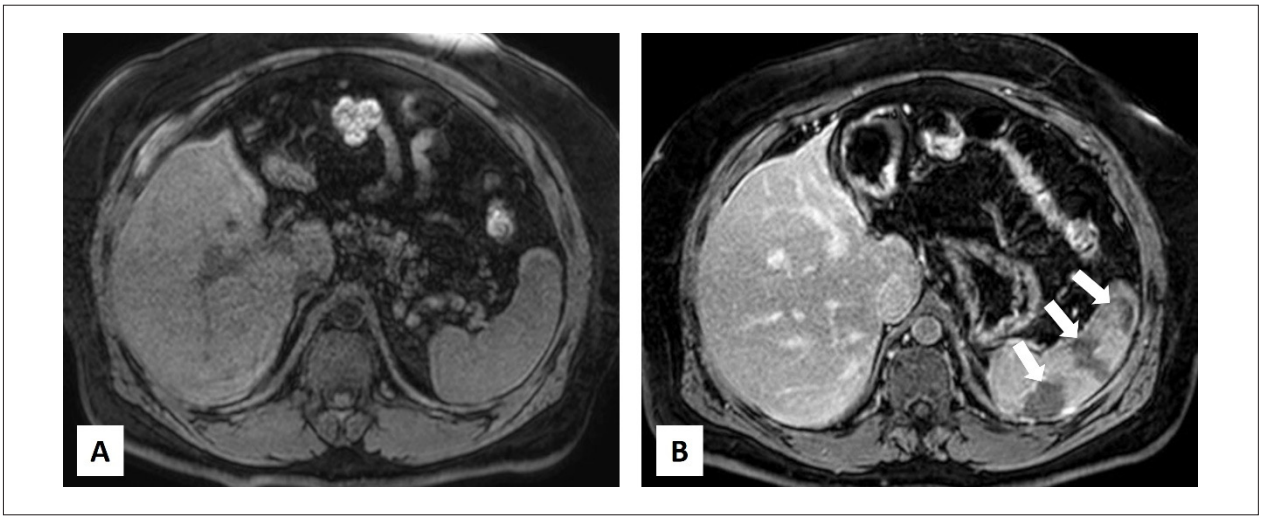

Figure 2 – *T1 weighted axial magnetic resonance image, with fat suppression before (A) and after (B) administration of paramagnetic contrast, which showed low uptake of the contrast (white arrows), compatible with areas of splenic infarction.*

embolism, including a long-tunnel PFO, hypermobile interatrial septum, prominent Eustachian valve or Chiari's network, a large right-to-left shunt during Valsalva maneuver, and a low angle between the PFO and the inferior vena cava. When two or more of these characteristics are detected by TEE, there is a strong association of PFO with thromboembolic events and therefore these patients will benefit from the PFO closure.[7]

The therapy adopted in the report was initially applied with the use of anticoagulant drugs and, later, percutaneous closure of the PFO, as already proposed by some studies.[8]

Paradoxical embolism with involvement of the splenic artery and association with pulmonary embolism implies the need for diagnostic investigation for a source of embolism, such as the interatrial shunt. In these circumstances, closure of the interatrial sept defect should be considered, in view of echocardiographic characteristics, in addition to a multidisciplinary approach on the anticoagulant therapy, aiming at preventing new thromboembolic events.

Author Contributions

Conception and design of the research: Vidal ABV; acquisition of data: Vidal ABV, Silva DB, Peres ARM, de Souza RL; analysis and interpretation of the data: Vidal ABV, Silva DB, Peres ARM, de Souza RL, Amorelli CES, Campedelli FL, Alves

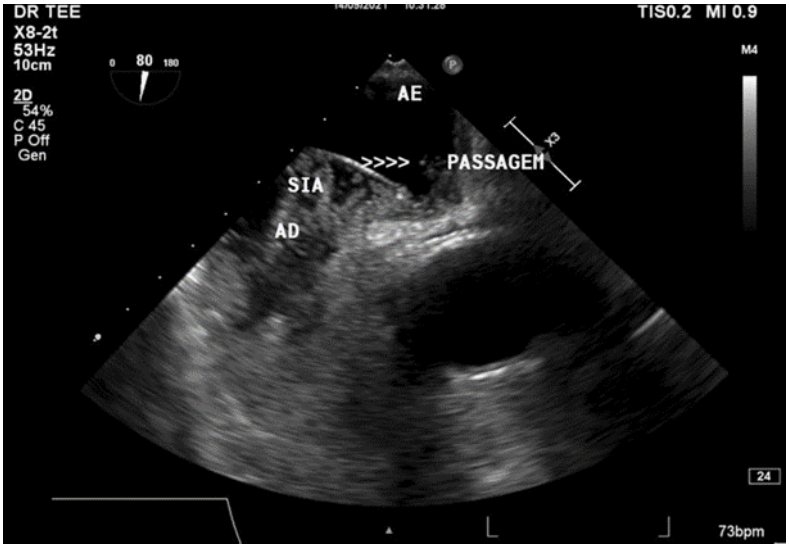

Figure 3 – *TEE (80º) showing passage of microbubbles (arrows), confirming the presence of PFO. LA: left atrium; RA: right atrium; IAS: interatrial septum.*

LM, de Oliveira FAC; writing of the manuscript: Vidal ABV, Silva DB; critical revision of the manuscript for intellectual content: Amorelli CES, Campedelli FL, Alves LM, de Oliveira FAC.

Potential Conflict of Interest

No potential conflict of interest relevant to this article was reported.

Sources of Funding

There were no external funding sources for this study.

Study Association

This study is not associated with any thesis or dissertation work.

Ethics Approval and Consent to Participate

This article does not contain any studies with human participants or animals performed by any of the authors.

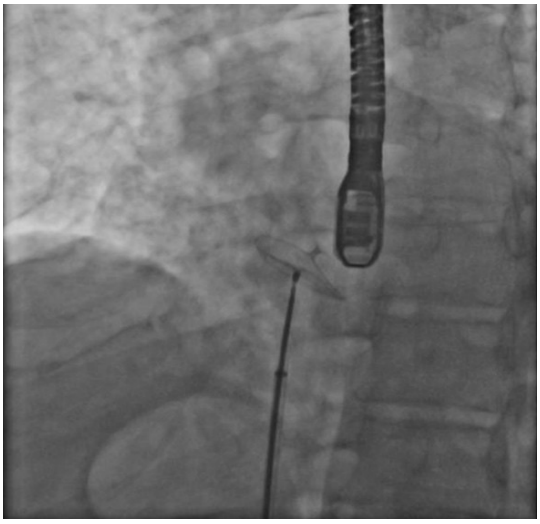

Figure 4 – *Implantation of a percutaneous closure device for PFO closure.*

References

1. Wieder MS, Blace N, Szlechter MM, Shulman E, Thankenchen J, Mbekeani JN. Central Retinal Artery Occlusion Associated with Patent Foramen Ovale: A Case Report and Literature Review. Arq Bras Oftalmol. 2021;84(5):494-8. doi: 10.5935/0004-2749.20210073.
2. Le Moigne E, Timsit S, Ben Salem D, Didier R, Jobic Y, Paleiron N, et al. Patent Foramen Ovale and Ischemic Stroke in Patients With Pulmonary Embolism: A Prospective Cohort Study. Ann Intern Med. 2019;170(11):756-63. doi: 10.7326/M18-3485.
3. Souto FMS, Faro FN, Silveira MFR, Barreto MA, Barreto-Filho JAS, Oliveira JLM, et al. Pulmonary Thromboembolism and Thrombus in Patent Foramen Ovale. Arq Bras Cardiol: Imagem Cardiovasc. 2014;27(1):29-31. doi: 10.5935/2318-8219.20140006.
4. Meier B, Kalesan B, Mattle HP, Khattab AA, Hildick-Smith D, Dudek D, et al. Percutaneous Closure of Patent Foramen Ovale in Cryptogenic Embolism. N Engl J Med. 2013;368(12):1083-91. doi: 10.1056/NEJMoa1211716.
5. Schmidt MR, Søndergaard L. Patent Foramen Ovale: A Villain in Pulmonary Embolism? Ann Intern Med. 2019;170(11):805-6. doi: 10.7326/M19-1089.
6. Lee PH, Song JK, Kim JS, Heo R, Lee S, Kim DH, et al. Cryptogenic Stroke and High-Risk Patent Foramen Ovale: The DEFENSE-PFO Trial. J Am Coll Cardiol. 2018;71(20):2335-42. doi: 10.1016/j.jacc.2018.02.046.
7. Nakayama R, Takaya Y, Akagi T, Watanabe N, Ikeda M, Nakagawa K, et al. Identification of High-Risk Patent Foramen Ovale Associated With Cryptogenic Stroke: Development of a Scoring System. J Am Soc Echocardiogr. 2019;32(7):811-16. doi: 10.1016/j.echo.2019.03.021.
8. Wilmshurst PT, Nightingale S, Walsh KP, Morrison WL. Effect on Migraine of Closure of Cardiac Right-to-Left Shunts to Prevent Recurrence of Decompression Illness or Stroke or for Haemodynamic Reasons. Lancet. 2000;356(9242):1648-51. doi: 10.1016/s0140-6736(00)03160-3.

Criss-Cross Heart: A Case Report

Mateus Oliveira Potratz,[1] Lorrayne Zonatele Garbo,[2] Kamila Pompermaier Pessimilio,[3] André Silveira Loss,[3] Crislane Belisario Ambrozim,[3] Ana Luiza Teixeira Albert Lima,[3] Danielle Lopes Rocha[3]

Hospital Universitário Cassiano Antônio de Moraes, Universidade Federal do Espírito Santo (UFES),[1] Vitória, ES – Brazil

Hospital Evangélico de Vila Velha,[2] Vila Velha, ES – Brazil

Hospital Estadual Infantil e Maternidade Alzir Bernardino Alves (HIMABA),[3] Vila Velha, ES – Brazil

Abstract

Criss-cross heart was first described in 1974. It is a rare congenital heart malformation that occurs in 8 cases per 1,000,000 children, and represents only 0.1% of congenital malformations. The diagnostic methods of choice are transthoracic echocardiography, cardiac magnetic resonance (CMR), computed tomography angiography (CT) and, sometimes, cardiac catheterization. This report describes the case of a newborn with a criss-cross heart in addition to double-outlet right ventricle (RV), with poorly positioned vessels, in addition to atrial septal defect (ASD), interventricular septal defect, tricuspid valve dysplasia and persistent left superior vena cava. The exact etiology of this malformation is not known, but it seems to occur due to rotation of the ventricles in their longitudinal axis, not accompanied by rotation of the atrial and atrioventricular (AV) valves. This movement produces abnormal ventricular inlets, determining that the RV be positioned on a superior plane and the left ventricle on an inferior plane. Although the exact cause of this anomaly is still unknown, it is believed that a genetic abnormality may be leading to these cases: mutation of the Cx43 gene. Diagnosis of the case concerned was given by transthoracic echocardiography and computed CT of the aorta and pulmonary arteries, which showed, in addition to the criss-cross heart, other abnormalities, such as double-outlet RV, large ASD and ventricular septal defect (VSD).

Introduction

Criss-cross heart was first described in 1974, although it had been reported in 1961.[1,2] It is a rare congenital heart malformation that occurs in 8 cases per 1,000,000 children, and represents only 0.1% of congenital malformations.[3,4]

Criss-cross heart appears when, during the embryonic period, the heart rotates around its own axis, resulting in an anterosuperior RV and a posteroinferior left ventricle. Due to the complex structural alteration, diagnosis is complicated, and the clinical picture depends on other congenital cardiac abnormalities, commonly present in cases of criss-cross heart.

The diagnostic methods of choice are transthoracic echocardiography, CMR imaging, computed CT and, occasionally, cardiac catheterization.[5] Transthoracic echocardiography is usually the first test to be performed. It identifies the position and morphology of the four chambers and AV valves and the connections between vessels and chambers.[6] Furthermore, in the performance of this method, there is, dynamically, the impression that the atrium empties into the contralateral ventricle due to the crossing of blood flows.[7,8] CMR imaging and computed CT provide more detailed information and on other planes, such as coronal, axial and sagittal positions.[9] Cardiac catheterization may be necessary to assess intracavitary or vessel pressures and oxygenation in different locations, in addition to ruling out septal defects not seen in other scans.[5]

The malformation regarding the rotation of the heart itself does not indicate a surgical approach, however, most cases are associated with other anatomic abnormalities, which need to be evaluated individually to determine the conduct. The most frequent associated malformations include: tricuspid valve and right ventricular hypoplasia, VSD, ventricular arterial discordance and pulmonary stenosis.[7]

In this report, we describe the case of a newborn with a criss-cross heart in addition to double-outlet RV, with poorly positioned vessels, in addition to ASD, interventricular septal defect, tricuspid valve dysplasia and persistent left superior vena cava.

Case report

Male child born on March 28, 2021, from home birth, was taken to a hospital in Colatina (ES) after birth, for evaluation. When examined by the attending physician, the heart test revealed an abnormality (saturation in the right upper limb = 92% and right lower limb = 92%). Transthoracic echocardiography was performed, suggesting a complex congenital heart disease with transposition of the great vessels with patent foramen ovale (PFO) ASD and large associated VSD.

Transferred to a reference pediatric cardiac surgery hospital in Vila Velha (ES) on March 30, 2021, for follow-up and treatment. Upon hospital admission to the pediatric intensive care unit (PICU), he had sucking issues, respiratory effort and drop in saturation during breastfeeding. On physical examination, he was afebrile, ruddy, acyanotic, diffuse toxic erythema, heart rate of 150 beats per minute, blood pressure of 60/35 mmHg in the right upper limb, 90/68 mmHg in the

Keywords

Congenital Heart Defects; Crisscross Heart; Heart Ventricles

Mailing Address: Mateus Oliveira Potratz •
Hospital Universitário Cassiano Antônio de Moraes. Av. Marechal Campos, 1355. Postal code: 29043-260. Santa Cecilia, Vitória, ES – Brazil
E-mail: mateusopotratz@hotmail.com
Manuscript received January 5,2022; revised October 27, 2022; accepted January 11, 2023
Editor responsible for the review: Karen Saori Shiraishi Sawamura

DOI: https://doi.org/10.36660/abcimg.2023282i

right lower limb, 79/47 mmHg in the left upper limb and 79/55 mmHg in the left lower limb, systolic ejection murmur ++/6+ in the left sternal border, in addition to mild subcostal retraction.

Transthoracic echocardiography was performed on March 31, 2021, which showed: situs solitus, levocardia; two-valve AV concordance with rotation of the AV connection and crossed ventricular inflow streams (Figures 1 and 2); double-outlet RV ventricular-arterial coupling (Figure 3), with poorly positioned vessels; wide fossa ovalis ASD, 5.4 mm in its largest measurement, no flow acceleration, mean gradient of 1.7 mmHg, left-right flow; interventricular septum with overriding greater than 50% and apparent double infundibulum; large inlet VSD, 10 mm, no significant gradient; moderate dilation of the right chambers and mild RV hypertrophy; preserved biventricular systolic function assessed by qualitative analysis; dysplastic tricuspid valve with straddling and moderate regurgitation of this valve allowing estimating right ventricular systolic pressure at 55 mmHg, 8.5 mm tricuspid annulus; trivalvular aortic valve anterior and to the right, no significant systolic gradient, mild regurgitation; trivalvular pulmonary valve with no significant systolic gradient at the time, mid-systolic notch and mild regurgitation; discrete stenosis in the left pulmonary artery; persistent left superior vena cava.

While in hospital, the child presented clinical and radiographic signs suggestive of pulmonary hyperflow. Adjustments were made to diuretic doses and computed CT of the thoracic aorta and pulmonary arteries was performed on April 8, 2021 for better anatomic evaluation and approach planning. The scan revealed: situs solitus; levocardia; concordant systemic and pulmonary venous couplings; luminal reduction of the ostium of the left internal pulmonary vein — 6.4 mm²; double RV outlet ventricular-arterial couplings (Figure 4); left ventricle inferior to the RV (criss-cross) (Figure 5); presence of a muscle band close to the aortic outflow tract; large inlet VSD; large ASD (Figure 6) and aortic arch on the left and abdominal aorta positioned on the left. Figure 7 reveals three-dimensional tomography reconstruction showing rotation of the ventricles around the largest axis and Figure 8 reveals normal AV couplings.

The patient underwent pulmonary artery banding cardiac surgery on April 20, 2021, uneventfully. In the immediate postoperative period, the patient developed supraventricular tachycardia, which improved after adjusting the temperature, required low-dose epinephrine, and presented oliguria requiring diuretic solution. The patient presented a positive outcome, allowing the diuretic solution and adrenaline to be suspended, and was extubated on April 22, 2021, uneventfully. Control transthoracic echocardiography on April 22, 2021 showed effective pulmonary banding.

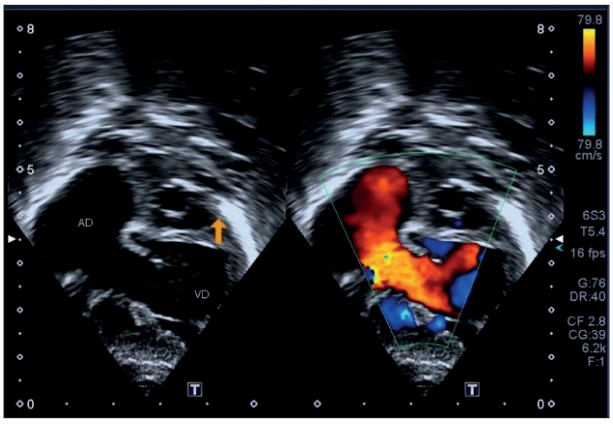

Figure 1 – *Echocardiographic image showing AD-RV connection rotation. RV: right ventricle; RA: right atrium.*

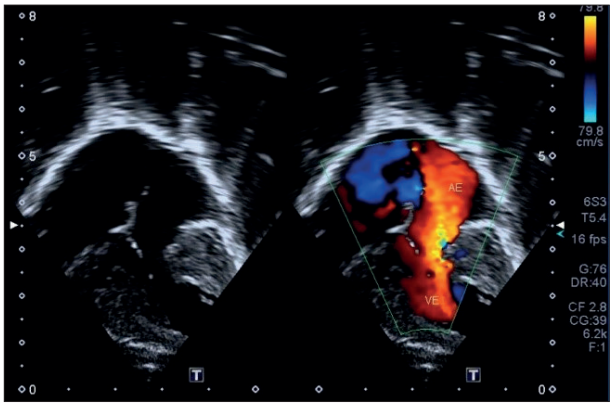

Figure 2 – *Echocardiographic image showing LA-LV connection rotation. LA: left atrium.*

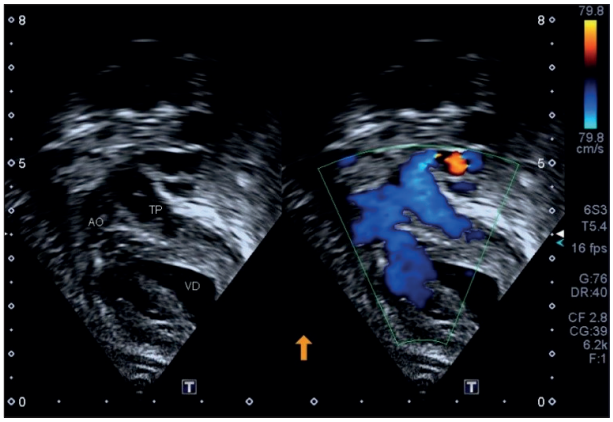

Figure 3 – *Echocardiographic image showing double outflow of the RV. RV: right ventricle; AO: aorta; PT: pulmonary trunk.*

Discussion

The exact etiology of this malformation is not known, but it seems to occur due to rotation of the ventricles around their longitudinal axis, not accompanied by atrial rotation and AV valve rotation. This movement produces abnormal ventricular inlets, determining that the RV be positioned on a superior plane and the left ventricle on an inferior plane.[10] The other anomalies normally found are hypoplasia of the right tricuspid valve, pulmonary stenosis, inlet VSD and abnormal ventricular-arterial coupling. Discordant coupling is more frequent, and double-outlet RV is rare.[10,11]

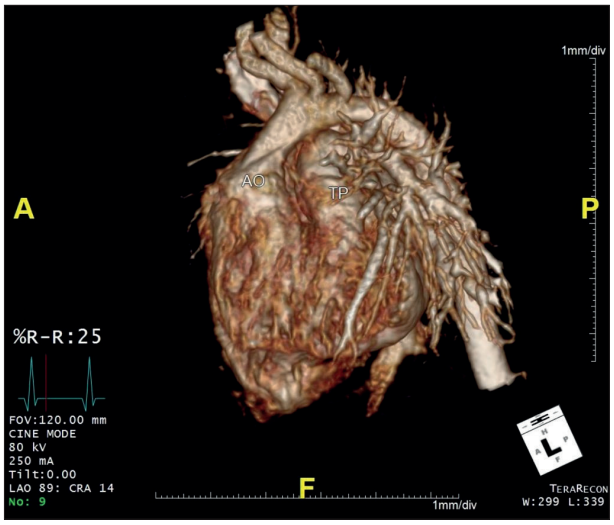

Figure 4 – *Double Outlet RV. AO: aorta; PT: pulmonary trunk.*

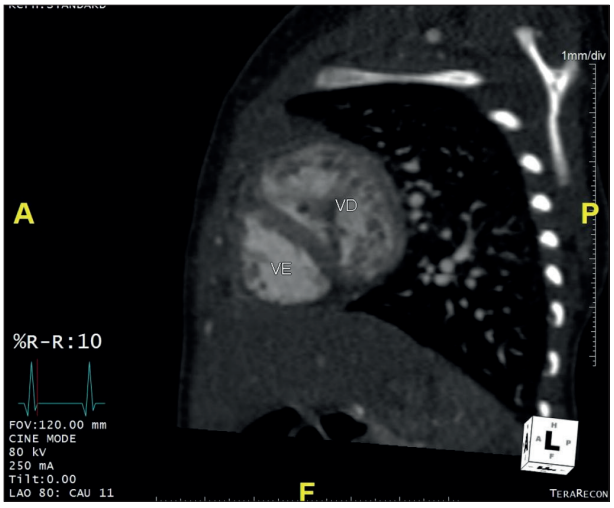

Figure 5 – *Left Ventricle Inferior to RV. RV: right ventricle; LV: left ventricle.*

Figure 6 – *Wide Interatrial Communication. RA: right atrium; LA: left atrium.*

Although the exact cause of this anomaly is not yet known, it is believed that a genetic abnormality may be leading to these cases — mutation of the Cx43 gene — and the exclusion of this gene would lead to a delay in the dextroposition of the heart, thus causing right ventricular defect, and not taking it into the correct position.[12]

The diagnosis of the case in question was given by through transthoracic echocardiography and computed CT of the aorta and pulmonary arteries, which showed, in addition to criss-cross heart, other abnormalities, such as double-outlet RV, and large ASD and VSD. Due to the presence of double-outlet RV, in view of the high systemic resistance leading to the flow preferentially through the pulmonary trunk, with exacerbated pulmonary hyperflow, it was decided to perform the banding of the pulmonary arteries in order to increase or, at least, equalize the pulmonary resistance and, thus, cause the blood to be ejected preferentially to the systemic arterial bed instead of the pulmonary venous bed, thus protecting the pulmonary arterial vasculature.[13] The procedure was uneventful, but, due to other neonatal problems, the child had to remain hospitalized after hospital discharge from a cardiovascular point of view, but remained hemodynamically stable and in room air, which demonstrates the effectiveness of the procedure performed, in addition to the echocardiography postoperatively. An outpatient follow-up schedule was created so that, in the future, the best therapeutic strategy could be defined.

Author Contributions

Conception and design of the research: Potratz MO, Garbo LZ, Pessimilio KP, Loss AS, Ambrozim CB, Lima ALTA, Rocha DL; acquisition of data and critical revision of the manuscript for intellectual content: Potratz MO, Garbo LZ, Rocha DL; writing of the manuscript: Lima ALTA.

Potential Conflict of Interest

No potential conflict of interest relevant to this article was reported.

Sources of Funding

There were no external funding sources for this study.

Study Association

This study is not associated with any thesis or dissertation work.

Ethics Approval and Consent to Participate

This article does not contain any studies with human participants or animals performed by any of the authors.

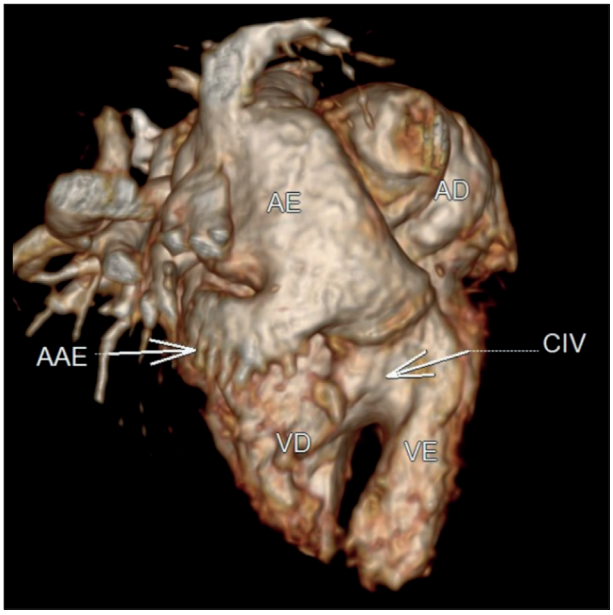

Figure 7 – *Three-dimensional tomography reconstruction showing the rotation of the ventricles in the major axis. RV: right ventricle; VSD: ventricular septal defect; LV: left ventricle; LA: left atrium; RA: right atrium; LAA: left atrial appendix.*

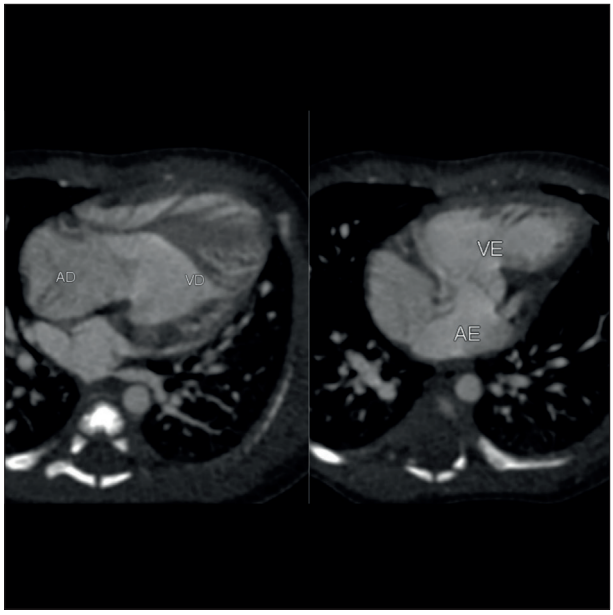

Figure 8 – *Tomography image showing normal AV connections. RV: right ventricle; RA: right atrium; LV: left ventricle; LA: left atrium.*

References

1. Anderson RH, Shinebourne EA, Gerlis LM. Criss-Cross Atrioventricular Relationships Producing Paradoxical Atrioventricular Concordance or Discordance. Their Significance to Nomenclature of Congenital Heart Disease. Circulation. 1974;50(1):176-80. doi: 10.1161/01.cir.50.1.176.
2. Lev M, Rowlatt UF. The Pathologic Anatomy of Mixed Levocardia. A Review of Thirteen Cases of Atrial or Ventricular Inversion with or Without Corrected Transposition. Am J Cardiol. 1961;8:216-63. doi: 10.1016/0002-9149(61)90209-0.
3. Ando M, Takao A, Cho E, Vehara K, Nihmura I. Criss-cross heart by abnormal rotation of bulboventricular loop: diagnostic considerations for complex cardiac anomaly. Proc Ped Circ Soc. 1974;4:82-3.
4. Fyler DC. Trends. In: Fyler DC, editor. Nanda's Pediatric Cardiology. Philadelphia: Hanley & Belfus; 1992. p. 273-80.
5. Robinson PJ, Kumpeng V, Macartney FJ. Cross Sectional Echocardiographic and Angiocardiographic Correlation in Criss Cross Hearts. Br Heart J. 1985;54(1):61-7. doi: 10.1136/hrt.54.1.61.
6. Wallis GA, Debich-Spicer D, Anderson RH. Congenitally Corrected Transposition. Orphanet J Rare Dis. 2011;6:22. doi: 10.1186/1750-1172-6-22.
7. Sanders S. Criss-Cross Heart. Paris: Orphanet Encyclopedia; 2003.
8. Valenzuela NJMB, Lucas E, Bomfim EJ. Criss-Cross Heart: Fetal Diagnose. Rev Bras Ecocardiogr Imagem Cardiovasc. 2009;22(2):51-6.
9. Link KM, Weesner KM, Formanek AG. MR Imaging of the Criss-Cross Heart. AJR Am J Roentgenol. 1989;152(4):809-12. doi: 10.2214/ajr.152.4.809.
10. Anderson RH, Smith A, Wilkinson JL. Disharmony between Atrioventricular Connections and Segmental Combinations: Unusual Variants of "Crisscross" Hearts. J Am Coll Cardiol. 1987;10(6):1274-7. doi: 10.1016/s0735-1097(87)80130-4.
11. Kim DY, Cho SR, Park SD, Chung HK. Double Outlet of Right in Criss-Cross Heart: Surgical Experience of One Case. Korean J Thorac Cardiovasc Surg. 1997;30:1242-6.
12. Ya J, Erdtsieck-Ernste EBHW, Boer PAJ, van Kempen MJA, Jongsma H, Gros D, et al. Heart Defects in Connexin 43-Deficient Mice. Circulation Research. 1998;82:360-6.
13. Barbero-Marcial M, Tamanati C, Jatene MB, Aiello VD, Baucia JA, Atik E, et al. Dupla Via de Saída do Ventrículo Direito com Comunicação Interventricular Não Relacionada: Resultados da Correção Cirúrgica com Técnica de Múltiplos Retalhos. Braz J Cardiovasc Surg.1997;12(2). doi: 10.1590/S0102-76381997000200009.

Case Report

Importance of Echocardiography in the Differential Diagnosis of Rheumatic Mitral Regurgitation in Children and Adolescents

Camila Magalhães Silva,[1] *Maik Arantes,*[1] *Fátima Derlene da Rocha Araújo,*[1] *Adriana Furletti Machado Guimarães,*[1] *Zilda Maria Alves Meira*[1]

Hospital das Clínicas da Universidade Federal de Minas Gerais,[1] *Belo Horizonte, MG – Brazil*

Introduction

Mitral regurgitation (MR) can be a result of abnormalities in different locations of the valve apparatus (cusps, annulus, tendinous cords and papillary muscles), being of acquired or congenital etiology.[1] MR can be classified as primary, when resulting from a deformity in the valve structure, or secondary, when related to another heart or systemic disease. In our field, the main cause of MR in students and adolescents is the acquired one. Rheumatic fever (RF) is among the causes, as well as bacterial endocarditis, which should be considered in the differential diagnosis.[2,3] However, congenital anomalies, such as mitral valve (MV) prolapse, mitral cleft (MC), parachute MV and, rarely, isolated cleft MV (ICMV) should be ruled out.[1,2] The etiological diagnosis of MR is very important to determine the proper treatment, once it can be clinical or surgical, with definitive correction of the lesion.

We present the report of a student whose clinical and echocardiographic scenario was first diagnosed as acute RF, showing the importance of echocardiography in the posterior differential diagnosis of MR.

Clinical case description

Male, 8-year-old student, was admitted in an intensive care unit presenting with rapid onset exhaustion, low fever and paleness. He denied articular involvement or abnormal movements. He reported previous episodes of pharyngotonsillitis unrelated to the current disease and denied previous hospitalization or regular pediatric follow-up. Negative family history of RF. At examination, his general status was compromised. He was feverish, acyanotic, anicteric, with no edema in the lower limbs, full and symmetrical peripheral pulses, moderate tachypnea, inspiratory crackles in lung bases and painful hepatomegaly. Cardiac auscultation showed three heart sounds, second hyper phonetic sounds, holosystolic murmur grade III-IV/VI, in a mitral area irradiating to the axilla. Laboratory examinations showed leukocytosis, increased C-reactive protein, increased velocity of hemossedimentation and high levels of anti-streptolysin O; blood cultures were negative. Thoracic X-ray showed moderate cardiomegaly in the left chambers, besides lung congestion. Electrocardiography showed sinus rhythm and overload of the left atrium. The first echocardiography diagnosed major MR, increased left chambers and pulmonary hypertension, which raised the possibility of possible rheumatic etiology. The patient was treated for rheumatic carditis with corticotherapy, as well as clinical treatment for heart failure. After discharge, he was referred to the pediatric cardiology outpatient clinic using penicillin G benzathine 1.200.000 UI applied every 21 days, furosemide, captopril and prednisone, remaining stable.

Echocardiographic control confirmed the diagnosis of major MR (Figure 1), increased left chambers, pulmonary hypertension (systolic pressure of the pulmonary artery estimated in 80 mmHg) and left ventricular systolic dysfunction (LVSD 67%). However, morphological evaluation of the MV did not show thickening nor reduction of the cuspid mobility (video); a discontinuity was visualized in the middle third of the anterior cuspid, measuring about 4 mm (Figure 2). There was no change in the aortic valve.

Mitral valvuloplasty was indicated and, during the surgical act, a cleft was identified in the anterior cuspid of the MV and enlargement of the valve ring. Cleft grafting was performed, as well as valve annulus plication, without intercurrences. In the follow-up, the child was asymptomatic, with no need for medications, normal cardiac auscultation and normalization of heart chamber dimensions, pulmonary pressure and presence of minimal MR jet.

Discussion

Rheumatic carditis corresponds to the most important manifestation of acute RF, occurring in about 40 to 70% of the cases. MV is the first to be affected in practically 100% of the cases of carditis, manifesting as MR in different grades.[2] Due to the epidemiology of the disease in our field, it should always be included in the differential diagnosis of acute heart failure and MR, especially in the pediatric age group.[2] For the diagnosis of the first RF outbreak two major manifestations, or one major and two minor manifestations, are necessary, besides the evidence of previous infection by group A streptococcus.[3,4] The child in

Keywords

Echocardiography; Mitral Valve Insufficiency; Rheumatic Fever; Diagnosis, Differential; Pediatrics

Mailing Address: Camila Magalhães Silva •
Avenida Alfredo Balena, 100, quinto andar, Postal code: 30130-100, Santa Efigênia, Belo Horizonte, MG – Brazil
E-mail: camila.magalhaes@live.com
Manuscript received October 19, 2022; revised manuscript January 27, 2023; accepted January 30, 2023
Editor responsible for the review: Daniela do Carmo Rassi Frota

DOI: https://doi.org/10.36660/abcimg. 2023360i

Contents

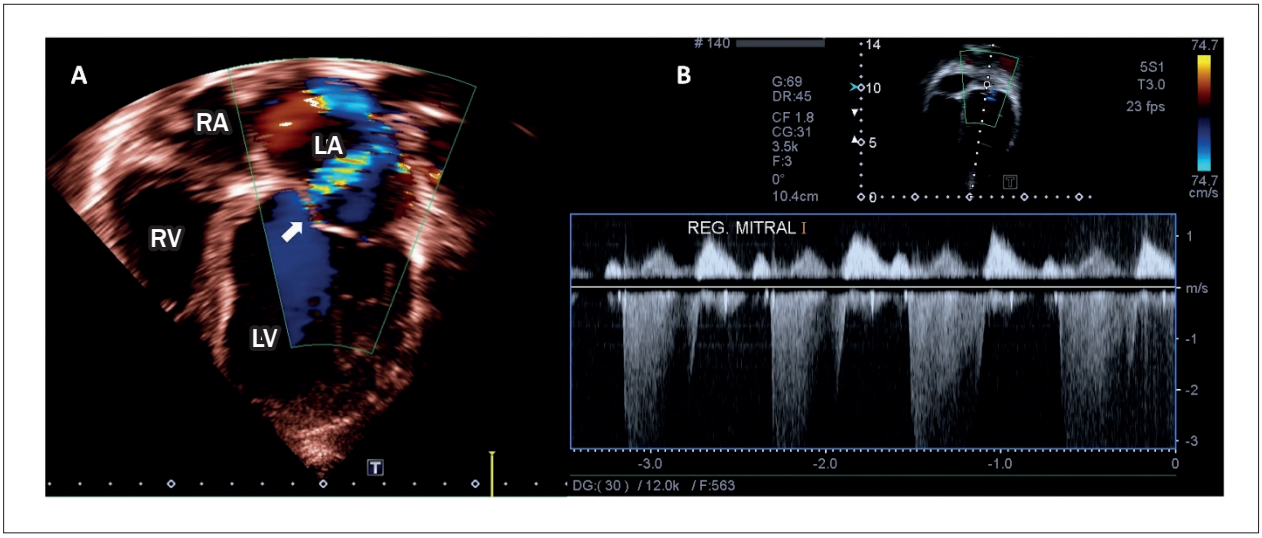

Figure 1 – *RA: right atrium; RV: right ventricle; LA: left atrium; LV: left ventricle; Arrow points to the location of the cleft with ColorDoppler image compatible with major MR.*

the report presented with a major manifestation (carditis) and two minor manifestations (fever and increased evidence of the inflammatory activity phase); previous streptococcia was proven by dosing the antistreptolysin O. Therefore, he was treated for heart failure due to acute rheumatic carditis. However, a detailed analysis of mitral morphology showed that the regurgitating jet originated from a flaw along the anterior cuspid and, for that, the most likely diagnosis would be the perforation of the secondary cuspid to bacterial endocarditis, fact that was not proven by the surgical finding that showed an aspect compatible with congenital cleft isolated from the MV.

ICMV is a rare congenital cause of MR with an incidence of 1:1340 in the pediatric population; it may occur both in the anterior and the posterior MV.[5] It can be isolated or in association with other congenital heart lesions, and the most common ones are interventricular communication, accessory chordaea in the left ventricle outflow, without obstruction, the ostium secundum interatrial communication and the persistence of the arterial channel.[6,7] When associated with other heart lesions, they can be more asymptomatic, and have an earlier diagnosis when compared to isolated cleft cases. However, after the advent of high resolution bidimensional echocardiography and the tridimensional echocardiography, the ICMV diagnosis has been earlier and more recurrent than in the past.[8]

This case shows how important the echocardiography is in the differential diagnosis of mitral valvulopathy, even in those patients who met the clinical criteria for RF, thus preventing a mistaken diagnosis and all of the implications related to secondary prophylaxis and late diagnosis of the true etiology.

Author Contributions

Conception and design of the research and critical revision of the manuscript for intellectual content: Araújo FDR e Meira ZMA; acquisition of data: Silva CM, Guimarães AFM, Araújo FDR, Meira ZMA, Arantes M; analysis and interpretation of the data: Guimarães AFM, Araújo FDR, Meira ZMA; writing of the manuscript: Silva CM, Araújo FDR, Meira ZMA, Arantes M.

Potential Conflict of Interest

No potential conflict of interest relevant to this article was reported.

Sources of Funding

There were no external funding sources for this study.

Study Association

This study is not associated with any thesis or dissertation work.

Ethics Approval and Consent to Participate

This article does not contain any studies with human participants or animals performed by any of the authors.

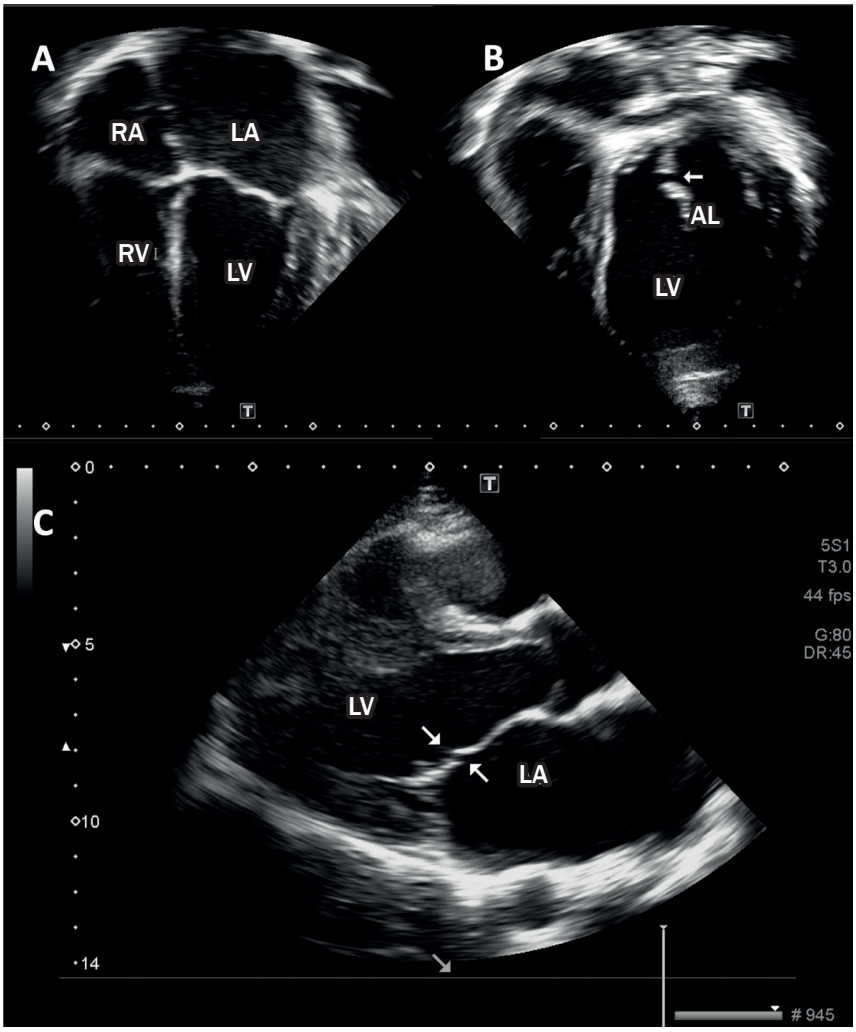

Figure 2 – *RA: right atrium; RV: right ventricle; LA: left atrium; LV: left ventricle; AL: mitral valve anterior leaflet. Arrow points to the cleft.*

References

1. Séguéla PE, Houyel L, Acar P. Congenital Malformations of the Mitral Valve. Arch Cardiovasc Dis. 2011;104(8-9):465-79. doi: 10.1016/j.acvd.2011.06.004.

2. Vahanian A, Beyersdorf F, Praz F, Milojevic M, Baldus S, Bauersachs J, et al. 2021 ESC/EACTS Guidelines for the Management of Valvular Heart Disease: Developed by the Task Force for the Management of Valvular Heart Disease of the European Society of Cardiology (ESC) and the European Association for Cardio-Thoracic Surgery (EACTS). Rev Esp Cardiol. 2022;75(6):524. doi: 10.1016/j.rec.2022.05.006.

3. Barbosa PJB, Müller RE, Latado AL, Achutti AC, Ramos AIO, Weksler C, et al. Brazilian Guidelines for the Diagnosis, Treatment and Prevention of Rheumatic Fever. Arq Bras Cardiol. 2009;93(3 Suppl 4):3-18. doi: 10.1590/S0066-782X2009002100001.

4. Gewitz MH, Baltimore RS, Tani LY, Sable CA, Shulman ST, Carapetis J, et al. Revision of the Jones Criteria for the Diagnosis of Acute Rheumatic Fever in the Era of Doppler Echocardiography: A Scientific Statement from the American Heart Association. Circulation. 2015;131(20):1806-18. doi: 10.1161/CIR.0000000000000205.

5. McDonald RW, Ott GY, Pantely GA. Cleft in the Anterior and Posterior Leaflet of the Mitral Valve: A Rare Anomaly. J Am Soc Echocardiogr. 1994;7(4):422-4. doi: 10.1016/s0894-7317(14)80204-6.

6. Hammiri AE, Drighil A, Benhaourech S. Spectrum of Cardiac Lesions Associated with Isolated Cleft Mitral Valve and their Impact on Therapeutic Choices. Arq Bras Cardiol. 2016;106(5):367-72. doi: 10.5935/abc.20160053.

7. García-Ropero Á, Cortés García M, Aldamiz Echevarría G, Farré Muncharaz J. Severe Mitral Regurgitation due to an Extraordinary Heart Defect. Interact Cardiovasc Thorac Surg. 2016;23(3):503-5. doi: 10.1093/icvts/ivw113.

8. Remenyi B, Gentles TL. Congenital Mitral Valve Lesions: Correlation between Morphology and Imaging. Ann Pediatr Cardiol. 2012;5(1):3-12. doi: 10.4103/0974-2069.93703.